DETERMINING THE BINDING KINETICS AND SIGNALLING EFFECTS OF CB1 AND CB2 RECEPTOR LIGANDS; A CLOSER LOOK AT RESIDENCE TIME AND FUNCTIONAL SELECTIVITY

eman ta zabal zazu

Universidad del País Vasco   Euskal Herriko Unibertsitatea

Department of Pharmacology

PhD thesis dissertation

Leire Borrega Román

Vitoria-Gasteiz, 2022

Supervisors:

Joan Sallés Alvira

Sergio Barrondo Lacarra

FINANCIAL SUPPORT

INDEX

ENGLISH VERSION

EUSKARAZKO BERTSIOA

LIST OF ABREVIATIONS

2-AG: 2-Arachidonoylglycerol

AEA: Anandamide

BCA: Bicinchoninic acid

BRET: Bioluminescence Resonance Energy transfer

BSA: Bovine serum albumin

CB1: Type 1 cannabinoid receptor

CB2: Type 2 cannabinoid receptor

CNS: Central nervous system

DERET: Diffusion-enhanced energy transfer

DMEM: Dulbecco's Modified Eagle Medium

DMSO: Dimethyl sulfoxide

EPS: Extrapyramidal side effects

FACS: Fluorescence activated cell sorting

FBS: Foetal bovine serum

FL: Fluorescent ligand

GPCR: G protein-coupled receptor

Gpp(NH)p: Guanyl-5'-yl imidodiphosphate

HBSS: Hanks' Balanced Salt solution

HD: Huntington's disease

mGsi: mini Gsi protein

NBD: Nitrobenzoxadiazole

Nluc: Manola luciferase

NTD: N-terminal domain

OD: Optical Density

OMA: Operational model of agonism

OMA: Operational model of agonism

PBS: Phosphate Buffer Solution

PEI: Polyethyleneimine

Rt: Residence time

RT: Room temperature

SEM: Standard error of the mean

THC: Tetrahydrocannabinol

TR-FRET: Time Resolved Foster Resonance energy transfer

WT: Wild type

βarr2: β-arrestin 2

1. INTRODUCTION AND AIMS

CB1 and CB2 receptors, key elements of the endocannabinoid system

The endocannabinoid system comprises the synthesis and degradation enzymes of endogenous cannabinoid compounds, and the receptors which recognize and signal upon the binding of these endocannabinoids. The CB1 receptor was first cloned in the 90's (Matsuda et al., 1990), after being proposed as the main receptor responsible for Δ9-THC effects, the main psychoactive constituent of marijuana (Devane et al., 1988). Some years later, a second type of cannabinoid receptor, CB2, was cloned from HL60 cells and detected at high levels in spleen macrophages (Munro et al., 1993). Although CB2 was considered as "the peripheral" cannabinoid receptor for many years, the development of more sensitive techniques led to the identification of this receptor in the brain. The CB2 receptor levels in the brain, however, are respectively much lower than CB1 levels (Liu et al., 2009; Onaivi et al., 2008; Van Sickle et al., 2005), which has been described as the most abundant G protein-coupled receptor (GPCR) in the brain (Katona et al., 1999).

Around the same time that cannabinoid receptors where discovered, anandamide (AEA), the first endogenous compound activating cannabinoid receptors was identified (Devane et al., 1992), followed by 2-AG (2-Arachidonoylglycerol) (Sugiura et al., 1995). Both 2-AG and AEA mediate important functions in the endocannabinoid system and remain the most widely studied endocannabinoids to date (Kano et al., 2009). Both of them are arachidonic acid derivates and they are synthetised "on demand", playing a role of modulators of the synaptic function in the brain by regulating neurotransmitter release by retrograde signalling (Zou & Kumar, 2018). Endocannabinoids are small lipophilic molecules which, unlike other neurotransmitters, are not stored in vesicles; they are directly released from cells in response to intracellular calcium concentration increases (Tsuboi et al., 2018). The synthesis of AEA and 2-AG is complex and can involve different biochemical pathways, which are not fully elucidated yet (Kano et al., 2009). However, the main synthesis route for 2-AG involves phospholipase C (PLC) and diacylglycerol lipase (DAGL). PLC hydrolyses membrane phospholipids and produces diacylglycerol, which is later converted to 2-AG by DAGLs action. The

primary synthetic route for AEA involves N-acyl-phosphatidylethanolamine (NAPE), which is the precursor of AEA and is metabolized by an specific phospholipase D (NAPE-PLD) (Devane et al., 1992; Mechoulam et al., 1995; Sugiura et al., 1995). The main degradation enzymes for AEA and 2-AG are fatty acid amide hydrolase (FAAH) and monoacylglycerol lipase (MAGL), respectively (Bisogno et al., 2003; Cravatt et al., 1996; Dinh et al., 2002; Okamoto et al., 2004). 2-AG acts as a full agonist of cannabinoid receptors, and its concentration in the brain is significatively higher than AEA, which has been described as a partial agonist (Baggelaar et al., 2018; Gonsiorek et al., 2000; Sugiura, 2009).

Although CB1 and CB2 were originally described as the main receptors mediating the cannabinoid action in the body, other receptors such as the orphan receptors GPR55, GPCR18 or GPR119 can also be activated or modulated by cannabinoids *in vitro* (R. G. Pertwee et al., 2010). Furthermore, the ion channel TRPV1 (Transient Receptor Potential Vanilloid 1) has been shown to be activated by AEA and 2-AG both *in vitro* and *in vivo* (De Petrocellis et al., 2017) (see review Di Marzo, 2018). The physiological relevance of these new receptors in the endocannabinoid action is still not fully characterised, and in some cases, controversial, but undoubtedly adds complexity to the understanding of the endocannabinoid system.

CB1 and CB2 receptors belong to the class A or rhodopsin like subfamily of G-protein coupled receptors, the largest class of GPCRs, accounting for ~80 % of membrane receptors in humans. GPCRs represents the largest family of integral membrane proteins, with more than 800 different GPCRs encoded in the human genome (Foord et al., 2005). Moreover, they constitute a family of important therapeutic targets, as ~33 % of all marketed drugs target these receptors (Santos et al., 2019).

GPCRs are also known as 7TM (7-transmembrane) receptors, as all of them share the common structural feature of 7 transmembrane domains looping inside and outside the cell, with an N-terminal in the extracellular part of the membrane and the intracellular C-terminal (Kobilka, 2007). Upon ligand binding, conformational changes of the protein structure lead to the activation of different effectors, modulating distinct intracellular signalling cascades.

The two cannabinoid receptors CB1 and CB2 show different distribution patterns in the human body; the CB1 is predominantly expressed in the central nervous system (CNS), whereas the CB2 subtype is mainly expressed in peripheral tissues related to the immune system (Khurana et al., 2017) such as the spleen and thymus (Galiègue et al., 1995; Munro et al., 1993).

Signalling through CB1 and CB2 receptors

The CB1 and CB2 receptors mainly couple to the inhibitory G protein ($G\alpha_{i/o}$), subsequently inhibiting adenylyl cyclase (AC) activity and reducing intracellular cAMP levels and protein kinase A-mediated signalling. Although coupling to $G\alpha_{i/o}$ is the canonical activation pathway that CB1 and CB2 mediate, their binding to other G proteins has also been described in some situations (Howlett, 1995).

Both CB1 and CB2 receptors can activate MAPK proteins (mitogen-activated protein kinase), as ERK1 and ERK2 (extracellular kinase 1 and 2), p38 and p42/p44, and c-Jun N-terminal kinase (JNK) through G-protein dependent mechanism. CB1 can also negatively regulate N- and P/ Q-type voltage-gated Ca^{2+} channels (VGCCs) and positively regulate A-type and inward-rectifying K^+ channels in some cells (Pertwee, 2005).

As well as signalling through activation of inhibitory G proteins, cannabinoid receptors can also signal through other effectors such as β-arrestins. Arrestin recruitment is promoted by the phosphorylation of intracellular domains of the receptor and leads to receptor desensitization and internalization processes, as well as activation of different kinases such as MAPKs or ERK1/2 (Shenoy & Lefkowitz, 2003). Both β-arrestin 1 and 2 have been described to be involved in the signalling upon CB1 and CB2 activation, although β-arrestin 2 coupling is thought to be stronger than β-arrestin 1 (Ibsen et al., 2019).

Therapeutic potential of CB1 and CB2 targeting drugs.

Although the levels of CB1 receptor in the periphery are comparatively lower than the CNS levels, they are present in tissues such as adipose tissue, liver and pancreas where they regulate important metabolic functions, and therefore, they represent a potential therapeutic target for many CNS and non-CNS related diseases (Pacher et al., 2006). Similarly, the CB2 expressed in the CNS, although

being present in notably lower levels than in the periphery, has important implications in a variety of neurological diseases including Alzheimer disease or Parkinson disease, where CB2 expression has found to be upregulated (Benito et al., 2003)(Gómez-Gálvez et al., 2016), thus becoming an interesting potential target for neurodegenerative disorders (Navarro et al., 2016).

For example, CB1 agonists are presented as potential drug candidates to treat Huntington's disease (HD). It has been described that CB1 receptor expression is downregulated in medium spiny projection neurons of the caudate and putamen (Denovan-Wright & Robertson, 2000; Glass et al., 2000; Van Laere et al., 2010). Moreover, the decrease of CB1 function has been demonstrated to contribute to the symptomatology of HD such as cognitive or motor impairment in animal models (Blázquez et al., 2015, 2011; Chiarlone et al., 2014). Therefore, CB1 agonists has been proposed as potential therapeutic targets for treating HD (Laprairie et al., 2016). Laprairie et al. (2016) demonstrated that some CB1 agonists contribute to the cell viability and corrected CB1 expression levels *in vitro* using ST*Hdh* medium spiny projection neuron cells. Furthermore, they hypothesized that compounds selectively activating $G_{i/o}$ dependant pathways over arrestins may be advantageous for treating HD (Laprairie et al., 2016, 2017).

Targeting CB1 and CB2 has also been proposed for alleviating the symptoms of schizophrenia (Kucerova et al., 2014). Alterations on the cannabinoid system, including changes in CB1 and CB2 expression have been described in patients with psychosis episodes. Several pre-clinical studies have demonstrated the effectiveness of cannabinoids for improving the symptomatology using animal models, although safety concerns and a poor risk-benefit balance has prevented the clinical use of cannabinoids up to date. Nevertheless, recent advances in understanding the role of CB2 receptor in the regulation of dopaminergic and glutamatergic systems suggest that treatments focusing specifically on CB2 modulation could be beneficial for early stage psychosis episodes, as well as the use of the allosteric modulator cannabidiol (CBD) (Cortez et al., 2020).

Some other potential therapeutic applications targeting cannabinoid receptors include the treatment of multiple sclerosis (Khan et al., 2022) or inflammatory and neuropathic pain (Guindon & Hohmann, 2008). Targeting cannabinoid receptors outside the nervous system has also been studied as a strategy for the

treatment of cardiac disease (Lu et al., 2019), obesity (Sullivan et al., 2021) or cancer (Hinz & Ramer, 2022).

Challenges targeting CB1 and CB2

Even though the cannabinoid system has been presented as a promising drug target for many different diseases, very few drugs targeting CB1 or CB2 receptors have reached the clinic to date. One example is the CB1 antagonist rimonabant which was marketed as a promising anti-obesity drug; however it was subsequently withdrawn from the market due to its severe neuropsychiatric adverse effects (Moreira & Crippa, 2009). Currently, Marinol® (dronabinol), Syndros® (dronabinol), and Cesamet® (nabilone) are the only FDA approved synthetic cannabinoids, which are used for treating nausea derived from cancer chemotherapy treatments and anorexia, which derive in weight loss, for AIDS patient (www.fda.gov).

The lack of success targeting these receptors can be partly explained by the challenge of designing selective drug candidates. Both cannabinoid receptors exhibit a high homology level, sharing 44% of their sequence at protein level in the whole sequence and sharing up to 68% identity in the transmembrane regions (Munro et al., 1993). The crystal structures solved for these two receptor subtypes in the last years (Hua et al., 2019; Xing et al., 2020) has provided valuable insights into the key residues implicated in the binding of ligands to these lipid binding GPCRs. The high degree of similarity described for their agonist binding pockets (Hua et al., 2020) makes the design of selective compounds a big challenge. Nevertheless, the combination of the recent structural information with new computational approaches has revealed new insights in the binding mode of specific compounds (Yang et al., 2020), presenting new strategies for successful drug design.

The drug-receptor binding process and the role of kinetics in drug action

The affinity of a ligand for a receptor is defined by the strength of the interaction between both species. The dissociation binding constant (K_d) is the pharmacological parameter to describe the affinity and express the concentration

of ligand or drug required to occupy half of the receptors when the binding reaches equilibrium.

The binding process of drug and receptors has been described by models that follows the law of mass action where the binding is considered a one-step reversible first-order reaction, where the reaction rate is proportional to the reactants concentration. Thereby, the drug-receptor complex [RL] formation rate (k_{obs}) will be proportional to the concentrations of both the receptor [R] and the drug molecule [L]. In this case, the [RL] formation will be dependent on the association constant rate (k_{on}), whereas the reverse reaction where both species unbound will be dictated by the dissociation constant rate (k_{off}). As the ligand forms complexes with the receptor, less [L] and [R] will be free to form new complexes, so the association will be slower as the binding occurs. When both complex formation and dissociation rate are equal ($[R] \cdot [L] \cdot k_{on} = [RL] \cdot k_{off}$), the system is in equilibrium and the division of rate constants will define the K_d affinity parameter ($K_d = k_{off}/k_{on}$).
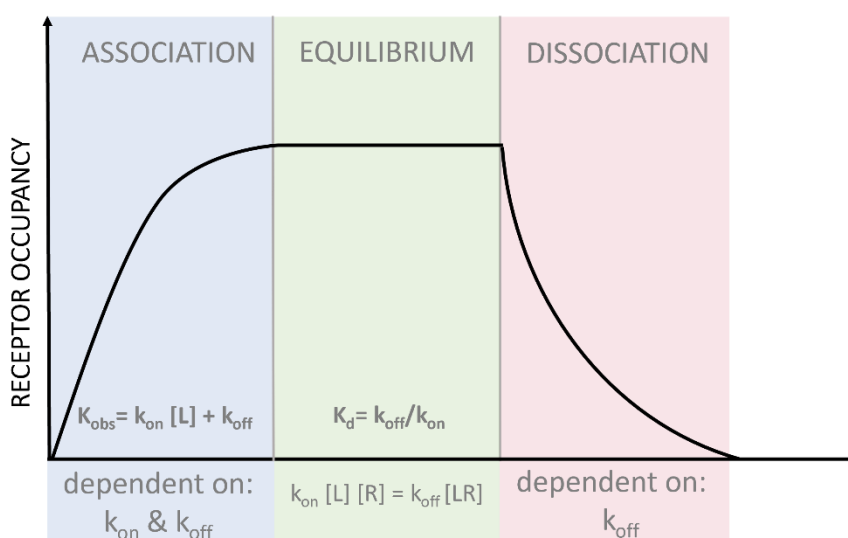
Figure 1. *Schematic representation of the ligand-receptor binding phases.*

While k_{on} is a second order rate constant and its units are reciprocal of concentration and time (M^{-1} min^{-1}), the dissociation rate is only dependant on time (min^{-1}), independently on the concentration of the ligand (see Figure 1). As both association and dissociation will simultaneously take place during the association phase, the observed association rate constant (k_{obs}) will define the binding rate that is observed with each ligand concentration, accounting for both

association and dissociation phenomena ($k_{obs}= (k_{on}$ x L$) + k_{off}$). Therefore, both k_{on} and k_{off} will be dictating the duration and shape of the association phase. In contrast, the dissociation phase will only be governed by the $koff$ parameter, that will be determinant of the time that a ligand remains bound to its target, or "residence time" (Rt), defined as the inverse of k_{off} (Rt=1/k_{off}).

Traditionally, K_d has been used as the main parameter to describe the ligand binding properties, and drug discovery programs have relied on this equilibrium constant in their search for potential drug candidates. However, as long as the body is an open system where equilibrium conditions may not be representative, the use of equilibrium parameters may not be appropriate. Moreover, it can be observed that infinite combinations of k_{on} and k_{off} can lead to the same binding affinity (K_d). Over the last decade, the interest in elucidating the implication of kinetics in drug action has been increasing, and efforts have been made to include the kinetic perspective in the drug development programs. As long as a drug will exert its action only when bound to the receptor and equilibrium conditions may not be reached in the physiology, the use of association and dissociation rates could significantly elucidate many aspects of drug action to translate them to in vivo (Copeland et al., 2006).

Many cases have been described where the binding kinetics seem to have a direct implication in drug action or toxicity. Although other phenomena as clearance rates, rebinding, or receptor turnover rate should also be considered to draw conclusions (Dahl & Akerud, 2013), today we are aware of many examples where a certain kinetic profile of drug-target interaction resulted in a better clinical outcome.

Long-residence times (slow k_{off}) has been shown to be desirable and prolong clinical effects in many cases (Guo et al., 2014). The second generation antihistamine bilastine, for instance, which exhibit long residence time, has a longer duration of action than other drugs blocking H1 receptor (Bosma et al., 2019). Candesartan, an angiotensin II type 1 (AT1) receptor antagonist used for the treatment of hypertension, has also shown improved clinical performance related to its long residence time (Fuchs et al., 2000). Another example is found in the use of CRF-1 antagonists (Fleck et al., 2012) for the treatment of sleep

disorders, where slow dissociation of such ligands result in an extended duration of action linked to increased drowsiness.

The drug tiotropium, used for the treatment of chronic obstructive pulmonary disease COPD constitutes another interesting example where kinetics play an important role modulating the drug action. In this case, the compound exhibits the same affinity (K_d) but selective kinetics profile for different muscarinic receptors, showing a ten-fold higher residence time toward the M3 muscarinic receptor (~10 h) than toward M2 (Casarosa et al., 2009; Sykes et al., 2012). In this case, the lower adverse effects of tiotropium, compared to other muscarinic agents, is considered a consequence of the long residence time in the on-target receptor M3 in comparison with the residence time shown in M2 (off-target).

Kinetic parameters have suggested to play an important role in the appearance of on-target adverse effects, as first described for antipsychotic drugs that target the dopamine D_2 receptor (Kapur & Seeman, 2000), where the short residence time of atypical antipsychotics such as clozapine were predicted to be associated with lower adverse effects, specifically reduced extrapyramidal side effects (EPS), while the longer receptor occupancy was proposed to be directly linked to the appearance of EPS. However, subsequent functional and binding studies using fluorescent tracers, suggest that k_{on} may also be influencing the clinical outcome as it directly affects rebinding and receptor reversal rates in the synaptic space (Sykes et al., 2017).

Even though the knowledge around cannabinoid receptors pharmacology has dramatically increased during the last decades, less attention has been paid to understanding the binding kinetics of compounds which bind both these receptor subtypes. A thorough examination of drugs binding kinetics, both in-vitro and in-vivo, can ultimately lead to a more complete understanding of their action. Additionally, this approach can help to explain improvements in clinical performance, be they related to drug efficacy or toxicity (Casarosa et al., 2009; Sykes et al., 2012, 2017; Tresadern et al., 2011).

Limitations for ligand-receptor binding kinetic characterization

Several approaches can be used to determine the kinetic association and dissociation rates of drugs binding to GPCRs. As individually labelling the

10

compounds of interest to study its binding properties is not feasible due to the increase cost that this would entail, the methodologies available rely on the competition of "cold" or not-labelled compounds with a tracer molecule. The model presented by Motulsky and Mahan (1984) is probably the most widely used methodology to assess the kinetic parameters of compounds. It consists of the monitorization of the tracer binding to our target receptor in the presence of different concentrations of the cold ligand that were simultaneously added before the binding starts. The competing cold ligand will change the binding profile of our tracer molecule depending on its association and dissociation rates, and therefore, the kinetic constants of the competing cold compounds can be estimated. It is necessary to accurately calculate the kinetic parameters of the tracer molecule in the absence of competitor in order to obtain the results for the tested cold compound parameters. Alternative approaches to the Motulsky and Mahan methodology has been used where the "delayed association" of a radioligand was monitored after preincubating the receptors with the cold ligand (Hara et al., 1995; Packeu et al., 2008, 2010)

Traditionally, radioligands have been used to assess the affinity and kinetic properties of drug-receptor binding (Dowling & Charlton, 2006; Ramsey et al., 2011; Sykes et al., 2010). However, the use of radioligands presents many drawbacks such as the increased risk associated with the manipulation of hazardous radioactive material and the increased experimental time and costs that are associated with these types of procedures. Indeed, the conditions under which radioligand competitions experiments are carried out are normally low throughput, and often carried out under non-physiological conditions. Furthermore, the traditional assay format presents difficulties in the characterisation of fast associating ligands (Georgi et al., 2019; Sykes et al., 2019), as the filtration step required for the separation of radioligand bound and unbound fraction, which makes difficult to acquire data of the early time points, necessary to assess the degree of competition between the tracer and the competitor.

The development of Scintillation Proximity Assays (SPA) allows to avoid the separation step that conventional radioligand technique requires, but bead settling can complicate the interpretation of early time points (Xia et al., 2016).

Moreover, even if homogeneous reading of the sample can be performed, this technique is still low throughput and difficult to apply to large compound series.

Surface Plasmon Resonance (SPR) techniques (Bocquet et al., 2015; Segala et al., 2015) or mass spectrometry (Massink et al., 2015) have been also used to study ligand binding kinetics as alternative methods that avoid the use of radiolabelled material, as they allow the detection of binding of non-labelled ligands. Nevertheless, purification of the GPCRs is necessary for SPR application, which constitutes the main limitation due to the poor stability of these proteins outside the lipidic membrane. On the other side, approaches using mass spectrometry are very labour intensive as filtration steps are necessary for each experimental point similar to the traditional radioligand assays (Ricart-Ortega et al., 2020).

During the last decade, methods based on resonance energy tranfer (RET) as TR-FRET (Schiele et al., 2015; Klein-Herenbrink et al., 2016) and BRET (Stoddart et al., 2018; Bouzo-Lorenzo et al., 2019) have been gaining more importance in the pharmacology field as useful strategies to study the ligand-receptor binding process. Methodologies based on resonance energy transfer present many advantages as homogeneous reading (no separation step is need) and precision in early time point readings, which is essential especially for kinetic studies.

Understanding efficacy of drugs on GPCRs from a molecular perspective.

The concept of efficacy has significantly evolved since it was first introduced by Stephenson (1956) as the ability of a drug to elicit a response upon binding to a receptor. The first proposed lock-and-key model, where the receptor would act as a switch capable of activating the cellular response upon ligand binding, became too simplistic given the dynamic nature of receptor proteins.

The first model that attempt to give a mechanistical explanation of receptor function was the "two-state model". According to this model, two receptor states (R, resting state and R*, activated state) in conformational equilibrium will be capable of binding the drug. While agonists would have preference for R*, antagonists will preferentially bind R, displacing this equilibrium to activated R* state (agonists) or resting R (antagonists).

12
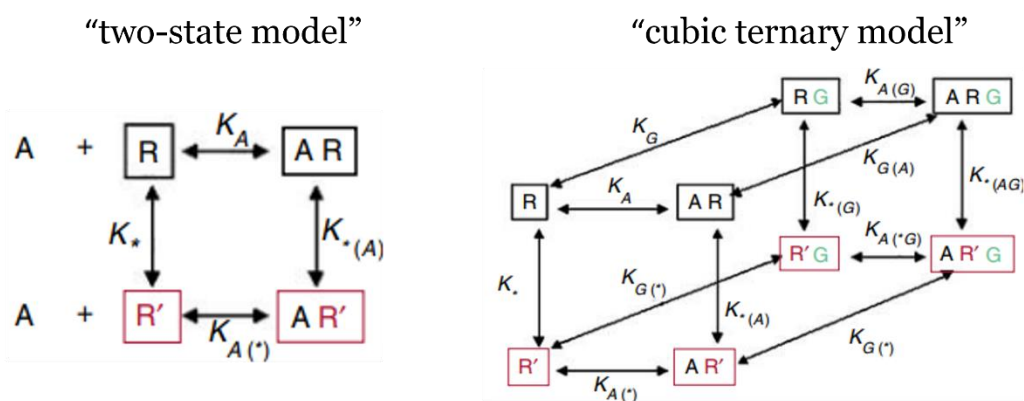
***Figure 2**. Different models of receptor activation by agonists. On the left, the reversible "two -state model" reflects the equilibrium between two states of the receptor, which can be shifted depending on the preference of the ligand A to bind R or R*. On the right, the more complex "cubic ternary model", where receptor's state is also influenced by the binding of intracellular G-proteins. Modified from (Rang, 2006).*

Later on, with the discovery of G-protein coupling to GPCRs as the first step of the signal transduction, the model evolved to the "ternary complex", including the G-protein as factor determining the different states of the receptor (Weiss et al., 1996). Schematic representations of the "two-state model" and the "cubic ternary model" are shown in Figure 2.

Although these models can work as approximations for defining efficacy, nowadays we know from protein thermodynamics that multiple conformations with a variety of affinity for effectors coexist (Weis & Kobilka, 2018). Moreover, the definition of "biased agonism" or the distinctive capability of ligands for activating certain responses further complicates the development of precise models to define drug action.

The operational model of agonist proposed by Black and Leff (Black & Leff, 1983) constitutes a valuable approach for defining and quantifying ligand bias and selective functionality and has been extensively applied during the last decades for profiling drug action. Nevertheless, this model presents an empirical approach for defining drug action from a quantitative perspective but lacks the capability of giving a mechanistic understanding of the receptor activation on a molecular level.

Moreover, the role of binding kinetics in the receptor activation process is yet unclear. Although in many cases specific kinetic features have been shown to derive in improved clinical outcomes (see section: The drug-receptor binding

process and the role of kinetics in drug action), the implication of kinetics in the receptor activation process is still a field to explore.

In the early 60s, Paton's "rate-theory" proposed that rather than receptor occupancy, the effect of a drug would be proportional to the number of the drug-receptor complexes formed (Paton, 1961). In this sense, the efficacy elicited by a drug would be strongly linked to the binding kinetics parameters. Paton hypothesized that after ligand binding and activation, it was necessary to "reset" the receptor by binding a new ligand before a new activation cycle could occur. According to this idea, fast dissociating drugs (high k_{off}, short residence time) will more efficiently activate the intracellular signalling, and slow dissociating ones (low k_{off}, long residence time) would be less efficacious.

More recently, aware of the limitations of describing the activation process as an equilibrium process, several efforts to develop models including the kinetic aspects has been made, (Kinzer-Ursem & Linderman, 2007; Shea et al., 2000; Waelbroeck et al., 1997). These models are derivations of the cubic ternary complex where kinetic aspects of the species formation are included. Nevertheless, these models do not specifically address the implication of ligand binding kinetic rates. However, it can be derived from their assumptions that oppositely to Paton's rate theory, long residence time ligands would be the ones displaying more efficacy, as the stabilization of the receptor for longer times would allow more G protein activation cycles, whereas fast off ligands may not stabilise the active conformations for enough time to produce the effector activation, so called "non-productive cycling".

Biased agonism

Biased agonism is defined as the ability of ligands to preferentially activate a signalling pathway at the expense of other.

Classically, the efficacy was seen as the ability to trigger an array of cell processes upon ligand binding to a receptor, and it was believed to be a monotonic response only varying in intensity. Until the 80s, pharmacological responses were measured as integrated outcomes derived from complex processes such as muscle contraction in isolated tissues, or biochemical measures such as cAMP accumulation. Nevertheless, with the development of heterologous systems and

the ability to perform a more detailed characterization of the cellular responses, different pathways and effectors interacting with GPCRs were discovered, and it became clear that the nature of the response could vary not only quantitatively. The observation of different activation patterns depending on the agonist used for receptor activation introduced the concept that the efficacy could also be described in qualitatively terms.
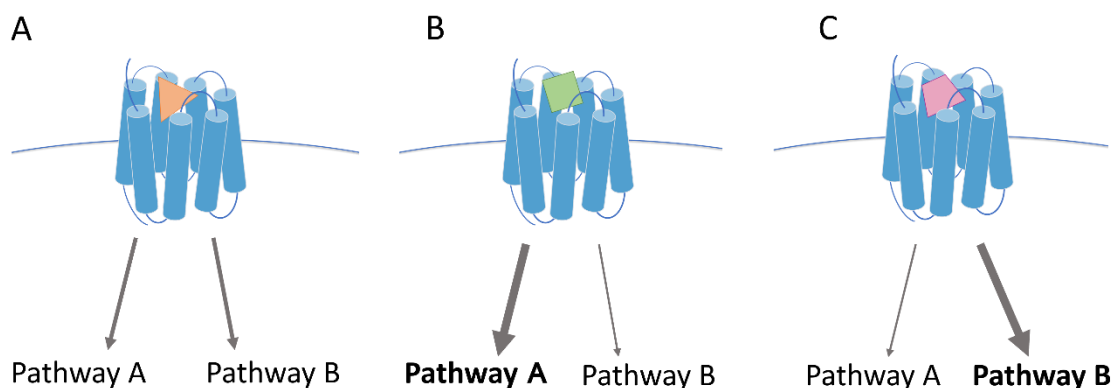
Figure 3. Schematic representation of ligand bias at GPCRs. Some ligands will not elicit a preferential activation of the different pathways and therefore will be balanced compounds (A). Some ligands can preferentially activate a certain pathway, and therefore bias the intracellular response triggered upon ligand binding (B and C).

This idea suggested that the receptor is not the minimum component that will dictate the intracellular processes activation, but rather than the receptor-ligand complex will be dictating the effect (see Figure 3). This new paradigm was presented along with the idea that not a single active conformation of the receptor exists, but several different conformations that will exhibit different ability to engage the distinct protein effectors. In this sense, GPCRs would act as allosteric proteins that can adopt several different conformations depending on the nature of the binding ligand, and act as communicating link to intracellular effector proteins differently. This distinct engagement to effectors is achieved through changes in the receptor conformation (induced fit) or through the stabilisation of different conformations of the protein (conformational selection) that coexist, rather than the classical active-inactive dichotomy scheme from the classical pharmacology models.

Therefore, a probabilistic model would describe a scenario where many different states or conformations would be present, showing a particular frequency

distribution (Onaran & Costa, 1997; Onaran et al., 2000). The equilibrium between different states will be altered upon the binding of a ligand, and therefore, the frequency distribution of the different receptor states will be altered. This model assumes that the binding of a ligand will favour some conformational states and preclude others, selectively changing the conformational landscape. While the classical receptor theory models account for two-state model or ternary models to mechanistically explain the link between ligand binding and efficacy, where the active-inactive receptor dichotomy exists, the probabilistic model presents many conformational states of the receptor and therefore, a more versatile paradigm to understand efficacy as a "pluridimensional" concept.
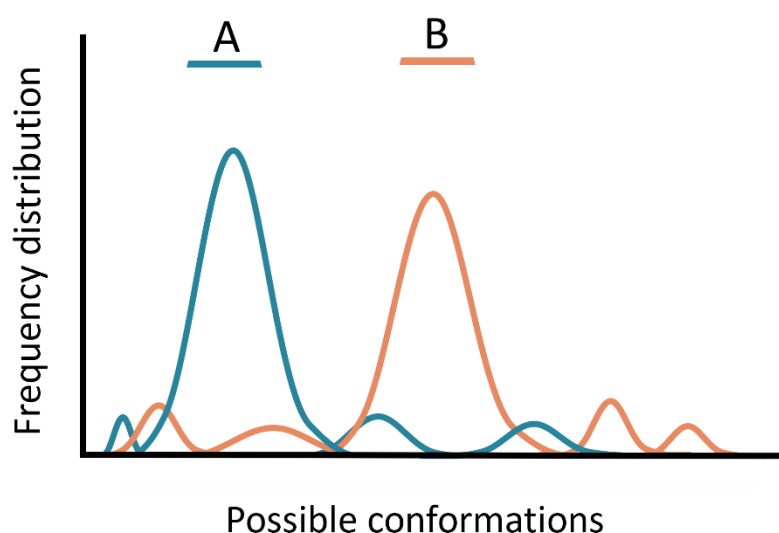
Figure 4. Frequency distribution of GPCR conformational states upon ligand binding. While ligand A may stabilise primarily conformations with more affinity to one effector (e.g G proteins), ligand B binding favour mostly different conformations that show greater affinity to other effector (e.g. arrestins).

According to this model, the quantity and type of conformation stabilised upon ligand binding will dictate the efficacy. As shown in **Figure 4**, some ligands will shift the distribution of conformations towards those interacting to G proteins, while the binding of a different ligand can favour different type of states that are more prone to interact with other effectors such as arrestins (Kenakin, 2004).

Biophysical studies carried out during the last decade have demonstrate the presence of diverse conformations in β2-adrenergic receptor (Manglik et al., 2015) and rhodopsin (Van Eps et al., 2017) in their inactive states. Moreover, the studies also showed how after activating the receptor with agonist or light in the

case of rhodopsin, an equilibrium shift occurred, but conformational heterogeneity remained. These studies showed the structural diversity of GPCRs in both their resting and stimulated states, consistent with the multiconformational model that attempts to explain the biased signalling (Gurevich & Gurevich, 2020).

The biased agonism concept generated great interest in the pharmacology field, as it presented new opportunities to selectively regulate cellular processes. Thereby, this phenomenon offers the opportunity to develop pathway selective therapies, that even targeting the same receptor, could selectively activate the signalling cascades of interest, which regulates the processed that derived in the desired effect. This could bring the opportunity to develop therapies targeting GPCRs and eliminating the side effects that would be consequence of different signalling pathway activation. Therefore, this potential benefit becomes especially important when on-target adverse effects have restricted or limited new drug therapies for a certain target. Ideally, drugs with a selected activation profile would lead to sophisticated treatments showing an improved clinical performance and avoiding the unwanted effects.

Opioids receptors are a clear example where biased ligands present an opportunity based on the different mechanism described for the analgesic and unwanted effects (Che et al., 2021). Some studies observed an enhanced analgesic effect with decreased side effects in β-arrestin 2 knock out mice (Bohn et al., 1999; Raehal et al., 2005). Therefore, it was suggested that the analgesia produced by targeting μ opioid receptors (μ-OR) was mediated by Gi activation, whereas side effects as tolerance, addiction and respiratory depression may be mediated by β-arrestin 2 recruitment.

In 2020, TRV130 (oliceridine) was approved by The Food and Drug Administration (FDA) as a G protein–biased agonist at μ-OR for treating moderate to acute pain. Nevertheless, understanding the cellular mechanisms that drive each effect in vivo is challenging due to the complexity and interplay of multiple factors in an organism and the better side-effect profile of TRV130 has been attributed to its partial agonism nature (Gillis et al., 2021) and not to the biased nature of the ligand.

Regarding the quantification of the bias displayed by agonist at a certain receptor, different strategies can de adopted for ranking the efficacy at the different cellular responses. The simplest method consists of using the EC_{50} potency values to characterise agonist activities when the compounds show maximal activation of the system and therefore, act as a full agonist. Nevertheless, this method is not appropriate when characterising ligands displaying submaximal effect, as both potency and E_{max} values describing the agonist activity needs to be accounted for a correct analysis of the agonists. The most extended approaches to characterise the bias activity of agonists are the comparison of relative activity ratios (RA) or "transduction coefficients" (τ/K_A) (Kenakin & Christopoulos, 2013). The relative activity is defined by the ratio of the maximal response to the EC_{50} value (RA = E_{max}/EC_{50}), and it is a useful measure to compare agonists activities among different pathways, taking into account both potency and maximal effect (Ehlert, 2008). The transduction coefficient (τ/K_A) was proposed by the operational model developed by Black and Leff (1983) for comparing agonists activities. The parameter τ integrates agonist efficacy, receptor density and coupling within the system. The use of both relative activities (RA) and transduction coefficients (τ/K_A) are widely accepted and used to characterise agonist activity at different pathways and asses bias (Kenakin & Christopoulos, 2013; Kolb et al., 2021). However, although the calculation of relative activity ratios (E_{max}/EC_{50}) is simpler, it is only useful when the dose-response curves analysed show a slope near to unity, which limit the use of this approach only to certain circumstances. In the rest of the cases, the operational model represents the most widely used method to rank agonist activities among different pathways.

Aims

Following the challenges discussed in previous sections, the main aims of this PhD are:

1. To develop a reliable method for the characterisation of cannabinoid compound binding kinetic properties to human CB1 and CB2 receptors.

2. To characterise the association and dissociation rates (k_{on} and k_{off}) of a series of cannabinoid compounds and therefore, determine the residence time of the selected cannabinoid compounds at CB1 and CB2 receptors using the model proposed by Motulsky and Mahan.

3. To characterise the signalling properties of the selected cannabinoid compounds upon binding at CB1 and CB2 receptors in β-arrestin 2 recruitment, miniG protein coupling, and internalization assays and calculate the bias of the compounds using the operational model.

4. To explore the relationship between residence time of cannabinoid agonists and signalling efficacy at CB1 and CB2 cannabinoid receptors.

2. MATERIALS AND METHODS

MATERIALS AND REAGENTS

Blasticidin HCl 10 mg/ml (Gibco, ref: 808854)

BSA: Bovine Serum Albumin (Sigma, ref: A7030)

Cell Dissociation non-enzymatic solution (Sigma, ref: C5789)

Dulbecco's Modified Eagle Medium (DMEM) (Sigma, ref: D6429)

EDTA purified grade, ≥98.5%, powder (Sigma)

EGTA purified grade ≥97% powder (Sigma)

Fluorescein Sodium salt (Sigma, ref: F6377)

Furimazine (AOBIOUS ref:36539)

G418- Geneticin (Gibco, ref: 10131035)

Hanks' Balanced Salt solution (Sigma, ref: H82G4)

$MgCl_2$ $6H_2O$ (Panreac, 131396)

OptiMEM (Gibco, ref: 11520386)

PEI linear, MW 25000, Transfection grade (PEI 25K) (Polysciences, ref: 23966-1)

Pierce™ BCA Protein Assay Kit (Thermo Scientific ™ ref: 23225)

Pluronic acid (Sigma, ref: P2443)

Poly-D-lysine hydrobromide (Sigma, ref: P6407)

SNAP-Surface® Alexa Fluor® 647 (New England Biolabs)

T-REx™-293 Cell Line (Invitrogen ref: R71007)

Trizma base (Sigma, T1503)

Trypan blue (Gibco ref:15250061)

Trypsin EDTA (0.25 %) (Gibco ref: 25200056)

Greiner CELLSTAR® cell culture 96 well plates (Merck ref:655098)
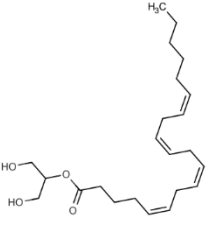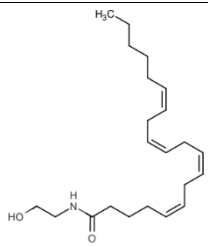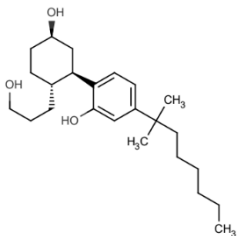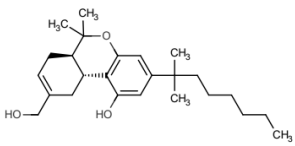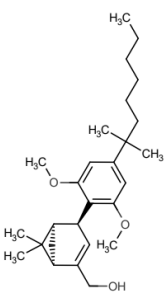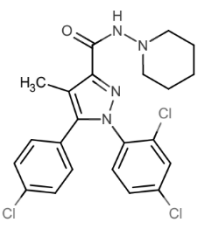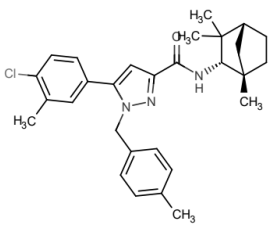
Zeocin ™ 100 mg/ml (Invitrogen)

Propylene 384 well storage plate, flat bottom, nonsterile (Falcon, ref: 353265)

BRAND™ 96-well plates (Fisher Scientific, ref: 10106131)

Rimonabant, HU210, CP55940, 2-AG, AEA, HU 308 were purchased from Tocris. SR144528 was purchased from Sigma.

	2-AG	Anandamide
Endogenous cannabinoids		
	CP 55940	HU-210
Non-selective agonists		
	HU-308	
CB2 selective agonist		
	Rimonabant	SR 144528
Inverse agonists		

METHODOLOGY

PLASMID GENERATION

SNAP-CB1, SNAP-CB1 $_{55\text{-}472}$, SNAP-CB1 $_{91\text{-}472}$, SNAP-CB2, SNAP-CB1-Nluc, SNAP-CB2-Nluc encoding plasmids were generated for the study. The DNA sequence for truncated and fused receptor proteins were cloned into pcDNA4/TO and modified via Gibson assembly (Gibson, 2011).

For N-terminal truncations of CB1, a two-fragment plasmid assembly was used (Heydenreich et al., 2017) whereby PCR oligonucleotides were designed such that Gibson assembly of the resulting DNA fragments would exclude the sequence for the truncated portion of the receptor. Two truncated variants of the human CB1 receptor were created, SNAP-CB1$_{55\text{-}472}$, and SNAP-CB1$_{91\text{-}472}$, by eliminating the first 54 and 90 amino acids from the N-terminus of its original human protein sequence respectively. The SNAP-CB2 receptor contained the whole protein sequence from the original human receptor.

Likewise, fusion of Nanoluc to the C-terminus of CB1 and CB2 receptors was performed by inserting the DNA sequence for a flexible GSSG peptide linker sequence followed by Nanoluc, between the C-terminal receptor residue and the stop codon.

All newly generated plasmids were verified by analytical restriction digest of the whole plasmid and subsequent agarose gel electrophoresis, as well as by Sangar sequencing covering the entirety of the coding sequence for the receptor constructs.

Plasmid amplification was carried out following standard procedures of transformation of *Escherichia Coli* TOP10 chemically competent cells with the plasmid of interest following with colony isolation in agar plates and growth using LB media. The plasmidic DNA was obtained from *E. coli* culture following standard methods using Macherey-Nagel™ NucleoBond™ Xtra Midi kit.

STABLE CELL LINES

HEK293-TREx™ cell line (Thermo Fisher Scientific) was used for the generation of stable cell lines. HEK293-TREx cell line uses the TREx expression system, for tetracycline-inducible expression of genes (Yao et al., 1998). These cells stably express the Tet repressor (TR) from the pcDNA™6/TR plasmid. The cells are transfected to express the gene of interest and dual selection is carried out using the vector-specific antibiotic and blasticidin for the maintenance of pcDNA™6/TR plasmid. In our case, the vectors used were pcDNA4/TO and Zeocin was used as the selection antibiotic for the maintenance of the plasmid encoding the protein of interest.
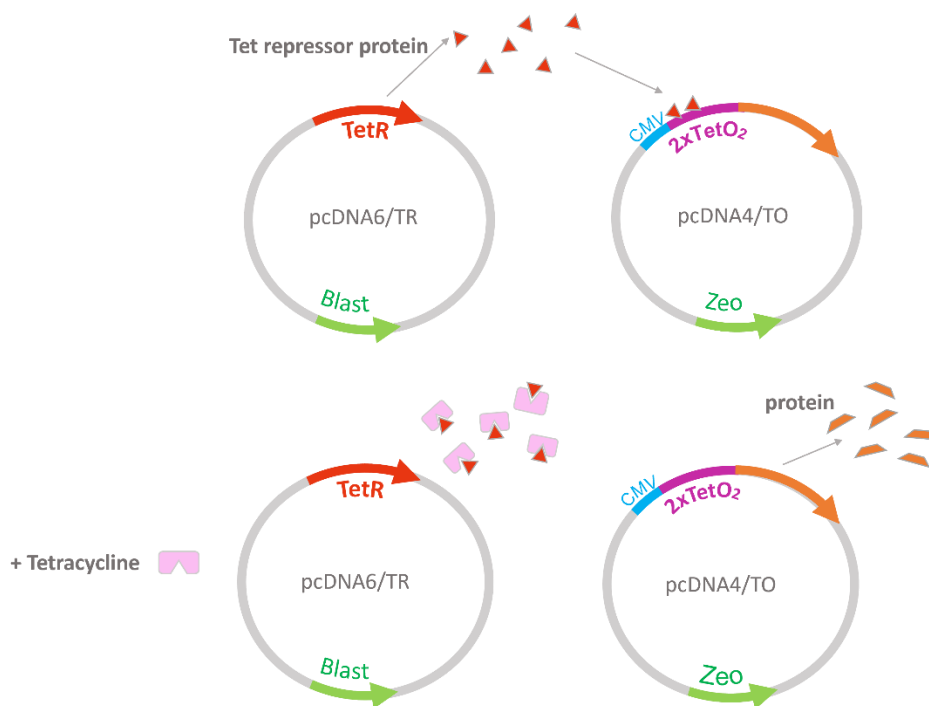
***Figure 5**. Schematic representation of TREx system. Transcription of the gene of interest (orange arrow) is repressed by Tet repressor protein in the absence of tetracycline. By adding tetracycline, the repressor cannot bind the tetracycline operator sequences (TetO2) and transcription of the sequence encoding the desired protein is promoted by CMV promoter.*

TREx system is a tetracycline mammalian expression system that has two tetracycline operator sites inserted after the CMV promoter. In the absence of tetracycline, the tetracycline repressor protein is synthetised from the pcDNA6/TR™ regulatory plasmid and will effectively block transcription initiation in the second plasmid (pcDNA4/TO) by binding to the TetO$_2$

tetracycline operator sites (Postle et al., 1984). When tetracycline is added to the cell culture media, it will bind and change the conformation of the repressor protein and prevent its binding to the $TetO_2$ sites, derepressing the transcription from the CMV promoter (see Figure 5). This system results in a high-level expression of the gene of interest.

Transfection protocol and selection of cells

For the transfection, HEK293-TRex cells were cultured in a T75 flask using Dulbecco's modified Eagle's medium (DMEM) supplemented with 10% FBS and Blasticidin (5 µg/ml). The transfection was carried out when the cells were in exponential growth phase (80-90 % confluent). A total amount of 5 µg DNA and 15 µg PEI were used for transfecting one T75 flask (DNA to PEI ratio 1:3). The DNA and PEI were diluted separately in 250 µl OptiMEM each and vortexed. The diluted DNA and PEI were mixed using 1:1 volume ratios (250 µl + 250 µl) and the mixture was incubated for 20 min at room temperature before adding to the cell culture. The culture media was replaced with 5 ml of fresh media containing DMEM supplemented with 10 % FBS 1h before transfecting the cells. Penicillin and Streptomycin in a final concentration of 100 I.U/ml and 100 µg/ml respectively were added to the media. The next day (~16h after transfection) the media was replaced with 15 ml of fresh warm media (DMEM + 10% FBS). Two days after transfection, the cells were subcultured (1:5 split). Media was aspirated, cells were washed with PBS and 2 ml of trypsin were added to the cells. The flask was incubated for 5 min at 37°C to allow the trypsin action. Cells were collected in ~5 ml of fresh media and centrifuged at 200 x rcf. The pellet obtained was resuspended in fresh media (DMEM + 10% FBS) and gently pipetted up and down 8-10 times to avoid clumps. 20 % of the volume was seed in a new T75 flask with a total volume of 15 ml of compete media (DMEM + 10% FBS) containing Blasticidin (5 µg/ml) and Zeozin (20 µg/ml) antibiotics for selection. The media containing the two antibiotics was replaced every 2-3 days until resistant colonies were achieved (2-3 weeks). The rest of the cells were frozen using DMEM + 10 % FBS + 5 %DMSO in 1 ml cryovial.

The above procedure was carried out for the generation of different cell lines. In the case of HEK TR-SNAP-CB1 full length and truncated versions and HEK TR-SNAP-CB2 expressing cell lines, the corresponding pcDNA4 was used and the

generated stably expressing cell lines were used to prepare membranes for ligand binding assays.

On the other hand, the HEKTR-SNAP-CB1-Nluc_βarr2-Venus and the HEKTR-SNAP-CB2-Nluc_βarr2-Venus cell lines were generated using a co-transfection were one of the plasmids (pcDNA4/TO) expressed the SNAP tagged CB1 or CB2 receptor with a Nanoluc fused to the C-terminal and a second plasmid (pcDNA3) encoded the biosensor and express resistance to G418 antibiotic (Geneticin). In this case, the biosensor was a β-arrestin 2 protein with a Venus fluorescent protein fused to its C-terminal. In the first case (HEKTR-SNAP-CB1-Nluc_βarr2-Venus cell line), the receptor:biosensor ratio used was 9:1 respecting the total DNA used for the transfection (5 μg) and the subsequent steps were carried out as previously explained with the addition of 250 μg/ml of G418 during the cell selection period. In the second case (HEKTR-SNAP-CB2-Nluc_βarr2-Venus) three different cell lines were created varying the receptor and biosensor encoding plasmids' ratios used in the co-transfection (1:3, 1:9 and 1:29 ratios of receptor to biosensor).

Fluorescence-Activated Cell Sorting (FACS)

HEKTR-SNAP-CB1-Nluc_βarr2-Venus stable cell line was sorted using Fluorescence-activated cell sorting, also known as FACS. The mixed population cell line generated was sorted by their level of biosensor (a β-arrestin 2 with a fused Venus) and receptor (a SNAP tagged CB1 receptor with a Nluc luciferase fused to its intracellular C-terminal). The biosensor level was assessed by the emission of the Venus protein, and the receptor level was assessed by labelling the SNAP tag fused to the extracellular N-terminal of the receptor with a substrate emitting in the red spectra.

In order to prepare the cells for the FACS, SNAP-Surface® Alexa Fluor® 647 red fluorescent cell impermeable substrate was used to label the SNAP tag fused to the receptor. HEK TR cell line was used as a negative control to account for the background staining when the SNAP tagged receptor was not present in the cell surface. The cells were cultured in T75 flasks with DMEM supplemented with 10% FBS; Blasticidin (5 μg/ml) was added to the HEK TR cell line and Blasticidin (5 μg/ml), Zeozin (20 μg/ml) and G418 (250 μg/ml) were added to the HEKTR-SNAP-CB1-Nluc_βarr2-Venus cell line to maintain the selective pressure. When

cells were 80-90 % confluent, tetracycline (1 µg/ml) was added to the media for 24 h to induce receptor protein expression. The media was replaced in the negative control and tested cell lines with 10 ml of DMEM + 10% FBS containing 1 µM of SNAP-Surface® Alexa Fluor® 647 and cells were incubated for 30 min at 37°C, 5% CO_2 in a humidified atmosphere. After that, the labelling media was discarded, and the cells were washed twice using 5 ml of PBS. The cells were detached using 2 ml of non-enzymatic cell dissociating media per flask and cells were collected in a tube containing complete media and centrifuged (200 x*g,* 5 min). The pellets obtained were gently resuspended and the cells were counted using trypan blue in the Countess™ 3 FL (Invitrogen) automated cell counter and 100,000 cells/ml suspensions were prepared in sterile Eppendorf tubes using DMEM + 10 % FBS + Penicillin (100 I.U) + Streptomycin (100 µg/ml).

The prepared labelled cell suspensions were sorted in the Flow Cytometry Facility at the University of Nottingham, using a Beckman Coulter Astrios EQ sterile cell sorter. Single cells were selected from different populations and plated into 96 well sterile culture plates. Media was regularly replaced, and the cells were seeded into 6-well plates first, and T25 flask and T75 flask later to expand the colonies when they had reached a high confluency in the plate (~90 %). The cells were grown until monoclonal cell lines were obtained.

TRANSIENT CELL LINES

HEK 293T/17 cells (ATCC, CRL-11268™) were used for transient transfections. The 293T/17 cell line is a derivative of the 293T (293tsA1609neo) cell line, from which the clone 17 was selected for his high transfectability. Two different plasmids encoding the biosensor (NES-Venus-mGsi or β-arrestin 2-Venus) and the receptor (either SNAP-CB1-Nluc and SNAP-CB2-Nluc) were used for transfecting the cells simultaneously. The biosensors were encoded in pcDNA3 plasmids whereas the receptors with Nluc fused to the C-terminal were encoded in pcDNA4/TO plasmids.

The transient transfections were carried out using plasmid DNA and PEI at a 1:3 ratio of total DNA to PEI. For testing different receptor:biosensor DNA ratios and 12 wells were transfected for each condition, using 1 µg DNA and 3 µg PEI . If less than 1 µg DNA was needed when combining receptor and biosensor plasmids,

sheared salmon sperm DNA (Invitrogen) was used to keep the total DNA constant through the test. The DNA and PEI were diluted in 100 μl of OptiMEM separately and vortexed. Diluted DNA was added to diluted PEI (100 μl + 100 μl) and vortexed. After 20 min of incubation at room temperature, the DNA-PEI mixture was added to 1.2 ml of cell suspension and mixed by inverting the tube several times. Finally, 100 μl of the cell suspension containing the transfection DNA-PEI mix was distributed in each well.

For a 96 well plate transfection, a proportional amount of total DNA (8 μg) and PEI (24 μg) were diluted separately to a final volume of 800 μl OptiMEM each and vortexed. The ratio of biosensor:receptor selected from previous test was 1:9, thus 0.8 ng of the biosensor and 7.2 ng of the receptor encoding plasmids were used for each 96 well transfection. The PEI solution was added to the DNA solution in 1:1 volume ratio (800 μl + 800 μl) and vortexed thoroughly. After a 20 min incubation period, the DNA-PEI mix was added to the 9.6 ml of cell suspension. The tube containing the cell suspension and the transfection mixture was inverted several times to ensure homogeneous mixing and the cell suspension was distributed in poly-D-lysine coated sterile 96 well plates adding 100 μl of the suspension to each well.

To prepare the cell suspension, a T75 flask of HEKT/17 cells in an exponential growth phase was used (~90% confluency). Media was aspirated and cells were washed with PBS before trypsin addition. 2 ml of trypsin were added to the T75 flask and incubated for 5 min at 37°C. Cells were collected in ~5 ml of fresh media and centrifuged at 200 x g. The pellet obtained was resuspended in fresh media (DMEM + 10% FBS) and gently pipetted up and down 8-10 times to avoid clumps. The cell concentration was calculated using trypan blue and Countess™ 3 FL (Invitrogen) automated cell counter and the volume was adjusted to prepare a cell suspension of 40,000 cells/ml with fresh warm media containing DMEM and 10% FBS.

The plate was incubated at 37 °C, in a humidified atmosphere with 5 % CO_2 for 48 h before performing the experiment to allow expression of proteins after transfection.

CELL LABELLING WITH TERBIUM CRYPTATE

HEK293-TREx cells stably expressing SNAP-CB1, SNAP- CB1$_{55-47}$, SNAP- CB1$_{91-472}$ or SNAP-CB2 were cultured in T175 flasks using DMEM supplemented with 10% fetal bovine serum and the selection antibiotics blasticidin (5 µg/ml) and zeocin (20 µg/ml). The receptor expression was induced by the addition of tetracyclin (1 µg/ml) to the cell culture when the cells had reached ~90% confluency to induce receptor expression prior to labelling with terbium cryptate. After 48h of tetracycline addition, medium was removed, and cells were washed twice: first using 5 ml of PBS and a second time using 5 ml of LABMED buffer. Then, 10 ml of Tag-lite labelling medium (LABMED) containing 100 nM of SNAP-Lumi4-Tb was added and incubated for 1h at 37 °C under 5 % CO2 to label the receptor with terbium cryptate (FRET donor)- the reaction between SNAP and terbium cryptate is represented in Figure 6.
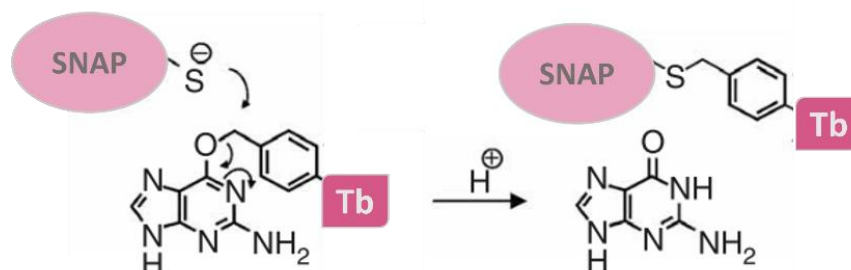
Figure 6*. Schematic representation of the covalent reaction between SNAP tag and terbium cryptate (Tb). A cysteine residue from the SNAP protein reacts with the benzylguanine conjugated terbium cryptate and the conjugated terbium is irreversibly transferred to the SNAP fusion protein.*

After, ~5 ml of PBS were used to wash the cells twice and cells were dissociated using 2 ml of non-enzymatic dissociation buffer. Cells were collected with media and centrifuged for 5 min (200 x *g*). Pellets were kept at -80 °C until membranes were prepared.

MEMBRANE PREPARATION FROM TERBIUM-LABELLED CELLS

Cell pellets were thawed using ice-cold buffer (10 mM HEPES and 10 mM EDTA, pH 7.4) and homogenization was conducted at 4°C using the Ultra-Turrax (Ika-Werk GmbH & Co. KG, Staufen, Germany). As shown in Figure 7, the cell homogenate was centrifuged at 1,200 x *g* for 5 min and the pellet obtained containing cell nuclei and other heavy organelle was discarded. The supernatant

31

obtained was then ultra-centrifuged at 48,000 x g, 4 °C, for 30 minutes (Beckman Avanti J-251 Ultracentrifuge; Beckman Coulter, Fullerton, USA). After discarding the supernatant, the pellet obtained was resuspended using the same buffer and homogenisation and ultra-centrifugation steps were carried out repeating the procedure described above. The pellet obtained was resuspended in a small volume of buffer containing 10 mM HEPES and 0.1 mM EDTA (pH 7.4). Determination of protein of the membrane preparation was carried out using the bicinchoninic acid assay kit (Sigma-Aldrich) and aliquots were prepared at ~5 mg/mL concentration and stored at -80 °C.
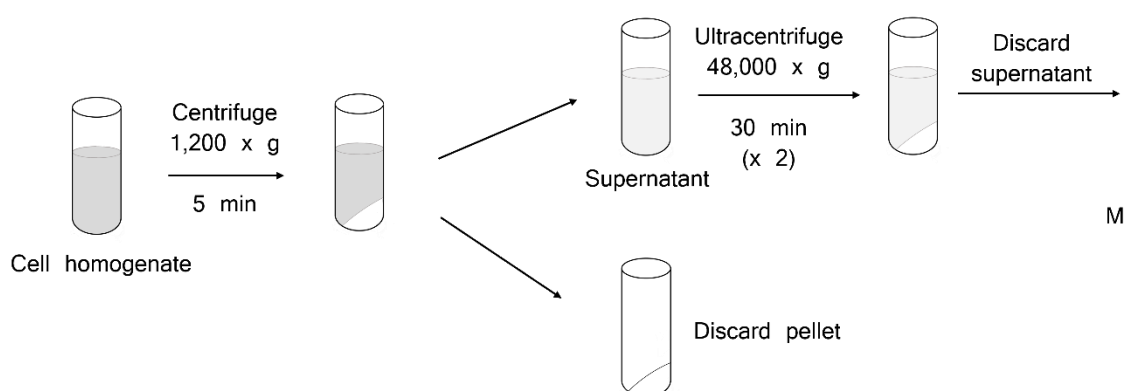
Figure 7. *Schematic diagram showing membrane preparation protocol from cell homogenate.*

PROTEIN DETERMINATION

Protein determination was conducted using the bicinchoninic acid assay kit (Thermo Scientific™) using BSA as a standard. The Bicinchoninic acid (BCA) method is a colorimetric detection used for the total protein quantification. This method relies in the biuret reaction (the $Cu2+$ reduction by proteins in an alkaline medium) and in the complexation of the formed $Cu+$ cations with BCA. Each reduced cuprous ion ($Cu+$) chelates two BCA molecules forming water soluble and purple-coloured complexes. The coloured product reaction exhibits a strong absorbance at 562 nm that display a linear correlation with the protein amount over a broad working range (20–2000 µg/ml).

Serial dilutions of BSA were prepared using the same buffer as the one used for the sample. Serial dilutions were carried out starting from the 2 mg/ml BSA stock to prepare 6 different BSA concentrations ranging from 0.1 to 1 mg/ml. 25 µL of each standard or unknown samples were pipetted into a 96 well plate. 200 µl of

Working Reagent (containing BCA and prepared following manufacturer instructions) were added in each well containing the sample. Blank samples were prepared adding 200 µL Working Reagent to 25 µL of the dilution buffer. After a 30 min incubation period at 37 °C, the plate was cooled down and the absorbance was read as optical density (OD) at 562 nm wavelength using the PHERAstar FSX plater reader (BMG Labtech). The OD values for each standard sample were plotted and a linear regression was fitted to the points, see Figure 8. Three measurements of the plate were carried out from monoplicate samples and r squared > 0.99 were accepted as valid fits.
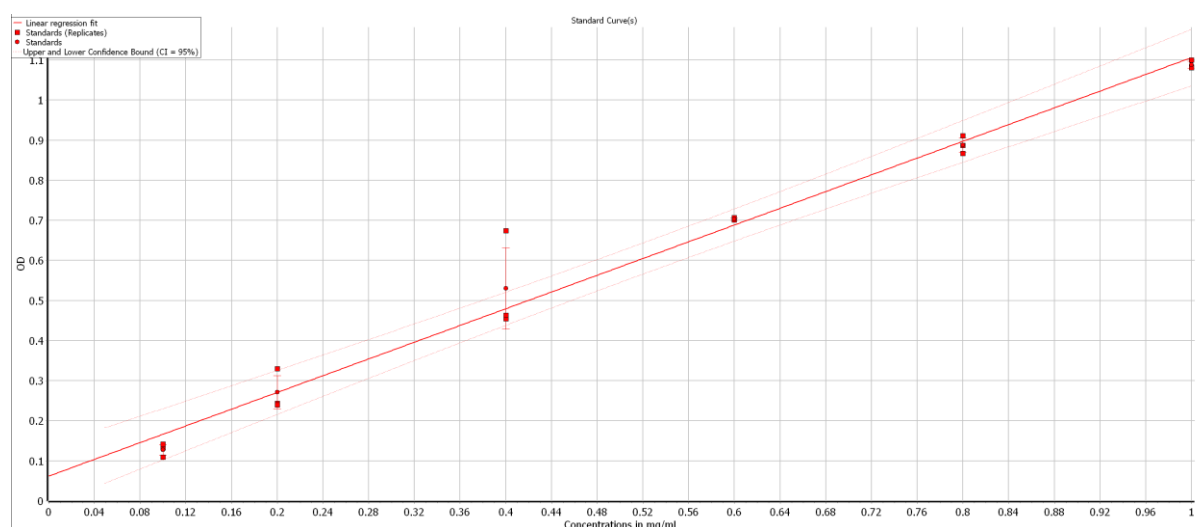
Figure 8. *Standard curve fit from standard BSA concentrations. Samples with 100, 200, 400, 600, 800, and 1000 µg/ml were used to fit the curve.*

The OD from the samples were substituted in the equation obtained from the linear regression fit and corrected by the dilution factor used to get the concentration estimation of our samples.

TR-FRET AND HTRF TECHNOLOGY

TR-FRET (Time-resolved fluorescence energy transfer) is the combination of Time-Resolved Fluorescence (TRF) with Försters Resonance Energy Transfer (FRET), that has been mainly used for the study of ligand-receptor binding events in the Pharmacology field.

FRET is named after Theodor Förster, the German scientist who originally described this energy transfer in the late 40s (Förster, 2012). In this phenomena, non-radiative energy is transferred between a donor and an acceptor molecule.

When the conditions for this to happen are present (distance between donor-acceptor pair < 10 nm and overlapping of donor emission and acceptor absorbance spectra) the transfer of energy occurs upon excitation of the donor molecule. When FRET occurs, the emission intensity of the donor is reduced while increasing the acceptor's emission intensity.
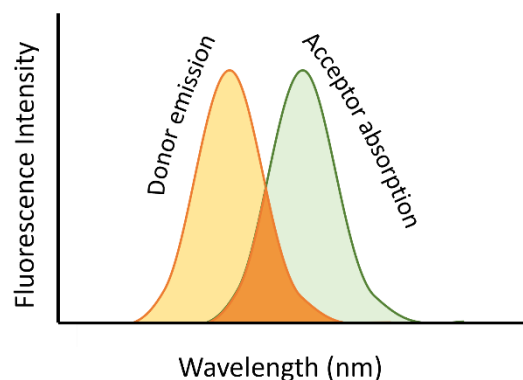
Figure 9. *Representation of the emission spectra and absorbance spectra of a "FRET pair". Energy transfer will happen when the two spectra overlap, leading to FRET.*

As shown in Figure 9, emission peaks of "FRET pairs" need to be far enough to selectively measure them but allowing significant donor emission and acceptor absorption spectral overlap to allow for an efficient energy transfer.

Time-resolved FRET allows a time delayed detection upon emission excitation by an energy source (usually a xenon lamp or laser). This enables the elimination of the short-lived background noise derived from scattered excitation light and autofluorescence. This is possible because the donor molecules used in TR-FRET are lanthanides, which shows up to milliseconds long emission lifetimes (Degorce et al., 2009). A schematic representation of time-resolved FRET is shown in Figure 10.

Lanthanides used as donors are either europium or terbium. As europium and terbium ions are only poorly fluorescent chelates, cryptates of these lanthanides are used to enhance their fluorescent properties for this purpose, as they enable both energy collection and transfer.
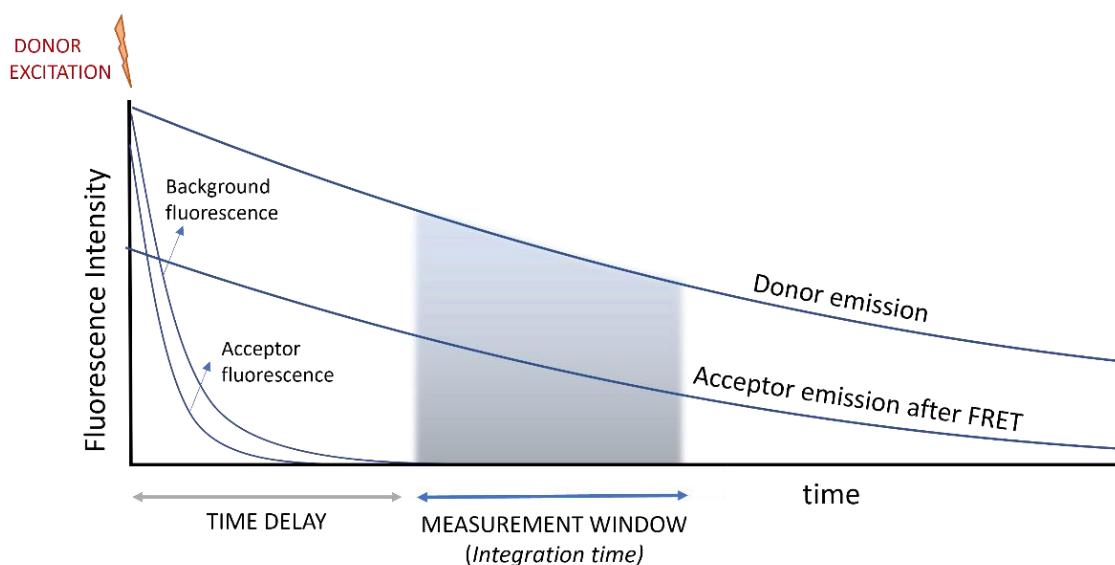
Figure 10. *Time-resolved FRET representation. The time delay from the sample excitation by the laser to the signal acquisition allows to discriminate the short-lived background fluorescence from the acceptor excitation or other components from the sample emitting fluorescence after excitation at 337 nm. The long-time emission of lanthanides (Europium or Terbium) acting as donors will continue transferring FRET energy to the acceptor and signal will be integrated in a delayed time window.*

Terbium has more adequate characteristics for its use in TR-FRET as a more than 10 times increased energy yield than europium, and a higher molar extinction coefficient. Unlike traditional fluorophores, the chelate/cryptate-lanthanide complex is extremely stable, which allows their use with a wide variety of assay buffers and conditions, and they undergo minimal photobleaching.

TR-FRET APPLICATION IN LIGAND BINDING ASSAYS

In order to benefit from the TR-FRET advantages when exploring ligand- receptor binding pharmacology, receptors need to be modified and a SNAP tag is usually placed in the extracellular N-terminal (see Figure 11). The SNAP tag is a derivative of O6-guanine nucleotide alkyl transferase, which can covalently react with fluorescent-conjugated benzyl guanine substrates (Keppler et al., 2003). This irreversible reaction will enable the labelling of receptors with a luminescent molecule acting as a donor for the FRET energy transfer (Maurel et al., 2008).

$$\textbf{HTRF emission ratio:} \ \frac{aceptor\ emission}{donor\ emission} \times 100$$
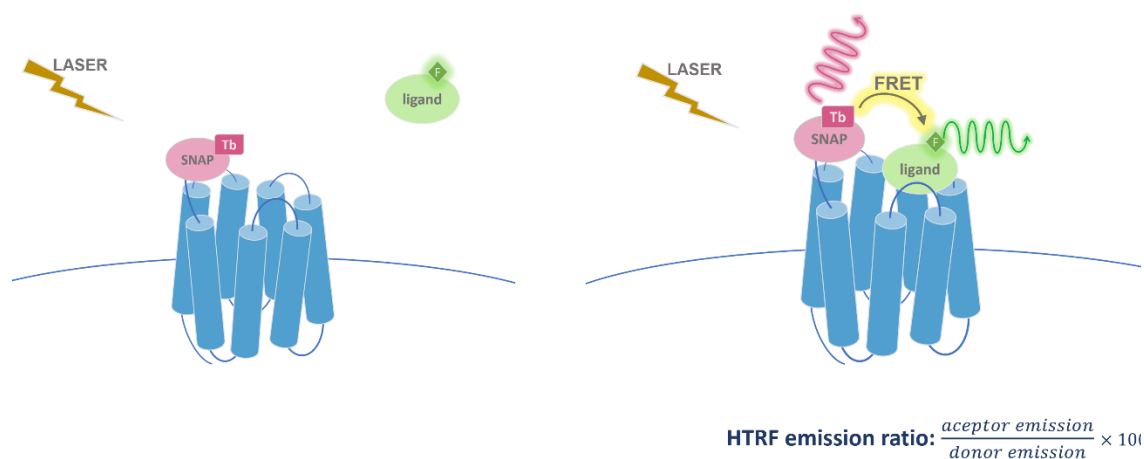
Figure 11. *Schematic representation of TR-FRET principle in ligand-receptor binding assays. The figure shows a GPCR labelled with Terbium (Tb) acting as a donor and a ligand with a fluorophore (F) as an acceptor. When the laser source excited the Terbium, it will transfer the energy to the acceptor and FRET will occur if the acceptor is in close proximity (< 10 nm). Acceptor emission after FRET occurs (green arrow) and donor emission (pink arrow) will be measured and HTRF emission ratio will be calculated.*

We applied this strategy for the detection of ligand binding to human cannabinoid receptors CB1 and CB2. It is worth mentioning that the CB1 receptor has a very long N-terminal extracellular domain, quite rare among class A GPCR family. This could have been a reason why the truncation of the aminoacidic sequence on its extracellular domain seems to be crucial to get a FRET signal for detecting ligand binding using FRET. The receptor protein sequence characteristics and binding pocket location will limit the use of this strategy for detection of ligand binding, as the close distance between the donor (located in the SNAP tagged fused to the receptor) and the fluorescent ligand acting as an acceptor is essential for getting a FRET signal.

A ratio of the integrated signals over time of the two emission peaks is measured to calculate the binding. The ratiometric measurement of the HTRF emission normalises the signal, eliminates medium interference, quenching, and volume or receptor variability between wells.

For the ligand-receptor binding experiments presented in this work, the PHERAstar FSX (BMG Labtech, Germany) plate reader has been used using dual emission filter settings in order to simultaneously detect the donor and acceptor emission at different wavelengths. The FRET was detected as HTRF ratio, dividing

the acceptor signal by the donor signal and multiplying by 10,000. The excitation source used in all the cases was a high energy laser that emitted at 337 nm, and the samples were excited with 4 flashes in each reading cycle.

MONITORIZATION OF DECAY CURVES

Decay curves of signal from donor and acceptor were monitored using the "decay curve monitoring" function in the PHERAstar FXS to ensure appropriate integration time values were chosen for the HTRF signal obtention. 1 μM of NBD (Nitrobenzoxadiazole) labelled ligand was used and HTRF intensity was measured every 20 μs after sample excitation with 20 laser flashes. The assay buffer used comprised Labmed, 5mM HEPES, 0.4% BSA and 0.02% pluronic acid (PH7.4). Membranes expressing SNAP-CB1 $_{91-472}$ previously labelled with the terbium donor were used and 1 μg of membranes were added in each well. HTRF signal was measured from a well containing 1 μM of NBD labelled ligand and a second well containing 3 μM of the inverse agonist rimonabant was measured to account for nonspecific binding. The specific HTRF ratio for each data point was calculated dividing the acceptor emission (520 nm) by the donor emission (620 nm) and multiplying by 10,000. White 384 well Optiplates were used with a final volume of 40 μl in each well.

MOTULSKY & MAHAN MODEL: KINETIC COMPETITION ASSOCIATION BINDING ASSAYS for the determination of kinetic parameters of unlabelled ligands

In order to assess the kinetic parameters of cold cannabinoid ligands, we applied the methodology described by Motulsky & Mahan (H. J. Motulsky & Mahan, 1984). Here, a mathematical model is described to estimate the kinetic parameters of unlabelled or "cold" ligands using association competition binding assays. Although traditionally radioactive isotope-labelled ligands have been used to perform this type of experiments, in this case, we use fluorescently labelled compounds as the tracer molecule, in order to benefit from the advantages of the TR-FRET technology i.e., no separation step need, lower assay volumes, high-throughput, possibility of accurate measurements of early time points. For this methodology, a range of different concentrations of cold ligand [B] are added to a

fixed concentration of the tracer molecule [L] simultaneously, thus the cold ligands act as competitor for the fluorescent ligand binding. This way, two different receptor complexes are formed, binding either the tracer [L] or the cold ligand [B].

$$[R] + [L] + [B] \;\underset{\leftarrow}{\rightarrow}\; [LR] + [BR] \qquad (2.\,1)$$

The rate of [LR] formation that will be measured will be dependent upon the kinetic properties of both ligands and the concentration of both the tracer [L] the cold competing ligand [B].

This approach allows the calculation of association and dissociation rates constants for unlabelled or "cold" ligands using the equations described by Motulsky and Mahan (1984):

$$K_A = k_1[L] + k_2$$

$$K_B = k_3[I] + k_4$$

$$S = \sqrt{((K_A - K_A)^2 + 4 \cdot k_1 \cdot k_3 \cdot L \cdot I \cdot 10^{-18})}$$

$$K_F = 0.5 * (K_A + K_B + S)$$

$$K_S = 0.5 * (K_A + K_B - S)$$

$$Q = \frac{Bmax * K_1 * L * 10^{-9}}{K_F - K_S}$$

$$Y = Q \cdot \left(\frac{k_4 \cdot (K_F - K_S)}{K_F \cdot K_S} + \frac{k_4 - K_F}{K_F} exp^{(-K_F \cdot X)} - \frac{k_4 - K_S}{K_S} exp^{(-K_S \cdot X)} \right) (2.\,2)$$

The following parameters of the equation: X = Time (min), Y = Specific binding (HTRF ratio 520nm/620nm*10,000), k_1 = k_{on} tracer (M^{-1} min^{-1}) and k_2 = k_{off} tracer (min^{-1}), L = concentration of tracer used (nM) and I = concentration of unlabelled ligand (nM) need to be fixed in order to calculate the association rate constant (k_3=k_{on} cold ligand) and dissociation rate constant (k_4=k_{off} cold ligand) of the unlabelled ligand, as well as B$_{max}$ (maximal specific binding at equilibrium as HTRF ratio 520 nm/620 nm *10,000).

38

The equilibrium dissociation constant (K_d) that defines the affinity of compounds is defined as follows:

$$Kd = \frac{Koff}{Kon} \qquad (2.3)$$

The k_{on} and k_{off} of cold compounds calculated from the kinetic Motulsky and Mahan approach are used to calculate the kinetic K_d.

CHARACTERIZATION OF THE TRACER: BINDING KINETICS AND EQUILIBRIUM AFFINITY

A pharmacological characterization of the tracer molecule used for the application of the Motulsky and Mahan competition association assay model is necessary where the kinetic parameters k_{on} (or k_1) and k_{off} (or k_2) are assessed accurately. Most of the receptor pharmacology models are developed from the "law of mass action", assuming that all ligands are equally free to bind the receptor ligand and that receptor and ligands will bind in a 1:1 stoichiometry in a readily reversible reaction.

$$[L] + [R] \quad \overset{kon}{\underset{koff}{\rightleftarrows}} \quad [LR] \qquad (2.4)$$
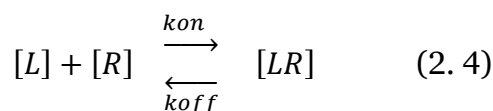
When the association rate equals the dissociation rates the system is said to be at equilibrium, and the equilibrium dissociation affinity constant is defined as K_d. The dissociation affinity constant Kd is calculated by dividing the k_{off} by the k_{on} parameters (i.e., $K_d = k_{off}/k_{on}$). Nevertheless, before equilibrium is reached, the rate of ligand-receptor complex formation i.e. [LR] formation, will be defined by the observed rate of association (k_{obs}) that will be dependent on the concentration of ligand and its association and dissociation rate constants k_{on} and k_{off}.

$$Kobs = [L] * kon + koff \qquad (2.5)$$

Thus, the kinetic parameters k_{on} and k_{off} of the fluorescent tracer can be determined using multiple tracer concentrations to generate different kinetic binding curves, where K_{obs} will depend on ligand concentration [L], but association and dissociation constant rates k_{on} and k_{off} will be shared parameters for all the association curves. The tracer binding over time will be fitted to the

equation that describes the pseudo-first order association kinetics of the interaction between a ligand and its receptor:

$$Y = Y_{max} * (1 - \exp(-1 * k\text{obs} * X)) \qquad (2.6)$$

Where Y is the level of receptor-tracer bound complex, Y_{max} is the level of tracer binding at equilibrium, X is in units of time (eg. min) and k_{obs} (min^{-1}) is the rate at which equilibrium is approached for each defined tracer concentration [L]. This globally fitted model of tracer binding allows to calculate k_{on} and k_{off} when defining the used tracer concentration [L] for each curve. The association and dissociation rates calculated are shared parameters for the multiple curves and independent of tracer concentration.

Furthermore, fitting each curve individually to the above exponential equation using the "one phase association" function in GraphPad Prism will allow the calculation of the specific k_{obs} obtained for each tracer ligand concentration.

The above calculations rely on the assumption that the free ligand concentration [L] remains unchanged throughout the course of binding e.g the amount of ligand depletion through the binding process should not be significant.

When the tracer binds to the receptor following the principles of law mass action, k_{obs} will linearly increase as a function of the used tracer concentration. The different k_{obs} values obtained from the "one-phase association" model can be fitted to a linear regression and the slope of the resulting line will correspond to the association constant rate k_{on}, and the y = 0 extrapolation of the plot will be indicative of dissociation constant rate k_{off} (H. Motulsky & Christopoulos, 2003; Sykes et al., 2010).

KINETIC ASSOCIATION BINDING EXPERIMENTS

Six different fluorescent ligand concentrations were used for the construction of kinetic association curves to CB1$_{91-472}$ and CB2 receptors. The dilutions were prepared in DMSO using 2-fold serial dilutions. Nonspecific binding was determined as the HTRF ratio detected in the presence of a high concentration of inverse agonist (3 μM Rimonabant for CB1 receptor or 1 μM SR 144,528 for CB2

receptor). Specific binding was determined by subtracting the nonspecific HTRF ratio from the total HTRF ratio.

Signal detection was conducted on a PHERAstar FSX (BMG Labtech, Germany) using dual emission HTRF filter settings to allow the signal acquisition from the donor and the acceptor simultaneously. The emission data were collected at different wavelength depending on the spectral characteristics of the fluorescent tracer used. In most of the cases, the fluorophores emitted in the green spectra and the emission of the acceptor were collected at 520 nm and the donor (terbium) emission was collected at 620 nm. In the case of MKA 138, due to its emission spectral characteristics, acceptor emission was collected at 570 nm whereas the donor emission was collected at 490 nm. The signal was acquired every 6 seconds and the integration time for the signal was set in 700 µs, with a delay of 100 µs from the laser excitation. HTRF ratios were obtained by dividing the acceptor signal by the donor signal and multiplying the obtained value by 10,000.

The assays were conducted in white 384-well Optiplate plates (Perkin Elmer). The membranes expressing terbium labelled SNAP-CB1$_{91\text{-}472}$ and SNAP-CB2 receptors were preincubated with 100 µM of GppNHp prior to the addition to the plate and automatic injectors were used to ensure early time point measurements. The final assay volume for each well was of 40 µL and 1 µg of membranes (in 20 µl volume) were added in each well.

The kinetic association binding experiments for the screening of fluorescent compounds was conducted at room temperature using LABMED buffer containing 5mM HEPES, 0.4% BSA and 0.02% pluronic acid (pH 7.4).

The characterization of the tracer of choice D77 for the Motulsky and Mahan model application was conducted at 37 °C and the buffer used comprised HBSS (Hanks Balance Salt Solution), 5mM HEPES, 0.5% BSA and 0.02% pluronic acid (pH 7.4).

For all the subsequent ligand binding assays using the fluorescent tracer D77 the assay buffer contained HBSS with 5mM Hepes, 0.4% BSA and 0.02 % Pluronic acid (pH 7.4).

Data were globally fitted using GraphPad Prism version 9.2 (San Diego, California USA) using the "Receptor binding-association kinetics" model to simultaneously calculate the k_{on} and k_{off} parameters for the different different tracers. In addition, data were also fitted using the "exponential-one phase association" model to obtain the k_{obs} values for each ligand concentration used.

SATURATION EXPERIMENTS

Total and nonspecific binding for the selected D77 fluorescent tracer to $CB1_{91-472}$ and CB2 receptors were assessed at equilibrium to allow the construction of saturation plots. The binding of the six tested concentrations was measured after 10 min of membrane addition to ensure equilibrium. A high energy laser lamp at 337 nm wavelength was used and the number of flashes was set to 4. Six consecutive reads were carried out for each point and the data were meaned. The integration time of the signal was set in 700 µs, with a delay of 100 µs to start after the laser flashes.

Saturation binding data were analysed using GraphPad Prism version 9.2 (San Diego, California USA) by "non-linear regression" equations.

The total and nonspecific binding data were fitted simultaneously using "one site-total and nonspecific binding" model. This analysis estimates a best-fit value for both the affinity (K_d) and the maximal level of specific binding (B_{max}) of the fluorescent ligand.

$$Total\ binding = (Bmax * [L])/(Kd + [L]) + (slope * [L]) + Background) \quad (2.7)$$

$$NSB = slope * [L] + Background \quad (2.8)$$

Where B_{max} is the maximal specific binding (measured as HTRF ratio), [L] is the concentration of fluorescent ligand in nM, K_d is the equilibrium dissociation constant in nM, *slope* is the slope of the linear nonspecific binding, and Background is the Y-axis intercept.

The specific binding was analyzed applying the "one site-specific binding" model that describes a rectangular hyperbola or binding isotherm:

$$\text{Specific binding} = \text{Bmax} * \frac{[L]}{Kd + [L]} \quad (2.9)$$

If the ligand- saturation phase is defined and the equilibrium dissociation constant (K_d) can be predicted accurately, it should match the K_d derived by the kinetic parameter obtained, when the ligand-receptor binding follows the law of mass action.

CHARACTERIZATION OF KINETIC PARAMETERS OF COLD COMPOUNDS

KINETIC COMPETITION ASSOCIATION BINDING EXPERIMENTS

The fluorescent ligand binding to the CB1$_{91-472}$ and CB2 receptor was assessed by HTRF detection and allow the construction of association kinetic curves in the absence or presence of a competing ligand.

The kinetic competition binding experiments were conducted using 600 nM and 900 nM of the D77 fluorescent tracer for CB1 and CB2 respectively. Seven different cannabinoid ligands were used to compete with the D77 fluorescent tracer for both receptors. Increasing concentrations of competing cannabinoid ligands were added and the data were collected every 8 s after membrane addition.

All the assays were conducted in white 384-well Optiplate plates (PerkinElmer) using the PHERAstar FSX microplate reader (BMG Labtech). The assay buffer comprised HBSS, 5 mM HEPES, 0.5% BSA and 0.02 % PA (pH 7.4). The dilutions of cannabinoid ligands were prepared from stock solutions in DMSO, and 3-fold serial dilutions were carried out using DMSO to ensure solubility. 0.5 μl of the competing compound dilutions were added in each well, thus the final DMSO in the well was 1.25 %. The nonspecific binding signal was calculated by the addition of 3 μM rimonabant and 1 μM SR144,528 for CB1 and CB2 respectively, and subtracted to each data point to calculate the specific binding.

Membranes were preincubated with 100 mM of GppNHp to ensure the absence of prebound G-proteins that could lead to two different populations of the receptor and thus the incorrect application of the Motulsky and Mahan model, as one unique ligand binding site is assumed in the model. Automatic injectors were used to add the membranes and ensure early time points could be measured with

accuracy in the plate reader. The final assay volume for each well was of 40 µL and 1 µg of membranes (in 20 µl volume) were added in each well.

HTRF ratios were obtained by dividing the acceptor signal from the fluorescent tracer (at a wavelength of 520 nm) by the donor signal of terbium (at 620 nm) and multiplied by 10,000. Data were globally fitted using GraphPad Prism version 9.2 (San Diego, California USA) to simultaneously calculate k_{on} and k_{off} of unlabelled compounds using the model "kinetics of competitive binding".

EQUILIBRIUM IC50 AND KI DETERMINATION FOR CANNABINOID LIGANDS

Equilibrium competition displacement binding data were obtained when the competition association experiments reached equilibrium (see previous section). The data obtained after 15 min of membrane addition to the plate was fitted to sigmoidal curves using a "one site binding" model to obtain log IC_{50} values. The IC_{50} (inhibitory concentration, 50%) parameter describes the concentration of competitor that results in binding halfway between Bottom and Top of the sigmoidal curve. The sigmoidal curve is defined with the following equation:

$$Y = \text{Bottom} + \frac{(\text{Top}-\text{Bottom})}{(1+10^{(X-\log IC50)})} \qquad (2.10)$$

Where X is the competitor concentration in logarithmic units and Bottom and Top are the specific binding (Y) value at the bottom plateau and top plateau.

The IC_{50} drug concentration obtained from the inhibition curves at equilibrium were converted to K_i values using the method of Cheng and Prusoff (Cheng & Prusoff, 1973). The K_i values are better estimations of drug potency as this parameter is dependent on IC_{50} and the concentration and affinity (K_d) of the tracer molecule used.

$$K_i = \frac{IC_{50}}{1+\frac{[L]}{K_d}} \qquad (2.11)$$

Where, IC_{50} (M) is the concentration of competing compound required to produce 50% inhibition of the tracer binding, L (M) is the concentration of tracer added and Kd (M) is the equilibrium dissociation constant of the tracer molecule for the receptor.

BRET

BRET or Bioluminescence Resonance Energy Transfer has been largely used in cell-based assay due to its versatility. This technique relies in the Resonance Energy Transfer between two molecules (Dale et al., 2019), similar to FRET. In this case, there is no need to perform an excitation of the sample to produce an excited state in the donor. A luciferase enzyme present in one of the two elements involved in the interaction will produce light that will excite the acceptor. Different enzymes can be used for BRET based assays, as Renilla luciferase (Rluc) or NanoLuc luciferase (Nluc). NanoLuc luciferase is the smallest size luciferase (19 kDa) and shows superior luminescence performance and stability over other luciferases, becoming the popular option for BRET assay reporters (Hall et al., 2012).

BRET APPLICATION FOR CELL SIGNALLING ASSAYS

In our experiments, we introduced a NanoLuc luciferase enzyme in the intracellular carboxyl terminal of the receptor that will produce light when reacting with furimazine (see Figure 12). On the other hand, the biosensors used mGsi and β-arrestin has been modified to introduce a Venus fluorescein protein that will act as an acceptor for the Resonance Energy Transfer.
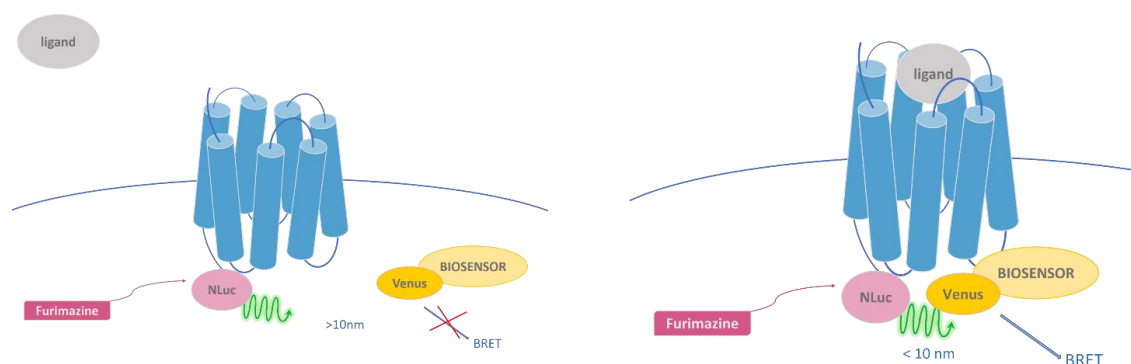
Figure 12. *Schematic representation of BRET assay principle for biosensor recruitment upon agonist stimulation in GPCRs. The GPCR has been modified fusing a Nluc in the intracellular C-terminal of the receptor, producing light when its substrate furimazine is present. The close interaction of the receptor with the biosensor with a Venus fluorescent protein will lead to energy transfer (BRET).*

mG$_{si}$ BINDING ASSAYS

mG$_{si}$ recruitment assays were conducted using transiently transfected HEK293 T/17 cells co-expressing both the receptor (with a Nluc fused to its intracellular terminal) and the mG$_{si}$ protein (fused to a Venus reporter miniG proteins are engineered alpha subunits of heterotrimeric G proteins that were originally used for stabilising the GPCR and aid in solving their structure in their active state (Carpenter & Tate, 2016). In the last years, their use has extended and different mini G proteins have been created in order to selectively bind the GPCR as different G alpha protein families (Nehmea et al., 2017). In this work, the mG$_{si}$ protein has been used as it is well characterised. This subtype of miniG protein mimics selectively the binding of G$_{i/o}$ subfamily G proteins, the primary G alpha proteins that has been described to bound cannabinoid CB1 and CB2 receptors.

The cells were transfected using a transfection in suspension protocol (see *TRANSIENT CELL LINES* section) in order to express the necessary elements to assess the mG$_{si}$ binding to the receptor using BRET and the assays were performed 48 h after the transfection to allow protein expression.

The cell media was aspirated, and cells were washed once using HBSS buffer before the assay buffer addition. The assay buffer contained HBSS, 5 mM HEPES and 0.5 % BSA (pH 7.4). Furimazine was added to the buffer to get a final 8 μM concentration just before the addition to the plate. The plate was introduced in the plate reader (preheated at 37 °C) and incubated for 15 min before compound addition to let the luminescence stabilise.

The compounds dilutions were prepared in U shaped polypropylene 96 well plates using the assay buffer with a 10 % DMSO to ensure compound solubility. The compounds were prepared using serial dilutions starting at a 10-fold concentration to the desired final plate concentration. The maximal concentrations in the assay plate were 50 μM for anandamide and 2-AG and 10 μM for all the rest of compounds. 5-fold serial dilutions were prepared.

The corresponding compound dilution was added to each well and data were collected every 60 s using a 450BP-550LP filter with a measuring interval time of 0.26 s for each well. These filters allow the detection of the light emitted in a range of wavelengths. In this case, the light produced by the donor (Nluc luciferase

reaction with furimazine) will be detected using the 450BP filter and 550LP will allow the collection of the signal coming from the Venus acceptor protein once the BRET occurs. BRET ratio was calculated dividing the acceptor signal (550LP) by the donor signal (450BP) and normalised to percentages using CP 55,940 maximal response as 100%.

Data were analysed using GraphPad Prism version 9.2 (San Diego, California USA) and was fitted to a sigmoidal curve using the "dose (log) vs response-three parameter" model were the Hill Slope is fitted to 1 using the following equation:

$$Y = Bottom + \frac{(Top - Bottom)}{1 + 10^{LogEC50 - X}} \quad (2.12)$$

Where Y is the response measured as BRET ratio normalised to percentages of CP 55,940 maximal response (100%), Bottom is the basal response without ligand stimulation (0 %) and Top is the maximal response for each given compound. EC50 is the concentration of agonist that gives a response halfway between Bottom and Top.

β-ARRESTIN 2 RECRUITMENT ASSAYS

β-arrestin2 recruitment assays were conducted using stable HEK TR cell lines co-expressing both the receptor (with a Nluc fused to its intracellular terminal) and the β-arrestin2 protein fused to a Venus reporter protein.

The HEK TR cell line expressing both the CB1 receptor and the biosensor (HEK TR-SNAP-CB1-Nluc_βarr2-Venus) was selected using FACS for the selection of the higher signal amplitude cell line. HEK TR-SNAP-CB2-Nluc_βarr2-Venus cell line was selected among three different stable cell lines created using different receptor to biosensor ratio to optimise the signal window.

The selected cell lines were induced using tetracycline 24 h prior to the assay for receptor protein expression. The cell media was aspirated, and cells were washed once using HBSS buffer before the assay buffer addition. The assay buffer contained HBSS, 5 mM HEPES and 0.5 % BSA (pH 7.4). Furimazine was added to the buffer to get a final 8 μM concentration just before the addition to the plate. The plate was introduced in the plate reader (preheated at 37ºC) and incubated for 15 min time to stabilise the luminescence.

The compounds dilutions were prepared in U shaped polypropylene 96 well plates using the assay buffer with a 10 % DMSO to ensure compound solubility. The compounds were prepared using serial dilutions starting at 10-fold concentrated to the desired final plate concentration. The maximal concentrations in the assay plate were 50 μM for anandamide and 2-AG and 10 μM for all the rest of compounds. 5-fold serial dilutions were prepared.

The corresponding compound dilution was added to each well and data were collected every 60 s using a 450BP-550LP filter and we selected a measuring interval time of 0.26 s for each well. These filters allow the detection of the light emitted in a range of wavelengths. In this case, the light produced by the donor (Nluc luciferase) will be detected using the 450BP filter and 550LP will allow the collection of signal coming from the Venus acceptor protein.

Data were analysed using GraphPad Prism version 9.2 (San Diego, California USA) and was fitted to a sigmoidal curve using the "dose (log) vs response" three parameter model where the Hill Slope is fitted to 1 using the equation $Y = Bottom + \frac{(Top - Bottom)}{1 + 10^{LogEC50 - X}}$ (2.12).

DERET FOR RECEPTOR INTERNALIZATION MONITORING

DERET or Diffusion-Enhanced Resonance Energy Transfer relies on the resonance transfer between a pair of donor and acceptor molecules under particular conditions. This technique has been applied for the study of internalization of receptors (Buenaventura et al., 2018; Roed et al., 2014), and has been described as a powerful method to monitor GPCR internalization in a dynamic and precise way (Levoye et al., 2015).

In this case, the acceptor molecule used is fluorescein, which will be present in the media in micromolar range concentrations. The donor molecule is terbium cryptate, that will be in the extracellular SNAP tag of the receptor. These conditions will enable to monitor a change in the donor emission depending on the receptor location respect to the acceptor molecule. The excess of acceptor molecules in the media will absorb part of the donor energy when the receptor is located in the membrane, producing a quenching effect, whereas the internalised receptors will emit the donor signal with no quenching effect from the

intracellular space (see Figure 13). This method allows to monitor the internalisation of receptor reflected as the DERET ratio, as the increase in the DERET ratio will be proportional to the internalization of labelled GPCRs.

DERET ratio: $\frac{620\ nm\ donor\ emission}{520\ nm\ acceptor\ emission} \times 10000$

Quenching→Low donor emission

↑ **DERET ratio:** $\frac{620\ nm\ donor\ emission}{520\ nm\ acceptor\ emission} \times 10000$
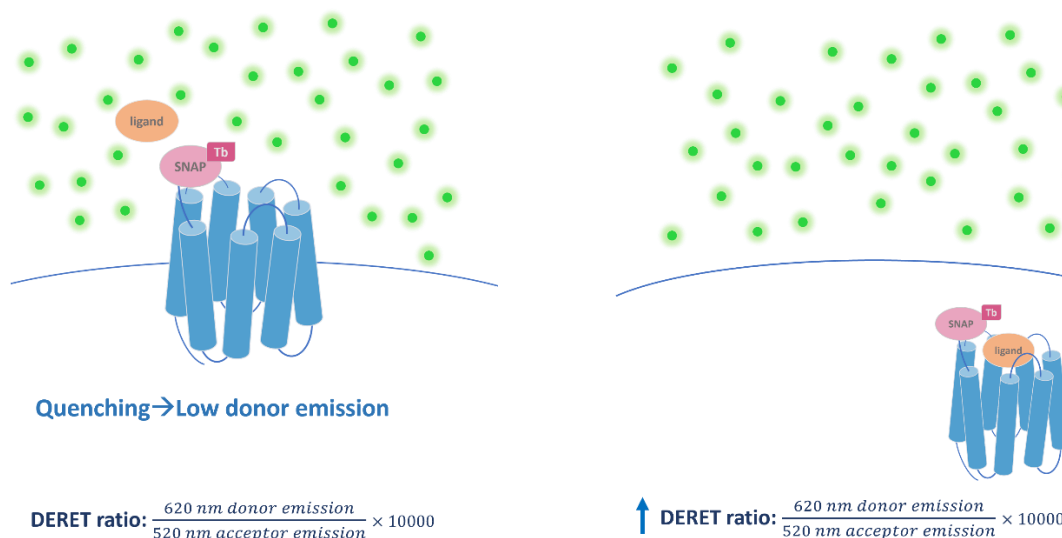
Figure 13. *Illustration of DERET principle for real-time internalisation monitoring of GPCRs. The surface receptors are labelled with Terbium (energy donor). The cells are incubated with a high concentration of fluorescein (acceptor molecule) in the extracellular matrix that will quench que Terbium signal coming from the receptor, thereby resulting in an overall low donor/acceptor ratio (DERET ratio). After ligand induced internalisation occurs, the Terbium emission will no longer be quenched due to the distance increase with the fluorescein acceptor molecule, resulting in an increase in the DERET ratio.*

INTERNALISATION MONITORING OF CB1 AND CB2 RECEPTORS UPON LIGAND STIMULATION

HEK TR stable cell lines for CB1 and CB2 expression were plated in 96 well plates, induced with tetracycline for protein expression and labelled with terbium cryptate before conducting the DERET internalization assays (see Figure 14).

HEK TR-SNAP-CB1 or HEK TR-SNAP-CB2 were cultured in T75 flasks with DMEM supplemented with 10% FBS, blasticidin (5 µg/ml) and zeozin (20 µg/ml) to maintain the selective pressure in the stable cell line. When the culture was in exponential growth phase (~90 % confluent) cells were detached using trypsin and seeded in poly-D-lysine coated sterile 96 well plates. The cells were detached using 2 ml of trypsin and cells were collected in a tube containing complete media and centrifuged (200 x*g,* 5 min). The pellets obtained were gently resuspended and cells were counted using trypan blue in the Countess™ 3 FL (Invitrogen)

49

automated cell counter. A 400,000 cells/ml cell suspension was prepared and 100 µl were seed per well, thus 40,000 cells per well. The media contained DMEM supplemented with 10% FBS and 1 µg/ml of Tetracycline to induce receptor expression.

After 48 h, media was aspirated, cells were washed with PBS and 50 µl of Labmed containing cell impermeable SNAP-Lumi4-Tb (100 nM) was added to each well to label the surface receptors. After 1 h incubation at 37°C, 5% CO_2 in a humidified atmosphere, cells were carefully washed three times with PBS and one time with HBSS before adding 90 µl of assay buffer. The assay buffer contained HBSS, HEPES 5mM and 0.5% BSA (PH 7.4). Fluorescein was added to the buffer just before the assay to achieve a final concentration of 30 µM in the wells. The 96 well plate was introduced in the plate reader (temperature was set at 37 °C) and 10 µl of the different ligand dilutions were added.

The different ligand concentrations were prepared in 10x concentration to the desired final concentration using serial dilutions in "U" shaped polypropylene plates. The buffer used for dilutions was the same used for the assay with the addition of 10% DMSO to ensure ligand solubility. The final DMSO concentration was 1% in the assay plate.

Figure 14. *Flowchart of DERET Internalisation assay preparation. The stable cell lines need to be induced with tetracycline for protein expression and labelled with terbium cryptate before each experiment.*

TR-FRET was monitored after ligand addition in a PHERAstar plate reader at 37 °C using the following settings: λ_{ex} = 337 nm, λ_{em} = 520 and 620 nm, integration time was set in 1500 µs for the 620 nm emission (with 1500 µs delay) and 400 µs for 520 nm emission (with 160 µs delay). DERET ratio was calculated dividing terbium donor signal at 620 nm by 520 nm signal and multiplied by 10,000. The assay plate was monitored every minute during 1 h after ligand addition, allowing the construction of curves showing the DERET ratio obtained over time. The basal internalisation level was monitored in a well containing only buffer and fluorescein and subtracted from the curves obtained for each ligand

concentration. Dose-response curves for ligands causing internalisation were constructed using the data at 15 min and data were normalised to CP 55,940 maximal internalisation (100 %). Data were fitted to a sigmoidal dose-response curve using GraphPad Prism 9 version and EC_{50} parameters and internalization percentage relative to CP 55,940 were obtained for each ligand.

BIAS CALCULATION

Ligand bias is described as the preference some ligands show for activating a signalling pathway over other. Bias was calculated for the agonists tested on mGsi coupling, β-arrestin 2 recruitment and internalization assays for both CB1 and CB2 receptor. We applied an operational analysis based on the operational model agonism (OMA) proposed by Black and Leff (Black & Leff, 1983), were the "transduction coefficient" or "transduction ratio" (τ/K_A) of the agonists are calculated for each pathway as a measure of the agonist activity for a certain response.

The τ/K_A transduction coefficient is the ratio between the efficacy (described with the τ parameter) and the equilibrium dissociation constant of the agonist-receptor complex (K_A) and represents a quantitative measure of the strength of a given agonist to activate a specific signalling pathway.

The analysis was performed based on van der Westhuizen et al. (Van Der Westhuizen et al., 2014), were (τ /KA) is defined as a single parameter, R:

$$E = \text{Basal} + \frac{(E_m - \text{Basal})}{1 + \left(\frac{\left(\frac{[A]}{10^{\log K_A}} + 1 \right)}{10^{\log R} \times [A]} \right)^n}$$

(2. 13)

Where E is the effect of the ligand for a particular response, *[A]* is the concentration of agonist, E_m is the system's maximal effect, Basal is the effect in the absence of agonist, *logK$_A$* indicates the logarithm of the functional equilibrium dissociation constant of the agonist, n is the slope of the transducer function that links occupancy to response, and *logR* is the logarithm of the "transduction coefficient" (or "transduction ratio"), τ/K_A, where τ is an index of the coupling efficiency of the agonist.

The assessment of bias was performed by comparing the activity of a ligand in a given pathway using a reference compound, in order to eliminate the system bias (Terry Kenakin & Christopoulos, 2013), which can otherwise influence the observed outcome. Therefore, we determined the relative effectiveness $\Delta \log(\tau/K_A)$ of an agonist to activate a certain pathway as follows:

$$\Delta \log\left(\frac{\tau}{K_A}\right)_{lig-path} = \log\left(\frac{\tau}{K_A}\right)_{ligand} - \log\left(\frac{\tau}{K_A}\right)_{reference} \quad (2.14)$$

The error for the calculated $\Delta \log(\tau/K_A)$ parameter was determined as described in (Soethoudt et al., 2018), from the SE associated from each $\log(\tau/K_A)$ or $\log R$ values as follows:

$$SEM\ \Delta \log\left(\frac{\tau}{K_A}\right) = \sqrt{SE \log\left(\frac{\tau}{K_A}\right)_{ligand}^2 + SE \log\left(\frac{\tau}{K_A}\right)_{reference}^2} \quad (2.15)$$

The log R values (equivalent to $\log(\tau/K_A)$) were calculated using GraphPad Prism version 9.2 (San Diego, California USA) as previously described in Soethoudt et al. (Soethoudt et al., 2017, supplemetary material). Data were analysed using a new user-defined "non-linear regression" equation:

A=10^X

operate1=((1+A)/((10^logR)*A))^n

operate2=((1+A/(10^logKA))/((10^LogR)*A))^n

Y1=basal+(Emax-basal)/(1+operate1)

Y2=basal+(Emax-basal)/(1+operate2)

<A:O>Y=Y1

<~A:O>Y=Y2

And "rules for initial values" tab was defined as follows:

LogR →-1.0 *(Value of X at YMID)

n →1.0

LogKA →1.0 *(Value of X at YMID)

basal →1.0 *YMIN

Emax →1.0 *YMAX

We fit the data obtained from the mGsi coupling and β-arrestin 2 recruitment to the above described equation. The reference compounds used to develop the bias calculations were 2-AG for CB1 and CP 55940 for CB2 receptor. Maximal response was constrained to 100 as data were already normalised with the reference agonists maximal response, n was set as a shared parameter and K_A values where constrained using the affinity data obtained from equilibrium displacement experiments. The log R values obtained from each independent experiment where used to calculate $\Delta \log (\tau/K_A)$.

For each agonist, the obtained $\Delta \log (\tau/K_A)$ values in the two studied responses (mGsi coupling and β-arrestin 2 recruitment) were then compared using two-way unpaired Student's t-test to account for statistical differences between the $\Delta\log (\tau/K_A)$ obtained for a single agonist between the two studied responses.

3. RESULTS

CB1 AND CB2 TR-FRET BASED KINETIC ASSAY DEVELOPMENT

LIGAND BINDING DETECTION USING FRET IN FULL LENGTH AND TRUNCATED CB1

To test FRET for detecting ligand-binding interaction at CB1 receptor, we chose an NBD labelled fluorescent ligand with a pyridine pharmacophore previously developed as tracer for the CB2 receptor (Gazzi et al., 2019) referred to as NBD-691 in this work. Although originally developed for CB2 binding purposes, it showed low receptor selectivity as it is usual for many cannabinoid compounds and reported binding to CB1 receptor in radioligand competition binding assays. Nevertheless, no FRET signal was detected using full length, terbium cryptate labelled SNAP-CB1 receptor.

The CB2 has a 28 amino acid residue N-terminal domain (NTD) whereas the CB1 receptor has a long NTD of 111 amino acids, which is quite unusual among class A GPCRs. As RET is strongly dependant on the donor an acceptor distance (Förster, 1948), the long NTD of CB1 could be the reason why the Terbium labelled SNAP tagged fused to it and the orthosteric binding site distance was long for energy transfer. Therefore, we reasoned that the elimination of part of the N-terminal will bring the SNAP tag closer to the orthosteric site, thus reducing the FRET pair distance and allowing the energy transfer between the donor and the acceptor.

Although N-terminal splicing variants show different signalling profiles when activating some pathways, their binding to cannabinoid compounds has been demonstrated to remain unchanged (Xiao et al., 2008). Therefore, we designed two truncated constructs based on the existing splicing variants to prove FRET (see Figure 15).

Two SNAP tagged CB1 variants were produced eliminating residues from the N-terminal extreme and named based on the amino acid residues remaining after truncation – $CB1_{51-472}$ and $CB1_{91-472}$.
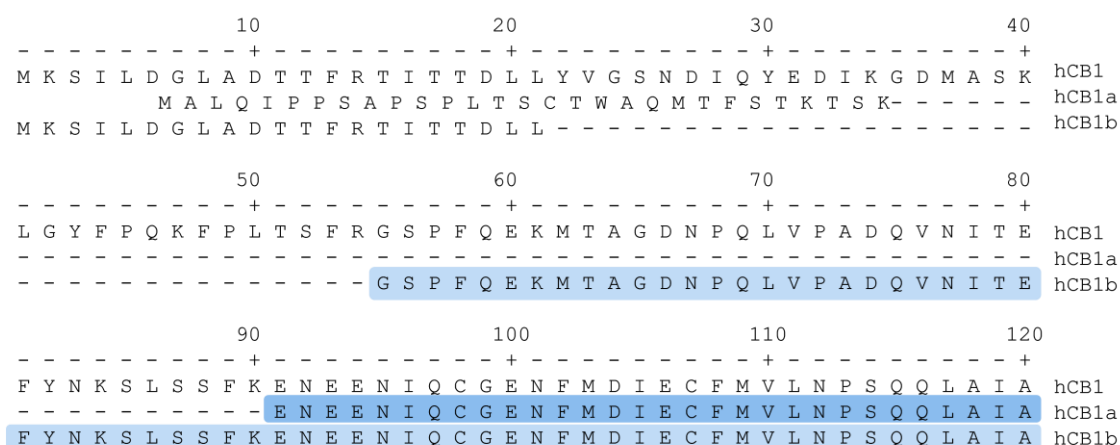
Figure 15. Amino acid sequence of the N-terminal of human cannabinoid receptor type 1 (hCB1) and its splicing variants hCB1a and hCB1b. The highlighted amino acids represent the N-terminal sequence of the truncated versions used (91-472 in dark blue, 55-472 in light blue). (Modified from Ryberg et al, 2005).

We tested the validity of the truncated variants of the receptor for TR-FRET experiments using 1 μM fluorescent NBD-691 ligand and comparing the HTRF emission obtained using the full length and truncated versions of the CB1 receptor.
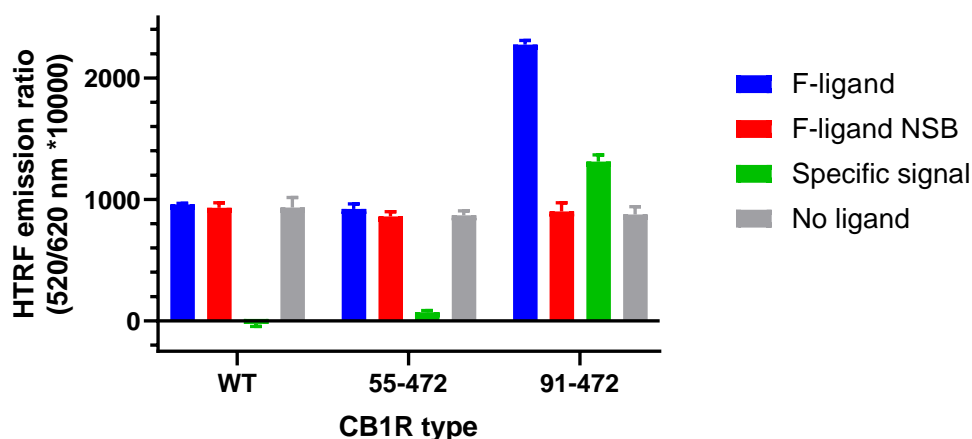
Figure 16. TR-FRET signal obtained for full-length (WT) and truncated CB1-receptor versions CB1$_{55-472}$ and CB1$_{91-472}$. The FRET signal obtained is indicated as HTRF ratio: in the absence of fluorescence ligand addition (No ligand, grey bars) and with 1 μM NBD-labelled ligand addition (F-ligand, blue bars). The nonspecific FRET was monitored using 1 μM of Rimonabant (red bars) and Specific signal (green bar) was calculated subtracting the nonspecific signal to the total signal (blue bars). Data shown are mean ± SEM of 3 experiments conducted independently.

The full length (WT) and the CB1 $_{55-472}$ truncated version show identical FRET signals with no specific HTRF detection and similar fluorescent detection in the

absence or presence of fluorescent tracer (see Figure 16). This indicates that the signal obtained reflects background HTRF and no ligand-receptor interaction was being detected.

Only the CB1 version with the first 90 aa eliminated from the sequence, $CB1_{91-472}$, displayed a TR-FRET signal indicative of ligand binding. Indeed, the non-specific binding signal was negligible as the FRET signal adding F-ligand with blocker (1 μM Rimonabant) was identical to the background FRET observed when no fluorescent ligand was present. Therefore, the truncated $CB1_{91-472}$ receptor was used in the binding studies employing TR-FRET.

BUFFER SELECTION

Three different buffers were tested with the aim of getting the best quality TR-FRET signal for the binding experiments. The effect of the buffer of choice was tested using a fluorescent ligand containing an Alexa Fluor 844 moiety, referred to as Alexa 841 in this work. The fluorescent ligand binding was tested in SNAP-$CB1_{91-472}$ expressing membranes previously labelled with the donor terbium cryptate. The buffers tested were:

•TRIS buffer: 50 mM Tris base, 3 mM MgCl2, 0.2 mM EGTA, 0.1% BSA, 0.02% Pluronic acid, pH 7.4

•HBSS buffer: Hanks Balanced Salt Solution, 5 mM HEPES, 0.5% BSA, 0.02% pluronic acid, pH 7.4

•LABMED buffer: Labmed buffer, 5 mM HEPES, 0.4% BSA, 0.02% pluronic acid, pH 7.4

Experiments were carried out at RT and the association of 6 different concentrations ranging from 31.25 nM to 1 μM was tested over 20 min. Nonspecific binding was monitored using 1 μM of Rimonabant and subtracted from the total binding to calculate specific binding.
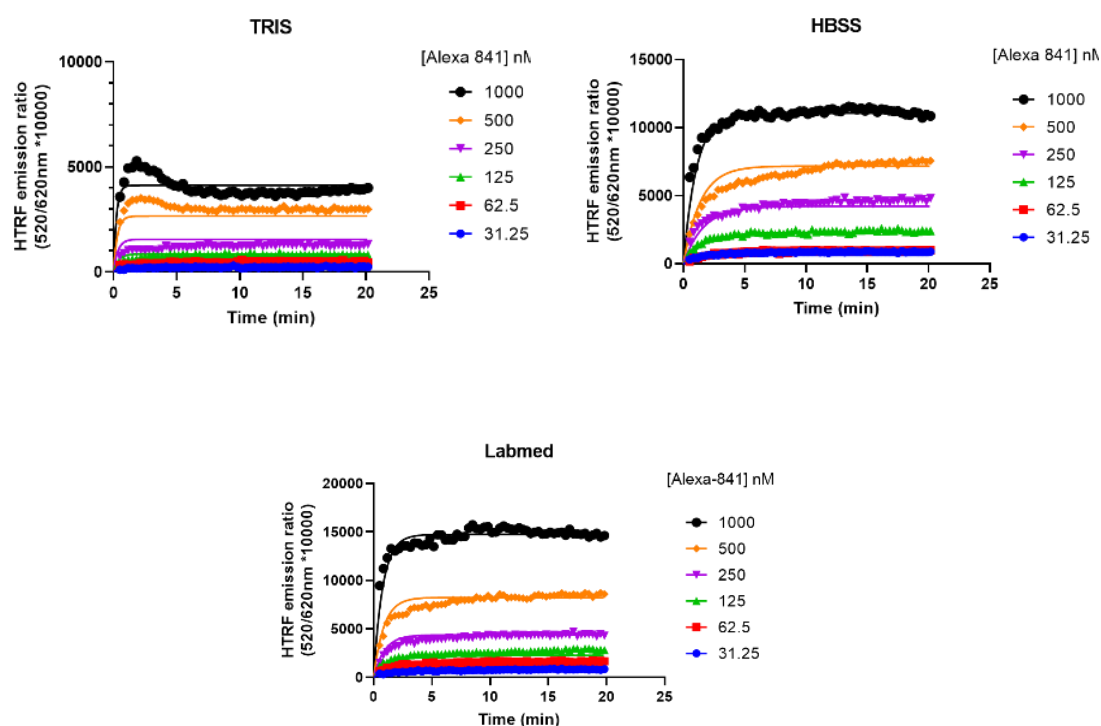
Figure 17. *Alexa 841 fluorescent ligand association binding curves at CB1 $_{91-472}$ receptor using different assay buffers. The graphs show specific binding expressed as HTRF emission ratio.*

As shown in Figure 17, the buffer utilised for the assay greatly influence the HTRF emission ratio obtained during the association of the fluorescent ligand. The fluorescent ligand binding using Labmed buffer shows wider assay window, displaying approximately 2 and 3 times higher HTRF ratio than HBSS buffer and Tris buffer respectively, when using the same fluorescent ligand concentration.

The fluorescent ligand binding using Tris buffer displayed an anomalous profile in the two higher concentrations tested, showing an artefactual increase in the HTRF ratio detected in the first minutes that start decaying after ~2 min and stabilises after 5 min of incubation. The binding profile obtained with Tris does not match the binding profile expected for a ligand-receptor binding experiment, therefore this buffer composition was not used in further experiments.

Both Labmed buffer and HBSS buffer displayed a good binding profile and HTRF detection window and thus will be used for the development of ligand binding assays in the subsequent experiments. The Labmed buffer (based on Tag-lite labelling media, Cisbio, Perkin Elmer) was developed for the efficient labelling of

SNAP tag with Terbium cryptate and its exact composition is currently not known as it is a propriety formulation. On the other hand, HBSS is a phosphate buffered solution that maintains physiological sodium ion concentration, and was also used in the development of the signalling assays.

PROTEIN QUANTITY

Different membrane protein amounts were tested in TR-FRET binding assays, thus the influence could be assessed and a rationale selection of the protein amount added to the assay plate could be made. We tested five different conditions where the membrane protein expressing $CB1_{91-472}$ in each well ranged from 18 ng to 1.5 µg and compared the HTRF ratio detection at 5 min when the binding had reached equilibrium conditions.
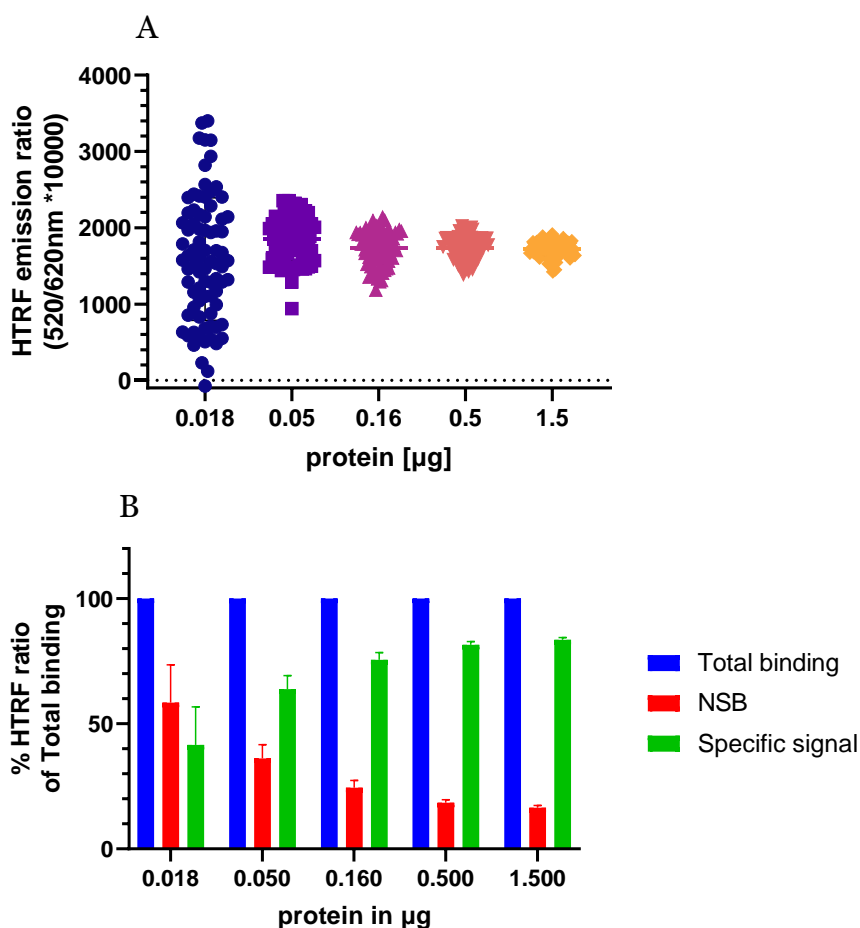
Figure 18. *Protein amount influence in the TR-FRET signal. Binding of 1 µM NDB-691 to $CB1_{91-472}$ receptor was measured as HTRF ratio at RT after reaching equilibrium (5 min).(A), the distribution of 80 consecutive reads of TR-FRET signal measured as Specific HTRF ratio using different $CB1_{91-472}$ expressing membrane protein amounts in the well. (B), NSB (Nonspecific signal, detected using 1 µM Rimonabant) and Specific signal as percentage of the total signal using different protein amounts is shown.*

It can be observed in Figure 18 (A) that small membrane protein amount addition leads to a lower precision in the signal acquisition and higher coefficient of variation. Whereas using 0.018 µg leads to a coefficient of variation (CV) of 50.5 %, increasing the protein amount to 0.05 and 0.16 µg leads to 15.8 % and 12.6 % CV respectively and using 0.5 or 1.5 µg significantly narrowed the data distribution, showing 8.8 % and 5.5 % of coefficient of variation. In addition, the specific binding signal percentage was significantly increased when using higher protein amounts, from 41 % using 0.018 µg protein to 81.6 % and 83.5 % using 0.5 and 1.5 µg respectively (Figure 18 B). Given the best specific signal percentage was obtained with the two top protein concentrations, $0.5 - 1$ µg protein were used in the subsequent binding experiments.

SCREENING AND CHARACTERIZATION FLUORESCENT CANNABINOID LIGANDS AT CB1 and CB2 RECEPTORS

In order to find a suitable fluorescent ligand to be used as a tracer in the kinetic association competition binding experiments and the subsequent application of the Motulsky & Mahan model, we studied the binding profiles of several fluorescent cannabinoid ligands.

As Georgi et al. explained in a very detailed manner, several factors will significantly influence the performance of the Motulsky & Mahan model, and many components of the assay needs to be carefully selected in order to achieve accurate and precise results (Georgi et al., 2019). One of the key elements that will impact the fit of the described model will be the binding kinetic characteristics of the tracer molecule: the association rate (k_{on}) and the dissociation rate (k_{off}). We performed an extensive fluorescent screening in order to characterise their affinity and kinetic properties, followed by a rational selection based on their binding properties.

The assay buffer contained Labmed with 5 mM Hepes, 0.4 % BSA and 0.02 % Pluronic acid. The experiments were conducted at RT, using 0.5 µg/well of cell membranes expressing either SNAP-CB1$_{91-472}$ or SNAP-CB2 receptor previously labelled with Terbium cryptate.

Experiments were carried out at RT and the association of 6 different concentrations were tested over 15 min. The fluorescent ligands concentrations

used for the binding assays were chosen from the affinity estimated in preliminary experiments, and ranged from 15.6 nM to 500 nM, from 31.2 nM to 1 µM or from 62.5 nM to 2 µM. Nonspecific binding was monitored using 1 µM of Rimonabant or SR 144,528 for CB1 and CB2 receptors respectively and subtracted from the total binding to calculate specific binding.

As shown in Figure 19 and Figure 20, the ligands show different binding properties to cannabinoid receptors CB1 and CB2. The ligands MKA 115 and MKA 136 show slow K_{on} when binding to both CB1 and CB2, and plateau was not obtained in the 15 min the binding was monitored, indicating that the time required for equilibrium was longer than the monitoring time. The slow association of MKA 115 and MKA 136 make them not suitable for their use in the Motulsky and Mahan model, as a fast association is desired in order to reach faster equilibrium when competing with the cold ligands. On the other hand, MKA 138, NBD 690, NBD 691, NBD 694 and NBD 698 show really fast association to CB1, although slightly slower to CB2 receptor. The fast Kon of these receptors make it not feasible to measure the binding in the association phase, before getting to equilibrium in their binding to CB1. Obtaining data from the association phase is crucial to apply the Kinetic competitive association model, as the absence of the data points before reaching equilibrium will lead to bad estimations of the tracer's kinetic parameters k_{on} and k_{off}, thus increasing the error when estimating the kinetic parameters of the cold compounds. The kinetic profile that MKA 138, NBD 690, NBD 691, NBD 694 and NBD 698 shown for the binding to CB2 can be suitable for the application of the Motulsky and Mahan modelling, as they exhibit moderately rapid association. However, a time-dependent decay of the HTRF ratio measured is observed for NBD 694 and NBD 698 binding to CB2. Although less pronounced, the same signal decay can be observed for the NBD 690 and NBD 691 binding to CB2 receptor.
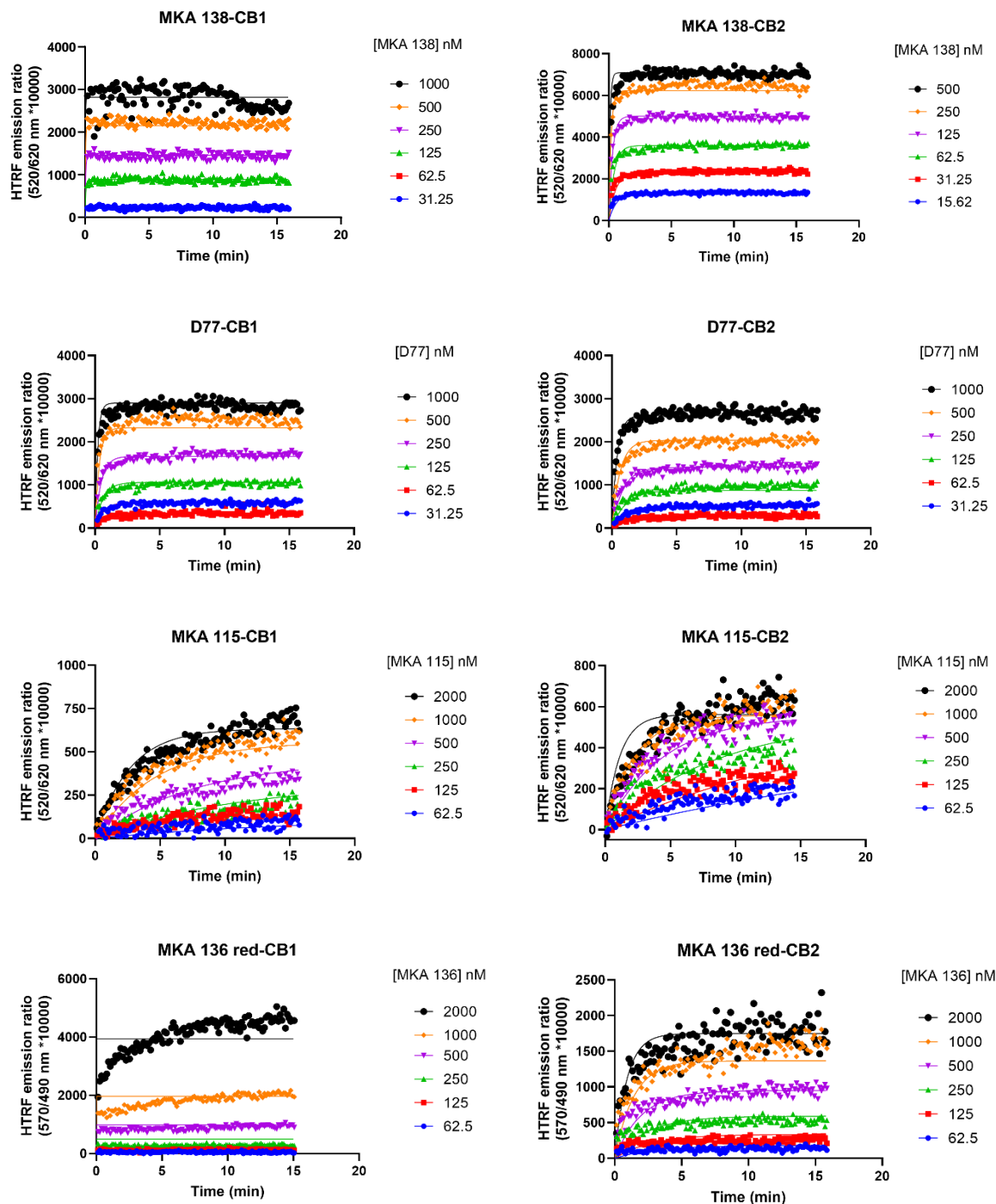
Figure 19. *Kinetic association binding curves of fluorescent cannabinoid ligands MKA 138, D77, MKA 115 and MKA 136 to receptor CB1 (left column) and CB2 (right column) expressing membranes. Representative graphs show specific binding expressed as HTRF emission ratio.*
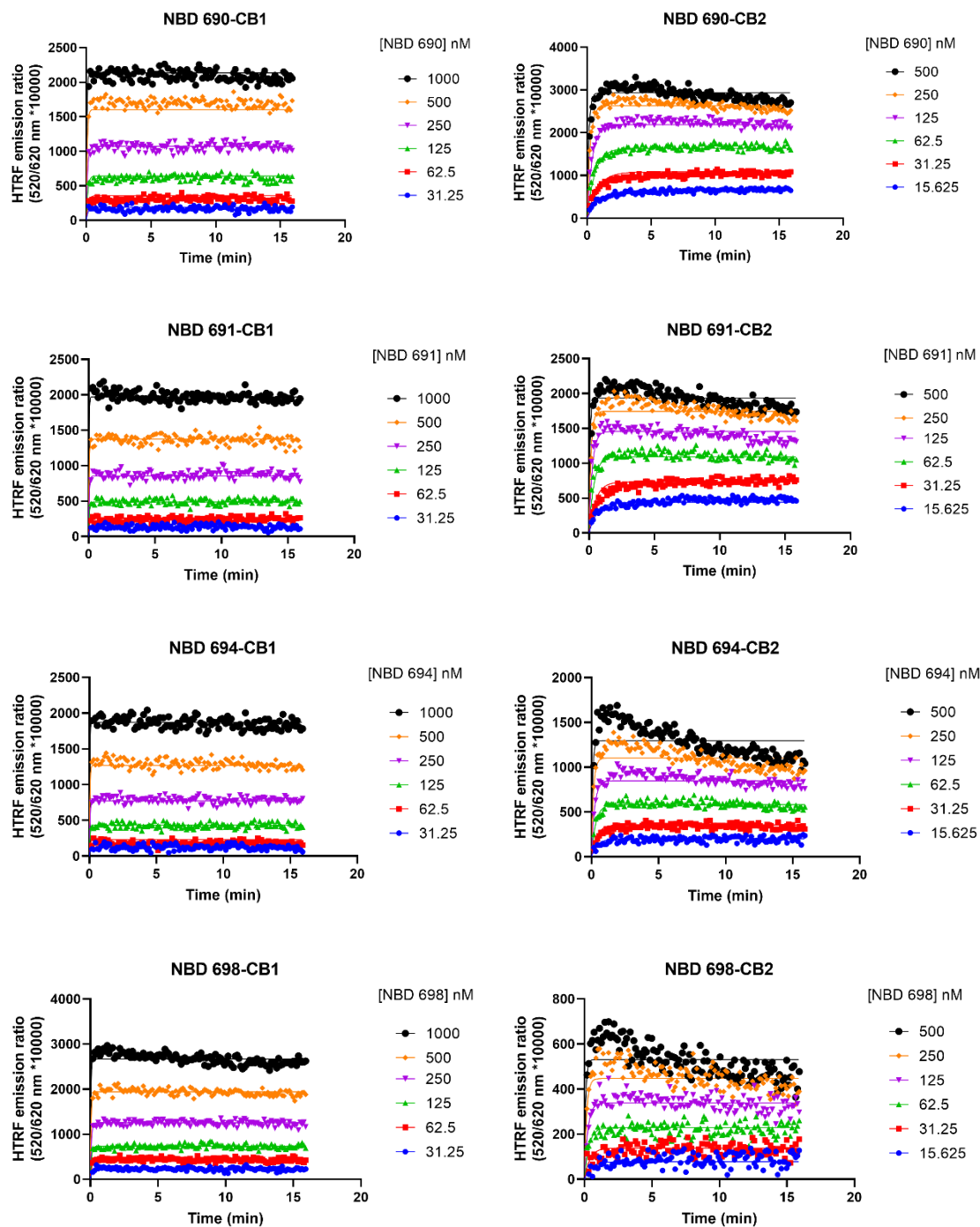
Figure 20. *Kinetic association binding curves of fluorescent cannabinoid ligands NBD 690, NBD 691, NBD 694 and NDB 698 to receptor CB1 (left column) and CB2 (right column) expressing membranes. Representative graphs show specific binding expressed as HTRF emission ratio.*

The D77 compound showed a moderately rapid association to both cannabinoid receptors, and the binding curves fitted very well to the one phase association model. Moreover, the HTRF signal was very stable over time and no decay was observed in the 15 min of binding monitorization. Therefore, the D77 fluorescent ligand was the selected tracer due to the ideal characteristics that it showed compared to the other screened compounds. In Table 1, we showed the affinity and association and dissociation constant of this fluorescent molecule at the two cannabinoid receptors CB1 and CB2.

Table 1
Pharmacological properties of D77 fluorescent ligand at CB1 and CB2 receptors at RT. All data are mean ± SEM, of 3 experiments (CB1 $_{91-472}$) or 4 experiments (CB2) conducted independently.

	CB1 $_{91-472}$	**CB2**
k_{on} **(M^{-1} min^{-1})**	$(3.61 \pm 0.07) \times 10^6$	$(1.63 \pm 0.1) \times 10^6$
k_{off} **(min^{-1})**	1.13 ± 0.07	0.57 ± 0.06
K_d **(nM)**	315 ± 24	348 ± 21

The association rate (k_{on}) of the D77 tracer was rapid, 3.61×10^6 and 1.63×10^6 M^{-1} min^{-1} for CB1 and CB2 binding respectively, which is adequate to the requirements for kinetic association competitive experiments used in the Motulsky and Mahan methodology. Nevertheless, the association phase could be successfully monitored, and several data points could be measured before reaching plateau indicating equilibrium, which is essential for the tracer used in the competitive experiments. Moreover, the D77 displays a moderately fast dissociation of 1.13 min^{-1} for CB1 and 0.57 min^{-1} for CB2, which is a positive feature of tracers and will contribute to a fast equilibration in the competition with the cold ligands.

DECAY CURVE MONITORING AND INTEGRATION TIME

D77 fluorescent tracer was synthetised based on Δ^8-THC structure and the fluorescent moiety conjugated to the molecule is NBD. Due to the different energy emission profiles fluorescent molecules displays, optimisation of the integration

time should be performed in order to maximize the signal obtainable. The emission decays of the donor terbium measured at 620 nm and the NBD acceptor measured at 520 nm were monitored following laser excitation (see Figure 21).
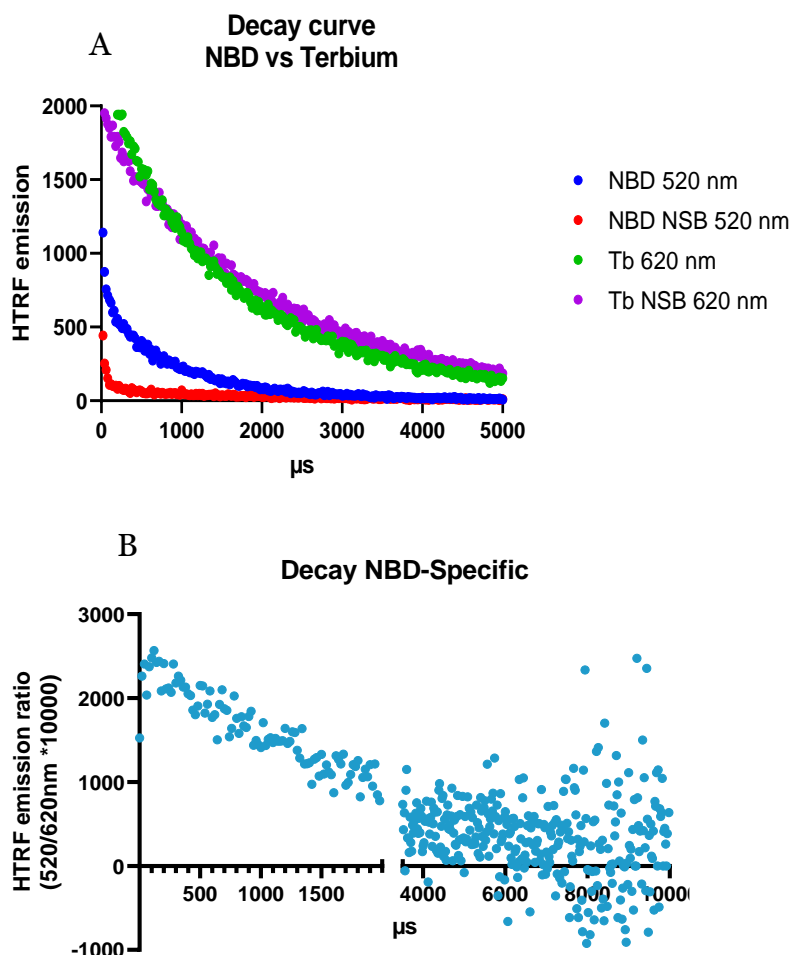
Figure 21*. A) Signal decay curves after laser excitation of the sample for the donor terbium and NBD acceptor. B) Specific signal decay over time was calculated from individual donor and acceptor emission signals at each time point after subtracting the Nonspecific (NSB) signal (1 μM Rimonabant). Each well contained 1 μM of NBD labelled ligand and ~0.5 μg of membranes expressing Tb-SNAP-CB1$_{91-472}$.*

The specific signal HTRF emission ratio drops with time after exciting the sample with the laser energy source, emitting ~50 % of the initial values after 1,500 μs. Three different integration times of the signal (100, 700 and 1,400 μs) were selected to study the influence of the obtained HTRF signal in each case. In all the cases, a delay of 100 μs from the laser excitation was set to avoid background fluorescence (see Figure 22).
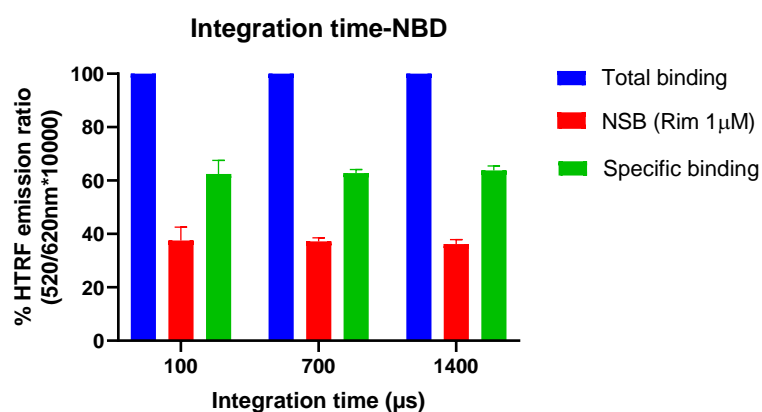
Figure 22. *Specific and Nonspecific binding (NSB) shown as percentage of total binding measured as HTRF ratio when using different integration times for the FRET signal. Error bars indicate SEM of six consecutive reads.*

The Specific HTRF signal was not significantly affected by the signal integration time, being ~60% of the total signal in the three cases. Even though the signal quality is not significantly affected by integration time, in this case, using the NBD fluorophore, this parameter is crucial for the HTRF data quality and should be monitored for each fluorophore in order to avoid high background levels in the assay, as it strongly affects the Specific and Nonspecific HTRF levels when using other fluorophores with different time decay profiles (Sykes et al., 2021).

The integration time of 700 μs was selected for the subsequent ligand binding experiments using the NBD labelled D77 tracer, as it gives more accurate HTRF values (lower SEM) than 100 μs integration time but will still enable fast reading cycles.

KINETIC PARAMETERS OF COLD CANNABINOID COMPOUNDS DETERMINED APPLYING THE MOTULSKY AND MAHAN MODEL

D77 TRACER CHARACTERIZATION UNDER PHYSIOLOGICAL CONDITIONS.

The selected fluorescent tracer D77 association binding profile to both cannabinoid receptors CB1 and CB2 was studied under physiological conditions. We measured the binding at 37 °C using HBSS buffer over a period of 5 min, using

six different concentrations of the fluorescent ligand D77 which ranged from 31.25 nM to 1 μM.
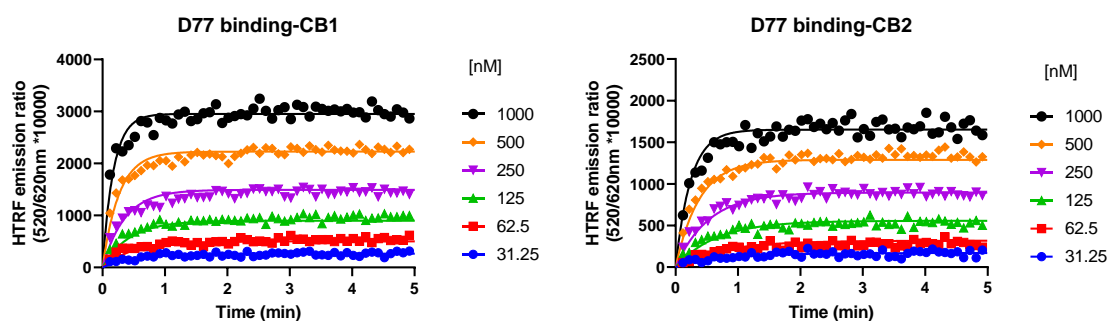
Figure 23. *D77 kinetic association binding curves to CB1 and CB2 cannabinoid receptors at 37 °C. Association binding curves using six concentrations of the fluorescent ligand D77 are shown for CB1 (left) and CB2 (right) receptors. Kinetic experiments report a K_d for D77 ligand of 437 ± 22 nM for CB1 and 370 ± 16 nM for CB2 receptor. Figures are representatives and data are expressed as mean ± SEM of 4 experiments conducted independently.*

The fluorescent ligand D77 shown in Figure 23 shows optimal binding characteristics at CB1 and CB2 making it an ideal tracer for the Motulsky and Mahan approach used to determine the kinetics of unlabelled compounds targeting these receptors. Although other fluorescent tracers for CB2 have been recently developed with higher affinity values (Gazzi et al., 2019) and proposed for their application of Motulsky and Mahan competitive binding, the faster k_{off} that D77 shows over the already described CB2 tracer SiR-6 (k_{off} 0.2 min^{-1}) will improve the assay performance with more accurate and precise estimates of the kinetic parameters of more rapidly dissociating compounds (Georgi et al., 2019).

The association rate constants are relatively slow for both receptors (k_{on-CB1}= (4.31 ± 0.19) x10^6 M^{-1} min^{-1}, k_{on-CB2} = (3.46 ± 0.22)x 10^6 M^{-1} min^{-1}), but compensated for by adding higher concentrations of tracer, but importantly it shows fast dissociation rate constants ($k_{off-CB1}$=1.87 ± 0.05 min^{-1} and $k_{off-CB2}$=1.13 ± 0.06 min^{-1}), meaning equilibrium is achieved fast with both receptors. Indeed, the D77 ligand shows a low non-specific binding signal at both receptors (Figure 24) and consequently a relatively high level of specific binding making it a useful tracer for competition studies and a practical alternative to the high affinity radioligands used in the past. Moreover, the binding signal of D77 measured as HTRF remains constant over time and we do not observe any decay associated with signal bleaching within the time of the signal acquisition.
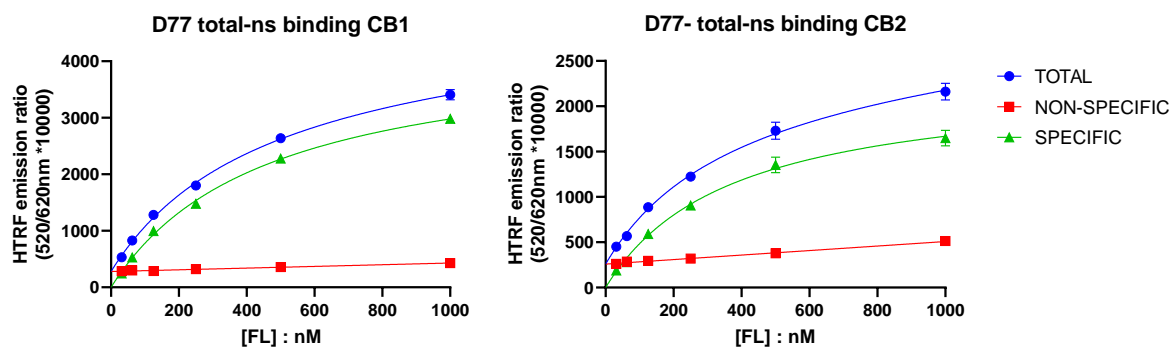
Figure 24. *Saturation binding curves at 5 min for D77 ligand binding to CB1 (left) and CB2 receptor (right). Total binding, non-specific binding, and specific signal saturation curves are shown as HTRF emission ratio. Non-specific binding was defined using 3 μM of rimonabant and 1 μM of SR144,528 for CB1 and CB2 receptors respectively. Figures are representatives and the mean ± SEM of six consecutive reads is represented in each point.*

The saturation plots indicate a saturating profile of the binding, and it can be observed the Nonspecific binding increases linearly with the increase of the tracer as it was expected. Moreover, the nonspecific levels remain low for both receptors, representing less than 25% of the total binding in both cases.

Table 2
Kinetic parameters k_{on} and k_{off} and Affinity of D77 fluorescent tracer at 37 °C calculated from kinetic association experiments (kinetic K_d) and from saturation experiments.

	k_{on} (M⁻¹ min⁻¹)	k_{off} (min⁻¹)
CB1	$(4.3 \pm 0.2) \times 10^6$	1.87 ± 0.05
CB2	$(3.5 \pm 0.2) \times 10^6$	1.13 ± 0.06
	Kinetic K_d (nM)	**Saturation K_d (nM)**
CB1	437 ± 22	427 ± 19
CB2	370 ± 16	380 ± 18

The affinity values (Kinetic K_d) were obtained from the kinetic parameters obtained from fitting the kinetic association data of the tested 6 concentrations of D77 ($K_d = k_{off}/k_{on}$). The K_d affinity parameter was also calculated from the fitting of specific binding data in equilibrium to a saturation model (see Figure 24). The affinity parameters obtained from both methods are detailed in Table 2 and show

good agreement, demonstrating the reliability of the kinetic data obtained from the kinetic association experiments.
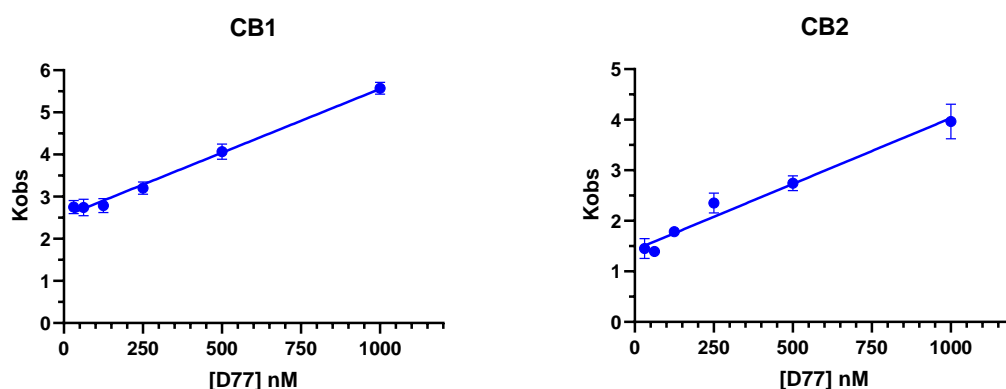
Figure 25. *Observed association rate constant (k_{obs}) obtained for each concentration of fluorescent tracer D77 fitted to a linear regression. Data plotted are mean ± SEM of 4 experiments conducted independently.*

As shown in Figure 25, The observed associated rate (k_{obs}) increases linearly with fluorescent ligand concentration, indicating that the binding follows the law of mass action (Motulsky & Christopoulos, 2003). The extrapolation of the fitted line to Y=0 yields to a estimation of k_{off} of 2.53 min^{-1} and 1.43 min^{-1} at CB1 and CB2 respectively and the slope indicates a $k_{on\text{-}CB1}$ = 3.03 x 10^6 M^{-1} min^{-1} and $k_{on\text{-}CB2}$ = 2.60 x 10^6 M^{-1} min^{-1}. These values are in good agreement with those obtained from global fitting of the D77 association binding curves (see Table 2).

MOTULSKY AND MAHAN MODEL

KINETIC PARAMETER DETERMINATION OF UNLABELLED CANNABINOID LIGANDS AT CB1 UNDER PHYSIOLOGICAL CONDITIONS

Competitive kinetic association experiments to CB1 receptor were carried out using the D77 fluorescent ligand as a tracer. The concentration of tracer used in the experiments was of 600 nM, approximately 1.5 x K_d. The association of the tracer ligand was monitored using TR-FRET in the competition with 7 different concentrations of each cold cannabinoid ligand. Data were globally fitted using the model "kinetics of competitive binding" in GraphPad Prism and association rate-k_{on} and dissociation rate-k_{off} were calculated for the different cannabinoid compounds.
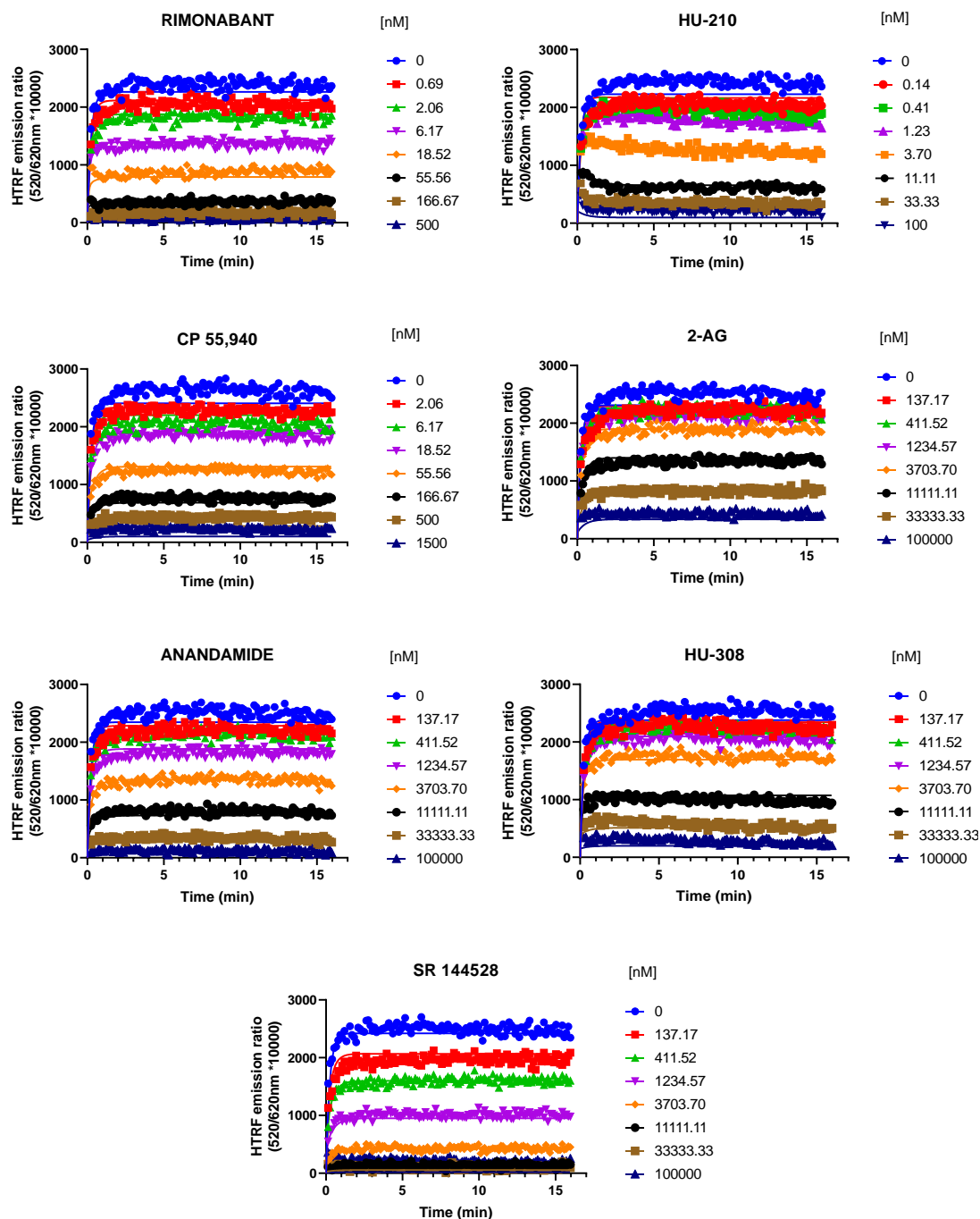
Figure 26: Competitive kinetic association curves of 7 cannabinoid ligands at CB1 (37 °C). *Experiments were conducted using increasing cannabinoid ligand concentrations that compete to the association of the tracer molecule D77 (600 nM). Data were globally fitted to the competition association model using GraphPad Prism 9 to simultaneously calculate k_{on} and k_{off}. Graphs are representatives of 4 experiments conducted independently.*

The competitive binding of the cold compounds resulted in curves (see Figure 26) showing a concentration dependant inhibition of the D77 tracer binding. The shape of the HU-210 competition curve showed the characteristic "overshoot" before reaching equilibrium, revealing the slow dissociation profile of the HU-210 compound relative to the tracer dissociation. The rest of the curves show a gradual increase of the D77 binding, indicating the faster dissociation of the competing compounds.

We report the kinetic parameters obtained from the competitive association binding experiments for the seven cannabinoid compounds selected. The kinetic association and dissociation rate constants (k_{on} and k_{off}) and residence times ($1/k_{off}$) were determined under physiological conditions (37 °C, physiological sodium concentration) and they are shown in Table 3.

Table 3
Kinetic parameters calculated from the Motulsky and Mahan experimental approach for the 7 cannabinoid compounds tested at CB1 at 37 °C. The data shown are mean ± SEM from 4 experiments conducted independently (except for 2-AG, N=3).

CB1 (37°C)	k_{on} (M^{-1} min^{-1})	k_{off} (min^{-1})	Residence time (Rt)	
			(min)	(s)
Rimonabant	$(5.0 \pm 0.5) \times 10^8$	2.2 ± 0.1	0.45 ± 0.03	**27 ± 2**
HU-210	$(3.8 \pm 0.1) \times 10^8$	0.85 ± 0.02	1.18 ± 0.03	**71 ± 2**
CP-55940	$(1.5 \pm 0.1) \times 10^8$	5.6 ± 0.3	0.18 ± 0.01	**10.8 ± 0.7**
2-AG (N=3)	$(1.4 \pm 0.5) \times 10^6$	6.7 ± 0.4	0.15 ± 0.01	**9.0 ± 0.5**
Anandamide	$(2.4 \pm 0.5) \times 10^6$	5.4 ± 0.6	0.19 ± 0.02	**12 ± 1**
HU-308	$(6.6 \pm 0.8) \times 10^5$	2.9 ± 0.3	0.35 ± 0.04	**21 ± 2**
SR144,528	$(1.4 \pm 0.2) \times 10^7$	5.0 ± 0.7	0.21 ± 0.03	**13 ± 2**

The faster associating compounds were Rimonabant, HU-210 and CP 55940, displaying a k_{on} of 5, 3.8, and 1.5 x10^8 M^{-1} min^{-1}. The two endocannabinoid compounds 2-AG and anandamide showed similar slower association rate constants (k_{on} 1.4 and 2.4 x10^6 M^{-1} min^{-1} respectively). The slowest associating compound was HU-308 with a k_{on} of 6.6 x10^5 M^{-1} min^{-1}, consistent with its lower affinity for CB1 receptor.

Regarding the dissociation profile of the compounds, the faster dissociating compounds where CP 55940, 2-AG, anandamide and SR 144528, therefore displaying the shorter residence times at the receptor of ~10 s. HU-210 showed the longer residence time (slowest k_{off}) of 71 s, followed by the inverse agonist Rimonabant (Rt= 27 s) and HU-308 (Rt= 21 s).

AFFINITY VALUES DERIVED FROM KINETIC PARAMETERS

The kinetic parameters obtained from the application of Motulsky and Mahan approach were used to calculate the kinetically derived affinity dissociation constant of the compounds tested by dividing the association and dissociation constants ($K_d=k_{off}/k_{on}$), shown in Table 4.

The non-selective agonist HU-210 showed the highest affinity for the CB1 R, with a K_d of 2.2 nM, followed by Rimonabant and CP 55940 with 4.6 and 37 nM respectively; the affinity of SR 144,528 was of 375 nM. The affinity of the two endocannabinoid compounds 2-AG and anandamide lay in the micromolar range (K_d 5.8 and 2.3 µM respectively). Similar to the endogenous cannabinoids, the compound HU-308, a CB2 selective agonist, showed low affinity with a K_d of 4.5 µM.

Table 4
Affinity values for the 7 cannabinoid compounds tested at CB1 at 37 °C. The equilibrium dissociation constant K_d was calculated from the kinetic parameters k_{on} and k_{off} obtained using the Motulsky and Mahan methodology. On the right column, the negative logarithmic transformation of the affinity values are shown as pK_d values. The data shown are mean ± SEM from 4 experiments conducted independently.

CB1 (37°C)	Kinetic K_d (nM)	pK_d (M)
Rimonabant	4.6 ± 0.6	8.35 ± 0.06
HU-210	2.23 ± 0.03	8.65 ± 0.01
CP-55940	37 ± 2	7.44 ± 0.03
2-AG (N=3)	5882 ± 1573	5.3± 0.1
Anandamide	2323 ± 172	5.64 ± 0.03
HU-308	4514 ± 76	5.34 ± 0.01
SR144,528	375 ± 12	6.43 ±0.01

KINETIC PARAMETER DETERMINATION OF UNLABELLED CANNABINOID LIGANDS AT CB2 RECEPTOR UNDER PHYSIOLOGICAL CONDITIONS

Competitive kinetic association experiments to CB2 receptor were carried out using the D77 fluorescent ligand as a tracer. The concentration of tracer used in the experiments was of 900 nM, approximately 2 x K_d. The association of the tracer ligand was monitored using TR-FRET in the competition with 7 different concentrations of each cold cannabinoid ligand. Data were globally fitted using the model "kinetics of competitive binding" in GraphPad Prism and association rate-k_{on} and dissociation rate-k_{off} were calculated for the different cannabinoid compounds.

The faster associating compounds at CB2 receptor were HU-210, CP 55940 and SR 144528, displaying a k_{on} of 2.6, 4.4, and 2.5 x10^8 M^{-1} min^{-1}, followed by HU-308, which displayed a k_{on} of 5.6 x10^7 M^{-1} min^{-1}. The two endocannabinoid compounds 2-AG and anandamide showed similar slower association rate constants (k_{on} 1.2 x10^7 and 9.7 x10^6 M^{-1} min^{-1} respectively), similar to rimonabant (k_{on} of 9 x10^6 M^{-1} min^{-1}).

Regarding the dissociation profile of the compounds, the faster dissociating compounds where 2-AG, rimonabant and anandamide, therefore displaying the shorter residence times at the receptor of ~4 s (2-AG) and ~10s. CP 55,940, HU-308 and SR 144,528 showed slower dissociation, with residence times of 33 s, 40 s and 87 s. The slowest dissociating compounds was HU-210, with a residence time of 20 min.

All the kinetic parameters (k_{on}, k_{off} and residence time) derived from the Motulsky and Mahan competitive association experiments at CB2 receptor (see **Figure 27**) can be found in Table 5.
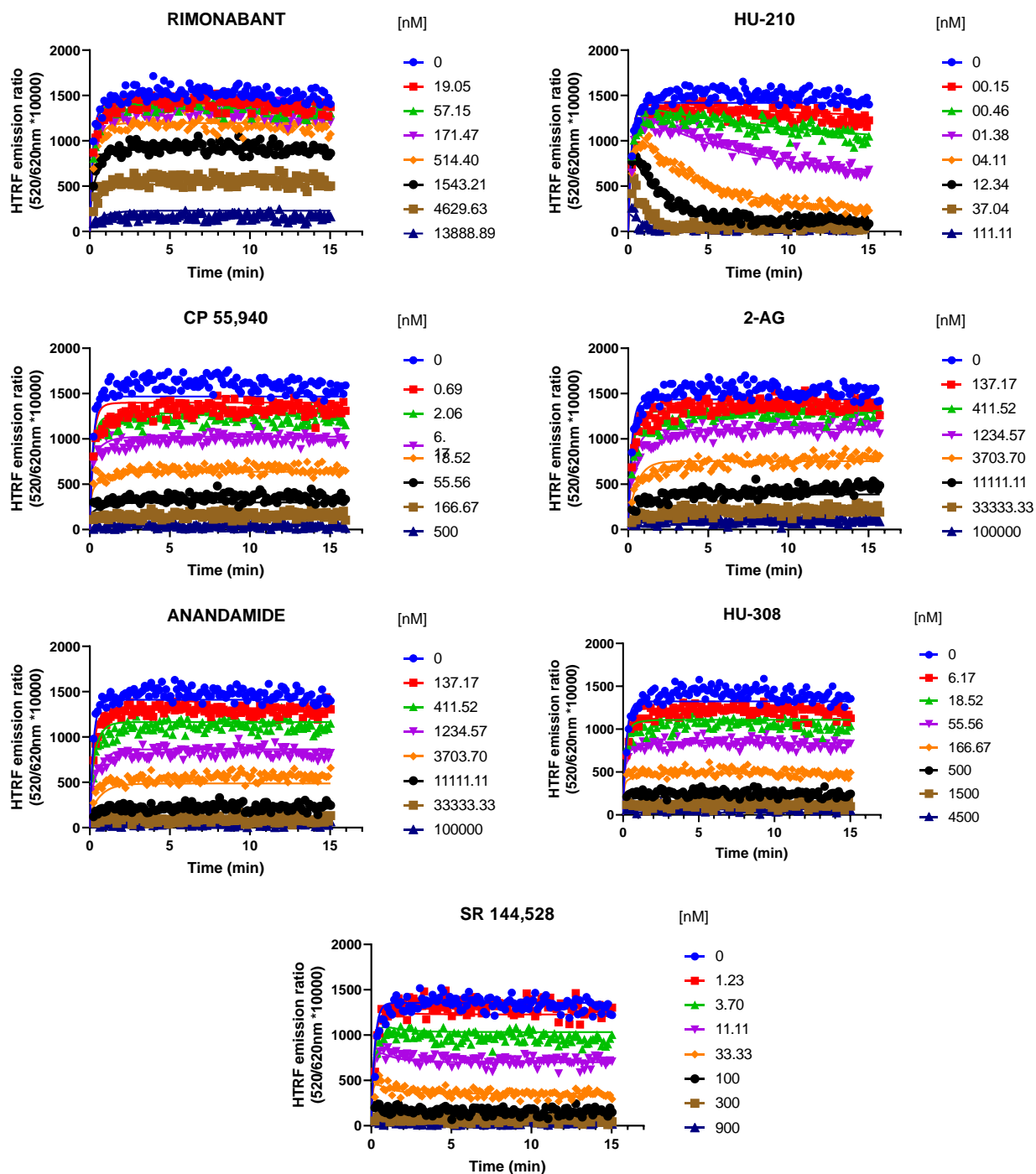
Figure 27. *Competitive kinetic association curves of 7 cannabinoid ligands at CB2. Experiments were conducted using increasing cannabinoid ligand concentrations that compete to the association of the tracer molecule D77 (900 nM). Data were globally fitted to the competition association model using GraphPad Prism 9 to simultaneously calculate k_{on} and k_{off}. Graphs are representatives of 4 experiments conducted independently.*

Table 5
Kinetic parameters calculated from the Motulsky and Mahan experimental approach for the 7 cannabinoid compounds tested for CB2 at 37°C. Data are expressed as mean ± SEM of 4 experiments conducted independently.

CB2 (37°C)	k_{on} (M^{-1} min^{-1})	k_{off} (min^{-1})	Residence time (Rt)	
			(min)	(s)
Rimonabant	$(9 \pm 1) \times 10^6$	6.4 ± 0.7	0.16 ± 0.02	10 ± 1
HU-210	$(2.6 \pm 0.2) \times 10^8$	0.051 ± 0.002	20 ± 1	1190 ± 67
CP-55940	$(4.4 \pm 0.5) \times 10^8$	1.9 ± 0.1	0.55 ± 0.04	33 ± 3
2-AG	$(1.2 \pm 0.2) \times 10^7$	14 ± 2	0.07 ± 0.01	4.4 ± 0.7
Anandamide	$(9.7 \pm 0.4) \times 10^6$	6.1 ± 0.7	0.17 ± 0.02	10 ± 1
HU-308	$(5.6 \pm 0.3) \times 10^7$	1.5 ± 0.1	0.66 ± 0.04	40 ± 2
SR144,528	$(2.5 \pm 0.2) \times 10^8$	0.69 ± 0.03	1.46 ± 0.07	87 ± 4

AFFINITY VALUES DERIVED FROM KINETIC PARAMETERS

The kinetic parameters obtained from the application of Motulsky and Mahan approach were used to calculate the kinetically derived affinity dissociation constant of the compounds tested by dividing the association and dissociation constants ($K_d = k_{off}/k_{on}$), as shown in Table 6.

Table 6.
Affinity values for the 7 cannabinoid compounds tested at CB2 at 37 °C. The equilibrium dissociation constant Kd was calculated from the kinetic parameters Kon and Koff obtained using the Motulsky and Mahan methodology. The data shown are mean ± SEM from 4 experiments conducted independently.

CB2	K_d (nM)	pK_d (M)
Rimonabant	701 ± 52	6.16 ± 0.03
HU-210	0.20 ± 0.02	9.71 ± 0.05
CP-55940	4.27 ± 0.24	8.37 ± 0.02
2-AG (N=3)	1213 ± 109	5.92 ± 0.04
Anandamide	632 ± 52	6.20 ± 0.04
HU-308	27.5 ± 1.5	7.56 ± 0.02
SR144,528	2.82 ± 0.16	8.55 ± 0.03

The non-selective agonist HU-210 showed the highest affinity for the CB2 receptor, with a K_d of 0.2 nM, followed by SR 144,528, CP 55940 and HU-308 with 2.8, 4.2 nM and 27.5 nM respectively. Rimonabant showed a K_d of 701 nM, similar to anandamide (632 nM). The compound with the lowest affinity was the endocannabinoid 2-AG, displaying a Kd of 1.2 µM.

KINETIC PARAMETERS AND EQUILIBIRUM AFFINITY

We performed a correlation analysis using the kinetic parameters (k_{on} and k_{off}) and the affinity for our set of compounds, in order to explore the role of association and dissociation constant rates in dictating the affinity that ligands display at CB1 and CB2 receptors.
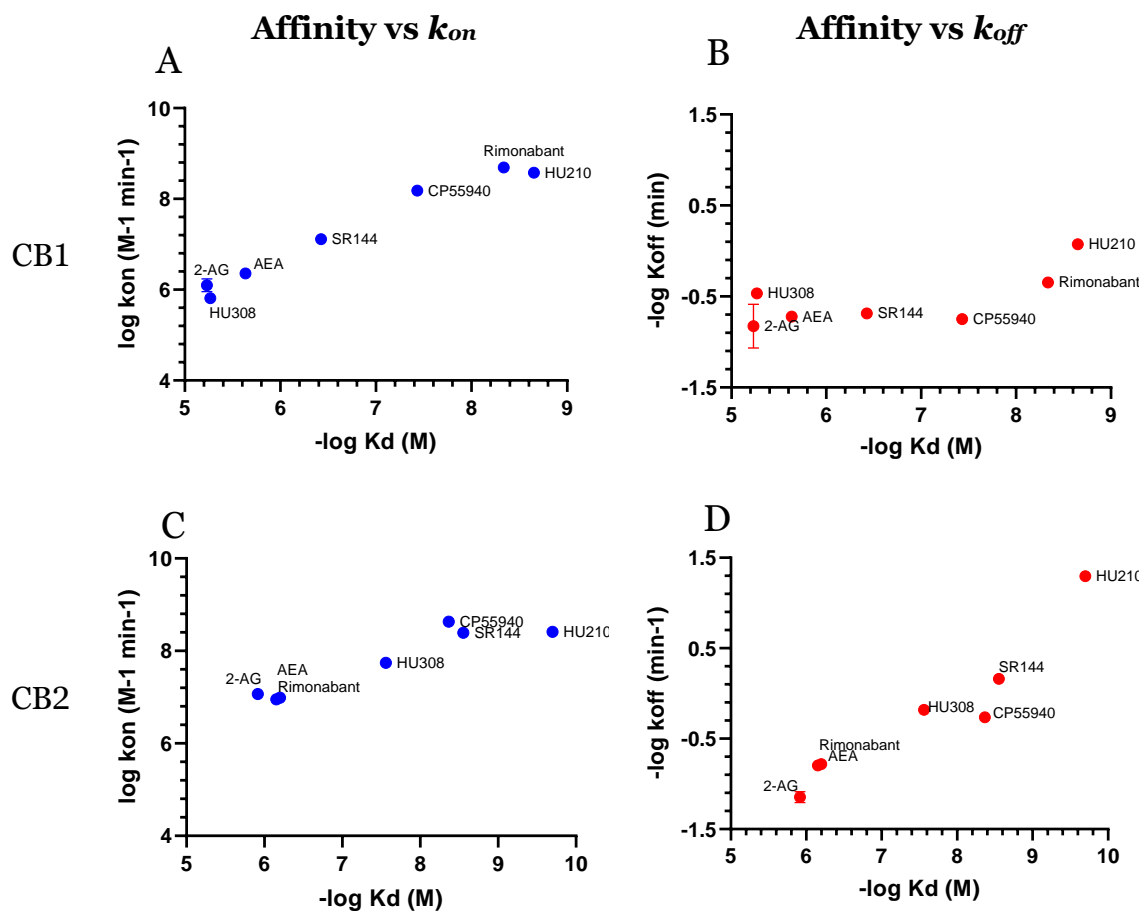
Figure 28. *Correlation plots of equilibrium and kinetic parameters of cannabinoid ligands at CB1 (A and B) and CB2 (C and D) measured at 37 °C. Correlation between negative logarithmic transformation of affinities (-log Kd) and logarithmic association rate (log kon) for CB1 (A) and CB2 (C). Correlation between negative logarithmic transformation of affinities (-log Kd) and negative logarithmic dissociation rates (-log koff) at CB1 (B) and CB2 (D). Correlation analysis was carried out using a Pearson correlation analysis (two-tails). Data shown are the mean and SEM of 4 independent experiments. P value was < 0.0001***(A) and 0.0023**(C) for the correlation of -logKd and log kon for CB1 and CB2 receptors respectively (Pearson coefficients CB1 -0.985 and CB2 -0.931). (B) -log koff and -log Kd does not show significant correlation at CB1 receptor (p value= 0.08). (D) -log koff and -log Kd show correlation at CB2 receptor with a p value = 0.0015**.*

The affinities and association rates of compounds show a strong correlation for both CB1 and CB2 receptors when performing a correlation analysis of their logarithmic transformations (pK_d vs log k_{on}), whereas the dissociation rates are only correlated with the affinity values for CB2 receptor, as no significant correlation was observed between pK_d and -log k_{off} values of compounds for CB1 receptor binding (see Figure 28). These results suggests that the k_{on}-association rate rather than k_{off}-dissociation rate is the dominant determinant of receptor affinity for CB1 receptor, whereas both k_{on} and k_{off} parameters are dictating the

affinity for the CB2 receptor binding. The correlation found between the affinity and dissociation rates for the CB2 receptor found with the selected compounds in this study is in contrast with the results published previously with a different set of compounds (Martella et al., 2017) where a no significant correlation was reported.

EQUILIBRIUM COMPETITION EXPERIMENTS

Equilibrium competition displacement experiments were carried out to calculate the equilibrium dissociation constant -pKi- of our set of cannabinoid compounds in equilibrium conditions. The D77 fluorescent tracer binding to CB1 and CB2 receptors was monitored using TR-FRET in presence of increasing amounts of cold cannabinoid ligands and IC$_{50}$ parameters were obtained from the derived curves, shown in Figure 29. The Cheng-Prusoff conversion equation was used to calculate Ki from IC$_{50}$ values derived from the curves.
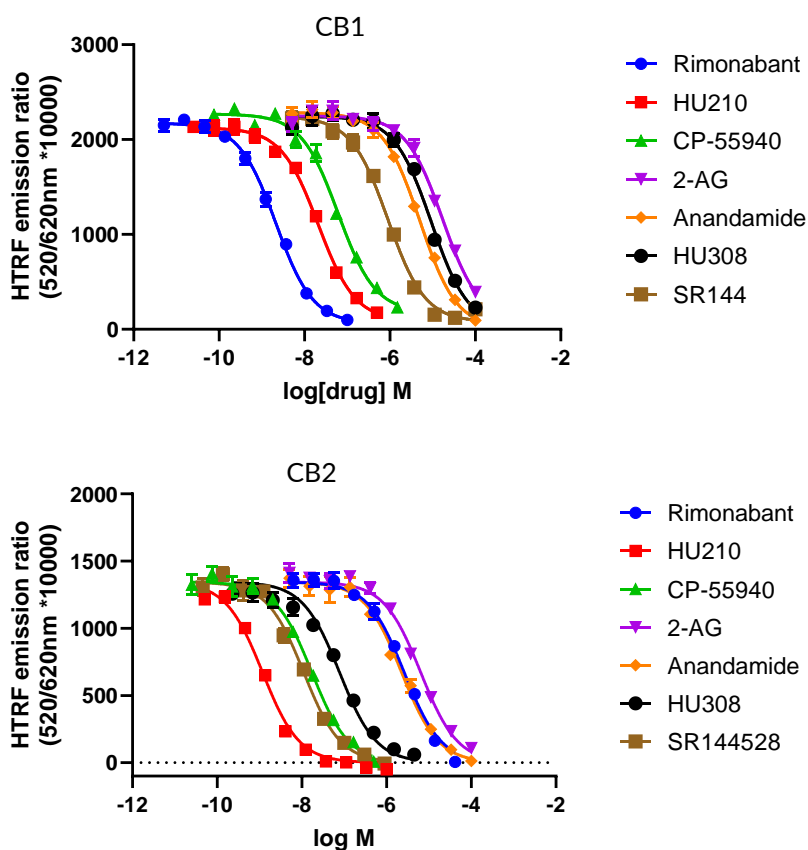
Figure 29. *Steady-state competition curves of D77 using 7 cannabinoid competing ligands at CB1 and CB2 receptor. 600 and 900 nM of the fluorescent molecule D77 was used for CB1 and CB2 respectively. Representative figures of the cannabinoid compounds competition to D77 are shown for both receptors at 37 °C after 15 min of membrane addition.*

Table 7
Equilibrium dissociation constant of the 7 cannabinnoid ligands tested expressed as pKi.
The data shown are mean ± SEM from 4 experiments conducted independently.

	pK_i	
	CB1	CB2
Rimonabant	8.98 ± 0.05	5.9 ± 0.1
HU210	8.0 ± 0.1	9.48 ± 0.08
CP 55,940	7.5 ± 0.3	8.2 ± 0.1
2-AG	5.1 ± 0.3	5.7 ± 0.2
Anandamide	5.59 ± 0.04	6.0 ± 0.1
HU 308	5.41 ± 0.02	7.5 ± 0.1
SR 144,528	6.43 ± 0.01	8.47 ± 0.09

COMPARISON BETWEEN KINETIC Kd AND COMPETITION DISPLACEMENT Ki VALUES

The equilibrium dissociation constants for the tested cannabinoid compounds were calculated from the kinetic association and dissociation rates from kinetic experiments (kinetic K_d; $K_d = k_{off}/k_{on}$) and from the equilibrium displacement data (K_i). Both values were compared for the binding of the tested compounds to both CB1 and CB2 receptors.
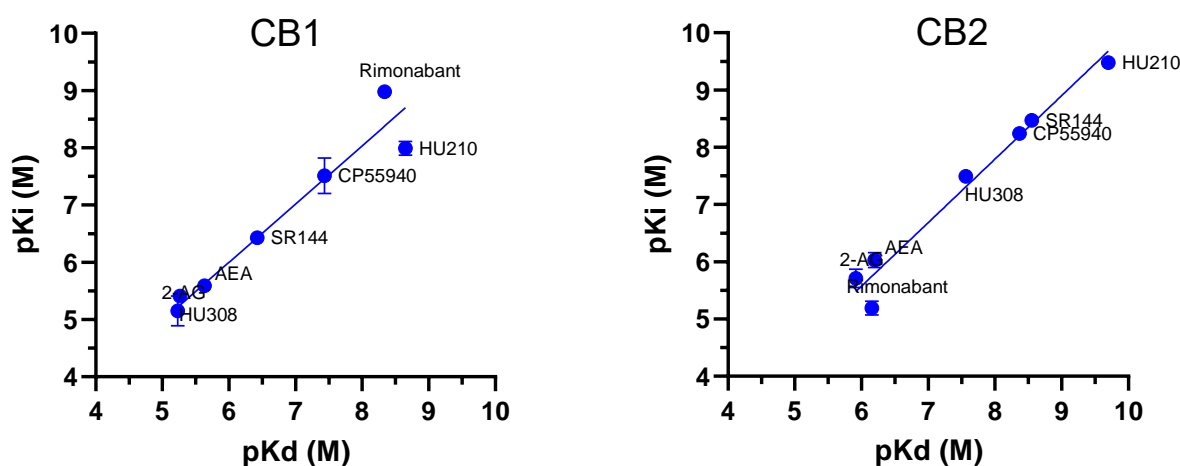
Figure 30. *Correlation between affinity values obtained from equilibrium displacement (pKi) and kinetic experiments (pKd) for the seven compounds tested at CB1 and CB2 receptors.*

As shown in Figure 30, the kinetic K_d affinity values generated showed a strong correlation with the K_i values obtained from the equilibrium displacement binding, obtaining a Pearson correlation coefficient of r=0.97 (P=0.0004) and r=0.98 (P<0.0001) for values at CB1 and CB2 respectively. These results showed that the association and dissociation rates obtained from the association competition experiments were good estimations that yield to very similar affinity values comparing to equilibrium data.

CANNABINOID SIGNALLING THROUGH β-ARRESTIN 2

STABLE CELL LINE CHARACTERISATION TO OPTIMISE ASSAY WINDOW AND PERFORMANCE

CB1 cell line

Different cell lines were sorted using FACS from the stable mixed-population cell line HEKTR-SNAP-CB1-Nluc_βarr2-Venus and were tested in β-arrestin2 recruitment BRET assays in order to select the clone with better assay window. Six different monoclonal cell lines were generated from different populations of cells, differing in their SNAP cell labelling intensity (indicating receptor membrane expression) and the Venus fluorescence intensity of the cells (indicative of β-arrestin2-Venus expression). Cells were selected from low (R8 and R11), medium (R9 and R12), or high (R10 or R13) biosensor expression cell subpopulations.
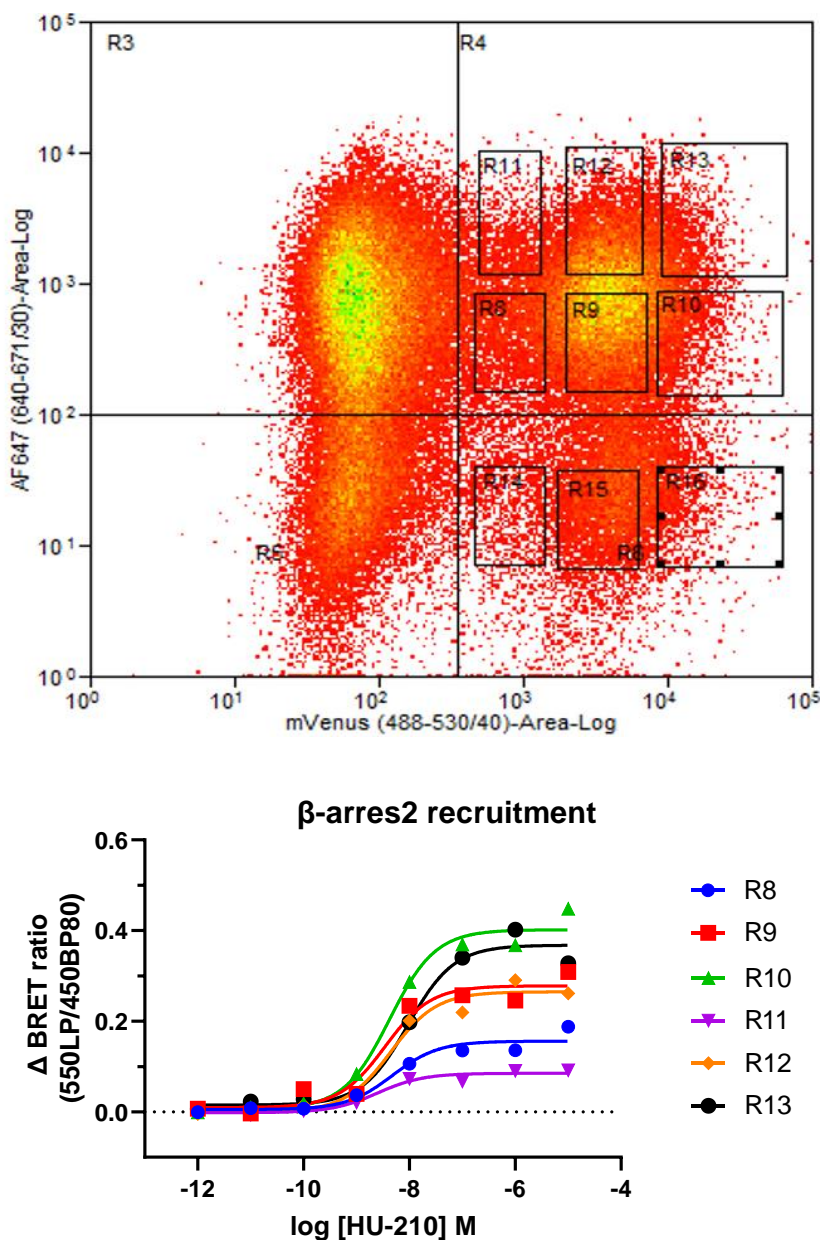
Figure 31. On the top, a graph representing the intensity of Venus and SNAP labelling of single cells of the mixed pool from the stable cell line HEKTR-SNAP-CB1-Nluc_βarr2-Venus analysed in the Flow Cytometry Facility (University of Nottingham). On the bottom, the dose-response curves of β-arrestin2 recruitment upon HU-210 cannabinoid agonist stimulation to CB1 receptor using BRET of monoclonal colonies obtained from each of the squares indicated in the top panel graph referred to as R8-R13.

The amplitude of the dose-response curves, and therefore the assay window for β-arrestin 2 differed among the cell lines obtained from the different subpopulations indicated above (see Figure 31). Cells with lower biosensor levels, and thus lower Venus intensity displayed a smaller assay window in β-arrestin2 recruitment BRET assays comparing to those with higher levels of biosensor, showing a direct relationship between biosensor expression and assay window. The assay window

that different cell lines displayed, as follows: R8/R11< R9/R12< R10/R13, is directly related with the Venus intensity obtained from the biosensor expressed in the cell lines.

In addition, cells from the populations with lower receptor expression R8, R9 and R10 showed slightly improved assay window comparing to the cell lines with similar Venus intensity but higher SNAP labelling R11, R12 and R13 respectively. These results indicate that a lower membrane expression of the CB1 receptor leads to an improved assay window when comparing similar biosensor (Venus-mGsi) levels, indicating that a low receptor/biosensor ratio is desirable for obtaining a good assay window.

The cell line from the R10 subpopulation was selected to study the recruitment of β-arrestin2 to CB1 receptors using BRET as it showed the wider assay window among the cell lines tested.

CB2 cell line

The three different cell lines generated using different receptor to biosensor ratios were tested in order to select the best performance in the assay.
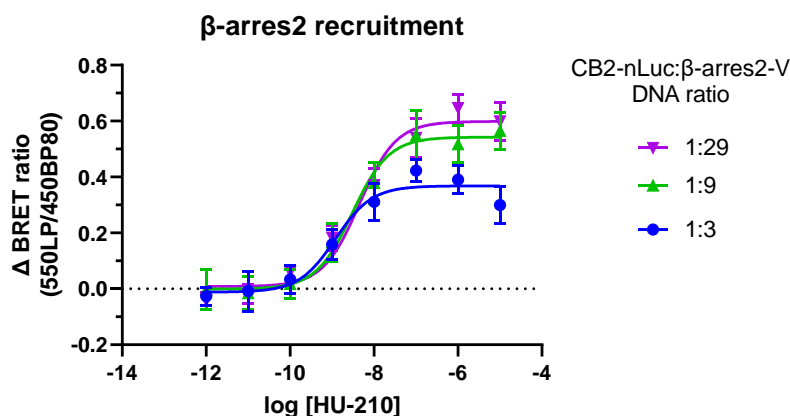
Figure 32. *Dose-response curves of β-arrestin2 recruitment upon HU-210 cannabinoid agonist using BRET in cell lines stably expressing CB2 receptor (HEKTR-SNAP-CB2-Nluc_βarr2-Venus). The cell lines were generated using different receptor to biosensor ratios as indicated in the legend.*

For the three curves generated, EC_{50} values were similar but a better assay window was observed as we incremented the biosensor ratio used for generating the stables cell lines (see Figure 32). The cell line generated with the DNA ratio of 1:29

receptor to biosensor was used as it displayed more accurate BRET ratio readouts and displayed the wider assay window.

β-ARRESTIN 2 RECRUITMENT TO CB1 AND CB2 RECEPTORS UPON CANNABINOID LIGAND STIMULATION.

The recruitment of β-arrestin 2 was studied in the stable HEK TR cell lines expressing CB1 or CB2 along with the β-arrestin 2 biosensor using BRET. The cannabinoid ligands were added in increasing concentrations reaching 10 µM in all cases, except for the two endocannabinoids 2-AG and AEA where the maximal concentration was 30 µM. BRET ratio signal was detected, and dose response curves were generated indicating the BRET ratio 15 min after the addition of ligands (see Figure 33).

At CB1 receptor, HU-210 compound showed the higher potency for inducing β-arrestin2 recruitment, and ~10 % higher maximal effect than the reference compound CP 55,940. The endogenous 2-AG and anandamide showed similar very weak potency for this signalling pathway, although their Emax is substantially different. Whereas anandamide appears as a partial agonist and showed an Emax of 70% of the effect elicited by CP 55,940 (100 %) at 50 µM, the maximal effect of 2-AG was 175% in relation to the effect induced by CP 55,940. It was not possible to define the top plateau of the 2-AG response due to the low solubility of the endocannabinoid compounds in aqueous buffer, but the estimation for the maximal effect when fitting the points to the sigmoidal dose-response curve suggest that the maximal effect could reach 200 %. Although rimonabant is defined as inverse agonist for CB1, no decrease of the basal signal was found for this pathway. The potency rank order for the β-arrestin2 recruitment upon agonist stimulation at CB1 receptors was as follows: HU-210≈ CP 55,940 > anandamide > 2-AG. Potency values and maximal effect values relative to CP 55,940 (100% effect) expressed as pEC_{50} and E_{max} can be found at Table 8.
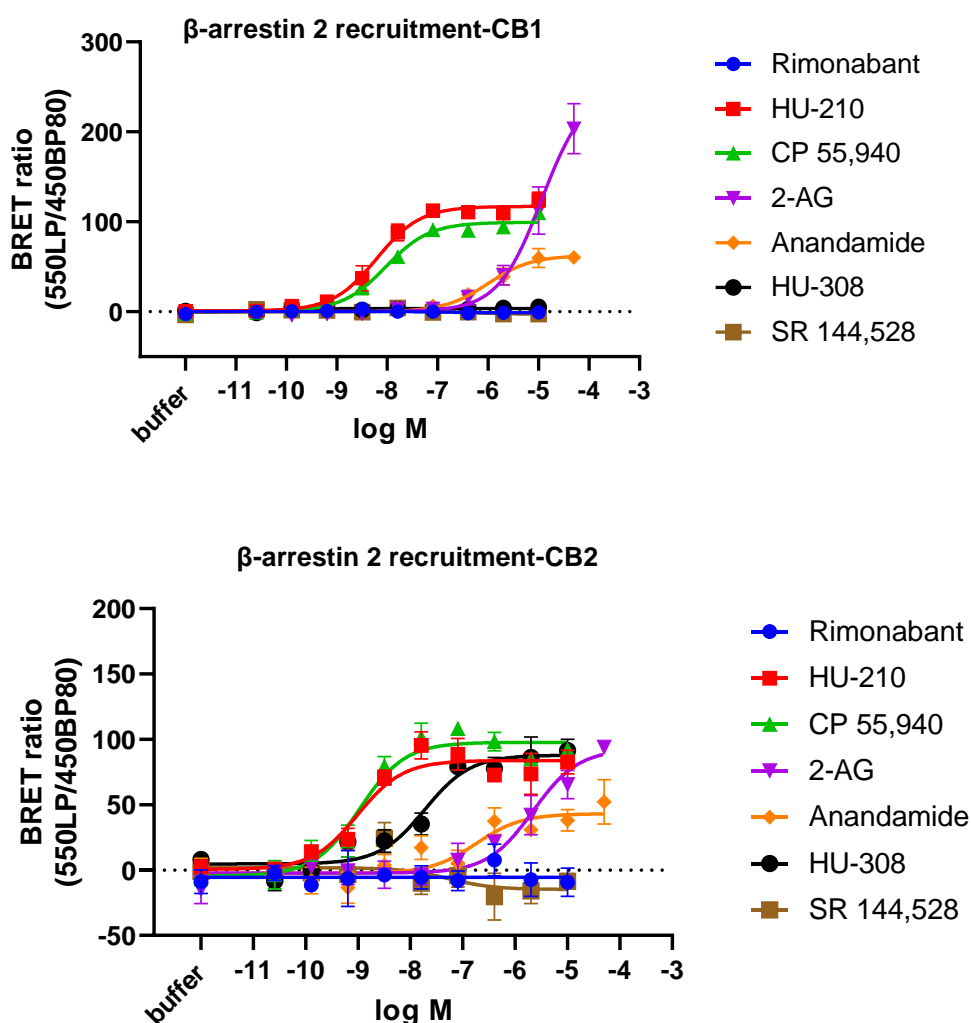
Figure 33. *β -arrestin2 recruitment to CB1 (top) and CB2 (bottom) upon cannabinoid ligand stimulation using 7 different cannabinoid compounds at 37°C. The BRET ratios obtained were normalised using the CP 55,940 as the reference agonist (100 % response). Data shown are mean ± SEM of ≥3 experiments conducted independently.*

At the CB2 receptor, HU-210 and CP 55,940 showed the highest potency for the activation of the β -arrestin2 recruitment. The E_{max} of HU-210 was ~90 % of the maximal response obtained with the reference compound CP 55,940. HU-308 showed lower potency and E_{max} than HU-210 and CP 55,940 compounds, producing a 77 % of the E_{max} obtained with CP 55,940. The two endogenous compounds showed the lower potency for the β -arrestin2 recruitment. However, anandamide showed the lower E_{max} among the 5 agonist studied whereas 2-AG appears to elicite the higher maximal (134 % of the reference CP 55,940) effect with low potency. The potency rank order for the β-arrestin 2 recruitment upon

agonist stimulation at CB2 receptors was as follows: HU-210≈CP 55,940 > HU 308 >anandamide> 2-AG.

Table 8
Potency values and maximal effect of agonist cannabinoid compounds expressed as pEC_{50} and E_{max} at CB1 and CB2 for β -arrestin2 recruitment response. E_{max} values are calculated relative to the effect elicited by CP 55,940 (100%). Data expressed are mean ± SEM of ≥3 experiments conducted independently.

CB1	pEC_{50}	E_{max}	CB2	pEC_{50}	E_{max}
HU-210	8.21 ± 0.15	114 ±3	HU-210	9.19 ± 0.17	77 ±8
CP 55,940	8.03 ± 0.17	100	CP 55,940	8.95 ± 0.16	100
2-AG	4.81 ± 0.23	212 ± 45	2-AG	5.6 ± 0.32	102 ± 9
AEA	5.70 ± 0.27	63 ±8	AEA	6.6 ± 0.65	44 ± 12
			HU-308	7.72 ± 0.23	89 ± 9

miniGsi COUPLING STUDIES TO CB1 AND CB2 RECEPTORS

The coupling of miniGsi biosensors was studied in HEK293 T17 cells transiently expressing CB1 or CB2 along with the mGsi biosensor using BRET. The cannabinoid ligands were added in increasing concentrations reaching 10 μM in all cases, except for the two endocannabinoids 2-AG and AEA where the maximal concentration was 30 μM. BRET ratio signal was detected, and dose response curves were generated indicating the BRET ratio 15 min after the addition of ligands (see Figure 34).

At CB1 receptor, both CP 55,940 and HU-210 exhibited full agonism for the mGsi coupling, as well as the endogenous 2-AG. Although anandamide shows higher potency for the mGsi coupling than 2-AG at CB1 receptor, the maximal response lay below the one elicited by the full agonist, only reaching ~80% of maximal response relative to CP 55940.
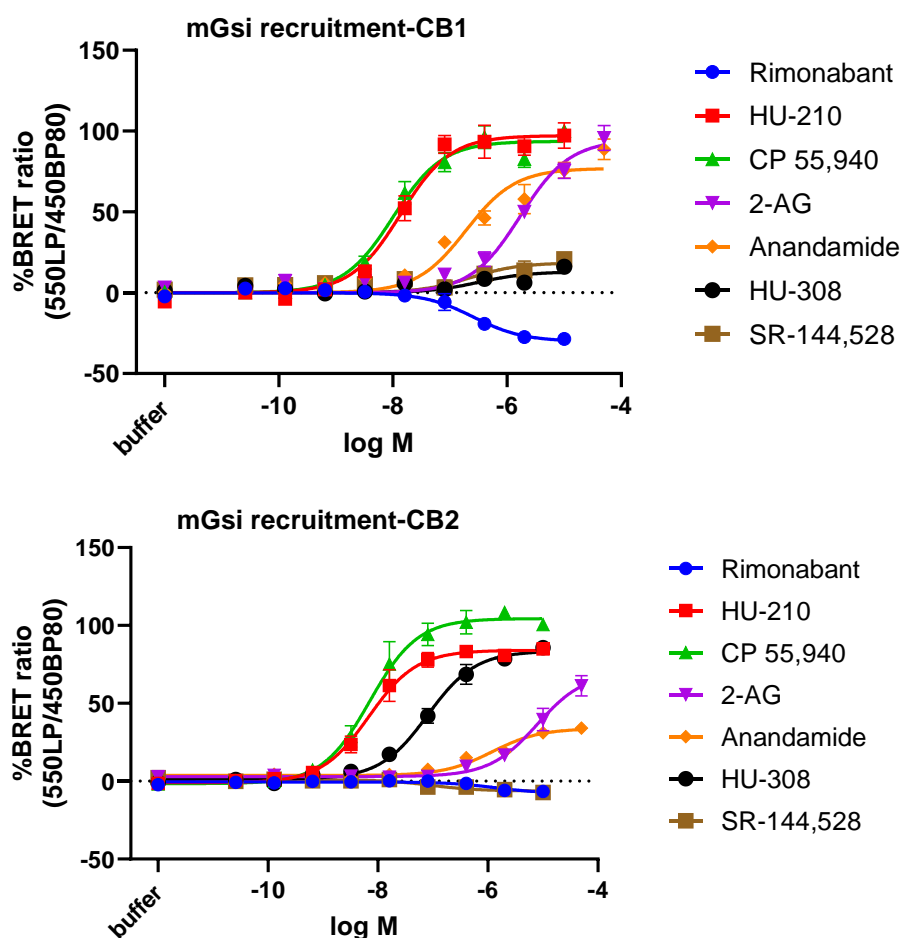
Figure 34*. Dose-response curves of CB1 (top) and CB2 (bottom) receptors of miniGsi recruitment upon ligand stimulation using BRET 15 min after ligand addition. The BRET ratios obtained were normalised using the CP 55,940 as the reference agonist (100 % response). Data shown are mean ± SEM of 4 experiments conducted independently.*

Rimonabant shows inverse agonist properties inhibiting the basal mGsi coupling by ~30% of its maximum, revealing strong constitutive activity of the CB1 receptor. The CB2 selective HU-308 and SR-144,528 elicit a very weak mGsi coupling at high concentrations, exhibiting weak partial agonism properties. Nevertheless, the increase in the BRET signal accounts for less than 20% of the response elicited by the full agonists and quantification of the EC_{50} values could not be performed with confidence. The potency values (pEC_{50}) for the activation of mGsi coupling for the tested cannabinoid agonist can be found in the Table 9. The potency rank order for the agonist inducing a mGsi coupling to CB1 receptors were as follows HU-210≈CP 55,940 > anandamide> 2-AG.

At CB2 receptor, only the CP 55,940 showed full agonism for the mGsi coupling activation, whereas HU-210, the two endocannabinoids 2-AG and anandamide

and HU-308 showed partial agonism by inducing a 80 %, 66 %, 30 % and 76 % of the maximal activation produced by the full agonist CP 55,940. The CB2 selective HU-308 shows a very similar maximal effect to the HU-210 compound, although here HU-308 is 10 times less potent than HU-210. The endogenous agonists 2-AG and anandamide showed low potency, similar to that at CB1 receptors, but with lower maximal effect. The inverse agonist SR 144,528 effect at CB2 shows that the constitutive activity for CB2 receptor in this system is relatively small as the decrease in the basal activation is marginal. Indeed, the weak effect of SR-144,528 causing a decrease in the basal effect is similar to the decrease induced by rimonabant. The potency rank order for the agonist inducing a mGsi coupling to CB2 receptors were as follows HU-210≈CP 55,940 > HU 308 >anandamide> 2-AG.

It can be observed that the E_{max} (maximal effect) that compounds induce when binding to the receptor varies among CB1 and CB2, but the potency rank order for the non-selective agonists are shared between the two systems.

Table 9
Potency values and maximal effect of agonist cannabinoid compounds expressed as pEC_{50} and E_{max} at CB1 and CB2 for mGsi coupling response. E_{max} values are calculated relative to the effect elicited by CP 55,940 (100%). Data expressed are mean ± SEM of 4 experiments conducted independently.

CB1	pEC_{50}	E_{max}	CB2	pEC_{50}	E_{max}
HU-210	7.91 ± 0.06	107 ± 8	HU-210	8.32 ± 0.03	80 ± 1
CP 55,940	8.00 ± 0.06	100	CP 55,940	8.29 ± 0.03	100
2-AG	5.66 ± 0.13	98 ± 8	2-AG	5.22 ± 0.08	66 ± 3
AEA	6.51 ± 0.15	78 ± 6	AEA	6.16 ± 0.13	30 ± 4
			HU-308	7.27 ± 0.08	76 ± 4

INTERNALISATION OF CB1 AND CB2 RECEPTORS UPON LIGAND STIMULATION

The internalisation of cannabinoid receptors was assessed in HEK TR cells expressing either CB1 and CB2 receptors after the stimulation with seven different cannabinoid ligand. The internalization process was assessed dynamically during 60 min using DERET or Diffusion Enhanced Resonance Energy Transfer.

The data obtained show that cannabinoid ligands described as agonist for each of the cannabinoid receptor produce a concentration dependent internalisation profile. Although the data were collected over 1 h after ligand addition, the shape of the curves suggest that the internalisation process has not reached equilibrium as the curves do not show a plateau within the first hour (see Figure 35 and Figure 36.)

Dose-response curves were generated using the data obtained after 15 min of ligand addition to determine the EC50 and maximal effect at that time (see Figure 37 and Figure 38). DERET data were normalised to CP 55,940 (100 % response) and basal internalization detected when no ligand was present was subtracted before plotting each curve.

The potency (pEC_{50}) and maximal effect (E_{max}) elicited by the agonists tested after 15 min of ligand addition can be found in Table 10.
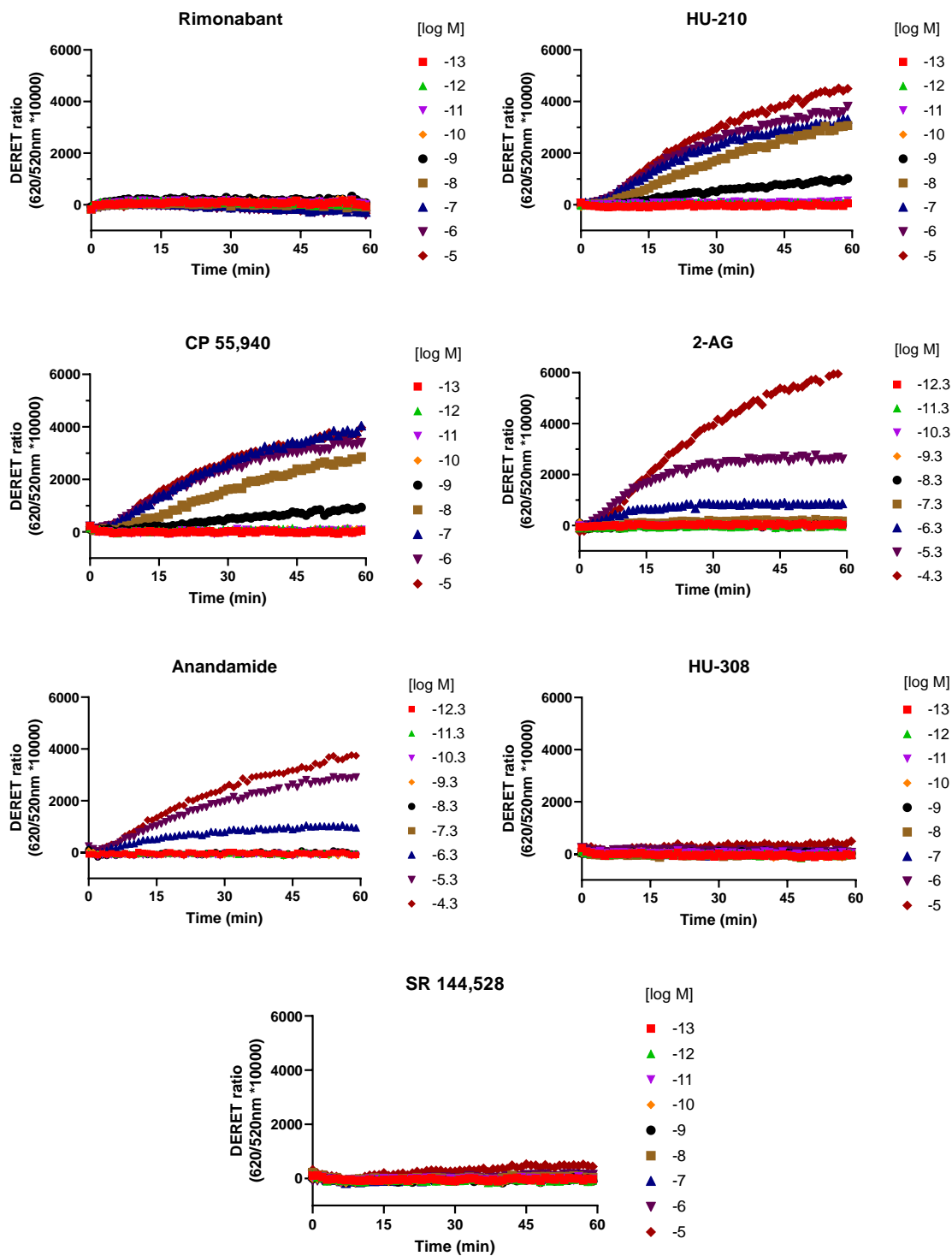
Figure 35. *Internalisation of the CB1 receptor measured over time at 37°C upon ligand stimulation. SNAP-CB1 receptors expressed at the cell surface were labelled with SNAP-Lumi4-Tb. Cells were subsequently incubated with an excess of acceptor (60 μM fluorescein) in the presence of different cannabinoid ligands. Constitutive basal internalisation was measured in the absence of ligands and subtracted from the obtained DERET values. Data are presented as representative of four experiments.*
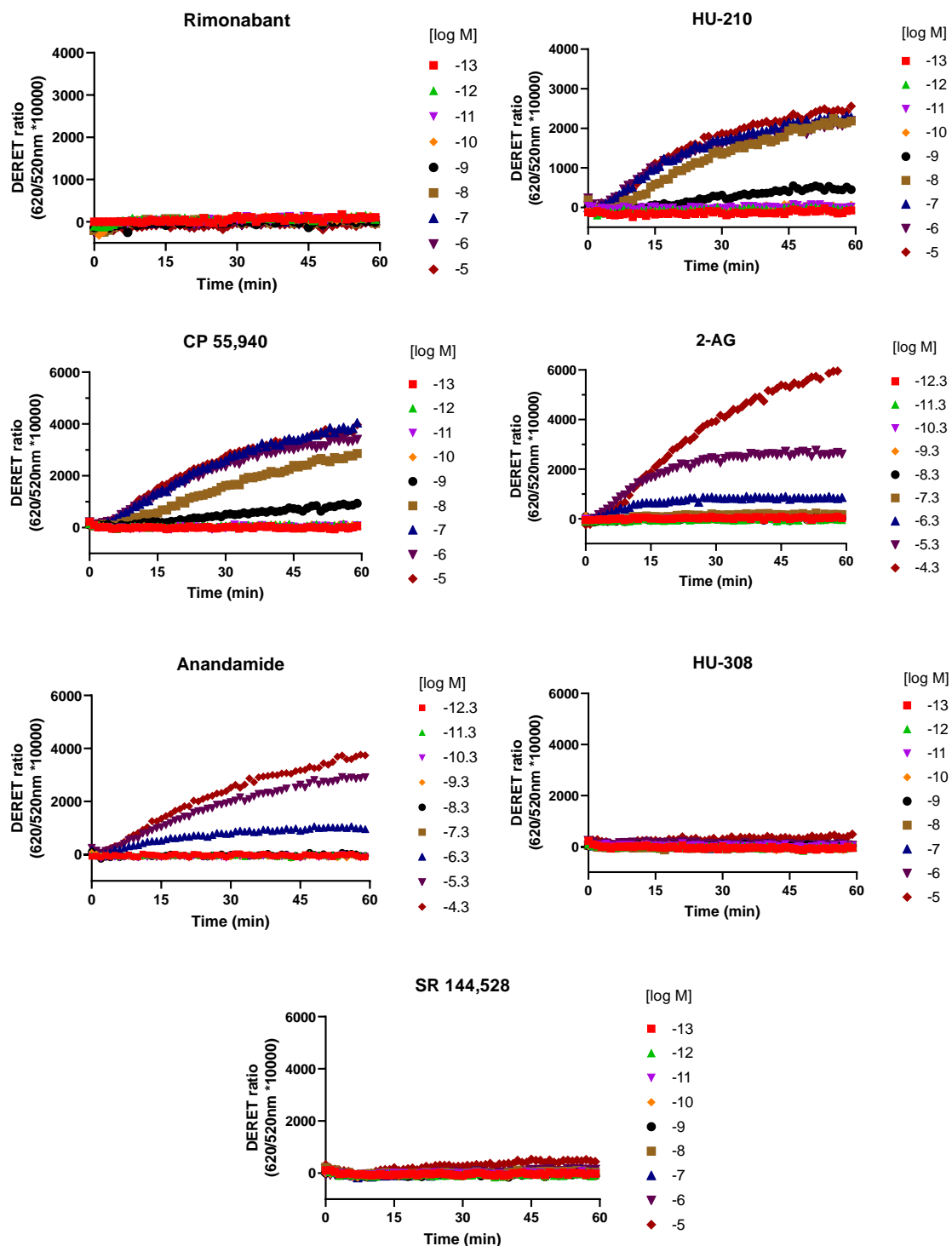
Figure 36. *Internalisation of the CB2 receptor measured over time at 37°C upon ligand stimulation. SNAP-CB1 receptors expressed at the cell surface were labeled with SNAP-Lumi4-Tb. Cells were subsequently incubated with an excess of acceptor (60 μM fluorescein) in the presence of different cannabinoid ligands. Constitutive basal internalisation was measured in the absence of ligands and subtracted from the obtained DERET values. Data are presented as representative of three to four experiments.*

In HEK TR- CB1 expressing cells, the endogenous 2-AG was the compound producing the higher internalization levels, 166 ± 16 % of the CP 55,940 response, although with low potency (EC50= 1.7 µM). Both HU-210 and anandamide produced an internalization level similar to CP 55,940 (104± 5 and 105±12, respectively), although HU-210 was ~25 times more potent for producing internalization of the CB1 receptors, with a potency similar to CP 55,940. HU-308 shows very weak internalization of CB1 receptor (~15%), as it is a CB2 selective compound that exhibit very low affinity for CB1 receptor. The inverse agonism activity of rimonabant can be observed with the decrease of DERET ratio, showing its capacity to reduce basal internalization.
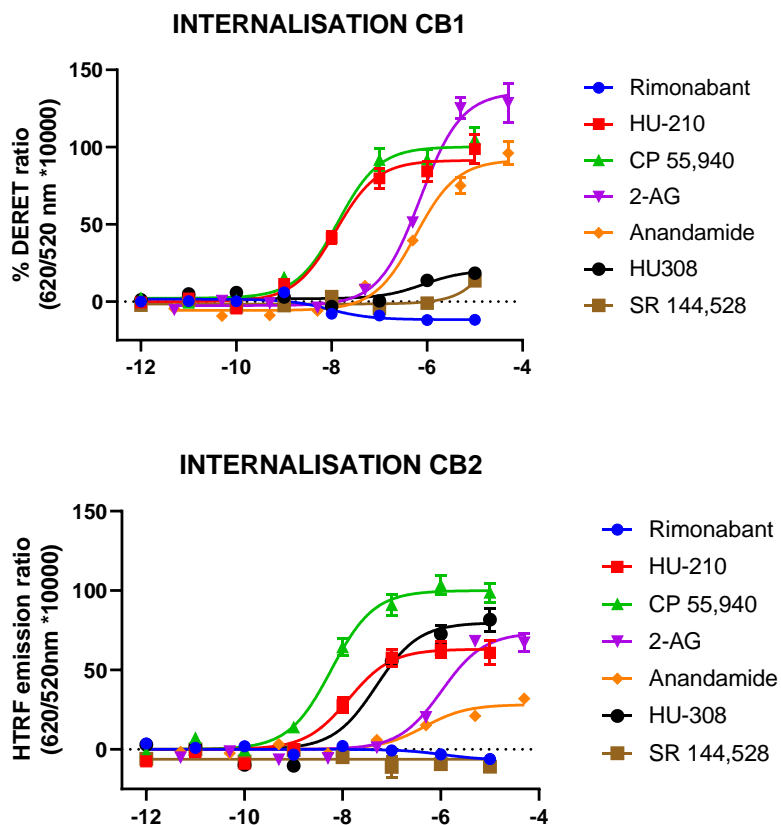
Figure 37. *Dose-response curves of the internalisation of CB1 and CB2 receptors expressed in HEK-TR cells after 15 min of ligand stimulation. Graphs shown are representatives of 4 experiments conducted independently. % DERET ratio is represented normalised to CP 55,940 response (100 % DERET ratio). Error bars represent SEM of 6 consecutive measurements.*

In HEK TR cells expressing CB2, CP 55940 was the most potent and efficacious compound producing internalization (EC_{50} 12 nM). The endogenous 2-AG and AEA only produced 80 and 20 % of internalization respectively (relative to CP 55,940), both showing low potency within the μM range. HU-210 only produced 64 % of internalization relative to CP 55,940, although they show very similar potency values (EC_{50} =16 nM and EC_{50} =13 nM for HU-210 and CP 55,940 respectively). HU-308 produced ~86 % internalization relative to CP 55,940 and showed a potency of EC_{50}=95nM.

Table 10
Potency values of agonist cannabinoid compounds expressed as pEC_{50} at CB1 and CB2 receptor internalisation response measured at 15 min after ligand addition. Data expressed are mean ± SEM of ≥4 experiments conducted independently.

CB1	pEC_{50}	E_{max}	CB2	pEC_{50}	E_{max}
HU-210	7.80 ± 0.07	104 ± 5	HU-210	7.80 ± 0.05	64 ± 5
CP 55,940	7.64 ± 0.08	100	CP 55,940	7.9 ± 0.2	100
2-AG	5.7 ± 0.1	166 ± 17	2-AG	5.9 ± 0.2	82 ± 4
AEA	6.4 ± 0.2	105 ± 12	AEA	5.6 ± 0.3	20 ± 5
			HU 308	7.02 ± 0.09	86 ± 4

BIAS OF CANNABINOID COMPOUNDS

We studied the bias of the cannabinoid agonists used in this study for the mGsi coupling, β-arrestin 2 recruitment and internalization pathways at CB1 and CB2 receptors. For the CB1 receptor, the activation of HU-210, CP 55940 and anandamide (AEA) was quantified. For the CB2 receptor, HU-210, 2-AG, AEA and HU-308 ligands were studied.

The data obtained from the three assays were fitted using the Operational Model in order to obtain log (τ/K_A) parameters for each ligand in the different studied responses. Transduction ratios (τ/K_A) obtained in different pathways were compared for each agonist relative to a reference compound. Therefore, the difference of the logarithmic transformation of the transduction ratio- $\Delta log(\tau/K_A)_{lig-ref}$ - was obtained for each ligand in a given pathway relative to the

reference. $\Delta \log(\tau /K_A)$ values were then used to calculate $\Delta\Delta\log(\tau /KA)_{1-2}$ and bias ($10^{\Delta\Delta\log (\tau/KA)_{1-2}}$), which are summarized in the Table 11.

$\Delta\Delta\log(\tau/KA)_{1-2}$ <0 will indicate the preference of the pathway 2 activation over pathway 1, whereas when the parameter is >0, will indicate a preference for the first pathway indicated. Bias is expressed as $10^{\Delta\Delta\log (\tau/KA)_{1-2}}$ and will indicate the magnitude of that preferential activation. In this sense, Bias=1 will be indicative of totally equilibrated pathways.

Table 11
*$\Delta\Delta\log(\tau /KA)_{1-2}$ and Bias ($10^{\Delta\Delta\log (\tau/KA)_{1-2}}$) values for cannabinoid agonists acting at CB1 and CB2. Values with * represent statistical significant $\Delta\Delta\log(\tau /KA)$ or Bias. The analysis was carried out using 2-AG as a reference compound for CB1 and CP 55,940 was used for CB2.*

CB1	mGsi-Intern		mGsi- β-arr2		β-arr2 -Intern	
	ΔΔlog(τ/KA)	Bias	ΔΔlog(τ/KA)	Bias	ΔΔlog(τ/KA)	Bias
2-AG (ref)	0	1	0	1	0	1
HU-210	0.82*	6.57*	-0.18	0.65	1.00*	9.97*
CP 55,940	0.81*	6.40*	0.11	1.28	0.70*	5.00*
AEA	0.65*	4.43*	0.28	1.92	0.36	2.31
CB2	mGsi-Intern		mGsi- β-arr2		β-arr2 -Intern	
	ΔΔlog(τ/KA)	Bias	ΔΔlog(τ/KA)	Bias	ΔΔlog(τ/KA)	Bias
CP 55,940 (ref)	0	1	0	1	0	1
HU-210	-0.24	0.57	0.24	1.75	-0.48*	0.33*
2-AG	-0.49*	0.32*	0.09	1.24	-0.58*	0.27*
AEA	-0.24	0.57	0.02	1.04	-0.26*	0.55*
HU-308	-0.34*	0.45*	-0.02	0.95	-0.32	0.47

All the compounds studied show a significant bias between some of the responses analysed. The compounds acting at CB1 receptor did not show any preference between the activation of mGsi and β-arrestin 2 recruitment, but all of them showed preference in inducing mGsi coupling comparing to internalization. The β-arrestin 2 recruitment was the preference induced response when comparing to

internalization on HU-210 and CP 55,940, although no statistical significance was found for AEA.

The agonists studied at CB2 receptor did not show any preference that was statistically significant between coupling mGsi and recruiting β-arrestin 2, similar to the observed in CB1 receptor. 2-AG and HU-308 showed preference for receptor internalization compared to mGsi coupling. HU-210, 2-AG and AEA exhibit preference in receptor internalization comparing to β-arrestin 2 recruitment.
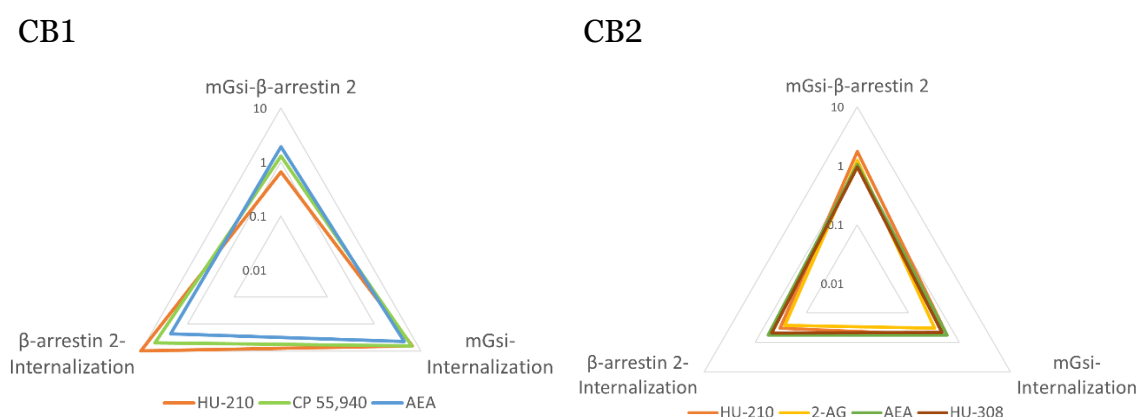
Figure 38. *Bias fingerprint relative to 2-AG for CB1 agonists (left) and CP 55,940 for CB2 agonists (right). Bias values ($10^{\Delta\Delta log\,(\tau/KA)_{1-2}}$) obtained for the agonists between the mGsi coupling, agonist induced internalization and β-arrestin 2 recruitment are represented as radar plots.*

It can be observed a general difference in the preference between the two receptors for activating one of the studied responses. Whereas at CB1 the statistically significant biased compounds show a preference for mGsi over internalization coupling or β-arrestin 2 recruitment, the opposite is observed for CB2 receptor, where the agonists show preference for internalization over β-arrestin 2 or mGsi coupling.

EXPLORING RESIDENCE TIME IMPLICATION IN EFFICACY

The efficacy (τ) values were calculated for each of the agonist from the log R (=log τ/K_A) derived from the Operational Model and their relationship to the residence time (Rt=$1/k_{off}$) was studied applying a Pearson correlation analysis (two-tails).

For CB1, the efficacy of four agonists- HU-210, CP 55,940, 2-AG and anandamide were calculated as τ for mGsi, β-arrestin 2 recruitment or internalization at 15 min of ligand stimulation. The analysis for CB2 includes the same agonists but also the HU-308 selective agonist, accounting for five compounds.

Using this correlation, we wanted to explore if the duration of the ligand–receptor complex of different agonists binding to CB1 and CB2 receptors may have an impact on the efficacy displayed to activate the studied responses.
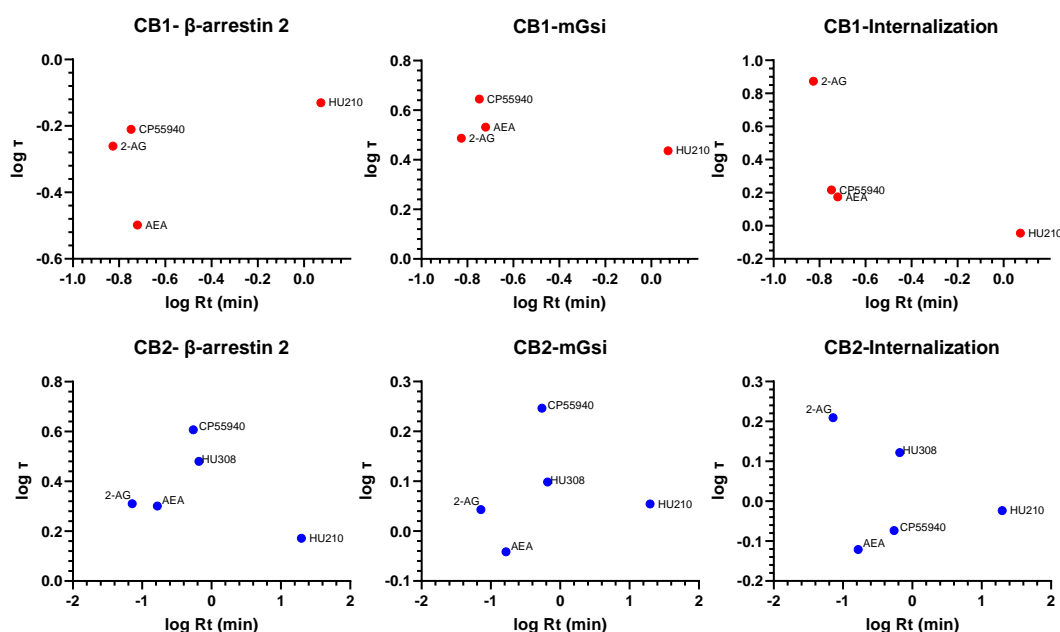
Figure 39. *Correlation plots of residence time (Rt) and efficacy (tau) at different responses of cannabinoid agonists acting at CB1 and CB2 receptors. Correlation analysis was carried out using a Pearson correlation analysis (two-tails) and the obtained R^2 values were β-arrestin 2 recruitment, mGsi coupling and internalization of 0.31, 0.38, and 0.45 at CB1 receptor and 0.11, 0.02 and 0.09 at CB2 receptor*

As it can be observed in Figure 39 , no significant correlation was found between the two parameters for the studied set of compounds. The data obtained for efficacy (τ) does not show significative correlation with the receptor-ligand complex duration, which is represented by Residence time (Rt).

4. DISCUSSION

CB1 AND CB2 TR-FRET BASED KINETIC ASSAY DEVELOPMENT

FRET in GPCRs with long N-terminal domain

Whereas class B and C GPCRs are characterized by a long N-terminal domain (NTD), most class A or rhodopsin-like receptors reveal shorter extracellular terminals (Gether, 2000). As shown in Figure 40, the N-terminal aminoacidic sequence rarely contains more than 100 aa for class A GPCRs. However, CB1 receptor contains an unusually long NTD among this subfamily, containing 111 amino acids and constituting more than the 25 % of its protein sequence.
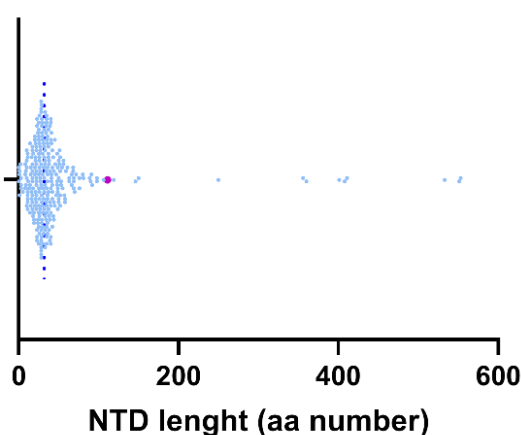
Figure 40. NTD length distribution of class A GPCRs. Each blue dot represents one single GPCR N-terminal amino acid (aa) number. CB1 receptor is highlighted in purple. (Data was obtained from GPCRdb database)

For both class B and class C receptors, containing an N-terminal domain of 100-150 amino acids (class B) and approximately 500-600 amino acids (class C), the N-terminal has been described as part of the ligand recognition and binding site in many cases (Bazarsuren et al., 2002; Grauschopf et al., 2000; O'Hara et al., 1993; Perrin et al., 2001). In contrast, this feature of NTDs has not been largely studied among class A GPCRs. The vasopresin V_{1a} receptor is one of the exceptions among class A GPCRs where the N-terminal has been described to be important for the ligand binding of agonists, where residues proximal to the transmembrane helix (TM1) were determined to be important for the binding affinity of agonists (Hawtin et al., 2005).

In the case of CB1, the affinity displayed by the different splice variants (where the N-terminal reveals different length and aa sequence) was very similar (Xiao et al., 2008), suggesting that the distal residues of the N-tail are not involved in the ligand binding process. Xiao et al. (2008) determined the affinity of CP 55940, methanandamide, 2-arachidonoyl glycerol, virodhamine, noladin ether, docosatetraenylethanolamide, and AM251 to the different human splice variants of CB1 receptor (CB1, CB1a and CB1b) by competition of agonist [^{3}H]-CP55940 binding using CHO cell membranes expressing the different receptor variants. A previous study conducted by Ryberg et al. (2005), showed no differences in the binding affinity of synthetic cannabinoids Δ9THC, CP 55940, WIN 55-212,2, HU-210 and SR141716 to the different splice variants. Nevertheless, Ryberg et al. observed a loss of affinity for endogenous compounds at CB1a and CB1b variants, although these results were not reproduced by Xiao et al. (2008), where the affinity was not significantly altered for both synthetic and endogenous compounds as previously mentioned. Moreover, no significative changes in the binding affinity of the CP 55,940 agonist were found when using N-truncated CB1 variants (Andersson et al., 2003). The role of the long N-tail is still unclear, but it has been speculated to play a role in the trafficking or maturation of the receptor (Andersson et al., 2003).

As we previously explained, the rationale behind the CB1 truncation variant used in this study was performed in light of the human CB1 splice variant sequences and the data already described (Ryberg et al., 2005; Shire et al., 1995). Although Ryberg et al. found differences in the dowstream signalling between the full-length and the splicing variants (Ryberg et al., 2005), no significant differences in signalling were found in a later study when a variety of cannabinoid ligands were investigated (Xiao et al., 2008). Nevertheless, both studies agreed that the N-terminal splice variants were not impacting the ligand-receptor binding process of synthetic cannabinoids, as no significant changes in affinity of compounds were found in both studies.

In the work presented here, we designed and used a truncated CB1 variant only for the ligand binding studies, whereas a full-lenght CB1 was used for the rest of assays, including miniG coupling, β-arrestin 2 recruitment and internalization. The truncation of CB1 was a requirement for the detection of a TR-FRET signal,

and thus, the only option for developing a fluorescence-based assay using HTRF. Although when the study was being conducted no fluorescence HTRF assay had been described for CB1 receptors, the group led by Franco recently published a work showing ligand binding detection in the human CB1 (Raïch et al., 2021). In their study, they use a novel fluorescent compound named CELT-335, but no data about the molecule has been published yet. This will help us to confirm if the rationale about the CB1 truncation developed in this work was correct or not when we assumed the long N-terminal was the limiting factor to obtain a distance small enough to let RET occur between the donor and the acceptor.

It is worth mentioning, that as it has been highlighted before, the kinetic features of the tracer binding to the receptor constitutes one of the main limitations in the successful determination of kinetic parameters of cold compounds using the Motulsky and Mahan approach (Georgi et al., 2019; Sykes et al., 2019). Therefore, even if the measurement of the binding of fluorescent molecule was possible in the mentioned work for equilibrium competition studies (Raïch et al., 2021), it will be still important to determine if the kinetic features of the novel CELT 335 would allow the development of a homogeneous kinetic assay using the full-length receptor.

Integration time in TR-FRET experiments

The fluorescent probe of choice for the binding studies carried out in this work was D77, which contains the NBD (Nitrobenzoxadiazole) fluorophore. As we present in the results, the specific signal obtained in the range of 100-700 μs integration time showed minimal variation for the NBD based probe. Nevertheless, we want to highlight that this parameter is crucial when working with FRET technique and needs to be carefully studied in order to get good quality data (Sykes et al., 2021). Signal detection with other fluorophores used for TR-FRET can be greatly influenced by the time window chosen for signal integration.
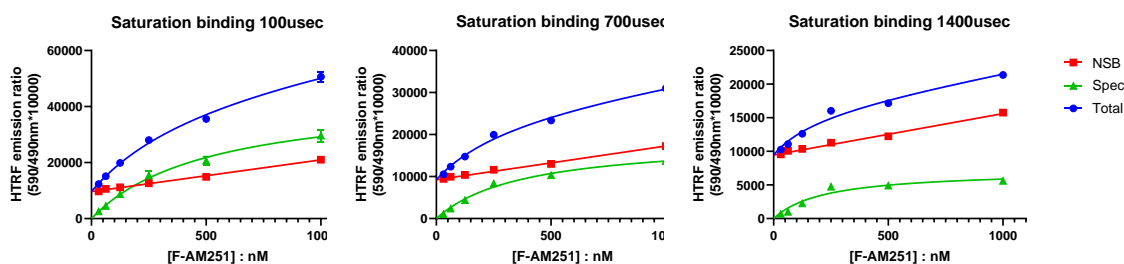
Figure 41. *Saturation binding curve showing total, nonspecific and specific binding of TAMRA labelled ligand binding to CB1 receptor.*
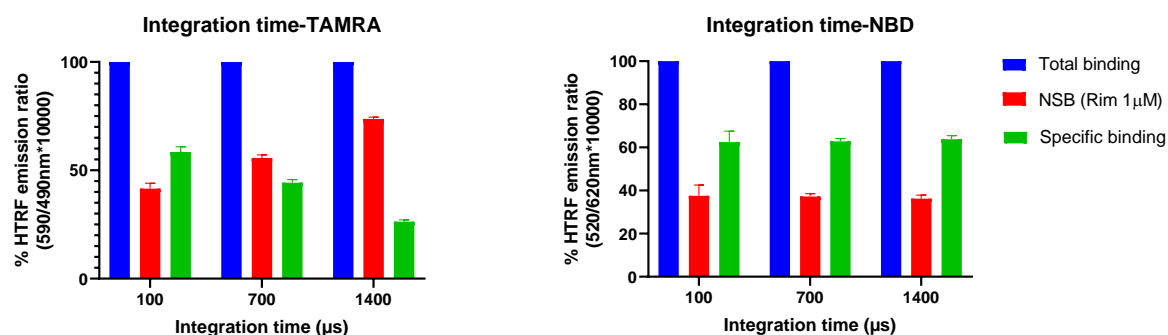
Figure 42. *Nonspecific (NSB) and Specific binding shown as percentages of total binding applying different integration time of the signal for NBD and TAMRA labelled fluorescent ligands.*

As an example, in Figure 41 we show the saturation plots obtained with a different fluorophore (TAMRA) to the one used in this study. In this particular case, the nonspecific signal obtained is greatly influenced by the integration time of the signal, thus becoming an important parameter for good quality signal detection. The more rapid decay after excitation of some fluorophores such as TAMRA highly influences the specificity of the signal acquired, and longer integration times significantly increases the nonspecific signal collection. It is shown in Figure 42 how the integration time affects NBD and TAMRA-based probes differently, strongly affecting the specific signal percentage only in TAMRA's case. The effect of the integration time parameter will strongly depend on the emission profile that each individual fluorophore displays, and therefore should be individually studied to optimise the TR-FRET assay performance (Sykes et al., 2021).

DETERMINATION OF KINETIC PARAMETERS OF CANNABINOID LIGANDS USING THE MOTULSKY AND MAHAN APPROACH.

In this work, we present a novel homogeneous TR-FRET competition association binding assay generated using D77, a nitrobenzoxadiazole (NBD)- labelled cannabinoid ligand to characterize CB1 and CB2 ligand kinetic parameters (association-rate-k_{on} and dissociation-rate-k_{off}) using the mathematical model of drug-receptor competition proposed by Motulsky and Mahan (Motulsky & Mahan, 1984).

We selected seven different cannabinoid compounds, the CB1 selective antagonist rimonabant, the CB2 selective antagonist SR144528, the two endocannabinoid ligands 2-arachidonoyl glycerol (2-AG) and anandamide (AEA), and the agonists HU-210, CP-55,940 and HU-308 and successfully derived their kinetic parameters using a novel fluorescent-based approach using a tracer based on THC named D77, under physiological conditions of temperature and sodium ion concentration. This assay constitutes a simple method to perform high-throughput *in vitro* screening of cannabinoid compounds to assess their ligand kinetics, and to explore the basis of selectivity between the two main cannabinoid GPCRs using the same probe.

The mathematical model presented by Motulsky and Mahan was developed based on previous works (Arányi, 1980; F. J. Ehlert et al., 1981; Weiland & Molinoff, 1981) that studied the ligand competition on receptors and how the apparent association rates of the tracer ligand were affected in the presence of competing molecules.

Although traditionally radioligands have been used to study ligand-receptor interactions and calculate pharmacological parameters, fluorescent based assays are becoming the new gold standard, and their use is hugely expanding over the last years. Even if both techniques are useful to determine the ligand-binding process at receptors as GPCRs, it is worth mentioning some issues that may arise when using fluorescent TR-FRET techniques. Compared to the classical radioligands, this methodology shows many advantages that make the

pharmacological research faster and extensible to high-throughput approaches that could be implemented in big screening processes in early drug discovery process. Also, they significantly lessen the risk associated when using radioactive material, and specially in kinetic studies, and they lead to further advantages as no separation process is necessary to get the binding measurement. Nevertheless, it is worth mentioning that attention should be paid to other issues such as ligand depletion, especially when using ligands with very high affinity (pM), where the free concentration can suffer a significant decrease during the binding process and prevent the correct application of the pharmacological binding models routinely used to quantify kinetic and equilibrium parameters. While in radioligand assays the ligand bound can be easily quantified, simply by detecting the radioligand that remains associated with the membrane after the binding reaction has been stopped, and comparing to the initial radioactivity values (which dictate the amount of radioligand added), such a determination cannot be achieved so easily using HTRF. This need to be taken into consideration when designing experiments and minimum membrane amounts and high tracer concentrations should be employed in order to avoid situations where the free ligand concentration is considerably changing during course of the assay. In our case, the tracer concentrations used are relatively high (600 nM and 900 nM for CB1 and CB2 kinetics assays respectively), thus ligand depletion should not be considered a problem.

Due to the low throughput of the traditional methods used to determine the association and dissociation rates, a dual-point competition association method has been previously used to characterise the kinetics of cannabinoid compounds at CB1 to improve the throughput of the assays. In this approach, the binding of a radioligand is measured in the presence or absence of the competing ligand, and two time points are measured. This method is based on the overshoot profile that slow-off compounds show when competing with a faster k_{off} compound. In this way, a KRI ("kinetic rate index") is obtained, which reflects the faster k_{off} (KRI <1) or slower k_{off} (KRI >1) compared to the kinetics of the used tracer (Guo et al., 2013). Nevertheless, this approach only gives semi-quantitative information about the kinetic profile of ligands and does not allow the precise estimation of k_{on}

and k$_{off}$. Moreover, early time points are not measured using this approach, which can be a problem for ranking slow dissociating compounds (Georgi et al., 2019).

D77 as the tracer of choice

As Sykes et al. extensively studied, the tracer kinetic characteristics play a decisive role in successfully predicting the kinetic parameters using the Motulsky and Mahan competitive binding approach, especially for low affinity and fast dissociating compounds. In their study, they predicted the reliability and accuracy of the kinetic assessment outcomes for a wide variety of scenarios using Monte Carlo simulations (Sykes et al., 2019), which were also validated including experimental TR-FRET data from D2 receptor binding using two distinct tracers. They concluded that tracers with a fast-dissociating profile (k_{off}=1-10 min^{-1}) would predict the kinetics of fast dissociating compounds accurately when applying the competitive association binding model proposed by Motulsky and Mahan (1984), while slower dissociating tracers would lead to less reliable data. The endogenous 2-AG and anandamide are the primary endogenous compounds mediating and regulating the endocannabinoid system, and their low affinity present a difficulty in characterising their kinetic properties due to the limitations that the tracer supposes in their estimation.

The availability of fluorescent compounds that are marketed nowadays is limited and often the classical parameter affinity is used to pharmacologically describe these tracer molecules. Nevertheless, it is important to note that in order to develop a useful and homogeneous assay capable of estimating the kinetic parameters of our non-labelled compounds, the critical parameters that will dictate the success of competitive experiments will be the association and dissociation rate of the tracer (Bosma, et al., 2019; Georgi et al., 2019; Sykes et al., 2019).

Kinetic characterization of cannabinoid compounds

In this work, we present the kinetic characterization of different fluorescently labelled cannabinoid compounds in human CB1 and CB2 receptors and their kinetic features in order to select the most appropriate to develop a novel homogeneous assay to study the kinetic characteristics of cannabinoid binding compounds using the Motulsky and Mahan approach. The D77 compound was

the tracer of choice due to the ideal kinetic profile that it showed when studying its binding to the cannabinoid receptors. Of note, our interest focuses in developing an assay capable of studying the kinetic parameters of cannabinoid compounds in conditions as relatable as possible to a physiological scenario. This has been an additional complication in our study, as physiological temperatures makes the association phase faster, complicating sometimes the measurements of the association phase before the binding reaches equilibrium. Nevertheless, we believe it is important to obtain data at physiological temperature and sodium ion concentration as this will enable a more realistic use of models where the ligand kinetic parameters play and important role as, for instance, rebinding processes in synaptic clefts (Sykes et al., 2017).

Furthermore, we determined the kinetic parameters at both 25°C (see Appendix A) and 37°C and important differences were found in the residence time of the compounds tested at CB1 and CB2, where HU-210, for example, displayed a difference in residence time of 30 min at CB2 between the two temperatures, being the residence time much longer at lower temperatures, as it can be expected from higher affinity values due to more slow association and dissociation processes.

To the best of our knowledge, only some antagonist kinetic profile has been determined to date for their CB1 binding (Xia et al., 2017, 2018). These studies conducted k_{on} and k_{off} parameter determination for rimonabant and other antagonists using competition association binding assays with [3H] CP55940 as a tracer. Nevertheless, they reported a residence time of 114 min for the radioligand tracer, which would result in limited accuracy of especially fast k_{off} compounds as it has been previously observed (Herenbrink et al., 2016; Sykes et al., 2019). However, all the compounds reported in Xia et al. (2017, 2018) had relatively slow dissociation profile.

Additionally, the CB2 ligand receptor kinetics has not been extensively studied either. As far as we can tell, only Heitman's lab developed a suitable radioligand specific for CB2, named [3H]-RO6957022 (Martella et al., 2017) and reported the kinetic constant of several ligands at CB2, including five that were also characterized in this work. The binding of their new radioligand shows high selectivity for CB2 receptor and an improved kinetic profile compared to

[^{3}H]-CP 55940. Moreover, it shows less nonspecific binding due to decreased lipophilicity.

The results showed in Martella et al. (2017) were similar to the ones reported in this study. They reported similar residence times at CB2 receptor (CP 55,940: 5 min; HU-308: 4.2 min; SR 144,528: 8.7 min; AEA: 1.4 min; 2-AG: 0.31 min) to the ones reported in this study (CP 55,940: 3.2 min; HU-308: 2.7 min; SR 144,528: 6.3 min; AEA: 0.8 min; 2-AG: 0.5 min). All the reported residence time values in this study were slightly shorter, except for the endocannabinoid 2-AG. Moreover, the kinetic K_d values reported in their study (Martella et al.: CP 55,940: 0.9 nM; HU-308: 21 nM; SR 144,528: 4.1 nM; AEA: 305 nM; 2-AG: 99 nM) were also similar to the ones in this work (CP 55,940: 2.8 nM; HU-308: 18 nM; SR 144,528: 1.9 nM; AEA: 872 nM; 2-AG: 446 nM). The endocannabinoid 2-AG was the compound with greater differences in affinity between both studies. Nevertheless, both studies were carried out under different conditions that can influence the kinetic parameter estimation. Martella et al. used a Tris HCl buffer and conducted their assay in the absence of GTP analogues. In our study, we used a HBSS based buffer and included GppNHp to ensure the absence of G-protein pre-coupled receptors. Moreover, Martella et al. used phenylmethylsulfonyl fluoride to prevent endocannabinoid degradation, which could explain the lower affinity we reported for 2-AG and AEA compared to their study.

Although Martella et al. showed a general good correlation of kinetically derived pK_d and pK_i (from displacement equilibrium binding studies), the pKi data they reported are lacking the pKi values of the two endocannabinoid compounds. Given the slower kinetic profile of their tracer (k_{off} 0.16 min-1) and the importance of getting early time points for low affinity fast-off compounds (Sykes et al., 2019), it is possible that kinetic data for those compounds did not yield accurate estimates given the necessary filtration step that prevents the measurements of very early time points. Furthermore, our kinetically derived pK_d and equilibrium displacement affinity data shows a very good correlation (25 °C AEA pK_d 6.06, pKi 6.03; 2-AG pK_d 6.3, pKi 6.23) corroborating the good impact of a fast k_{off} tracer and early time point measurement for the correct fit of kinetic parameters of low affinity compounds (Sykes et al., 2019).

The affinity data derived from kinetic parameters show a very good correlation with the equilibrium displacement data ($K_{d(kin)}$ vs pKi CB1 r= 0.96 P=0.0004 and CB2 r=0.98 P<0.0001). Nevertheless, rimonabant and HU-210 compounds showed a noticeable difference between kinetically derived K_d and pKi at CB1 (see Figure 30), which are the slowest dissociating compounds from CB1. In this case, a slower k_{off} of the tracer (k_{off} D77 CB1: 1.9 min^{-1}) would be desirable, as it has shown to estimate slow k_{off} compound rates more accurately for slower dissociating compounds (Georgi et al., 2019).

Kinetic parameters and equilibrium affinity

We explored the correlation between the association and dissociation rate values and affinity parameters for the cannabinoid compounds binding to CB1 and CB2 receptors. Interestingly, a strong correlation was found between k_{on} and affinity for compounds acting at CB1, suggesting that the association is the main parameter determining the affinity of compounds binding to CB1. The k_{on} values for CB1 binding showed a difference of three orders of magnitude from the slowest associating compound to the most rapid. This observation contrasts with the general assumption that association for binary complex formation is diffusion limited (Tummino & Copeland, 2008).

For compounds binding to CB2, both k_{on} and k_{off} parameters correlated with affinity. However, in contrast to what was observed for CB1, a stronger correlation was found for dissociation constant rate parameters, suggesting that k_{off} is in this case, the main parameter dictating affinity of compounds binding to CB2.

BIAS DETERMINATION AT CB1 and CB2 receptors

Biased signalling analysis was carried out using the Operational Model of agonism (OMA) developed by Black and Leff (1983). The Operational model allows to rank the agonists based on their efficacy and it has been extensively used for describing and quantifying agonism during the last decades. In this work, we compared the efficacy of cannabinoid agonist compounds for miniGsi coupling, β-arrestin 2 recruitment, and internalization at the two cannabinoid receptors CB1 and CB2. Other studies that have assessed bias used downstream readouts, such as phosphorilation of ERK (pERK) or inhibition of forskolin-dependent cAMP

production. Nevertheless, mGsi and β-arrestins directly interact with the receptor and reveal information that could be more useful for understanding the mechanistic implications of receptor-signal activation. Moreover, different effectors can simultaneosly impact in pERK and cAMP production, therefore the interpretation on how the receptor interacts with direct effectors can be confusing.

The operational model proposed by Black and Leff introduced the parameter τ, which describes "operational efficacy" or the strength that an agonist displays to produce a certain response. Since the efficacy is a relative term and will be dependent on the system we are working on, a reference compound is always used to quantify bias in a relative manner, in order to eliminate what is called "system bias". Ideally, the reference compound should be a "balanced compound", displaying similar potencies across the studied pathways and a full agonist exerting the maximal effect possible in the system (E_{max}) (Kolb et al., 2021).

β-arrestin 2 recruitment

We performed β-arrestin 2 recruitment assays to CB1 and CB2 receptors upon ligand stimulation using a BRET based methodology. Like most GPCRs, CB1 and CB2 receptors recruits arrestins upon activation. Cannabinoid receptors activate β-arrestin 2 which leads to the desensitization and internalization of the receptor (Daigle et al., 2008; Gyombolai et al., 2013; Kouznetsova et al., 2002). Although their interaction with arrestin is relatively weak comparing with other GPCRs, β-arrestin 2 has shown greater affinity for binding the CB1 receptor (Gyombolai et al., 2013) than β-arrestin 1.

Accordingly to other studies, we measured that 2-AG produce a high level of arrestin recruitment upon CB1 binding comparing to CP 55,940 and AEA (Ibsen et al., 2019), although with low potency (Gyombolai et al., 2013). Our 2-AG estimulated β-arrestin recruitment also shows discrepancies with Soethoudt et al. (2017), because the maximal effect they reported was significantly lower than the one elicited by CP 55,940, whereas we reported 212 % using CP 55,940 maximal response as reference (100 %). Nevertheless, they maximal concentration they assayed was 10 μM whereas we reached 30 μM due to the low potency that 2-AG displays at cannabinoid receptors.

For agonists acting at CB2, our data was in line with the efficacies and potency values reported in previous studies for CP 55,940, AEA, 2-AG and HU-308 (Ibsen et al., 2019; Soethoudt et al., 2017). In our study, CP 55,940, 2-AG and HU-308 acted as full agonists for β-arrestin 2 recruitment whereas HU-210 and AEA acted as partial agonists, with an Emax of 74 % and 44 % relative to CP (100 %).

In contrast with the study carried out by Soethoudt et al. (2017), we did not observe constitutive arrestin recruitment that could be reversed by inverse agonists in either CB1 or CB2 receptors.

mGsi coupling studies

We effectively measured the agonist-induced mGsi (mini Gs/i) coupling to CB1 and CB2 receptors using a BRET based methodology. For this aim, mGsi proteins are used as conformation-specific biosensors that bind the receptor in its active conformation state for coupling heterotrimeric $G\alpha_{i/o}$ proteins (Nehmea et al., 2017; Oberhauser & Stoeber, 2022).

The first mini-G protein was developed by the Tate's group (Carpenter & Tate, 2016) for stabilising receptors binding to adenylate cyclase stimulating G protein $G\alpha_s$. The initial aim of mini-G proteins was to facilitate the structural determination of GPCRs in their active conformation using X-ray crystallography, developing a soluble small protein that would bind the GPCRs in the absence of βγ subunits. The rationale behind their design was the observation that GTPase domain of Gαs subunits was responsible of most of the contacts between the β2AR and heterotrimeric Gs (Rasmussen et al., 2011). Therefore, the alpha helical domain was eliminated from the α subunit and a mutation in the C-terminal was introduced in the α 5 helix stabilizing receptor–mini G complexes in the presence of guanine nucleotides, thus preventing their dissociation from the active GPCR. Mutations were also introduced to eliminate the βγ binding surface and to increase their solubility and stability (Carpenter & Tate, 2016).

Mini G proteins mimic the function of nucleotide-empty G protein heterotrimers that display a very short half-life due to rapid dissociation from βγ G protein subunits (Carpenter & Tate, 2016). In this sense, they act as allosteric modulators of G-proteins, inducing an affinity shift comparable to the shift observed with heterotrimeric G proteins (Wan et al., 2018).

The first mini-G construct (mini Gs, 22 kDa) was further modified and different mini-G proteins were created and validated as conformation-specific detectors specifically mimicking the binding from different Gα protein families. This was possible because the mutations and deletions introduced in the first place to generate mGs constructs were carried out in conserved residues among all α subunits (Nehmea et al., 2017). Therefore, mini Gs was further modified by introducing 9 mutations into the α5 helix to switch its specificity to that of Gi1, creating the mGsi chimera used in this study.

Even though the mini-Gsi used in this work was developed with the aim of mimicking αi1, its ability to resemble the coupling of other $α_{i/o}$ members has not been assessed yet. In this sense, even if this construct has shown to exhibit selectivity for G $α_{i/o}$ members, the selectivity among the different α subtypes is still unknown. As a consequence, as different $Gα_{i/o}$ protein members have been described to couple cannabinoid receptors (Michelle Glass & Northup, 1999; Mukhopadhyay & Howlett, 2005) in an agonist-dependant manner, data from mGsi coupling should be carefully interpreted, as mGsi coupling does not necessarily represent the binding to different members of the $Gα_{i/o}$ family.

The mGsi coupling was assessed at CB1 and CB2 receptors at 15 min from ligand stimulation. For CB1, CP 55,940, HU-210 and 2-AG acted as full agonists, whereas anandamide showed partial agonism properties, only reaching ~80% of the maximal activation. For CB2 receptor, only CP 55,940 showed full agonism properties, whereas HU-210 and HU-308 and the two endocannabinoids acted as partial agonists. Of note, the coupling elicited by the endocannabinoids 2-AG and AEA was weak, coupling only 30 % and 65 % of the maximal coupling induced by CP 55,940 respectively.

Internalization of cannabinoid receptors

We studied the agonist induced internalization of CB1 and CB2 cannabinoid receptors using a method based on DERET (Diffusion Enhanced Resonance Energy Transfer) used previously to study the internalization of other GPCRs (Buenaventura et al., 2018; Roed et al., 2014). While other methods relied on preparation of samples at different time points (Grimsey et al., 2008; Hislop & von Zastrow, 2011), involving several steps for receptor labelling (either with

antibodies or biotinylating them) followed by several sample manipulation steps before signal acquisition (fixation of cells for microscopy with several washing step or cell lysate preparations for subsequent detection of biotinylated receptors), the technique used here allows the dynamic quantification of internalisation over time from a single sample. In this sense, this method constitutes a sensitive and reliable method for studying receptor internalization.

We monitored the internalization during 1 h after ligand addition and the curves obtained suggested that internalization was still occurring. Nevertheless, we studied the dose-response curves at 15 min from ligand addition, in order to maintain the same criteria for all the studied responses and assess the functional selectivity using the same time point readout in all the cases, following the recently published recommendations regarding bias assessment (Kolb et al., 2021).

Bias of cannabinoid agonists acting at CB1 and CB2 receptors

In our study, 2-AG and CP 55,940 were used as reference agonists for quantifying biased signalling at CB1 and CB2 respectively. 2-AG was the compound causing maximal effect at CB1 in the studied pathways, although it showed lower potency in arrestin recruitment at CB1 (pEC_{50}: 4.8) comparing to mGsi and Internalization assays (pEC_{50}: ~5.6). Previous bias studies at CB1 has also reported their values using 2-AG as a reference compound (Khajehali et al., 2015; Zhu et al., 2020) as a perfectly balanced compound is not always feasible. In the case of CB2 receptor, the reference compound selected, CP 55940 acted as full agonist in the three studied responses with similar potency values.

The bias was assessed by comparing the transduction coefficients ($\log (\tau/KA)$) calculated for each ligand relative to a reference compound for each of the responses studied at a specific time point (15 min). Our results reported that all of the studied agonists showed preference for activating some of the responses, confirming the biased that has previously been described for agonists acting at the cannabinoid receptors CB1 (Khajehali et al., 2015; Laprairie et al., 2014) and CB2 (Shoemaker et al., 2005; Soethoudt et al., 2017) in different systems. Nevertheless, the results of the bias analysis carried out in this study cannot be directly compared to previous reported data, as different pathways have been

analysed in other studies, usually reporting downstream signals as inhibition of forskolin induced cAMP production or stimulated ERK phosphorylation.

Our results report no preference for the agonist studied between mGsi coupling and β-arrestin 2 recruitment either at CB1 or CB2 receptors. In contrast, a preference for mGsi over internalization was estimated for HU-210, CP 55,940 and AEA relative to 2-AG at CB1, and also a preference for β-arrestin 2 over internalization for HU-210 and CP 55,940. Nevertheless, it should be noted that the analysis was carried out using 2-AG as the reference compound, which shows a lower potency on β-arrestin 2 assay, which can impact on the results reported.

When studying the bias at CB2 receptor, we observed that all the agonists displaying significance in the bias calculation showed preference to internalize the receptor over β-arrestin 2 recruitment (2-AG and HU-308) or mGsi recruitment (2-AG, HU-210 and AEA) relative to the reference agonist CP 55,940.

Exploring residence time implications in efficacy

Increasing interest concerning the kinetic aspects around GPCRs has emerged during the last years, including different contexts. As we have previously mentioned in the introduction, many studies support the idea that ligand-binding kinetics can have a direct impact on the clinical performance of drug action, leading to a sustained action due long-term receptor occupancy for some long-residence time drugs or, in other cases such as antipsychotics, a diminution of adverse effects has been attributed to fast dissociating compounds.

Furthermore, it has also been hypothesized that the kinetic features of ligand-receptor binding could have a direct implication on the effectiveness on a molecular level, by differentially changing the energy landscape and therefore stabilising conformations that would lead to the activation of certain pathways (Herenbrink et al., 2016).

In this work, we explore if the ligand-receptor complex duration, represented by the residence time concept, will play a decisive role in the efficacy that the ligands display for activating different signalling pathways at CB1 and CB2 receptors. We could not stablish a relationship between the residence time and the effectiveness that those ligands displayed in the studied signalling assays. Nevertheless, it has

been described how residence time of agonists is directly correlated with the effectiveness in other GPCRs. For example, Sykes at al. (2009) showed how the responses of seven muscarinic agonists acting at M3 muscarinic receptors at calcium release and [35S]-GTPγS assays were correlated with the residence time those ligands displayed (Sykes et al., 2009). In particular, they showed that short residence time agonists were less effective in producing the responses, whereas agonists displaying longer residence times displayed a stronger response in those assays, showing a very good correlation between k_{off} and intrinsic activity or tau values for the mentioned responses. In another study where ten adenosine agonists acting at A2A receptors were studied, the residence times were also correlated with the intrinsic efficacies of those ligands at cAMP production and impedance assays (Guo et al., 2014). Interestingly, the receptor-ligand complex duration was proposed to be important for explaining the loss of activity of the partial agonist clonidine at α2A adrenergic receptors located at noradrenergic terminals (autoreceptors) on noradrenaline release experiments using tritiated noradrenaline (Hoeren et al., 2008). In this case, the loss of efficacy of clonidine at lower temperatures was proposed to be due to a short ligand-receptor complex duration in comparison with the full agonists UK 14,304, insufficient to elicit an activation of the receptor. The study of Hoeren et al. (2008) also points out the differential changes that temperature elicits in k_{on} and k_{off} depending on the agonist. In particular, a reduction in affinity was observed with lower temperatures for clonidine, because the k_{off} reduction (57 %) could not compensate for the association rate reduction (74 %) at lower temperatures, whereas the reduction of both parameters in a similar way lead to similar affinity values for the full agonist UK 14,304 (Hoeren et al., 2008).

Hoeren at al. (2008) proposed the "activation interval" as a possible explanation for the differences in efficacy of the tested agonists. They proposed that ligands with shorter residence times that the "activation interval" would lead to short receptor-ligand complex stabilisation times, insufficient for the activation, and thus will be less efficacious in activating a certain response.

It should be noted that the aforementioned studies where a correlation was observed between efficacies and residence times often use readouts from

downstream processes, and not direct effector engagement as we performed here with the mGsi assay or arrestin recruitment assay.

The GPCR-G protein interaction has been described to be a rapid process (~40 ms)(Lohse et al., 2008), as well as arrestin-GPCR interaction (Nuber et al., 2016) that will not exceed the residence times of our cannabinoid compounds. Nevertheless, the intracellular signalling cascade map is still incomplete, and the active receptor-ligand complex duration may be a limiting step affecting and dictating the rates of other events yet unexplored in the downstream signalling of cannabinoid receptors, where the contact length with the active receptor conformation may be defining the signalling through those effectors.

It is worth mentioning, that even similar conditions were used to assess the kinetic parameters and the response in the signalling assays, we used GppNHp in order to eliminate the G-protein pre-coupled population of CB1 and CB2 receptors. The presence of different population of GPCRs (coupled and uncoupled to G-proteins) could lead to difficulties in interpreting the data from the binding assays. In this sense, the kinetic parameters were assessed in a low-affinity CB1 and CB2 population. However, it is plausible that different type of receptor conformations coexists in the cellular systems where we carried out the signalling assays, and different kinetic on and off rates are operating due to diverse receptor conformation.

The agonist we tested in this work for CB1 and CB2 receptors show preference for some signalling pathways over other, although none of them showed strong bias as it has been described for other agonists. Additionally, all the displayed preferences were towards the same signalling pathways. Probably, this homogeneity is due to the low number of agonists that comprised this work. However, it would be interesting to further explore if the receptor-ligand complex duration can influence the bias fingerprint of cannabinoid compounds exploring the kinetic parameters that distinct agonists display. In particular, the ligand-receptor complex duration may be a parameter influencing the conformational landscape, thereby favouring the stabilization of certain conformations over others. In that case, the residence time would influence the preferential engagement to some effectors over others, by changing the frequency distribution of the different active conformations.

5.CONCLUSIONS

Based on the experimental results obtained in the present PhD Thesis, the following conclusions were drawn:

1. We generated a novel homogeneous TR-FRET assay capable of determining the kinetic parameters of cannabinoid ligands binding to the main two GPCRs in the cannabinoid system, CB1 and CB2, under physiological conditions.

    1.1. The novel fluorescent ligand D77 shows ideal kinetic profile for its use as a tracer in Motulsky and Mahan competition model for both CB1 and CB2 receptors, showing a moderate affinity and a rapid dissociation profile.

    1.2. The assay generated constitutes the first fluorescent-based high throughput HTRF methodology for the determination of kinetic parameters of cannabinoid compounds, which could be implemented in large-scale kinetic characterisation.

    1.3. In order to obtain a FRET signal for the binding to human CB1 receptor, a truncated version -$CB1_{91-472}$- where the first 90 amino acids were deleted was used.

2. We successfully characterised the kinetic association and dissociation constant rates (k_{on} and k_{off}) of a set of seven cannabinoid compounds at CB1 and CB2 receptors, including the low affinity endocannabinoids 2-AG and anandamide.

    2.1. The kinetically derived affinity values strongly correlated with the K_i values obtained by equilibrium competition experiments, which is indicative of the good performance of the Motulsky and Mahan kinetic assay.

    2.2. The methodology developed allowed the kinetic characterization at physiological temperature (37 °C). In this way, the obtained kinetic parameters can be correlated to the different responses analysed in cells that are generally measured at 37 °C.

    2.3. At CB1 receptor, the association rate constant k_{on} appears to be the principal parameter dictating the affinity, whereas both k_{on} and k_{off} are correlated with the affinity at CB2 receptors for our set of compounds.

3. We characterized the responses elicited by the agonist compounds in terms of β-arrestin 2 recruitment, mGsi coupling, and internalization and applied the operational model to assess the bias. We observed that cannabinoid responses upon binding at CB1 and CB2 receptors can be biased, although none of the studied compounds exhibited strong selectivity in preferentially activating a pathway.

3.1. The potency rank order of the agonists tested for the β-arrestin 2 recruitment and mGsi coupling at CB1 receptors was as follows: HU-210≈CP55,940 > anandamide > 2-AG. At CB2, the potency rank order was HU-210≈CP 55,940 > HU 308 >anandamide> 2-AG.

3.2. The potency rank order for the agonist inducing internalization at CB1 receptors was as follows HU-210≈CP 55,940 > anandamide> 2-AG. At CB2, the potency rank order was HU-210≈CP 55,940 > HU 308 >anandamide≈2-AG.

3.3. Although the compounds showed very similar potency ranks in the three responses we measured, the maximal efficacy of the compounds changed over the pathways. At CB1, CP 55,940 and HU-210 only acted as full agonists in mGsi coupling, whereas 2-AG exerted the maximal effect for β -arrestin 2 binding and internalization. At CB2, CP 55,940 acted as a full agonist in all the cases, whereas 2-AG also showed full agonist behaviour in β -arrestin 2 recruitment.

4. After examining the compounds selected for this study, we cannot affirm that ligand binding kinetics or residence time has a direct influence on the efficacy (τ) exerted upon CB1 and CB2 receptor activation.

4.1. Log τ values correlated poorly with the residence time of the compounds, with R^2 values for β -arrestin 2 recruitment, mGsi coupling and internalization of 0.31, 0.38, and 0.45 at CB1 receptor and 0.11, 0.02 and 0.09 at CB2 receptor.

4.2. Nevertheless, the number of cannabinoid agonist compounds used in this work is limited, therefore, future studies using a broader number of agonists will allow to further explore the role of kinetics in efficacy at cannabinoid receptors.

REFERENCES

Andersson, H., D'Antona, A. M., Kendall, D. A., Von Heijne, G., & Chin, C. N. (2003). Membrane assembly of the cannabinoid receptor 1: Impact of a long N-terminal tail. *Molecular Pharmacology*, *64*(3), 570–577. https://doi.org/10.1124/mol.64.3.570

Arányi, P. (1980). Kinetics of the hormone-receptor interaction competition experiments with slowly equilibrating ligands. *Biochimica et Biophysica Acta*, *628*, 220–227.

Baggelaar, M. P., Maccarrone, M., & van der Stelt, M. (2018). 2-Arachidonoylglycerol: A signaling lipid with manifold actions in the brain. *Progress in Lipid Research*, *71*(November 2017), 1–17. https://doi.org/10.1016/j.plipres.2018.05.002

Bazarsuren, A., Grauschopf, U., Wozny, M., Reusch, D., Hoffmann, E., Schaefer, W., Panzner, S., & Rudolph, R. (2002). In vitro folding, functional characterization, and disulfide pattern of the extracellular domain of human GLP-1 receptor. *Biophysical Chemistry*, *96*(2–3), 305–318. https://doi.org/10.1016/S0301-4622(02)00023-6

Benito, C., Núñez, E., Tolón, R. M., Carrier, E. J., Rábano, A., Hillard, C. J., & Romero, J. (2003). Cannabinoid CB2 Receptors and Fatty Acid Amide Hydrolase Are Selectively Overexpressed in Neuritic Plaque-Associated Glia in Alzheimer's Disease Brains. *Journal of Neuroscience*, *23*(35), 11136–11141. https://doi.org/10.1523/jneurosci.23-35-11136.2003

Bisogno, T., Howell, F., Williams, G., Minassi, A., Cascio, M. G., Ligresti, A., Matias, I., Schiano-Moriello, A., Paul, P., Williams, E. J., Gangadbaran, U., Hobbs, C., Di Marzo, V., & Doherty, P. (2003). Cloning of the first sn1-DAG lipases points to the spatial and temporal regulation of endocannabinoid signaling in the brain. *Journal of Cell Biology*, *163*(3), 463–468. https://doi.org/10.1083/jcb.200305129

Black, J. W., & Leff, P. (1983). Operational models of pharmacological agonism. *Proceedings of the Royal Society of London. Series B, Biological Sciences*,

220(1219), 141–162. https://doi.org/10.1098/rspb.1983.0093

Blázquez, C., Chiarlone, A., Bellocchio, L., Resel, E., Pruunsild, P., García-Rincón, D., Sendtner, M., Timmusk, T., Lutz, B., Galve-Roperh, I., & Guzmán, M. (2015). The CB1 cannabinoid receptor signals striatal neuroprotection via a PI3K/Akt/mTORC1/BDNF pathway. *Cell Death and Differentiation*, *22*(10), 1618–1629. https://doi.org/10.1038/cdd.2015.11

Blázquez, Cristina, Chiarlone, A., Sagredo, O., Aguado, T., Pazos, M. R., Resel, E., Palazuelos, J., Julien, B., Salazar, M., Börner, C., Benito, C., Carrasco, C., Diez-Zaera, M., Paoletti, P., Díaz-Hernández, M., Ruiz, C., Sendtner, M., Lucas, J. J., De Yébenes, J. G., … Guzmán, M. (2011). Loss of striatal type 1 cannabinoid receptors is a key pathogenic factor in Huntington's disease. *Brain*, *134*(1), 119–136. https://doi.org/10.1093/brain/awq278

Bocquet, N., Kohler, J., Hug, M. N., Kusznir, E. A., Rufer, A. C., Dawson, R. J., Hennig, M., Ruf, A., Huber, W., & Huber, S. (2015). Real-time monitoring of binding events on a thermostabilized human A2A receptor embedded in a lipid bilayer by surface plasmon resonance. *Biochimica et Biophysica Acta - Biomembranes*, *1848*(5), 1224–1233. https://doi.org/10.1016/j.bbamem.2015.02.014

Bohn, L. M., Lefkowitz, R. J., Gainetdinov, R. R., Peppel, K., Caron, M. G., & Lin, F. T. (1999). Enhanced morphine analgesia in mice lacking β-arrestin 2. *Science*, *286*(5449), 2495–2498. https://doi.org/10.1126/science.286.5449.2495

Bosma, R., Stoddart, L. A., Georgi, V., Bouzo-Lorenzo, M., Bushby, N., Inkoom, L., Waring, M. J., Briddon, S. J., Vischer, H. F., Sheppard, R. J., Fernández-Montalván, A., Hill, S. J., & Leurs, R. (2019). Probe dependency in the determination of ligand binding kinetics at a prototypical G protein-coupled receptor. *Scientific Reports*, *9*(1), 1–13. https://doi.org/10.1038/s41598-019-44025-5

Bosma, R., Wang, Z., Kooistra, A. J., Bushby, N., Kuhne, S., Van Den Bor, J., Waring, M. J., De Graaf, C., De Esch, I. J., Vischer, H. F., Sheppard, R. J., Wijtmans, M., & Leurs, R. (2019). Route to prolonged residence time at the

histamine H1 receptor: Growing from desloratadine to rupatadine. *Journal of Medicinal Chemistry*, *62*(14), 6630–6644. https://doi.org/10.1021/acs.jmedchem.9b00447

Buenaventura, T., Kanda, N., Douzenis, P. C., Jones, B., Bloom, S. R., Chabosseau, P., Corrêa, I. R., Bosco, D., Piemonti, L., Marchetti, P., Johnson, P. R., Shapiro, A. M. J., Rutter, G. A., & Tomas, A. (2018). A targeted RNAi screen identifies endocytic trafficking factors that control GLP-1 receptor signaling in pancreatic β-cells. *Diabetes*, *67*(3), 385–399. https://doi.org/10.2337/db17-0639

Carpenter, B., & Tate, C. G. (2016). Engineering a minimal G protein to facilitate crystallisation of G protein-coupled receptors in their active conformation. *Protein Engineering, Design and Selection*, *29*(12), 583–593. https://doi.org/10.1093/protein/gzw049

Casarosa, P, Tautermann, C., Kiechle, T., Pieper, M., & Gantner, F. (2009). *Understanding the Mechanism of Long Duration of Action of Tiotropium: Insight into Its Interaction with the Human M3 Receptor.* A1917. https://doi.org/10.1164/ajrccm-conference.2009.179.1_meetingabstracts.a1917

Casarosa, Paola, Bouyssou, T., Germeyer, S., Schnapp, A., Gantner, F., & Pieper, M. (2009). Preclinical evaluation of long-acting muscarinic antagonists: Comparison of tiotropium and investigational drugs. *Journal of Pharmacology and Experimental Therapeutics*, *330*(2), 660–668. https://doi.org/10.1124/jpet.109.152470

Che, T., Agnihotri, H. D., Shukla, A. K., & Roth, B. L. (2021). Biased ligands at opioid receptors: Current status and future directions. *Science Signaling*, *14*(677), 1–11. https://doi.org/10.1126/scisignal.aav0320

Cheng, Y.-C., & Prusoff, W. H. (1973). Relationship between the inhibition constant (KI) and the concentration of inhibitor which causes 50 per cent inhibition (I50) of an enzymatic reaction. *Biochemical Pharmacology*, *22*(23), 3099–3108. https://doi.org/10.1016/0006-2952(73)90196-2

Chiarlone, A., Bellocchio, L., Blázquez, C., Resel, E., Soria-Gómez, E., Cannich, A.,

Ferrero, J. J., Sagredo, O., Benito, C., Romero, J., Sánchez-Prieto, J., Lutz, B., Fernández-Ruiz, J., Galve-Roperh, I., & Guzmán, M. (2014). A restricted population of CB1 cannabinoid receptors with neuroprotective activity. *Proceedings of the National Academy of Sciences of the United States of America*, *111*(22), 8257–8262. https://doi.org/10.1073/pnas.1400988111

Copeland, R. A., Pompliano, D. L., & Meek, T. D. (2006). Drug-target residence time and its implications for lead optimization. *Nature Reviews Drug Discovery*, *5*(9), 730–739. https://doi.org/10.1038/nrd2082

Cortez, I. L., Rodrigues da Silva, N., Guimarães, F. S., & Gomes, F. V. (2020). Are CB2 Receptors a New Target for Schizophrenia Treatment? In *Frontiers in Psychiatry* (Vol. 11). https://doi.org/10.3389/fpsyt.2020.587154

Cravatt, B. F., Giang, D. K., Mayfield, S. P., Boger, D. L., Lerner, R. A., & Gilula, N. B. (1996). Molecular characterization of an enzyme that degrades neuromodulatory fatty-acid amides. *Nature*, *384*(6604), 83–87. https://doi.org/10.1038/384083a0

Dahl, G., & Akerud, T. (2013). Pharmacokinetics and the drug-target residence time concept. *Drug Discovery Today*, *18*(15–16), 697–707. https://doi.org/10.1016/j.drudis.2013.02.010

Daigle, T. L., Kwok, M. L., & Mackie, K. (2008). Regulation of CB1 cannabinoid receptor internalization by a promiscuous phosphorylation-dependent mechanism. *Journal of Neurochemistry*, *106*(1), 70–82. https://doi.org/10.1111/j.1471-4159.2008.05336.x

Dale, N. C., Johnstone, E. K. M., White, C. W., & Pfleger, K. D. G. (2019). NanoBRET: The bright future of proximity-based assays. *Frontiers in Bioengineering and Biotechnology*, *7*(MAR), 1–13. https://doi.org/10.3389/fbioe.2019.00056

De Petrocellis, L., Nabissi, M., Santoni, G., & Ligresti, A. (2017). Actions and Regulation of Ionotropic Cannabinoid Receptors. In D. Kendall & S. P. H. B. T.-A. in P. Alexander (Eds.), *Cannabinoid Pharmacology* (Vol. 80, pp. 249–289). Academic Press. https://doi.org/https://doi.org/10.1016/bs.apha.2017.04.001

Degorce, F., Card, A., Soh, S., Trinquet, E., Knapik, G. P., & Xie, B. (2009). HTRF: A Technology Tailored for Drug Discovery –A Review of Theoretical Aspects and Recent Applications. *Current Chemical Genomics*, *3*, 22–32.

Denovan-Wright, E. M., & Robertson, H. A. (2000). Cannabinoid receptor messenger RNA levels decrease in a subset of neurons of the lateral striatum, cortex and hippocampus of transgenic Huntington's disease mice. *Neuroscience*, *98*(4), 705–713. https://doi.org/https://doi.org/10.1016/S0306-4522(00)00157-3

Devane, W. A., Dysarz, F. A., Johnson, M. R., Melvin, L. S., & Howlett, A. C. (1988). Determination and characterization of a cannabinoid receptor in rat brain. *Molecular Pharmacology*, *34*(5), 605–613.

Devane, W., Hanus, L., Breuer, A., Pertwee, R., Stevenson, L., Griffin, G., Gibson, D., Mandelbaum, A., & Etinger, A. (1992). Isolation and Structure of a Brain Constituent That Binds to the Cannabinoid Receptor. *Science*, *258*(December), 1946–1949.

Di Marzo, V. (2018). New approaches and challenges to targeting the endocannabinoid system. *Nature Reviews Drug Discovery*, *17*(9), 623–639. https://doi.org/10.1038/nrd.2018.115

Dinh, T. P., Carpenter, D., Leslie, F. M., Freund, T. F., Katona, I., Sensi, S. L., Kathuria, S., & Piomelli, D. (2002). Brain monoglyceride lipase participating in endocannabinoid inactivation. *Proceedings of the National Academy of Sciences of the United States of America*, *99*(16), 10819–10824. https://doi.org/10.1073/pnas.152334899

Dowling, M. R., & Charlton, S. J. (2006). Quantifying the association and dissociation rates of unlabelled antagonists at the muscarinic M 3 receptor. *British Journal of Pharmacology*, *148*(7), 927–937. https://doi.org/10.1038/sj.bjp.0706819

Ehlert, F. J., Roeske, W. R., & Yamamura, H. I. (1981). Mathematical analysis of the kinetics of competitive inhibition in neurotransmitter receptor binding assays. *Molecular Pharmacology*, *19*(3), 367–371.

Ehlert, Frederick J. (2008). On the analysis of ligand-directed signaling at G

protein-coupled receptors. *Naunyn-Schmiedeberg's Archives of Pharmacology*, *377*(4–6), 549–577. https://doi.org/10.1007/s00210-008-0260-4

Fleck, B. A., Hoare, S. R. J., Pick, R. R., Bradbury, M. J., & Grigoriadis, D. E. (2012). Binding kinetics redefine the antagonist pharmacology of the corticotropin-releasing factor type 1 receptor. *Journal of Pharmacology and Experimental Therapeutics*, *341*(2), 518–531. https://doi.org/10.1124/jpet.111.188714

Foord, S. M., Bonner, T. I., Neubig, R. R., Rosser, E. M., Pin, J. P., Davenport, A. P., Spedding, M., & Harmar, A. J. (2005). International Union of Pharmacology. XLVI. G protein-coupled receptor list. *Pharmacological Reviews*, *57*(2), 279–288. https://doi.org/10.1124/pr.57.2.5

Förster, T. (1948). *Zwischenmolekulare Energiewanderung und Fluoreszenz* (pp. 55–75). Annals of Physics.

Förster, T. (2012). Energy migration and fluorescence. *Journal of Biomedical Optics*, *17*(1), 011002. https://doi.org/10.1117/1.jbo.17.1.011002

Fuchs, B., Breithaupt-Grögler, K., Belz, G. G., Roll, S., Malerczyk, C., Herrmann, V., Spahn-Langguth, H., & Mutschler, E. (2000). Comparative Pharmacodynamics and Pharmacokinetics of Candesartan and Losartan in Man. *Journal of Pharmacy and Pharmacology*, *52*(9), 1075–1083. https://doi.org/10.1211/0022357001774994

Galiègue, S., Mary, S., Marchand, J., Dussossoy, D., Carrière, D., Carayon, P., Bouaboula, M., Shire, D., LE Fur, G., & Casellas, P. (1995). Expression of Central and Peripheral Cannabinoid Receptors in Human Immune Tissues and Leukocyte Subpopulations. *European Journal of Biochemistry*, *232*(1), 54–61. https://doi.org/10.1111/j.1432-1033.1995.tb20780.x

Gazzi, T., Brennecke, B., Atz, K., Korn, C., Sykes, D., Sarott, R. C., Westphal, M. V., Pfaff, P., Weise, M., Mostinski, Y., Hoare, B. L., Miljuš, T., Mexi, M., Guba, W., Alker, A., Rufer, A. C., Kusznir, E. A., Huber, S., Raposo, C., … Nazaré, M. (2019). Drug derived fluorescent probes for the specific visualization of cannabinoid type 2 receptor - A toolbox approach. *ChemRxiv*, 1–14.

https://doi.org/10.26434/chemrxiv.10283027

Georgi, V., Dubrovskiy, A., Steigele, S., & Fernández-Montalván, A. E. (2019). Considerations for improved performance of competition association assays analysed with the Motulsky–Mahan's "kinetics of competitive binding" model. *British Journal of Pharmacology*, *176*(24), 4731–4744. https://doi.org/10.1111/bph.14841

Gether, U. (2000). Uncovering molecular mechanisms involved in activation of G protein-coupled receptors. *Endocrine Reviews*, *21*(1), 90–113. https://doi.org/10.1210/edrv.21.1.0390

Gibson, D. G. (2011). Enzymatic assembly of overlapping DNA fragments. *Methods in Enzymology*, *498*(January), 349–361. https://doi.org/10.1016/B978-0-12-385120-8.00015-2

Gillis, A., Gondin, A. B., Kliewer, A., Sanchez, J., Lim, H. D., Alamein, C., Manandhar, P., Santiago, M., Fritzwanker, S., Schmiedel, F., Katte, T. A., Reekie, T., Grimsey, N. L., Kassiou, M., Kellam, B., Krasel, C., Halls, M. L., Connor, M., Lane, J. R., … Canals, M. (2021). Low intrinsic efficacy for G protein activation can explain the improved side effect profiles of new opioid agonists (Science Signaling (2021) DOI: 10.1126/scisignal.aaz3140). *Science Signaling*, *14*(670). https://doi.org/10.1126/scisignal.abf9803

Glass, M, Dragunow, M., & Faull, R. L. (2000). The pattern of neurodegeneration in Huntington's disease: a comparative study of cannabinoid, dopamine, adenosine and GABA(A) receptor alterations in the human basal ganglia in Huntington's disease. *Neuroscience*, *97*(3), 505–519. https://doi.org/10.1016/s0306-4522(00)00008-7

Glass, Michelle, & Northup, J. K. (1999). Agonist selective regulation of G proteins by cannabinoid CB1 and CB2 receptors. *Molecular Pharmacology*, *56*(6), 1362–1369. https://doi.org/10.1124/mol.56.6.1362

Gómez-Gálvez, Y., Palomo-Garo, C., Fernández-Ruiz, J., & García, C. (2016). Potential of the cannabinoid CB2 receptor as a pharmacological target against inflammation in Parkinson's disease. *Progress in Neuro-Psychopharmacology and Biological Psychiatry*, *64*, 200–208.

https://doi.org/10.1016/j.pnpbp.2015.03.017

Gonsiorek, W., Lunn, C., Fan, X., Narula, S., Lundell, D., & Hipkin, R. W. (2000). Endocannabinoid 2-arachidonyl glycerol is a full agonist through human type 2 cannabinoid receptor: Antagonism by anandamide. *Molecular Pharmacology*, *57*(5), 1045–1050.

Grauschopf, U., Lilie, H., Honold, K., Wozny, M., Reusch, D., Esswein, A., Schäfer, W., Rücknagel, K. P., & Rudolph, R. (2000). The N-terminal fragment of human parathyroid hormone receptor 1 constitutes a hormone binding domain and reveals a distinct disulfide pattern. *Biochemistry*, *39*(30), 8878–8887. https://doi.org/10.1021/bi0001426

Grimsey, N. L., Narayan, P. J., Dragunow, M., & Glass, M. (2008). A novel high-throughput assay for the quantitative assessment of receptor trafficking. *Clinical and Experimental Pharmacology and Physiology*, *35*(11), 1377–1382. https://doi.org/10.1111/j.1440-1681.2008.04991.x

Guindon, J., & Hohmann, A. G. (2008). Cannabinoid CB 2 receptors: A therapeutic target for the treatment of inflammatory and neuropathic pain. *British Journal of Pharmacology*, *153*(2), 319–334. https://doi.org/10.1038/sj.bjp.0707531

Guo, D., Hillger, J. M., Ijzerman, A. P., & Heitman, L. H. (2014). Drug-Target Residence Time-A Case for G Protein-Coupled Receptors Ligand-receptor binding kinetics View project Label-free technologies and personalized medicine View project Drug-Target Residence Time-A Case for G Protein-Coupled Receptors. *Med. Res. Rev*, *34*(4), 856–892. https://doi.org/10.1002/med.21307

Guo, D., van Dorp, E. J. H. H., Mulder-Krieger, T., Van Veldhoven, J. P. D. D., Brussee, J., Ijzerman, A. P., & Heitman, L. H. (2013). Dual-point competition association assay: A fast and high-throughput kinetic screening method for assessing ligand-receptor binding kinetics. *Journal of Biomolecular Screening*, *18*(3), 309–320. https://doi.org/10.1177/1087057112464776

Gurevich, V. V., & Gurevich, E. V. (2020). Biased GPCR signaling: possible mechanisms and inherent limitations. *Pharmacology and Therapeutics*,

211. https://doi.org/10.1016/j.pharmthera.2020.107540.Biased

Gyombolai, P., Boros, E., Hunyady, L., & Turu, G. (2013). Differential β-arrestin2 requirements for constitutive and agonist-induced internalization of the CB1 cannabinoid receptor. *Molecular and Cellular Endocrinology, 372*(1–2), 116–127. https://doi.org/10.1016/j.mce.2013.03.013

Hall, M. P., Unch, J., Binkowski, B. F., Valley, M. P., Butler, B. L., Wood, M. G., Otto, P., Zimmerman, K., Vidugiris, G., MacHleidt, T., Robers, M. B., Benink, H. A., Eggers, C. T., Slater, M. R., Meisenheimer, P. L., Klaubert, D. H., Fan, F., Encell, L. P., & Wood, K. V. (2012). Engineered luciferase reporter from a deep sea shrimp utilizing a novel imidazopyrazinone substrate. *ACS Chemical Biology, 7*(11), 1848–1857. https://doi.org/10.1021/cb3002478

Hara, M., Kiyama, R., Nakajima, S., Kawabata, T., Kawakami, M., Ohtani, K., Itazaki, K., Fujishita, T., & Fujimoto, M. (1995). Kinetic studies on the interaction of nonlabeled antagonists with the angiotensin II receptor. *European Journal of Pharmacology, 289*(2), 267–273. https://doi.org/10.1016/0922-4106(95)90103-5

Hawtin, S. R., Wesley, V. J., Simms, J., Argent, C. C. H., Latif, K., & Wheatley, M. (2005). The N-terminal juxtamembrane segment of the V1a vasopressin receptor provides two independent epitopes required for high-affinity agonist binding and signaling. *Molecular Endocrinology, 19*(11), 2871–2881. https://doi.org/10.1210/me.2005-0148

Herenbrink, C. K., Sykes, D. A., Donthamsetti, P., Canals, M., Coudrat, T., Shonberg, J., Scammells, P. J., Capuano, B., Sexton, P. M., Charlton, S. J., Javitch, J. A., Christopoulos, A., & Lane, J. R. (2016). The role of kinetic context in apparent biased agonism at GPCRs. *Nature Communications, 7*, 1–14. https://doi.org/10.1038/ncomms10842

Heydenreich, F. M., Miljuš, T., Jaussi, R., Benoit, R., Milić, D., & Veprintsev, D. B. (2017). High-throughput mutagenesis using a two-fragment PCR approach. *Scientific Reports, 7*(1), 1–11. https://doi.org/10.1038/s41598-017-07010-4

Hinz, B., & Ramer, R. (2022). Cannabinoids as anticancer drugs:current status of

preclinical research. *British Journal of Cancer*.

Hislop, J. N., & von Zastrow, M. (2011). Analysis of GPCR Localization and Trafficking James. *Methods Mol Biol.*, *746*, 425–440. https://doi.org/10.1007/978-1-61779-126-0

Hoeren, M., Brawek, B., Mantovani, M., Löffler, M., Steffens, M., Van Velthoven, V., & Feuerstein, T. J. (2008). Partial agonism at the human α2A-autoreceptor: Role of binding duration. *Naunyn-Schmiedeberg's Archives of Pharmacology*, *378*(1), 17–26. https://doi.org/10.1007/s00210-008-0295-6

Howlett, A. C. (1995). Pharmacology of cannabinoid receptors. *Annual Review of Pharmacology and Toxicology*, *35*, 607–634.

Hua, T., Li, X., Wu, L., Iliopoulos-Tsoutsouvas, C., Wang, Y., Wu, M., Shen, L., Johnston, C. A., Nikas, S. P., Song, F., Song, X., Yuan, S., Sun, Q., Wu, Y., Jiang, S., Grim, T. W., Benchama, O., Stahl, E. L., Zvonok, N., … Liu, Z. J. (2020). Activation and Signaling Mechanism Revealed by Cannabinoid Receptor-Gi Complex Structures. *Cell*, *180*(4), 655-665.e18. https://doi.org/10.1016/j.cell.2020.01.008

Hua, T., Vemuri, K., Ho, J. H., Wu, Y., Wu, L., Popov, P., Benchama, O., Zvonok, N., Locke, K., Qu, L., Han, G. W., Iyer, M. R., Cinar, R., Coffey, N. J., Wang, J., Wu, M., Katritch, V., Zhao, S., Kunos, G., … Liu, Z. J. (2019). Crystal Structure of the Human Cannabinoid Receptor CB2. *Cell*, *176*(3). https://doi.org/10.1016/j.cell.2018.12.011

Ibsen, M. S., Finlay, D. B., Patel, M., Javitch, J. A., Glass, M., & Grimsey, N. L. (2019). Cannabinoid CB1 and CB2 receptor-mediated arrestin translocation: Species, subtype, and agonist-dependence. *Frontiers in Pharmacology*, *10*(APR), 1–18. https://doi.org/10.3389/fphar.2019.00350

Kano, M., Ohno-Shosaku, T., Hashimotodani, Y., Uchigashima, M., & Watanabe, M. (2009). Endocannabinoid-mediated control of synaptic transmission. *Physiological Reviews*, *89*(1), 309–380. https://doi.org/10.1152/physrev.00019.2008

Kapur, S., & Seeman, P. (2000). Antipsychotic agents differ in how fast they come

off the dopamine D2 receptors. Implications for atypical antipsychotic action. *Journal of Psychiatry and Neuroscience*, *25*(2), 161–166.

Katona, I., Sperlágh, B., Sík, A., Käfalvi, A., Vizi, E. S., Mackie, K., & Freund, T. F. (1999). Presynaptically located CB1 cannabinoid receptors regulate GABA release from axon terminals of specific hippocampal interneurons. *Journal of Neuroscience*, *19*(11), 4544–4558. https://doi.org/10.1523/jneurosci.19-11-04544.1999

Kenakin, Terry. (2004). Principles: Receptor theory in pharmacology. *Trends in Pharmacological Sciences*, *25*(4), 186–192. https://doi.org/10.1016/j.tips.2004.02.012

Kenakin, Terry, & Christopoulos, A. (2013). Signalling bias in new drug discovery: Detection, quantification and therapeutic impact. *Nature Reviews Drug Discovery*, *12*(3), 205–216. https://doi.org/10.1038/nrd3954

Keppler, A., Gendreizig, S., Gronemeyer, T., Pick, H., Vogel, H., & Johnsson, K. (2003). A general method for the covalent labeling of fusion proteins with small molecules in vivo. *Nature Biotechnology*, *21*(1), 86–89. https://doi.org/10.1038/nbt765

Khajehali, E., Malone, D. T., Glass, M., Sexton, P. M., Christopoulos, A., & Leach, K. (2015). Biased agonism and biased allosteric modulation at the CB1 cannabinoid receptors. *Molecular Pharmacology*, *88*(2), 368–379. https://doi.org/10.1124/mol.115.099192

Khan, H., Ghori, F. K., Ghani, U., Javed, A., & Zahid, S. (2022). Cannabinoid and endocannabinoid system: a promising therapeutic intervention for multiple sclerosis. In *Molecular Biology Reports*. https://doi.org/10.1007/s11033-022-07223-5

Khurana, L., Mackie, K., Piomelli, D., & Kendall, D. A. (2017). Modulation of CB1 cannabinoid receptor by allosteric ligands: Pharmacology and therapeutic opportunities. In *Neuropharmacology* (Vol. 124, pp. 3–12). Elsevier Ltd. https://doi.org/10.1016/j.neuropharm.2017.05.018

Kinzer-Ursem, T. L., & Linderman, J. J. (2007). Both ligand- and cell-specific parameters control ligand agonism in a kinetic model of G protein-coupled

receptor signaling. *PLoS Computational Biology*, *3*(1), 0084–0094. https://doi.org/10.1371/journal.pcbi.0030006

Kobilka, B. K. (2007). G Protein Coupled Receptor Structure and Activation Brian. *Biochimica et Biophysica Acta*, *1748*(4), 794–807. https://www.ncbi.nlm.nih.gov/pmc/articles/PMC3624763/pdf/nihms4127 28.pdf

Kolb, P., Gloriam, D., Breinholt, S., Bouvier, M., Ehlert, F., Hill, S. J., Martemyanov, K., & Neubig, R. (2021). *International Union of Basic and Clinical Pharmacology . Recommendations for GPCR ligand bias*. 1–27.

Kouznetsova, M., Kelley, B., Shen, M., & Thayer, S. A. (2002). Desensitization of cannabinoid-mediated presynaptic inhibition of neurotransmission between rat hippocampal neurons in culture. *Molecular Pharmacology*, *61*(3), 477–485. https://doi.org/10.1124/mol.61.3.477

Kucerova, J., Tabiova, K., Drago, F., & Micale, V. (2014). Therapeutic potential of cannabinoids in Schizophrenia. *Recent Recent Patents on CNS Drug Discovery*, *9*(7), 13–25. https://doi.org/10.1016/j.biopsych.2015.11.018

Laprairie, R. B., Bagher, A. M., & Denovan-Wright, E. M. (2017). Cannabinoid receptor ligand bias: implications in the central nervous system. *Current Opinion in Pharmacology*, *32*, 32–43. https://doi.org/10.1016/j.coph.2016.10.005

Laprairie, R. B., Bagher, A. M., Kelly, M. E. M., & Denovan-Wright, E. M. (2016). Biased type 1 cannabinoid receptor signaling influences neuronal viability in a cell culture model of huntington diseases. In *Molecular Pharmacology* (Vol. 89, Issue 3, pp. 364–375). https://doi.org/10.1124/mol.115.101980

Laprairie, R. B., Bagher, A. M., Kelly, M. E. M., Dupré, D. J., & Denovan-Wright, E. M. (2014). Type 1 cannabinoid receptor ligands display functional selectivity in a cell culture model of striatal medium spiny projection neurons. *Journal of Biological Chemistry*, *289*(36), 24845–24862. https://doi.org/10.1074/jbc.M114.557025

Levoye, A., Zwier, J. M., Jaracz-Ros, A., Klipfel, L., Cottet, M., Maurel, D., Bdioui, S., Balabanian, K., Prézeau, L., Trinquet, E., Durroux, T., & Bachelerie, F.

(2015). A broad G protein-coupled receptor internalization assay that combines SNAP-tag labeling, diffusion-enhanced resonance energy transfer, and a highly emissive terbium cryptate. *Frontiers in Endocrinology*, *6*(NOV). https://doi.org/10.3389/fendo.2015.00167

Liu, Q. R., Pan, C. H., Hishimoto, A., Li, C. Y., Xi, Z. X., Llorente-Berzal, A., Viveros, M. P., Ishiguro, H., Arinami, T., Onaivi, E. S., & Uhl, G. R. (2009). Species differences in cannabinoid receptor 2 (CNR2 gene): Identification of novel human and rodent CB2 isoforms, differential tissue expression and regulation by cannabinoid receptor ligands. *Genes, Brain and Behavior*, *8*(5), 519–530. https://doi.org/10.1111/j.1601-183X.2009.00498.x

Lohse, M. J., Nikolaev, V. O., Hein, P., Hoffmann, C., Vilardaga, J. P., & Bünemann, M. (2008). Optical techniques to analyze real-time activation and signaling of G-protein-coupled receptors. *Trends in Pharmacological Sciences*, *29*(3), 159–165. https://doi.org/10.1016/j.tips.2007.12.002

Lu, Y., Lee, D. I., Roy Chowdhury, S., Lu, P., Kamboj, A., Anderson, C. M., Fernyhough, P., & Anderson, H. D. (2019). Activation of Cannabinoid Receptors Attenuates Endothelin-1-Induced Mitochondrial Dysfunction in Rat Ventricular Myocytes. *Journal of Cardiovascular Pharmacology*, *75*(1), 54–63. https://doi.org/10.1097/FJC.0000000000000758

Manglik, A., Kim, T. H., Masureel, M., Altenbach, C., Yang, Z., Hilger, D., Lerch, M. T., Kobilka, T. S., Thian, F. S., Hubbell, W. L., Prosser, R. S., & Kobilka, B. K. (2015). Structural Insights into the Dynamic Process of β2-Adrenergic Receptor Signaling. *Cell*, *161*(5), 1101–1111. https://doi.org/10.1016/j.cell.2015.04.043

Martella, A., Sijben, H., Rufer, A. C., Grether, U., Fingerle, J., Ullmer, C., Hartung, T., IJzerman, A. P., Van Der Stelt, M., & Heitman, L. H. (2017). A novel selective inverse agonist of the CB2 receptor as a radiolabeled tool compound for kinetic binding studies. *Molecular Pharmacology*, *92*(4), 389–400. https://doi.org/10.1124/mol.117.108605

Massink, A., Holzheimer, M., Hölscher, A., Louvel, J., Guo, D., Spijksma, G., Hankemeier, T., & IJzerman, A. P. (2015). Mass spectrometry-based ligand

binding assays on adenosine A1 and A2A receptors. *Purinergic Signalling*, *11*(4), 581–594. https://doi.org/10.1007/s11302-015-9477-0

Matsuda, L. A., Lolait, S. J., Brownstein, M. J., Young, A. C., & Bonner, T. I. (1990). Structure of a cannabinoid receptor and functional expression of the cloned cDNA. *Nature*, *346*(6284), 561–564. https://doi.org/10.1038/346561a0

Maurel, D., Comps-Agrar, L., Brock, C., Rives, M. L., Bourrier, E., Ayoub, M. A., Bazin, H., Tinel, N., Durroux, T., Prézeau, L., Trinquet, E., & Pin, J. P. (2008). Cell-surface protein-protein interaction analysis with time-resolved FRET and snap-tag technologies: Application to GPCR oligomerization. *Nature Methods*, *5*(6), 561–567. https://doi.org/10.1038/nmeth.1213

Mechoulam, R., Ben-Shabat, S., Hanus, L., Ligumsky, M., Kaminski, N. E., Schatz, A. R., Gopher, A., Almog, S., Martin, B. R., Compton, D. R., Pertwee, R. G., Griffin, G., Bayewitch, M., Barg, J., & Vogel, Z. (1995). Identification of an endogenous 2-monoglyceride, present in canine gut, that binds to cannabinoid receptors. *Biochemical Pharmacology*, *50*(1), 83–90. https://doi.org/https://doi.org/10.1016/0006-2952(95)00109-D

Moreira, F. A., & Crippa, J. A. S. (2009). The psychiatric side-effects of rimonabant. *Revista Brasileira de Psiquiatria*, *31*(2), 145–153. https://doi.org/10.1590/S1516-44462009000200012

Motulsky, H., & Christopoulos, A. (2003). Fitting Models to Biological Data Using Linear and Nonlinear Regression.Fitting curves with GraphPad Prism. *GraphPad Prism Software Inc., San Diego,California.*, 296–297.

Motulsky, H. J., & Mahan, L. C. (1984). The kinetics of competitive radioligand binding predicted by the law of mass action. *Molecular Pharmacology*, *25*(1), 1–9.

Mukhopadhyay, S., & Howlett, A. C. (2005). Chemically distinct ligands promote differential CB1 cannabinoid receptor-Gi protein interactions. *Molecular Pharmacology*, *67*(6), 2016–2024. https://doi.org/10.1124/mol.104.003558

Munro, S., Thomas, K. L., & Abu-Shaar, M. (1993). Molecular characterization of

a peripheral receptor for cannabinoids. *Nature*, *365*(6441), 61–65. https://doi.org/10.1038/365061a0

Navarro, G., Morales, P., Rodríguez-Cueto, C., Fernández-Ruiz, J., Jagerovic, N., & Franco, R. (2016). Targeting cannabinoid CB2 receptors in the central nervous system. Medicinal chemistry approaches with focus on neurodegenerative disorders. *Frontiers in Neuroscience*, *10*(SEP), 1–11. https://doi.org/10.3389/fnins.2016.00406

Nehmea, R., Carpenter, B., Singhal, A., Strege, A., Edwards, P. C., White, C. F., Du, H., Grisshammer, R., & Tate, C. G. (2017). Mini-G proteins: Novel tools for studying GPCRs in their active conformation. *PLoS ONE*, *12*(4), e0175642. https://doi.org/10.1371/journal.pone.0175642

Nuber, S., Zabel, U., Lorenz, K., Nuber, A., Milligan, G., Tobin, A. B., Lohse, M. J., & Hoffmann, C. (2016). β-Arrestin biosensors reveal a rapid, receptor-dependent activation/deactivation cycle. *Nature*, *531*(7596), 661–664. https://doi.org/10.1038/nature17198

O'Hara, P. J., Sheppard, P. O., Thógersen, H., Venezia, D., Haldeman, B. A., McGrane, V., Houamed, K. M., Thomsen, C., Gilbert, T. L., & Mulvihill, E. R. (1993). The ligand-binding domain in metabotropic glutamate receptors is related to bacterial periplasmic binding proteins. *Neuron*, *11*(1), 41–52. https://doi.org/10.1016/0896-6273(93)90269-W

Oberhauser, L., & Stoeber, M. (2022). Biosensors Monitor Ligand-Selective Effects at Kappa Opioid Receptors. *Handbook of Experimental Pharmacology*, *271*, 65–82. https://doi.org/10.1007/164_2020_427

Okamoto, Y., Morishita, J., Tsuboi, K., Tonai, T., & Ueda, N. (2004). Molecular Characterization of a Phospholipase D Generating Anandamide and Its Congeners. *Journal of Biological Chemistry*, *279*(7), 5298–5305. https://doi.org/10.1074/jbc.M306642200

Onaivi, E. S., Ishiguro, H., Gong, J. P., Patel, S., Meozzi, P. A., Myers, L., Perchuk, A., Mora, Z., Tagliaferro, P. A., Gardner, E., Brusco, A., Akinshola, B. E., Hope, B., Lujilde, J., Inada, T., Iwasaki, S., Macharia, D., Teasenfitz, L., Arinami, T., & Uhl, G. R. (2008). Brain neuronal CB2 cannabinoid receptors

in drug abuse and depression: From mice to human subjects. *PLoS ONE*, *3*(2). https://doi.org/10.1371/journal.pone.0001640

Onaran, H. Ongun, & Costa, T. (1997). Agonist efficacy and allosteric models of receptor action. *Annals of the New York Academy of Sciences*, *812*, 98–115. https://doi.org/10.1111/j.1749-6632.1997.tb48150.x

Onaran, H.O., Scheer, A., Cotecchia, S., & Costa, T. (2000). A Look at Receptor Efficacy. From the Signalling Network of the Cell to the Intramolecular Motion of the Receptor. In T. Kenakin & J. Angus (Eds.), *The Pharmacology of Functional, Biochemical, and Recombinant Receptor Systems. Handbook of Experimental Pharmacology* (Vol. 148, pp. 217–280).

Pacher, P., Bátkai, S., & Kunos, G. (2006). The endocannabinoid system as an emerging target of pharmacotherapy. In *Pharmacological Reviews* (Vol. 58, Issue 3, pp. 389–462). https://doi.org/10.1124/pr.58.3.2

Packeu, A., De Backer, J. P., Van Liefde, I., Vanderheyden, P. M. L., & Vauquelin, G. (2008). Antagonist-radioligand binding to D2L-receptors in intact cells. *Biochemical Pharmacology*, *75*(11), 2192–2203. https://doi.org/10.1016/j.bcp.2008.03.001

Packeu, A., Wennerberg, M., Balendran, A., & Vauquelin, G. (2010). Estimation of the dissociation rate of unlabelled ligand-receptor complexes by a "two-step" competition binding approach. *British Journal of Pharmacology*, *161*(6), 1311–1328. https://doi.org/10.1111/j.1476-5381.2010.00931.x

Paton, W. D. M. (1961). A theory of drug action based on the rate of drug-receptor combination. *Proceedings of the Royal Society of London. Series B. Biological Sciences*, *154*(954), 21–69. https://doi.org/10.1098/rspb.1961.0020

Perrin, M. H., Fischer, W. H., Kunitake, K. S., Craig, A. G., Koerber, S. C., Cervini, L. A., Rivier, J. E., Groppe, J. C., Greenwald, J., Nielsen, S. M., & Vale, W. W. (2001). Expression, Purification, and Characterization of a Soluble Form of the First Extracellular Domain of the Human Type 1 Corticotropin Releasing Factor Receptor. *Journal of Biological Chemistry*, *276*(34), 31528–31534. https://doi.org/10.1074/jbc.M101838200

Pertwee, R. G., Howlett, A. C., Abood, M. E., Alexander, S. P. H., Di Marzo, V., Elphick, M. R., Greasley, P. J., Hansen, H. S., Kunos, G., Mackie, K., Mechoulam, R., & Ross, R. A. (2010). International Union of Basic and Clinical Pharmacology. LXXIX. Cannabinoid receptors and their ligands: Beyond CB1 and CB2. In *Pharmacological Reviews* (Vol. 62, Issue 4, pp. 588–631). https://doi.org/10.1124/pr.110.003004

Pertwee, Roger G. (2005). Cannabinoids. In *Annals of Clinical Biochemistry: International Journal of Laboratory Medicine*. https://doi.org/10.1177/000456328302000420

Postle, K., Nguyen, T. T., & Bertrand, K. P. (1984). Nucleotide sequence of the repressor gene of the TN10 tetracycline resistance determinant. *Nucleic Acids Research*, *12*(12), 4849–4863. https://doi.org/10.1093/nar/12.12.4849

Raehal, K. M., Walker, J. K. L., & Bohn, L. M. (2005). Morphine side effects in β-arrestin 2 knockout mice. *Journal of Pharmacology and Experimental Therapeutics*, *314*(3), 1195–1201. https://doi.org/10.1124/jpet.105.087254

Raïch, I., Rivas-Santisteban, R., Lillo, A., Lillo, J., Reyes-Resina, I., Nadal, X., Ferreiro-Vera, C., de Medina, V. S., Majellaro, M., Sotelo, E., Navarro, G., & Franco, R. (2021). Similarities and differences upon binding of naturally occurring Δ9-tetrahydrocannabinol-derivatives to cannabinoid CB1 and CB2 receptors. *Pharmacological Research*, *174*. https://doi.org/10.1016/j.phrs.2021.105970

Ramsey, S. J., Attkins, N. J., Fish, R., & Van Der Graaf, P. H. (2011). Quantitative pharmacological analysis of antagonist binding kinetics at CRF 1 receptors in vitro and in vivo. *British Journal of Pharmacology*, *164*(3), 992–1007. https://doi.org/10.1111/j.1476-5381.2011.01390.x

Rang, H. P. (2006). The receptor concept: Pharmacology's big idea. *British Journal of Pharmacology*, *147*(SUPPL. 1), 9–16. https://doi.org/10.1038/sj.bjp.0706457

Rasmussen, S. G. F., DeVree, B. T., Zou, Y., Kruse, A. C., Chung, K. Y., Kobilka, T.

S., Thian, F. S., Chae, P. S., Pardon, E., Calinski, D., Mathiesen, J. M., Shah, S. T. A., Lyons, J. A., Caffrey, M., Gellman, S. H., Steyaert, J., Skiniotis, G., Weis, W. I., Sunahara, R. K., & Kobilka, B. K. (2011). Crystal structure of the β2 adrenergic receptor-Gs protein complex. *Nature*, *477*(7366), 549–555. https://doi.org/10.1038/nature10361

Ricart-Ortega, M., Berizzi, A. E., Catena, J., Malhaire, F., Muñoz, L., Serra, C., Lebon, G., Goudet, C., & Llebaria, A. (2020). Development and validation of a mass spectrometry binding assay for mGlu5 receptor. *Analytical and Bioanalytical Chemistry*, *412*(22), 5525–5535. https://doi.org/10.1007/s00216-020-02772-9

Roed, S. N., Wismann, P., Underwood, C. R., Kulahin, N., Iversen, H., Cappelen, K. A., Schäffer, L., Lehtonen, J., Hecksher-Soerensen, J., Secher, A., Mathiesen, J. M., Bräuner-Osborne, H., Whistler, J. L., Knudsen, S. M., & Waldhoer, M. (2014). Real-time trafficking and signaling of the glucagon-like peptide-1 receptor. *Molecular and Cellular Endocrinology*, *382*(2), 938–949. https://doi.org/10.1016/j.mce.2013.11.010

Ryberg, E., Vu, H. K., Larsson, N., Groblewski, T., Hjorth, S., Elebring, T., Sjögren, S., & Greasley, P. J. (2005). Identification and characterisation of a novel splice variant of the human CB1 receptor. *FEBS Letters*, *579*(1), 259–264. https://doi.org/10.1016/j.febslet.2004.11.085

Santos, R., Ursu, O., Gaulton, A., Bento, A. P., Donadi, R. S., Bologa, G., Karlsson, A., Al-lazikani, B., Hersey, A., & Oprea, T. I. (2019). A comprehensive map of molecular drug targets. *Nature Reviews Drug Discovery*, *16*(1), 19–34. https://doi.org/10.1038/nrd.2016.230.A

Segala, E., Errey, J. C., Fiez-Vandal, C., Zhukov, A., & Cooke, R. M. (2015). Biosensor-based affinities and binding kinetics of small molecule antagonists to the adenosine A2A receptor reconstituted in HDL like particles. In *FEBS Letters* (Vol. 589, Issue 13, pp. 1399–1405). https://doi.org/10.1016/j.febslet.2015.04.030

Shea, L. D., Neubig, R. R., & Linderman, J. J. (2000). Timing is everything: The role of kinetics in G protein activation. *Life Sciences*, *68*(6), 647–658.

https://doi.org/10.1016/S0024-3205(00)00977-2

Shenoy, S. K., & Lefkowitz, R. J. (2003). Multifaceted roles of β-arrestins in the regulation of seven-membrane-spanning receptor trafficking and signalling. *Biochemical Journal*, *375*(3), 503–515. https://doi.org/10.1042/BJ20031076

Shoemaker, J. L., Ruckle, M. B., Mayeux, P. R., & Prather, P. L. (2005). Agonist-directed trafficking of response by endocannabinoids acting at CB2 receptors. *Journal of Pharmacology and Experimental Therapeutics*, *315*(2), 828–838. https://doi.org/10.1124/jpet.105.089474

Soethoudt, M., Grether, U., Fingerle, J., Grim, T. W., Fezza, F., De Petrocellis, L., Ullmer, C., Rothenhäusler, B., Perret, C., Van Gils, N., Finlay, D., Macdonald, C., Chicca, A., Gens, M. D., Stuart, J., De Vries, H., Mastrangelo, N., Xia, L., Alachouzos, G., … Van Der Stelt, M. (2017). Cannabinoid CB2 receptor ligand profiling reveals biased signalling and off-target activity. *Nature Communications*, *8.* https://doi.org/10.1038/ncomms13958

Soethoudt, M., Hoorens, M. W. H., Doelman, W., Martella, A., van der Stelt, M., & Heitman, L. H. (2018). Structure-kinetic relationship studies of cannabinoid CB2 receptor agonists reveal substituent-specific lipophilic effects on residence time. *Biochemical Pharmacology*, *152*(March), 129–142. https://doi.org/10.1016/j.bcp.2018.03.018

Stephenson, R. P. (1956). A modification of receptor theory. *British Journal of Pharmacology*, *11*(4), 379–393. https://doi.org/10.1111/j.1476-5381.1997.tb06783.x

Sugiura, T. (2009). Physiological roles of 2-arachidonoylglycerol, an endogenous cannabinoid receptor ligand. *BioFactors (Oxford, England)*, *35*(1), 88–97. https://doi.org/10.1002/biof.18

Sugiura, T., Kondo, S., Sukagawa, A., Nakane, S., Shinoda, A., Itoh, K., Yamashita, A., & Waku, K. (1995). 2-Arachidonoylgylcerol: A Possible Endogenous Cannabinoid Receptor Ligand in Brain. *Biochemical and Biophysical Research Communications*, *215*(1), 89–97. https://doi.org/https://doi.org/10.1006/bbrc.1995.2437

REFERENCES

Sullivan, S. E. O., Yates, A. S., & Porter, R. K. (2021). *Molecular Target for Modulating Body Weight in Man. 1*, 1–15.

Sykes, D. A., Borrega-Roman, L., Harwood, C. R., Hoare, B., Lochray, J. M., Gazzi, T., Briddon, S. J., Nazaré, M., Grether, U., Hill, S. J., Charlton, S. J., & Veprintsev, D. B. (2021). Kinetic Profiling of Ligands and Fragments Binding to GPCRs by TR-FRET. *Topics in Medicinal Chemistry, 37*(May), 1–32. https://doi.org/10.1007/7355_2021_120

Sykes, D. A., Dowling, M. R., & Charlton, S. J. (2009). Exploring the mechanism of agonist efficacy: A relationship between efficacy and agonist dissociation rate at the muscarinic M3 receptor. *Molecular Pharmacology, 76*(3), 543–551. https://doi.org/10.1124/mol.108.054452

Sykes, D. A., Dowling, M. R., & Charlton, S. J. (2010). *Measuring Receptor Target Coverage : A Radioligand Competition Binding Protocol for Assessing the Association and Dissociation Rates of Unlabeled Compounds. September*, 1–30. https://doi.org/10.1002/0471141755.ph0914s50

Sykes, D. A., Dowling, M. R., Leighton-Davies, J., Kent, T. C., Fawcett, L., Renard, E., Trifilieff, A., & Charlton, S. J. (2012). The influence of receptor kinetics on the onset and duration of action and the therapeutic index of NVA237 and tiotropium. *Journal of Pharmacology and Experimental Therapeutics, 343*(2), 520–528. https://doi.org/10.1124/jpet.112.194456

Sykes, D. A., Jain, P., & Charlton, S. J. (2019). Investigating the influence of tracer kinetics on competition-kinetic association binding assays: Identifying the optimal conditions for assessing the kinetics of low-affinity compounds. *Molecular Pharmacology, 96*(4), 418. https://doi.org/10.1124/mol.119.116764err

Sykes, D. A., Moore, H., Stott, L., Holliday, N., Javitch, J. A., Robert Lane, J., & Charlton, S. J. (2017). Extrapyramidal side effects of antipsychotics are linked to their association kinetics at dopamine D2 receptors. *Nature Communications, 8*(1), 1–12. https://doi.org/10.1038/s41467-017-00716-z

Sykes, D. A., Stoddart, L. A., Kilpatrick, L. E., & Hill, S. J. (2019). Binding kinetics

of ligands acting at GPCRs. In *Molecular and Cellular Endocrinology* (Vol. 485, pp. 9–19). Elsevier Ireland Ltd. https://doi.org/10.1016/j.mce.2019.01.018

Tresadern, G., Bartolome, J. M., MacDonald, G. J., & Langlois, X. (2011). Molecular properties affecting fast dissociation from the D2 receptor. *Bioorganic and Medicinal Chemistry*, *19*(7), 2231–2241. https://doi.org/10.1016/j.bmc.2011.02.033

Tsuboi, K., Uyama, T., Okamoto, Y., & Ueda, N. (2018). Endocannabinoids and related N-acylethanolamines: Biological activities and metabolism Makoto Murakami. *Inflammation and Regeneration*, *38*(1), 1–10. https://doi.org/10.1186/s41232-018-0086-5

Tummino, P. J., & Copeland, R. A. (2008). Residence time of receptor-ligand complexes and its effect on biological function. *Biochemistry*, *47*(32), 8465. https://doi.org/10.1021/bi801226m

Van Der Westhuizen, E. T., Breton, B., Christopoulos, A., & Bouvier, M. (2014). Quantification of ligand bias for clinically relevant b2-adrenergic receptor ligands: Implications for drug taxonomy s. *Molecular Pharmacology*, *85*(3), 492–509. https://doi.org/10.1124/mol.113.088880

Van Eps, N., Caro, L. N., Morizumi, T., Kusnetzow, A. K., Szczepek, M., Hofmann, K. P., Bayburt, T. H., Sligar, S. G., Ernst, O. P., & Hubbell, W. L. (2017). Conformational equilibria of light-activated rhodopsin in nanodiscs. *Proceedings of the National Academy of Sciences of the United States of America*, *114*(16), E3268–E3275. https://doi.org/10.1073/pnas.1620405114

Van Laere, K., Casteels, C., Dhollander, I., Goffin, K., Grachev, I., Bormans, G., & Vandenberghe, W. (2010). Widespread decrease of type 1 cannabinoid receptor availability in Huntington disease in vivo. *Journal of Nuclear Medicine*, *51*(9), 1413–1417. https://doi.org/10.2967/jnumed.110.077156

Van Sickle, M. D., Duncan, M., Kingsley, P. J., Mouihate, A., Urbani, P., Mackie, K., Stella, N., Makriyannis, A., Piomelli, D., Davison, J. S., Marnett, L. J., Di Marzo, V., Pittman, Q. J., Patel, K. D., & Sharkey, K. A. (2005). Identification

and functional characterization of brainstem cannabinoid CB2 receptors. *Science*, *310*, 329–332. https://doi.org/10.1126/science.1115740

Waelbroeck, M., Boufrahi, L., & Swillens, S. (1997). Seven helix receptors are enzymes catalysing G protein activation. What is the agonist K(act)? *Journal of Theoretical Biology*, *187*(1), 15–37. https://doi.org/10.1006/jtbi.1997.0411

Wan, Q., Okashah, N., Inoue, A., Nehme, R., Carpenter, B., Tate, C. G., & Lambert, N. A. (2018). Mini G protein probes for active G protein– coupled receptors (GPCRs) in live cells. *Journal of Biological Chemistry*, *293*(19), 7466–7473. https://doi.org/10.1074/jbc.RA118.001975

Weiland, G. A., & Molinoff, P. B. (1981). Quantitative analysis of drug-receptor interactions: I. Determination of kinetic and equilibrium properties. *Life Sciences*, *29*(4), 313–330. https://doi.org/10.1016/0024-3205(81)90324-6

Weis, W. I., & Kobilka, B. K. (2018). The Molecular Basis of G Protein-Coupled Receptor Activation. *Annual Review of Biochemistry*. http://doi.org/10.1146/annurev-biochem-060614-033910

Weiss, J. M., Morgan, P. H., Lutz, M. W., & Kenakin, T. P. (1996). The cubic ternary complex receptor-occupancy model. III. Resurrecting efficacy. *Journal of Theoretical Biology*, *181*(4), 381–397. https://doi.org/10.1006/jtbi.1996.0139

Xia, L., De Vries, H., Lenselink, E. B., Louvel, J., Waring, M. J., Cheng, L., Pahlén, S., Petersson, M. J., Schell, P., Olsson, R. I., Heitman, L. H., Sheppard, R. J., & Ijzerman, A. P. (2017). Structure-Affinity Relationships and Structure-Kinetic Relationships of 1,2-Diarylimidazol-4-carboxamide Derivatives as Human Cannabinoid 1 Receptor Antagonists. *Journal of Medicinal Chemistry*, *60*(23), 9545–9564. https://doi.org/10.1021/acs.jmedchem.7b00861

Xia, L., de Vries, H., Yang, X., Lenselink, E. B., Kyrizaki, A., Barth, F., Louvel, J., Dreyer, M. K., van der Es, D., IJzerman, A. P., & Heitman, L. H. (2018). Kinetics of human cannabinoid 1 (CB1) receptor antagonists: Structure-kinetics relationships (SKR) and implications for insurmountable

antagonism. *Biochemical Pharmacology*, *151*, 166–179. https://doi.org/10.1016/j.bcp.2017.10.014

Xiao, J. C., Jewell, J. P., Lin, L. S., Hagmann, W. K., Fong, T. M., & Shen, C. P. (2008). Similar in vitro pharmacology of human cannabinoid CB1 receptor variants expressed in CHO cells. *Brain Research*, *1238*, 36–43. https://doi.org/10.1016/j.brainres.2008.08.027

Xing, C., Zhuang, Y., Xu, T. H., Feng, Z., Zhou, X. E., Chen, M., Wang, L., Meng, X., Xue, Y., Wang, J., Liu, H., McGuire, T. F., Zhao, G., Melcher, K., Zhang, C., Xu, H. E., & Xie, X. Q. (2020). Cryo-EM Structure of the Human Cannabinoid Receptor CB2-Gi Signaling Complex. *Cell*, *180*(4), 645-654.e13. https://doi.org/10.1016/j.cell.2020.01.007

Yang, J. F., Williams, A. H., Penthala, N. R., Prather, P. L., Crooks, P. A., & Zhan, C. G. (2020). Binding Modes and Selectivity of Cannabinoid 1 (CB1) and Cannabinoid 2 (CB2) Receptor Ligands. *ACS Chemical Neuroscience*, *11*(20), 3455–3463. https://doi.org/10.1021/acschemneuro.0c00551

Yao, F., Svensjö, T., Winkler, T., Lu, M., Eriksson, C., & Eriksson, E. (1998). Tetracycline repressor, tetR, rather than the tetR-mammalian cell transcription factor fusion derivatives, regulates inducible gene expression in mammalian cells. *Human Gene Therapy*, *9*(13), 1939–1950. https://doi.org/10.1089/hum.1998.9.13-1939

Zhu, X., Finlay, D. B., Glass, M., & Duffull, S. B. (2020). Evaluation of the profiles of CB 1 cannabinoid receptor signalling bias using joint kinetic modelling . *British Journal of Pharmacology*, *March*, 1–15. https://doi.org/10.1111/bph.15066

Zou, S., & Kumar, U. (2018). Cannabinoid receptors and the endocannabinoid system: Signaling and function in the central nervous system. *International Journal of Molecular Sciences*, *19*(3). https://doi.org/10.3390/ijms19030833

APPENDIX A

KINETIC PARAMETERS OF UNLABELLED CANNABINOID LIGANDS AT CB1 AT ROOM TEMPERATURE

The kinetic parameters of the cannabinoid compounds tested were also determined at room temperature (25 °C) following the Motulsky and Mahan approach and using the D77 fluorescent ligand as the tracer (600 nM). The association of the tracer ligand was monitored using TR-FRET in the competition with 7 different concentrations of each cold cannabinoid ligand. Data were globally fitted using the model "kinetics of competitive binding" in GraphPad Prism and association rate-k_{on} and dissociation rate-k_{off} were calculated for the different cannabinoid compounds, which are found in Table 12.

Table 12
Kinetic parameters calculated from the Motulsky and Mahan experimental approach for the 7 cannabinoid compounds tested for CB1 at room temperature (25°C). Data are expressed as mean ± SEM of 4 experiments conducted independently.

CB1 (25°C)	k_{on} (M^{-1} min^{-1})	k_{off} (min^{-1})	Residence time (Rt)	
			(min)	(s)
Rimonabant	$(1.2 \pm 0.2) \times 10^8$	0.36 ± 0.03	2.9 ± 0.2	**171 ± 14**
HU-210	$(1.64 \pm 0.08) \times 10^8$	0.376 ± 0.004	2.66 ± 0.03	**160 ± 2**
CP-55940	$(1.0 \pm 0.1) \times 10^8$	2.4 ± 0.2	0.42 ± 0.03	**25 ± 2**
2-AG	$(1.2 \pm 0.2) \times 10^6$	4.8 ± 0.8	0.22 ± 0.03	**13 ± 2**
Anandamide	$(1.4 \pm 0.2) \times 10^6$	3.8 ± 0.5	0.27 ± 0.03	**17 ± 2**
HU-308 (N=3)	$(4.0 \pm 0.5) \times 10^5$	1.7 ± 0.2	0.60 ± 0.08	**36 ± 5**
SR144,528	$(1.2 \pm 0.2) \times 10^7$	2.3 ± 0.2	0.44 ± 0.04	**26 ± 3**

AFFINITY VALUES DERIVED FROM KINETIC PARAMETERS

The kinetic parameters obtained from the application of Motulsky and Mahan approach were used to calculate the kinetically derived affinity dissociation constant of the compounds tested by dividing the association and dissociation constants ($K_d = k_{off}/k_{on}$), shown in Table 13.

Table 13
Affinity values for the 7 cannabinoid compounds tested at CB2 at 25 °C. The equilibrium dissociation constant Kd was calculated from the kinetic parameters k_{on} and k_{off} obtained using the Motulsky and Mahan methodology. The data shown are mean ± SEM from 4 experiments conducted independently.

CB1 (25 °C)	K_d (nM)	pK_d (M)
Rimonabant	3.2 ± 0.2	8.5 ± 0.03
HU-210	2.3 ± 0.1	8.64 ± 0.02
CP-55940	25 ± 2	7.61 ± 0.03
2-AG	4237 ± 728	5.40 ± 0.08
Anandamide	2710 ± 73	5.57 ± 0.01
HU-308 (N=3)	4308 ± 50	5.366 ± 0.005
SR144,528	190 ± 10	6.72 ±0.02

KINETIC PARAMETERS OF UNLABELLED CANNABINOID LIGANDS AT CB2 AT ROOM TEMPERATURE

The kinetic parameters of the cannabinoid compounds tested were also determined at room temperature (25 °C) following the Motulsky and Mahan approach and using the D77 fluorescent ligand as the tracer (900 nM). The

association of the tracer ligand was monitored using TR-FRET in the competition with 7 different concentrations of each cold cannabinoid ligand. Data were globally fitted using the model "kinetics of competitive binding" in GraphPad Prism and association rate-k_{on} and dissociation rate-k_{off} were calculated for the different cannabinoid compounds, which are shown in Table 14.

Table 14
Kinetic parameters calculated from the Motulsky and Mahan experimental approach for the 7 cannabinoid compounds tested for CB2 at room temperature (25°C). Data are expressed as mean ± SEM of 4 experiments conducted independently.

CB2 (25 °C)	k_{on} (M^{-1} min^{-1})	k_{off} (min^{-1})	Residence time (Rt)	
			(min)	(s)
Rimonabant	$(2.0 \pm 0.3) \times 10^6$	2.0 ± 0.3	0.54 ± 0.08	**32 ± 5**
HU-210	$(6.42 \pm 0.3) \times 10^7$	0.024 ± 0.005	50 ± 13	**2971 ± 772**
CP-55940	$(1.1 \pm 0.1) \times 10^8$	0.33 ± 0.05	3.2 ± 0.4	**191 ± 23**
2-AG	$(6 \pm 2) \times 10^6$	2.5 ± 0.6	0.5 ± 0.1	**29 ± 7**
Anandamide	$(1.4 \pm 0.2) \times 10^6$	1.27 ± 0.2	0.8 ± 0.1	**51 ± 8**
HU-308	$(2.5 \pm 0.4) \times 10^7$	0.42 ± 0.05	2.7 ± 0.2	**164 ± 12**
SR144,528	$(8.5 \pm 0.4) \times 10^6$	0.16 ± 0.01	6.3 ± 0.4	**379 ± 27**

AFFINITY VALUES DERIVED FROM KINETIC PARAMETERS

The kinetic parameters obtained from the application of Motulsky and Mahan approach were used to calculate the kinetically derived affinity dissociation constant of the compounds tested by dividing the association and dissociation constants ($K_d = k_{off}/k_{on}$), shown in Table 15.

Table 15
Affinity values for the 7 cannabinoid compounds tested at CB2 at 25 °C. The equilibrium dissociation constant Kd was calculated from the kinetic parameters k_{on} and k_{off} obtained using the Motulsky and Mahan methodology. The data shown are mean ± SEM from 4 experiments conducted independently.

CB2 (25 °C)	K_d (nM)	pK_d (M)
Rimonabant	1008 ± 95	6.00 ± 0.04
HU-210	0.38 ± 0.08	9.46 ± 0.12
CP-55940	2.8 ± 0.1	8.55 ± 0.01
2-AG	446 ± 57	6.36 ± 0.06
Anandamide	872 ± 31	6.06 ± 0.02
HU-308	18 ± 3	7.75 ± 0.08
SR144,528	1.9 ± 0.2	8.73 ± 0.05

LIGANDO KANNABINOIDEEN LOTURA-ZINETIKAK ETA SEINALEZTAPENA CB1 ETA CB2 HARTZAILEETARA LOTZEAN; FINKAPEN DENBORA ETA SELEKTIBITATE FUNTZIONALA GERTUAGOTIK AZTERTZEN

1. SARRERA ETA HELBURUAK

CB1 eta CB2 hartzaileak eta endokannabinoide sistema

Endokannabinoide sistema osatzen duten elementuen artean konposatu kannabinoideen sintesian eta degradazioan parte hartzen duten entzimak eta konposatu endokannabinoideak antzeman eta lotzen dituzten hartzaileak aurkitu daitezke. Hartzaile kannabinoide nagusiak CB1 eta CB2 hartzaileak dira, endogenoki sortutako kannabinoideak (endokannabinoideak) lotu ostean seinaleztapena eragingo dutenak. CB1 hartzailea marihuanaren Δ9-THC osagai psikoaktiboaren efektuak eragiten zituen elementua zela proposatu zen (Devane et al., 1988) eta 90eko hamarkadan klonatu zen lehendabiziko aldiz (Matsuda et al., 1990),. Urte batzuk beranduago, bigarren hartzaile kannabinoide mota klonatu zen, CB2 hartzailea (Munro et al., 1993). CB2 hartzailea HL60 zeluletatik klonatu zen, eta barean aurkitzen diren makrofagoetan maila altuetan espresatzen zela ikusi zen. Hasiera batean, CB2 hartzailea periferikoa zela uste zen, eta bere presentzia immunitate sistemarekin erlazionatutako organoetara mugatzen zela. Dena den, gaur egun badakigu, garatutako tekniken sentsibilitatea hobetuz joan delako, CB2 hartzailea nerbio sistema zentralean ere aurki daitekeela. Dena dela, CB1 hartzailearekin konparatuta, garunean aurkitu daitekeen CB2 hartzaileen maila baxua da (Liu et al., 2009; Onaivi et al., 2008; Van Sickle et al., 2005). Izan ere, CB1 da garunean espresatzen den G-proteinei lotutako hartzaile (GPCR) ugariena (Katona et al., 1999).

Hartzaile kannabinoideak aurkitu eta berehala, hauei lotzen ziren konposatuak ere identifikatu ziren, hau da, endokannabinoideak. Anandamida (AEA) izan zen lehen identifikatu zen konposatu endokannabinoidea (Devane et al., 1992), eta ondoren, 2-AG (2-arakidonilglizerola) (Sugiura et al., 1995). Bi konposatu hauek funtzio garrantzitsuak betetzen dituzte endokannabinoide sisteman, eta gaur egun arte gehien ikertu diren endokannabinoideak dira (Kano et al., 2009). 2-AG eta anandamida azido arakidonikotik eratorritako konposatuak dira eta modulazio sinaptikoan parte hartzen dute, neurotransmisoreen askapena erregulatuz atzera-seinaleztapenaren bidez (Zou & Kumar, 2018). Endokannabinoideak molekula txiki eta lipofilikoak dira, eta ez dira besikuletan gordetzen beste neurotransmisore batzuen moduan, baizik eta behar direnean sintetizatzen dira zelula barneko kaltzio mailak igotzen direnean (Tsuboi et al., 2018). Anadamida eta 2-AG endokannabinoideen sintesia bide desberdinak

155

jarraituz sintetizatu daitezke, oraindik argitzeke dauden biosintesi bideen bidez (Kano et al., 2009). Dena den, 2-AG sintesirako bide nagusia C fosfolipasa (PLC) eta diazilglizerol lipasa (DAGL) entzimen bitartez ematen da. PLC-k mintzeko fosfolipidoak hidrolizatzen duenean diazilglizerola sortzen da; ondoren, DAGL-aren bidez 2-AG sortzen da. Bestalde, anandamida sortzeko NAPE (N-azil fosfatidiletanolamina) aitzindaria metabolizatzen da fosfolipasa espezifiko baten bidez (NAPE-PLD) (Devane et al., 1992; Mechoulam et al., 1995; Sugiura et al., 1995). Anandamidaren degradazioan eragiten duen entzima garrantzitsuena gantz azido amida hidrolasa (FAAH) da, eta 2-AG degradazioan, berriz, monoazilglizerol lipasa (MAGL) (Bisogno et al., 2003; Cravatt et al., 1996; Dinh et al., 2002; Okamoto et al., 2004). 2-AG agonista total moduan eragiten du hartzaile kannabinoideetan eta bere mailak anandamidarenak baino altuagoak dira garunean. Anandamida, bestalde, hartzaile kannabinoideen agonista partzial moduan deskribatu izan da (Baggelaar et al., 2018; Gonsiorek et al., 2000; Sugiura, 2009).

CB1 eta CB2 hartzaileak deskribatu dira endokannabinoideen ekintza bideratzen duten hartzaile nagusiak bezala. Dena den, gaur egun badakigu beste hartzaile batzuk ere gai direla endokannabinoideak lotzeko, hala nola, GPR55, GPR19 ala GPR119 hartzaileak gai dira endokannabinoideak *in vitro* lotzeko (Pertwee et al., 2010). Gainera, 2-AG-k eta AEA-k TRPV 1 (*Transient Receptor Potential Vanilloid 1*) hartzailea aktibatzeko gaitasuna erakutsi dute *in vitro* nahiz *in vivo* (De Petrocellis et al., 2017) (ikusi Di Marzo, 2018 berrikuspena). Hartzaile hauek fisiologikoki duten garrantzia argi ez egon arren, konplexutasuna gehitzen dute endokannabinoide sistema ulertzeko orduan.

CB1 eta CB2 hartzaileak G proteinei lotutako hartzaileak dira (GPCR: *G protein-coupled receptors*) eta A klasean sailkatzen dira (errodopsina antzeko hartzaileak). GPCRen familia oso handia da, 800 GPCR hartzaile desberdin inguru kodetzen ditu giza genomak (Foord et al., 2005). Gainera, itu terapeutiko oso garrantzitsuak dira hartzaile mota hauek, izan ere, komertzializatutako farmakoen heren batek GPCR familiako kideren bat erabiltzen du itu moduan (Santos et al., 2019).

GPCR hartzaileek 7 mintz-zeharreko domeinu dituzte, eta 7TM hartzaile bezala ere ezagutzen dira (7TM: *7-transmembrane receptors*). Izan ere, mintz

156

plasmatikoa zelula barrualdera eta kanpoaldera zazpi alditan zeharkatzen duten domeinu proteikoek osatzen dute hartzaile bakoitza. Zelula kanpoaldean, N-terminala kokatzen da, eta zelula barnealdean, C-terminala (Kobilka, 2007). Hartzaile batek ligando bat lotzen duenean, konformazio aldaketak emango dira egituran eta mezulari desberdinak aktibatuko dira, zelula barneko seinaleztapen bide desberdinak aktibatuz.

CB1 eta CB2 hartzaileak modu desberdinean banatzen dira gizakietan. CB1 hartzailea batez ere nerbio sistema zentralean azaltzen da (Katona et al., 1999), eta CB2 hartzailea, berriz, immunitate sistemarekin erlazionatutako ehunetan azaltzen da gehien bat (Khurana et al., 2017), hala nola, barea eta timoan (Galiègue et al., 1995; Munro et al., 1993).

Seinaleztapena CB1 eta CB2 hartzaileen bidez

CB1 eta CB2 hartzaileak batez ere G proteina inhibitzaileetara lotzen dira ($G\alpha_{i/o}$), adenilil ziklatoa (AC) inhibituz eta zelula barneko AMP zikliko (AMPz) mailak jeitsiaraziz. Seinaleztapen kanonikoa $G\alpha_{i/o}$ bidez ematen den arren, CB1 eta CB2 hartzaileak beste familietako G proteinetara lotu daitezkeela deskribatu da zenbait kasuetan (Howlett, 1995).

Bi hartzaile kannabinoideek MAPK proteinak (mitogenoak aktibatutako proteina kinasa) aktibatzeko gaitasuna dute, adibidez ERK1 eta ERK2 (*extracellular kinase 1 and 2*), p38 eta p42/p44, edota JNK (c-Jun N-terminaleko kinasa) G-proteinen bidezko mekanismoen bitartez. Gainera, CB1ek ahalmena dauka N eta P/ Q-motako boltai menpeko kaltzio kanalak negatiboki erregulatzeko eta A-motako eta potasio zuzentzaileak diren kanalak positiboki erregulatzeko zelula batzuetan (Pertwee, 2005).

CB1 eta CB2 hartzaile kannabinoideek posible dute beste mezulari batzuen bidez seinaleztatzea G-proteinen bidez gain, esaterako, β-arrestina proteinen bidez. Hartzailearen zelula barneko domeinuak fosforilatzean arrestinen lotzea ahalbidetzen da, zelulen desensitizazioa eta internalizazio prozesuekin erlazionatzen dena, eta baita MAPK kinasa edo ERK1/2 aktibazioarekin (Shenoy & Lefkowitz, 2003). β-arrestina 1 eta 2 lotu daitezke CB1 eta CB2 hartzaileetara, baina β-arrestina 2-ren lotura sendoagoa dela deskribatu da β-arrestina 1-ekin konparatuta (Ibsen et al., 2019).

CB1 eta CB2 hartzaileak itu terapeutiko gisa duten potentziala

CB1 hartzailearen mailak batez ere altuak dira nerbio sistema zentralean (NSZ) eta CB2 hartzailearenak, berriz, zenbait ehun periferikoetan. Hala ere, CB1 hartzailea beste ehun batzuetan aurkitu daiteke ere, hala nola ehun adiposoan, gibelean edota pankrean, non funtzio oso garrantzitsuak erregulatzen dituen. Hori dela eta, NSZ-arekin erlazionatutako gaixotasunak nahiz beste gaixotasun batzuk tratatzeko itu potentzial gisa deskribatu da (Pacher et al., 2006). Antzeko moduan, CB2 hartzailea batez ere ehun periferikoetan espresatzen den arren eta NSZ-an mailak baxuak diren arren, garrantzitsua da zenbait gaixotasunen garapenean, adibidez, Alzheimer edo Parkinsonean (Benito et al., 2003)(Gómez-Gálvez et al., 2016). Ondorioz, CB2 hartzailea itu interesgarri bat bihurtu da gaixotasun neurologikoen tratamendurako (Navarro et al., 2016).

Adibidez, CB1 hartzailearen agonistak Huntington gaixotasunaren tratamendurako proposatu dira. Deskribatu izan da nola CB1 hartzailearen gainespresioa ematen den garuneko zenbait lokalizazioetan aurkitzen diren neurona proiekzio arantzadunetan (Denovan-Wright & Robertson, 2000; Glass et al., 2000; Van Laere et al., 2010). Gainera, animali ereduetan CB1-aren funtzioaren gutxitzeak gaixotasunaren bilakaeran ematen diren sintomatologia antzekoa eragiten duela ikusi da, adibidez, limitazio kognitibo edo motoreak (Blázquez et al., 2015, 2011; Chiarlone et al., 2014). Hortaz, CB1 hartzailearen agonistak proposatu dira tratamendu potentzial moduan Huntington gaixotasunean azaltzen diren sintomatologia murrizteko helburuarekin (Laprairie et al., 2016). Laprairie et lankideek (2016) erakutsi dute nola CB1 agonistek zelula biziraupenean lagundu dezaketen eta baita CB1 espresio maila normalen berrezarpena bultzatzen dutela *in vitro* STDdh zelula lerroan. Gainera, ikerlari horien hipotesiaren arabera, $G_{i/o}$ menpeko bideak aktibatzeko gaitasun selektiboa duten konposatuek zenbait abantaila aurkeztu ditzakete Huntington gaixotasuna tratatzeko orduan (Laprairie et al., 2016, 2017).

CB1 eta CB2 hartzaileak itu terapeutiko moduan proposatu dira ere eskizofrenian agertzen den sintomatologia tratatzeko (Kucerova et al., 2014). Psikosi gertaerak jasan dituzten pazienteetan CB1 eta CB2 espresio mailen aldaketak ikusten dira.

Animali ereduetan gauzatutako zenbait ikerketa preklinikoek erakutsi dute konposatu kannabinoideek lagundu dezaketela eskizofrenian agertzen den sintomatologia murrizten. Hala ere, askotan segurtasun profil ahula erakusten dute ikertutako konposatu kannabinoideak, eta honek kannabinoideen erabilera mugatu du klinikan. Den dela, aurrera pausoak eman dira CB2 hartzaileek sistema dopaminergiko eta glutamatergikoa erregulatzeko duten rola ulertzen, eta beraz, bereziki CB2 hartzailean eragiten duten konposatuak erabilgarriak izan daitezkeela proposatu da, bereziki lehen gertaera psikotikoak jasaten ari diren pazienteetan. Cannabidiola (CBD) bezalako modulatzaile alosterikoen erabilera ere proposatu da eskizofrenian agertzen den sintomatologia arintzeko (Cortez et al., 2020).

Kannabinoideen erabilera potentziala ez da mugatzen bakarrik aldez aurretik aipatutako kasuetara, izan ere, beste erabilera ugari ikertzen ari dira. Esaterako, esklerosi anizkoitzaren tratamenduan (Khan et al., 2022) edo min neuropatikoan (Guindon & Hohmann, 2008) erabilgarriak izan daitezkeela proposatu da. Hartzaile kannabinoideak itu farmakologiko moduan ere proposatu dira bihotz-gaixotasunak tratatzeko (Lu et al., 2019), obesitatea (Sullivan et al., 2021) edota kantzerra (Hinz & Ramer, 2022).

CB1 eta CB2 itu farmakologiko moduan erabiltzeko erronkak

Nahiz eta endokannabinoide sistema oso itu terapeutiko interesgarria izan gaixotasun desberdinen tratamendurako, CB1 edota CB2 hartzaileak itu bezala dituzten oso farmako gutxi iritsi dira klinikara gaur egun arte. Adibide bezala, rimonabant izeneko farmakoa dugu, obesitatea tratatzeko merkaturatu zena. Dena dela, oso eragin desiragaitz neuropsikiatriko larriak sortzen zituen eta merkatutik kendu behar izan zuten honen eraginez (Moreira & Crippa, 2009).

Gaur egun, FDA-k bakarrik hiru kannabinoide sintetiko ditu onartuta erabilera klinikorako: Marinol® (dronabinol), Syndros® (dronabinol), eta Cesamet® (nabilona). Hauek, kimioterapiarekin erlazionatutako emesia tratatzeko erabiltzen dira, eta baita anorexia tratatzeko HIESa (Hartutako Immuno Eskasiaren Sindromea) duten pazienteetan (www.fda.gov).

Farmako kannabinoideen garapenak orain arte izan duen arrakasta baxua izan da. Honen arrazoietako bat, konposatu selektiboak garatzeko zailtasuna da

(Munro et al., 1993), izan ere, bi hartzaileek duten homologia maila oso altua da (% 44 proteina mailan eta % 68 mintz-zeharreko sekuentzietan). Dena den, azken urteetan aurrerapen handiak ematen ari dira hartzaile kannabinoideen ikerkuntza arloan. Adibidez, bi hartzaile hauen kristal egiturak azaldu dira (Hua et al., 2019; Xing et al., 2020) eta honek informazio oso erabilgarria deskribatu du ligandoen loturan inplikatutako ondarrei dagokionez. Bi hartzaileetan, lotura gunean azaltzen diren aminoazido ondarrak oso antzekoak dira (Hua et al., 2020), beraz, zaila da konposatu selektiboak garatzea. Dena den, egiturari buruzko informazio berria beste metodo konputazionalekin konbinatuz informazio baliagarria lortu da ligandoak lotzeko moduaren inguruan (Yang et al., 2020), eta ondorioz, estrategia berriak agertzen ari dira konposatu kannabinoideen sintesirako.

Farmako eta hartzailearen arteko lotura prozesua eta zinetikaren papera farmakoen ekintzan

Ligando batek hartzaile batekiko duen afinitateak, ligando eta hartzailearen arteko loturaren sendotasuna deskribatzen du. Lotura disoziazio konstantea (K_d) da afinitatea deskribatzen duen parametroa. Honek, oreka egoerara iristean hartzaile kopuruaren erdiak ligando batekin lotuta egoteko behar den ligando konzentrazioa deskribatzen du.

Hartzaile eta farmako baten arteko lotura deskribatzeko erabiltzen diren ereduak masa akzioaren legean oinarrituz sortu dira. Eredu hauetan, lotura pauso bakarrean eta modu itzulgarrian ematen den lehen mailako erreakzio bat kontsideratzen da, eta erreakzioaren abiadura proportzionala izango da erreakzioan parte hartzen duten elementuekiko. Hau da, hartzaile-ligando konplexuaren [RL] sorkuntza abiadurak (k_{obs}) proportzionaltasuna mantenduko du hartzaile [R] eta ligando [L] kontzentrazioekin. Kasu honetan, [RL] konplexuaren formakuntza asoziazio konstante abiaduraren menpekoa izango da (k_{on}). Alderantzizko erreakzioa, non [RL] konplexua banandu eta [R] eta [L] produktuak sortuko diren, berriz, disoziazio abiaduraren menpekoa izango da (k_{off}).

160

Ligandoak hartzailearekin konplexuak sortzen ditduen einean, [L] eta [R] askeen kopurua txikiagoa izango da, eta beraz, asoziazioa geldoagoa izango da lotura prozesua aurrera doan joan ahala. Konplexuen sorrera eta disoziazio abiadurak berdintzen direnean ($[R] \cdot [L] \cdot k_{on} = [RL] \cdot k_{off}$), sistemak oreka lortuko du eta disoziazio eta asoziazio abiadura konstantearen arteko zatiketak definituko du K_d afinitate parametroa ($K_d=k_{off}/k_{on}$).
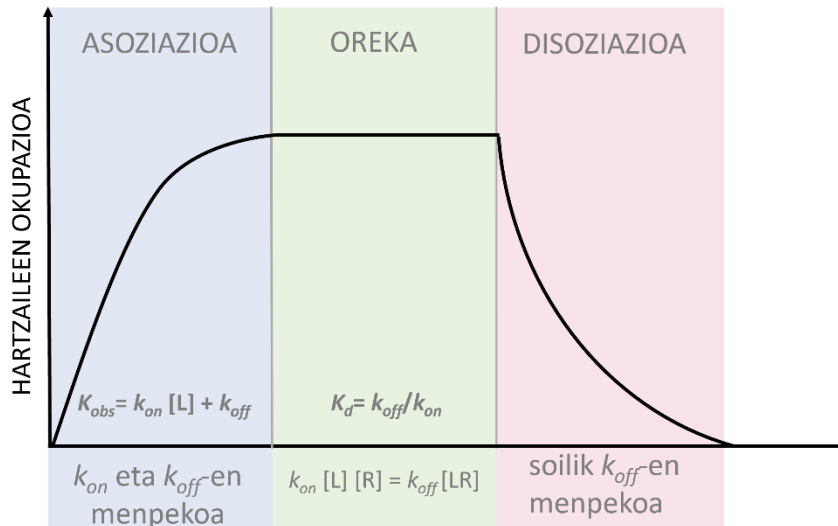
1. irudia. *Hartzaile eta ligandoen arteko lotura faseen irudikapen eskematikoa.*

Asoziazio abiadura konstantea (k_{on}) bigarren mailako konstantea da, eta bere unitateak kontzentrazio eta denboraren alderantzizkoak dira (M^{-1} min^{-1}). Disoziazio abiadura konstantea (k_{off}), berriz, soilik denboraren menpekoa da (min^{-1}), eta ligando kontzentrazioarekiko ez du menpekotasunik (ikusi 1. irudia). Asoziazio fasean aldi berean asoziazio eta disoziazio prozesuak emango direnez, behatutako asoziazio konstanteak (k_{obs}) definituko du ligando kontzentrazio desberdinekin behatuko den asoziazioa, bi fenomenoak kontuan izanik ($k_{obs}= (k_{on} \times L) + k_{off}$). Hori dela eta, k_{on} and k_{off}-en menpekoa izango da asoziazio fasearen iraupena eta forma. Disoziazio fasea, aldiz, k_{off} parametroaren menpekoa izango da soilik. Disoziazio abiadura konstanteak (k_{off}) definituko du ligandoak hartzaileari lotuta emango duen denbora, hau da, finkapen denbora (Rt= "*residence time*"), k_{off}-en alderantzizkoa den parametroa (Rt=1/k_{off}).

Tradizioz, K_d parametro nagusi gisa erabili izan da ligando eta hartzaileen arteko lotura deskribatzeko, eta farmakoak aurkitzeko programek oreka-konstante horretan konfiantza izan dute hautagaiak bilatzeko orduan. Hala ere, gorputza

sistema ireki bat da, eta baliteke oreka-baldintzak adierazgarriak ez izatea fisiologia mailan. Bestalde, ikus daiteke k_{on} eta k_{off} konbinazio desberdin infinituek afinitate bera (K_d) eragin dezaketela. Azken hamarkadan, gero eta interes handiagoa dago zinetikak farmakoen ekintzan duen inplikazioa ikasteko, eta ahaleginak egin dira farmakoen garapen-programetan ikuspegi zinetikoa sartzeko. Farmako bat hartzailera lotzean, oreka-baldintzak lortzen ez badira, asoziazio eta disoziazio konstanteak nabarmen argitu ditzakete farmakoen ekintzaren alderdi ugari *in vivo* (Copeland et al., 2006).

Kasu askotan deskribatu izan da loturaren parametro zinetikoek eragin zuzena dutela farmakoen ekintzan edo toxikotasunean. Gaur egun baditugu adibide ugari non profil zinetiko berezi bat duten farmakoek, abantailak aurkeztu dituzten zinetika desberdinak zituzten beste farmako batzuekin konparatuta.

Finkapen denbora luzea duten farmako batzuek (k_{off} *geldoa*) efektu klinikoa luzaroan mantentzeko erabilgarriak direla ikusi da zenbait kasuetan (Guo et al., 2014). Bilastina, esaterako, finkapen denbora luzea duen bigarren belaunaldiko antihistaminikoa da eta H1 hartzailea blokeatzen duten beste farmako batzuekin alderatuta, ekintza klinikoa luzaroan mantentzen du (Bosma et al., 2019). Candesartan, hipertentsioa tratatzeko erabiltzen den II-angiotensina 1 motako (AT1) hartzailearen antagonista da eta klinikan duen erantzun ona bere finkapen denbora luzeagatik dela ere pentsatzen da (Fuchs et al., 2000). Beste adibide bat lo arazoak tratatzeko erabiltzen den CRF-1 antagonista da (Fleck et al., 2012). Kasu honetan ere, bere disoziazio motelak abantaila bat suposatzen du efektu klinikoa denbora luzeagoan mantentzeko.

Biriketako gaixotasun buxatzaile kronikoa (BGBK) tratatzeko erabiltzen den tiotropioa beste adibide interesgarri bat da, non zinetikak eragin garrantzitsua duen farmakoaren ekintzan. Kasu horretan, tiotropio konposatuak afinitate (K_d) berdina du, baina profil zinetiko selektiboa, hartzaile muskariniko desberdinentzat, baina finkapen denbora hamar aldiz handiagoa da M3 (~10 h) hartzailean M2an baino (Casarosa et al., 2009; Sykes et al., 2012). Kasu honetan, tiotropioak eragin desiragaitz profil hobeagoa aurkezten du beste farmako muskariniko batzuekin alderatuta. Profil kliniko hau, M3 hartzailean (eragin klinikoaren arduraduna) duen finkapen denbora luzeagatik dela proposatu da, M2 hartzailean (eragin desiragaitzen eragilea) duenarekin konparatuta.

162

Parametro zinetikoek eragina izan ditzakete ere efektu terapeutikoaren erantzulea den itu berbera denean eragin desiragaitzen erantzule, D2 dopamina-hartzailean eragiten duten antipsikotikoentzat deskribatu den bezala (Kapur & Seeman, 2000). Kasu honetan, antipsikotiko atipikoen finkapen-denbora laburra (klozapina konposatuarena, esaterako) eragin kaltegarri txikiagoekin erlazionatzen da. Modu honetan, D2 hartzailean finkapen denbora (k_{off} azkarra) duten antipsikotikoek, erantzun terapeutiko ona dute eta eragin desiragaitz gutxiago, finkapen denbora luzea duten antipsikotikoekin alderatuz.

Nahiz eta azken hamarkadetan nabarmen handitu den hartzaile kannabinoideen farmakologiari buruzko ezagutza, arreta gutxiago jarri zaio CB1 eta CB2 hartzaile horiei lotzen zaizkien konposatuen alderdi zinetikoak ikasteari. Farmakoak (*in vitro* nahiz *in vivo*) lotzeko zinetikaren azterketa sakona egiteak, azken batean, haren ekintza hobeto ulertzeko lagungarria izan daiteke. Gainera, ikuspegi horrek alderdi klinikoan hobekuntzak izaten lagundu dezake, bai farmakoen eraginkortasunarekin eta baita toxikotasunarekin zerikusia dutenak (Casarosa et al., 2009; Sykes et al., 2012, 2017; Tresadern et al., 2011).

Ligando eta hartzailearen arteko lotura zinetikak determinatzeko limitazioak

Zenbait estrategia erabili daitezke GPCRekin lotzen diren ligandoen parametro zinetikoak zehazteko. Zinetikoki aztertu nahi diren konposatuen banakako markaketa (radioisotopo edo fluoroforo bidez) ezinezkoa da praktikan, horrek kostu ikaragarria suposatuko bailuke. Hori dela eta, erabiltzen diren metodologia gehienek markatutako ligando batekin lehiatzen duten markatu gabeko ligando "hotz"-en azterketa inplikatzen du. Motulsky eta Mahan zientzialariek (Motulsky & Mahan, 1984) aurkeztutako proposamena da, seguruenik, konposatuen parametro zinetikoak ebaluatzeko metodorik erabiliena. Markatutako ligando baten eta hartzailearen arteko lotura monitorizatzean datza, hartzaile berera lotzeko lehiatzen duten ligando hotzen konzentrazio desberdinene presentzian. Kasu honetan, hartzailera lotzeko lehiatuko duten bi ligandoak (markatutakoa eta hotza) aldi berean gehitzen dira eta markatutako ligandoaren lotura neurtzen da. Markatu gabeko ligando hotzen presentziak aldatu egingo du markatutako ligandoaren lotura profila, hau da, bere k_{on} eta k_{off} parametroak, eta, beraz,

lehiatzen duten ligando hotzen parametro zinetikoak determinatu daitezke. Lehenik eta behin, beharrezkoa da markatutako molekularen parametro zinetikoak zehaztasunez kalkulatzea lehiaketarik ez dagoenean, ondoren ligando lehiakorren parametro zinetikoak kalkulatu ahal izateko. Motulsky eta Mahan metodologiaren ordezko ikuspegiak ere erabili izan dira ligando hotzen zinetikak kalkulatzeko. Proposatutako beste metodologia horiek oinarria markatutako ligandoaren loturan ematen den geldotzea da, hartzailea ligando hotzekin preinkubatu ondoren (Hara et al., 1995; Packeu et al., 2008, 2010).

Tradizionalki, erradioligandoak erabili izan dira ligandoek hartzaileekiko duten afinitatea eta propietate zinetikoak aztertzeko (Dowling & Charlton, 2006; Ramsey et al., 2011; Sykes et al., 2010). Hala ere, erradioligandoak erabiltzeak eragozpen asko ditu, hala nola, material erradioaktibo arriskutsuen manipulazioari lotutako arriskua eta prozedura horiei lotutako denbora eta kostu altuak. Gainera, esperimentu horien formatu tradizionalak zailtasunak aurkezten ditu zinetika azkarra duten ligandoen parametroak aztertzeko (Georgi et al., 2019; Sykes et al., 2019). Izan ere, esperimentu hauek aurrera eramateko ezinbestekoa da iragazketa prozesu bat, non hartzaileari lotutako eta lotu gabeko erradioligando frakzioa bereizten diren, eta horrek zaildu egiten du hasierako denbora tartearen datu zehatzak lortzea, bereziki garrantzitsuak direnak Motulsky eta Mahan eredua erabiliz datu zehatz eta fidagarriak lortzeko.

Azken hamarkadan zehar, TR-FRET (Schiele et al., 2015; Klein-Herenbrink et al., 2016) eta BRET (Stoddart et al., 2018; Bouzo-Lorenzo et al., 2019) bezalako erresonantzia energiaren transferentzian (RET: "*resonance energy transfer*") oinarritutako metodoek garrantzi handia izatea lortu dute farmakologia arloko ikerketan. Erresonantzia energia transferentzian oinarritutako metodologiek abantaila asko aurkezten dituzte, hala nola, irakurketa homogeneoa lortzen da (ez da bereizketarik egin behar lotutako eta lotu gabeko ligandoen artean) eta denbora goiztiarreko puntuak doitasun handiz eskuratzea ahalbidetzen dute, funtsezkoa dena ligandoen azterketa zinetikorako.

GPCR-tan eragiten duten farmakoen eraginkortasuna ulertzen ikuspegi molekular batetik

Eraginkortasunaren kontzeptua nabarmen aldatu da Stephenson-ek (1956) lehen aldiz hau azaldu zuenetik. Honek, gai aktibo batek hartzaile batekin elkartzean erantzun bat eragiteko duen ahalmena bezala deskribatu zuen eraginkortasuna. Proposatutako lehenengo sarraila eta giltza ereduan, hartzaileak ligandoarekin lotzean erantzun zelularra aktibatzeko gai den etengailu gisa jokatuko luke. Dena den, ikuspegi hau oso sinplista zela azaldu zen, proteina hartzaileen izaera dinamikoa dela eta.

Hartzaileen funtzioaren azalpen mekanizista eman nahi izan zuen lehen eredua "*two-state model*" izan zen, non hartzailearen bi egoera desberdinen arteko oreka deskribatzen zen (ikusi 2.irudia). Eredu horren arabera, hartzailearen bi egoerak (R, atseden-egoera eta R*, egoera aktibatua) konformazio-orekan egonik, gai izango dira farmakoa lotzeko. Agonistek R* nahiago duten bitartean, antagonistek R lotzeko joera izango dute, eta oreka hori R* egoera aktibatura (agonistak) edo R atseden egoerara (antagonistak) mugituko dute ligandoek.
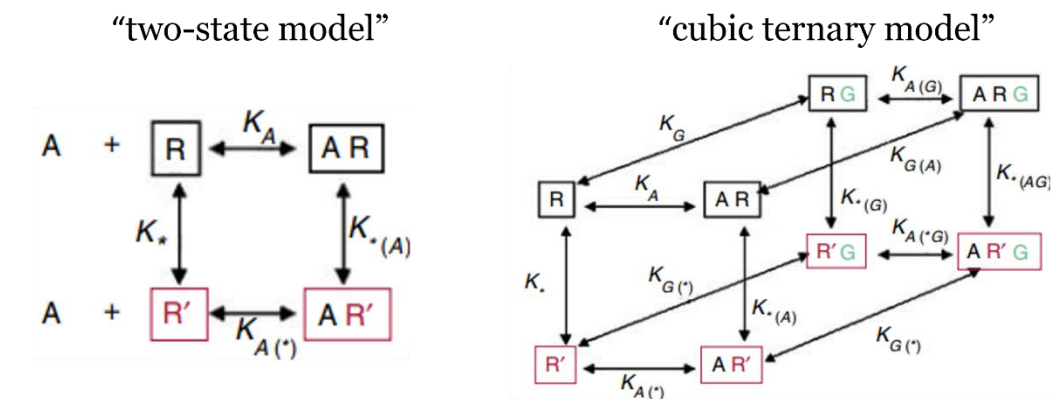
2. irudia. *Hartzailearen aktibazioa azaltzeko eredu desberdinak. Ezkerrean, "two-state model" ereduak itzulgarriak diren hartzailearen bi egoeren arteko oreka islatzen du; oreka hori aldatu daiteke A ligandoak R edo R* elkartzeko duen lehentasunaren arabera. Eskuinean, "cubic ternary model" eredua, non zelula barneko G proteinen elkarketak ere eragina duen hartzailearen egoeran. Rang, 2006-tik eraldatua.*

Ondoren, ereduak eboluzionatu zuen seinaleen transdukzioaren lehen urrats gisa hartzaileak G proteinetara akoplatzen zela ikusi zenean, eta G proteinek

hartzailearen egoeran efektua izango zuten elementu gisa proposatu ziren (Weiss et al., 1996)

Eredu horiek eraginkortasuna definitzeko hurbilketa gisa erabili badaiteke ere, gaur egun badakigu, proteina termodinamikan egindako azterketengatik, hartzaileen konformazio desberdin ugari egon daitezkeela orekan (Weis & Kobilka, 2018). Gainera, "bideratutako agonismoa" ("*biased agonism*") fenomenoak, oraindik gehiago konplikatzen du GPCR hartzaileen ekintza mekanismoa ulertzea maila molekularrean. Bideratutako agonismoak deskribatzen duena honakoa da: ligando batek seinaleztapen bideren bat aktibatzeko izan dezaketen lehentasuna edo joera beste batzuen gainetik, hartzaile batera lotzen denean. Ikuspegi honek GPCR hartzaileen aktibazioak duen konplexutasun maila agerian jartzen du, eta zaildu egiten du eredu berrien garapena.

Black and Leff zientzialariek (Black & Leff, 1983) proposatutako agonista eredu operazionala ikuspegi baliotsua da bideratutako agonismoa (selektibitate funtzionala izenarekin ere ezagutzen dena) definitu eta kuantifikatzeko, eta azken hamarkadetan asko aplikatu da farmakoen eraginkortasuna ikasteko. Hala ere, eredu horrek ikuspegi enpirikoa baino ez du, eta farmakoen ekintza kuantifikatzeko erabilgarria izan arren, ez du gaitasunik hartzaileak maila molekularrean duen aktibazioa mekanikoki ulertu eta deskribatzeko.

Gainera, hartzailearen aktibazio prozesuan lotura zinetikak duen eragina ez dago argi oraindik. Nahiz eta kasu askotan frogatu den ezaugarri zinetiko espezifikoak emaitza kliniko hobeekin erlazionatzen direla, zinetikaren inplikazioa hartzailearen aktibazio prozesuan aztertu beharreko alderdia izaten jarraitzen du.

1960ko hamarkadaren hasieran, Paton-ek proposatu zuen, sortzen ziren farmako-hartzaile konplexu zenbakiek definituko zutela farmako baten eraginkortasuna, hartzaileen okupazio maila ordez (Paton, 1961). Proposatzen zenaren arabera, farmako baten eraginkortasuna estu lotuta egongo litzateke lotura parametro zinetikoekin, hauek mugatuko baitute sortzen eta disoziatzen diren ligando-hartzaile konplexu zenbakia. Paton-ek hipotesi hau proposatu zuen: ligandoa elkartu eta hartzailea aktibatu ondoren, beharrezkoa izango litzateke hartzailea "berrezartzea", beste ligando bat elkartuz, aktibazio-ziklo berri bat

166

sortu aurretik. Ideia horren arabera, disoziazio azkarra duten farmakoek (k_{off} azkarra, finkapen-denbora laburra) modu eraginkorrago batean aktibatuko dituzte zelula barneko seinaleak, eta disoziazio moteleko farmakoek (k_{off} geldoa, finkapen-denbora luzea) eraginkortasun txikiagoa izango lukete.

Aktibazio-prozesua oreka-prozesu gisa deskribatzeko mugez jabeturik, zenbait ahalegin egin dira alderdi zinetikoak kontuan hartzen dituzten ereduak garatzeko (Kinzer-Ursem & Linderman, 2007; Shea et al., 2000; Waelbroeck et al., 1997). Eredu horiek modelo ternariotik eratortzen dira, non espezieen eraketaren alderdi zinetikoak ere kontuan hartzen diren. Hala ere, eredu horiek ez dute bereziki kontuan hartzen ligando-hartzaile loturaren alderdi zinetikoa. Proposamen hauetatik ondorioztatu daiteke, Paton-en ereduaren kontra, finkapen-denbora luzeko ligandoek erakutsiko luketela eraginkortasun handiena; izan ere, hartzailea denbora tarte luzeago batean zehar egonkortzeak G proteina aktibatzeko ziklo gehiago ahalbidetuko lituzke, eta finkapen denbora motza dutenek, berriz, ez lituzkete hartzaileak egonkortuko efektoreen aktibazioa eragiteko behar beste denboraz.

Bideratutako agonismoa

Bideratutako agonismoa edo selektibitate funtzionala ligandoek seinaleztapen bide bat lehentasunez aktibatzeko duten gaitasuna da, beste bide batzuen gainetik.

Kontzeptu hau garatu aurretik, hartzailearen aktibazioa era monotonikoan ikusten zen, non eraginkortasunaren intentsitatea besterik ez zitekeen aldatu, baina ez honen izaera kualitatiboa. 80ko hamarkadara arte, prozesu konplexuen ondorioz integratutako eragin gisa neurtzen ziren erantzun farmakologikoak, hala nola muskulu-uzkurdura ehun isolatuetan, edo neurri biokimikoak (AMPz metaketa, esaterako). Hala ere, sistema heterologoen garapena eman zenean eta erantzun zelularren karakterizazio zehatzagoa egiteko gaitasuna dela eta, GPCRekin elkarreragiten duten hainbat bide eta efektu aurkitu ziren. Honekin argi geratu zen hartzaileak aktibatzean ematen den erantzunaren izaera ez zela kuantitatiboki bakarrik aldatzen. Hartzailea aktibatzeko erabilitako agonistaren araberako aktibazio-patroi desberdinak behatzean, eraginkortasunaren kontzeptua ere termino kualitatiboetan deskribatu zitekeela ondorioztatu zen.
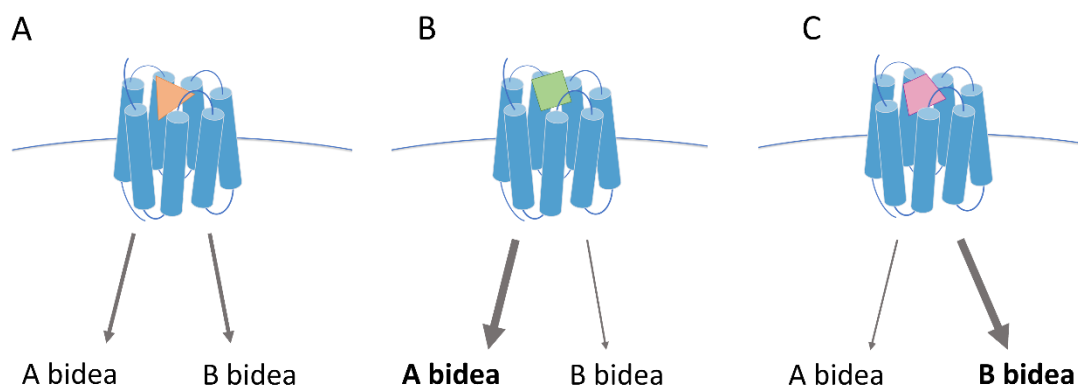
3. irudia. *Bideratutako agonismoaren irudikapen eskematikoa GPCRetan. Zenbait ligandoek ez dute lehentasunik aurkeztuko bide desberdinen aktibazioa pizteko orduan eta, beraz, konposatu orekatuak izango dira(A). Beste ligando batzuek, berriz, bide jakin bat aktiba dezakete lehentasunez, eta, beraz, ligandoa lotzean hartzaileek eragindako zelula barneko erantzuna bideratu dezakete, bide jakin bat lehentasunez aktibatuz beste baten aurrean (B eta C).*

Ideia horrek iradokitzen du hartzailea ez dela zelula barneko prozesuen aktibazioa determinatzeko gutxieneko osagaia, baizik eta hartzaile-ligando konplexua dela eragina definituko duena (ikusi 3. irudia). Paradigma berri hori ideia honekin batera aurkeztu zen: ez dago hartzailearen konformazio aktibo bakar bat, konformazio desberdin ugari baizik, eta horiek ahalmen desberdina izango dute proteina efektoreak aktibatzeko. Alde horretatik, GPCRek proteina alosteriko gisa jardungo lukete. Proteina horiek zenbait konformazio desberdin har ditzakete lotutako ligandoaren izaeraren arabera, eta zelula barneko proteina efektoreekiko lotura komunikatzaile gisa jardun, modu desberdinean. Efektoreen aktibazio desberdin hori lortzeko, ligandoa hartzailera lotzen denean aldaketak eragiten dira hartzailearen konformazioan (induzitutako konformazioa) edota orekan dauden proteinaren konformazio desberdinak egonkortzen dira (konformazio hautapena). Honek, ikuspegi konplexuago batetik aurkezten du GPCRen aktibazioa, farmakologia klasikoak deskribatutako eskema dikotomikoaren ordez, non hartzaileek aktibo edo inaktibo egoerak soilik izan ditzaketen.

Beraz, probabilitate eredu batek GPCRen egoera edo konformazio desberdin asko izango lituzkeen eszenatoki bat deskribatuko luke, maiztasun-banaketa partikularra erakutsiz (Onaran & Costa, 1997; Onaran et al., 2000). Egoera

desberdinen arteko oreka aldatu egingo da ligando bat lotzean, eta, beraz, hartzaileen konformazio posibleen maiztasunaren banaketa aldatu egingo da. Eredu horren arabera, ligando bat elkartzeak konformazio egoera batzuei mesede egingo die eta beste batzuk baztertuko ditu, aurkitu daitezkeen konformazioen paisaia selektiboki aldatuz. Hartzailearen teoriaren eredu klasikoak aurkezten duen ikuspegitik urrun, eredu probabilistikoak hartzailearen konformazio egoera ugari hartzen ditu kontuan, eta, beraz, paradigma zabalagoa aurkezten du, eraginkortasunaren kontzeptua dimentsio ugari dituen elementu gisa ulertzeko.
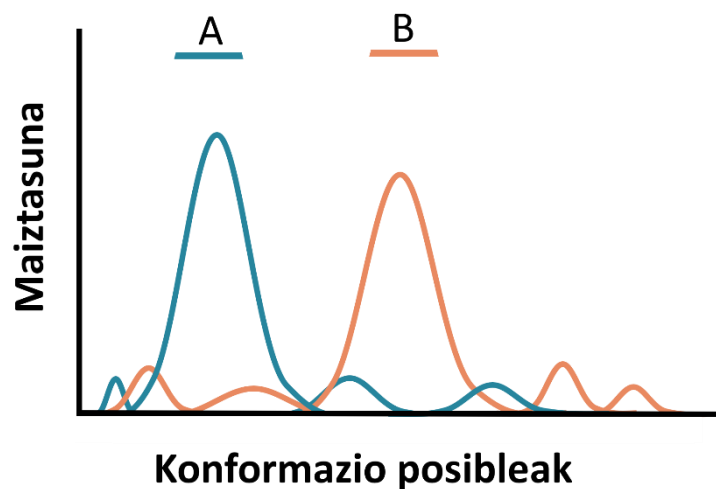
4. irudia. *GPCR-en konformazio-egoeren maiztasunen banaketa ligandoa lotzean. A ligandoak batez ere efektore batekiko afinitate handiagoa aurkezten duten konformazioak egonkortuko lituzke (adibidez, G proteinak); B ligandoak, berriz, beste efektore batekiko afinitate handiagoa duten konformazioak egonkortuko lituzke (adibidez, arrestinak).*

Eredu horren arabera, ligandoaren lotura ematean egonkortutako hartzailearen konformazio motak eta honen maiztasunak zehaztuko luke eraginkortasuna. 4. irudian ikusi daitekeenez, zenbait ligandok aldatu egingo dute konformazioen banaketa G proteinekin lotuko diren konformazio egoerak egonkortuz; ligando desberdin bat elkartzean, berriz, beste efektore batzuk (arrestinak, esaterako) aktibatzeko joera handiagoa duten zenbait hartzaileen konformazioak sor daitezke (Kenakin, 2004).

Azken hamarkadan egindako azterketa biofisikoek frogatu dute β2 hartzaile adrenergikoaren era askotako konformazioak ematen direla aldi berean (Manglik et al., 2015), eta fenomeno berdina ikusi da baita rodopsina hartzailearekin (Van

Eps et al., 2017) beren egoera ez-aktiboetan. Gainera, azterketek erakutsi zuten hartzailea agonistarekin edo argiarekin aktibatu ondoren ere konformazio heterogeneotasuna jarraitzen zuela nahiz eta oreka egoera aldatu. Azterketa horiek GPCRen konformazioen aniztasuna erakutsi zuten, bai atseden egoeran dauden hartzaileetan, bai aktibatutako hartzaileetan ere. Ikusitako konformazioen aniztasun hori selektibitate funtzionala azaltzeko eredu probabilistikoak planteatutakoarekin bat etorriko litzateke (Gurevich & Gurevich, 2020).

Bideratutako agonismoaren kontzeptuak interes handia sortu zuen farmakologiaren arloan, zelula prozesuak selektiboki aktibatzeko aukera berriak aurkeztu baitzituen. Gainera, fenomeno horrek terapia selektiboagoak garatzeko aukera eman dezake, hartzaileak modu selektiboan aktibatuz, nahi den efektua eragiten duen seinale kaskaden aktibazioa soilik emateko. Horrek aukera eman dezake GPCRei zuzendutako terapia hobeagoak garatzeko eta seinaleztapen bide batzuk aktibatzearen ondoriozko albo-ondorioak ezabatzeko. Beraz, onura hori bereziki garrantzitsua da eragin desiragaitzen agerpenak terapia farmakologiko berrien garapena mugatu duten kasuetan. Selektiboki aukeratutako aktibazio-profila duten farmakoek tratamendu sofistikatuak suposatuko lituzkete, jarduera kliniko hobea izateko eta nahi ez diren ondorioak saihesteko.

Agonistek eragiten duten bideratutako agonismoaren kuantifikazioari dagokionez, zenbait estrategia har daitezke erantzun zelularren eraginkortasuna sailkatzeko. Agonistak sailkatzeko metodorik sinpleena EC_{50} potentzia balioak erabiltzea da, konposatuek sistemaren aktibazio maximoa dutenean eta, beraz, agonista oso gisa jarduten dutenean. Hala ere, metodo hori ez da egokia efektu partziala duten ligandoak karakterizatzeko; izan ere, agonisten efektua deskribatzen duten potentziaren balioak eta E_{max}-en balioak (E_{max}: efektu maximoa) kontuan hartu behar dira agonistak behar bezala aztertzeko. Agonisten bideratutako erantzuna karakterizatzeko estrategia hedatuenak aktibitate erlatiboaren (RA: *relative activity*) edo "transdukzio-koefizienteen" (τ/K_A) arteko erlazioen konparazioa dira (Kenakin & Christopoulos, 2013). Aktibitate erlatiboa erantzun maximoaren eta EC_{50} balioaren arteko erlazioaren bidez definitzen da ($RA = E_{max}/EC_{50}$), eta neurri erabilgarria da bide desberdinen arteko agonisten efektuak alderatzeko, potentzia eta efektu maximoa kontuan hartuta (Ehlert,

2008). Black eta Leff zientzialariek (1973) garatutako eredu operazionalak transdukzio-koefizientea (τ/K_A) proposatu zuen agonisten efektuak konparatzeko. τ parametroak agonistak sisteman duen barne eraginkortasuna, hartzailearen dentsitatea eta akoplamendua integratzen ditu. Bi metodoak, aktibitate erlatiboak (RA) eta transdukzio-koefizienteak (τ/KA) kontuan hartzen dituztenak, asko erabiltzen dira gaur egun agonisten efektuak ebaluatzeko eta bideratutako agonismoa kuantifikatzeko (Kenakin & Christopoulos, 2013; Kolb et al., 2021). Hala ere, nahiz eta aktibitate erlatiboaren erlazioen kalkulua (E_{max}/EC_{50}) sinpleagoa izan, aztertutako dosi-erantzun kurbek unitatetik gertu dagoen malda dutenean baino ez da erabilgarria, eta horrek metodo honen erabilera egoera jakin batzuetara soilik mugatzen du. Orokorrean, beraz, eredu operazionala da bide ezberdinen artean agonisten efektuak sailkatzeko metodorik erabiliena.

Helburuak

Aurreko ataleta aurkezten diren erronkak behin azalduta, doktoretza tesi honen helburu nagusiak hauek dira:

1. Metodo fidagarri bat garatzea, konposatu kannabinoideen propietate zinetikoak karakterizatzeko giza CB1 eta CB2 hartzaileekin lotzean.

2. Konposatu kannabinoideen asoziazio eta disoziazio abiadura konstanteak (k_{on} eta k_{off}) karakterizatzea, eta, beraz, konposatu kannabinoideak CB1 eta CB2 hartzaileetan duten finkapen denbora zehaztea, Motulskyk eta Mahanek proposatutako eredua erabiliz.

3. Konposatu kannabinoide agonisten seinaleztapen propietateak karakterizatzea CB1 eta CB2 hartzaileekin lotzean. Horretarako, ligando agonistek eragindako β-arrestina 2 erreklumendua, miniG proteinen akoplamendua eta hartzaileen internalizazioa neurtzeko gai diren entseguak garatzea, eta konposatuen selektibitate funtzionala kalkulatzea, eredu operazionala erabiliz.

4. CB1 eta CB2 hartzaile kannabinoide agonisten finkapen denboraren eta seinaleztapenaren eraginkortasunaren arteko erlazioa aztertzea karakterizatutako seinaleztapen bide desberdinetan.

2. METODOLOGIA

PLASMIDOEN PRESTAKETA

SNAP-CB1, SNAP-CB1 $_{55-472}$, SNAP-CB1 $_{91-472}$, SNAP-CB2, SNAP-CB1-Nluc, eta SNAP-CB2-Nluc kodetzen duten plasmidoak prestatu ziren. Proteina desberdinen DNA sekuentziak pcDNA4/TO plasmidoan klonatu ziren Gibson metodoa erabiliz (Gibson, 2011).

Modu honetan, CB1 eta CB2 hartzailearen sekuentzia osoa espresatzen zuten plasmidoak sortu ziren, eta baita CB1 hartzailearen bi aldaera desberdin espresatzen zutenak, N-muturreko lehen 54 edo 90 aminoazidoak ezabatuz (SNAP-CB1 $_{55-472}$ eta SNAP-CB1 $_{91-472}$, hurrenez hurren). Hartzaile guztiek, SNAP fusio proteina ere espresatzen zuten bere N-muturrean.

Bestalde, Nanoluc fusio proteina bere C-muturrean espresatzen zuten CB1 eta CB2 hartzaileak kodetzen zituzten plasmidoak ere sortu ziren metodo berdina jarraituz. Kasu honetan, GSSG peptido sekuentzia malgua txertatu zen hartzailearen C-muturra eta Nanoluc proteinaren artean.

Prestatutako plasmido guztien sekuentziak zuzenak zirela egiaztatu zen errestrikzio entzimen bitarteko digestio bidez eta agarosazko gel elektroforesi bitartez aztertuz. Gainera, Sangar sekuenziazioa erabilli zen plasmidoen sekuentziak zuzenak zirela egiaztatzeko.

ZELULA LERRO EGONKORRAK

HEK293-TREx™ zelula lerroa (Thermo Fisher Scientific) erabili zen zelula lerro egonkorrak sortzeko. HEK293-TREx zelula lerroak TetR tetraziklinaren aurkako erresistentzia geneen erregulatzailea duen plasmidoa espresatzen du. Modu honetan, pcDNA™6/TR plasmidoak kodetutako Tet proteina errepresorea (TR) sintetizatzen da eta honek, pcDNA4/TO plasmidoan kodetutako proteinaren transkripzioa geldiaraziko du TetR-ek kontrolatutako geneetan. Tetraziklina antibiotikoa erabiltzen denean, ordea, Tet proteinaren konformazioa aldatzen da, eta pcDNA4/TO plasmidoak kodetzen duen sekuentziaren transkripzioa ez da oztopatuko. Modu honetan, tetraziklina bidez kontrolatzen da geneen espresioa erabilitako bigarren bektorean (ikusi 5. irudia).

Sistema honek blastizidina eta zeozina antibiotikoak beharrezkoak ditu bi bektoreen presioa selektiboa mantentzeko. Horrela, blastizidinaren bitartez

pcDNA™6/TR plasmidoaren egonkortasuna bermatzen da gure zelula lerroan, eta zeozinaren bitartez pcDNA4/TO-rena. Izan ere, plasmido hauek badituzte antibiotiko hauekiko erresistentzia geneak.

Sistema honen bitartez, gure intereseko proteinen espresio maila altuak lortzen dira.
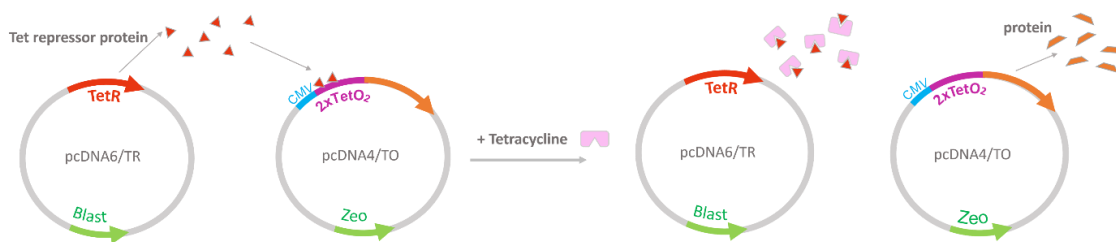
5. irudia. *TREx sistemaren eskema. Gure intereseko genearen transkripzioa (gezi laranja) Tet proteina errepresoaren bitartez galarazten da tetraziklina ez dagoenean. Tetraziklina erabiltzean, ordea, errepresore proteinak ezin izango du TetO2 sekuentzia operadorera lotu eta genearen espresioa emango da.*

Transfekzio protokoloa

HEK293-TRex zelulak FBS % 10an eta blastizidina 5 µg/ml osagarri gisara duen DMEM medio osoan inkubatu ziren 37 °C-tara % 5-ko CO2-a duen atmosfera hezean. Zelulen transfekzioa HEK293-TRex zelulak fase exponentzialean zeudenean (% 80-90 konfluentzian) burutu zen T75 ontzietan. Zelulei medio aldatu zitzaien transfekzioa burutu baino 1 h lehenago, eta % 10 FBS, penizilina 100 I.U/ml eta estreptomizina 100 µg/ml osagarri giza zituen 5 ml DMEM-ekin inkubatu ziren zelulak. Transfekzioak burutzeko erabilitako DNA:PEI ratioa 1:3-koa izan zen. Guztira, 5 µg DNA eta 15 µg PEI erabili ziren 75 cm²-ko ontzi bakoitza transfektatzeko. DNA 250 µl OptiMEM-arekin nahastu zen eta PEI, beste 250 µl OptiMEM-arekin. DNA eta PEI diluzioak nahastu ziren eta giro tenperaturan 20 minutuz inkubatu ondoren, zelulen gainean isuri zen nahastea.

Hurrengo egunean, (transfekzioa burutu zenetik ~16 h igaro zirenenan), zelulen medioa aldatu zen eta 15 ml medio berri (DMEM + 10% FBS) gehitu zitzaien kultiboei. Bigarren egunean, kultiboak kutxa berrietan erein ziren 1:5 banaketa burutu ostean, hau da, itsatsitako zelulak tripsinarekin tratatu eta % 20a kultibo kutxa berrian erein zen. Erabili zen medioa % 10 FBS, blastizidina (5 µg/ml) eta zeozina (20 µg/ml) antibiotikoak osagarri gisa zituen DMEM izan zen. Medioa 2-3 egunero aldatu zen, kolonia erresistenteak lortu ziren arte (2-3 aste).

Azaldutako prozedura zelula lerro desberdinak sortzeko erabili zen. Alde batetik, HEK TR-SNAP-CB1 (sekuentzia osoko hartzailea eta trunkazioa zuten aldaerak) eta HEK TR-SNAP-CB2 zelula lerroak ligando-hartzaile lotura entseguak burutzeko mintzen prestaketarako erabili ziren. Bestalde, HEKTR-SNAP-CB1-Nluc_βarr2-Venus eta HEKTR-SNAP-CB2-Nluc_βarr2-Venus zelula lerro egonkorrak ere sortu ziren, kasu honetan bi DNA desberdinen kotransfekzioa burutuz. Erabilitako plasmidoek SNAP N-muturrean atxikia eta Nanoluc C-muturrera atxikia zuen CB1 edo CB2 hartzailea (pcDNA4/TO) eta Venus proteina C-muturrean atxikita zuen β-arrestin 2 biosentsorea kodetzen zuten (pcDNA3).

ZELULA LERRO IRAGANKORRAK

HEK 293T/17 zelulak (ATCC, CRL-11268™) erabili ziren transfekzio iragankorrak burutzeko. Bi plasmido desberdin erabili ziren aldi berean: batak biosentsorea kodetzen zuen (NES-Venus-mGsi edo β-arrestin 2-Venus), eta besteak, hartzailea SNAP-CB1-Nluc edo SNAP-CB2-Nluc). Biosentsorea kodetzen zuten plasmidoak pcDNA3 motakoak ziren, eta biosentsoarea kodetzen zutenak, aldiz, pcDNA4/TO plasmidoak.

Transfekzioak burutzeko erabilitako DNA:PEI ratioa 1:3-koa izan zen. Hartzaile eta biosentsore desberdinen ratioak prestatu ziren eta 96 putzuko plakako 12 putzu transfektatu ziren kondizio bakoitzarekin, 1 µg DNA eta 3 µg PEI erabiliz. Guztira 1 µg DNA baino gutxiago erabili behar bazen, zatitutako izokin esperma DNA (Invitrogen) erabili zen DNA kantitatea konstante mantentzeko baldintza guztietan. DNA 100 µl OptiMEM-ean nahastu zen, eta PEI beste 100 µl OptiMEM-ean. Diluitutako DNA eta PEI nahastu ziren eta 20 minutuz inkubatu ziren giro tenperaturan. DNA-PEI nahasketak 1.2 ml zelula suspentsio batera gehitu ziren eta tutua zenbait aldiz biratu zen transfekzio medioa era homogeneoan sakabanatzeko. Azkenik, zelula suspentsioa putzuetan erein zen, 100 µl gehituz putzu bakoitzean. Plakak, poli-D-lisinarekin estalitakoak eta esterilak ziren, zelulen kultiborako aproposak.

Plaka osoa transfektatzeko, prozedura berdina erabili zen DNA eta PEI kantitate proportzionalak erabiliz (DNA 8 µg eta PEI 24 µg). Aurreko entseguak kontuan hartuta, aukeratu zen hartzaile:biosentsore ratio aproposa 1:9-koa izan zen,

beraz, hartzailea eta biosentsorea kodetzen zuten 0.8 ng eta 7.2 ng plasmido erabili ziren, hurrenez hurren, plaka oso bat transfektatzeko.

Zelula suspentsioa prestatzeko fase exponentzialeean zegoen HEKT/17 zeluen T75 ontzi bat erabili zen, ~% 90 konfluentzia zuelarik. Tripsinarekin tratatu eta zelulak jaso ostean, zelulen konzentrazioa kalkulatzen zen tripan urdina erabiliz, zelula kontatzeko gailu elektronikoan (Countess™ 3 FL (Invitrogen)). Azkenik, beharrezko medio kantitatea (% 10 FBS zuen DMEM) gehitu zen 40,000 zelula/ml-ko suspenstsioa lortzeko

Transfektatutako kultibo plakak 37 °C-tan inkubatu ziren, % 5eko CO_2-a duen atmosfera hezean. Transfekzioa burutu zenetik 48 h igarotakoan burutu ziren esperimentuak, proteinen espresioa ahalbidetzeko.

ZELULEN MARKAKETA TERBIO KRIPATOA ERABILIZ

SNAP-CB1, SNAP- $CB1_{55-47}$, SNAP- $CB1_{91-472}$ edo SNAP-CB2 modu egonkorrean espresatzen zituzten HEK293-TREx zelula lerroen kultiboa T175 ontzietan prestatu zen, % 10 FBS eta blastizidina (5 µg/ml) eta zeozina (20 µg/ml) antibiotikoak osagarri bezala zituen DMEM medioan. Hartzaileen espresioa tetraziklina antibiotikoa (1 µg/ml) erabiliz induzitu zen zelulen kultiboak ~ % 90-ko konfluentzia zutenean. Tetraziklina gehitu eta 48 h igarotakoan, zelulen medioa baztertu eta bitan garbitu ziren itsatsitako zelulak: lehenengo 5 ml PBSrekin eta ondoren 5 ml LABMED tanpoiarekin. Ondoren, 100 nM SNAP-Lumi4-Tb zuen Tag-lite (LABMED) tanpoia gehitu zen zelulen ontzietara eta 1 orduz inkubatu ziren 37 °C-tara, % 5 CO2-arekin eta giro hezean, hartzaileen SNAP molekula terbioarekin markatzeko (FRET energia emailea), 6. irudian agertzen den erreakzioa emanez.
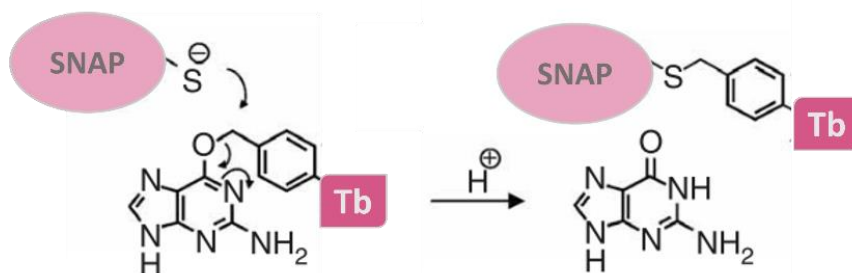

6. irudia. *SNAP proteinaren eta terbioaren (Tb) arteko erreakzio kobalentearen eskema. SNAP proteinaren zisteinak terbioarekin konjokatutako benzilguaninarekin erreakzionatu ostean, terbioa SNAP proteinara lotzen da lotura kobalente baten bidez.*

Ondoren, ~5 ml PBS erabili ziren bitan zelulak garbitzeko eta zelulak tanpoi ez-entzimatiko bat erabiliz jaso ziren. Jasotako zelulak DMEM medioarekin zentrifugatu ziren 5 minutuz 200 x g-tara, eta lortutatako zelula pellet-a -80 °C-tara gorde zen mintz prestaketa burutu arte.

ZELULA MINTZEN PRESTAKETA TERBIOAREKIN MARKATUTAKO ZELULAK ERABILIZ

Zelula pelletak desizoztu ziren izotzean murgildutako tanpoi hotza erabiliz (10 mM HEPES eta 10 mM EDTA, pH 7.4). Zelulen homogenizazioa 4°C-tan burutu zen Ultra-Turrax (Ika-Werk GmbH & Co. KG, Staufen, Germany) erabiliz. Ondoren, homogenizatutako zelulak 5 minutuz zentrifugatu ziren 1,200 x g indarrarekin. Lehen zentrifugazio honen ostean lortutako pelleta zelula nukleoak eta bestelako mintz astunaz osatuta, baztertu egin zen. Lortutako gainjalkina ultrazentrifugazio bidez prozesatu genuen 48,000 x g-ko indarrarekin (Beckman Avanti J-251 Ultracentrifuge; Beckman Coulter, Fullerton, USA). Gainjalkina baztertu ostean, ultrazentrifugazio bitartez lortutako pelleta berriro homogezitu genuen tanpoi berriarekin Ultra-Turrax erabiliz, eta bigarren ultrazentrifugazio ziklo bat (30 minutuz 4 °C-tan, 48,000 x g) burutu genuen. Mintzak lortzeko prozesuaren eskema aurki daiteke 7. irudian.
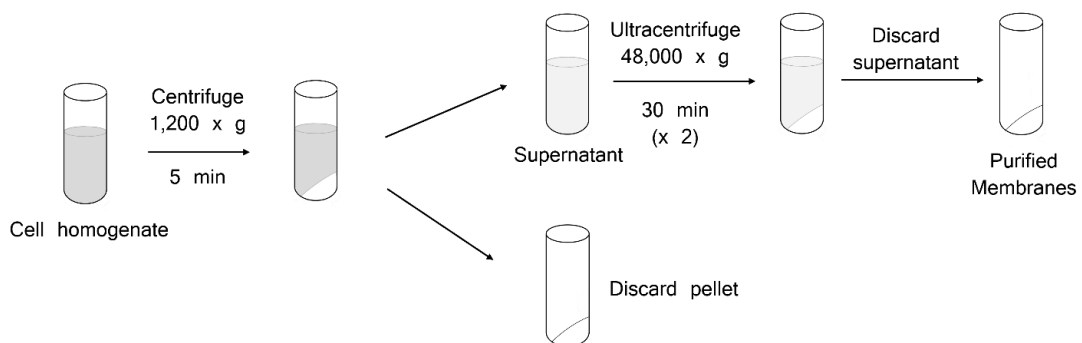
7. irudia. *Zelula homogenatutik habiatuta mintz prestaketa burutzeko pausoen eskema orokorra.*

Lortutako pelletari tanpoi bolumen txiki bat gehitu genion (10 mM HEPES eta 0.1 mM EDTA, pH 7.4) eta pipeta erabiliz suspentsio homogeneoo bat lortu arte nahastu genuen. Ondoren, gure laginaren proteina kantitatea neurtu genuen

azido bizinkonikoaren metodoan oinarritutako zuen kit erabiliz (Sigma-Aldrich). Behin proteina kantitatea kalkulatuta, 5 mg/ml-ko kontzentrazioa zuten mintz alikuotak prestatu eta -80 °C-tan gorde genituen.

TR-FRET teknologia

TR-FRET (*Time-resolved fluorescence energy transfer*) ligando eta hartzaileen arteko lotura ikasteko erabili izan den metodoa da farmakologia arloan. Metodo honek TRF (*Time-Resolved Fluorescence*) eta FRET (*Försters Resonance Energy Transfer* konbinatzen ditu.

FRET (Försters Resonance Energy Transfer) fenomenoa Theodor Förster zientzialari alemaniarrak deskribatu zuen 40ko hamarkadan lehen aldiz (Förster, 2012). Fenomeno honetan, energia ez-erradiatiboaren transferentzia ematen da energia-emaile eta energia-hartzaile diren bi molekulen artean. Energia tranferentzia hau eman dadin zenbait baldintza bete behar dira: alde batetik, bi molekulen arteko distantzia < 10 nm izan beharko da, eta bestetik, hartzaile eta emailearen xurgapen espektroak gainezartzea ezinbestekoa izango da. Baldintza hauek betetzean, FRET fenomenoa gertatuko da, eta energia-emaileak igorritako energiaren intentsitatea txikitu egingo da, eta energia-hartzailearena handituko da.

FRET pareen energia espektro tontorrak selektiboki neurtzeko hauek banunduta agertu beharko dira, baina aldi berean ezinbestekoa izango da bi espektroak gainezartzea bi molekulen arteko energia transferentzia eraginkorra izan dadin, 8.irudian irudikatzen den moduan.
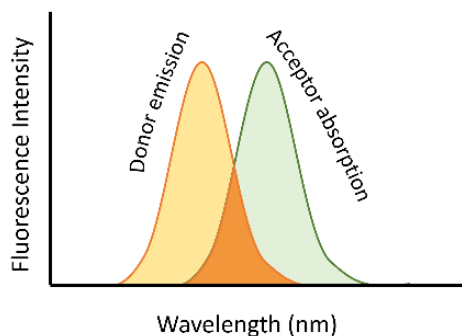
8. irudia. *"FRET parea" osatzen duten bi molekulen emisio eta xurgapen espektroen errepresentazioa. Bi espektroen gainezartzeak baimenduko du FRET energia transferentzia ematea.*

TR-FRET teknikari esker, desiragarriak ez diren autofluoreszentzia eta bestelako seinaleen biltzea eragozten da. Teknika honekin, denbora atzerapaen batekin neurtzen da laginaren emisioa hau laser edo xenon iturriekin kitzikatu ostean (ikusi 9.irudia). Horrela, lagina kitzikatu eta berehalakoan sortu daitezkeen zarata seinaleak saihesten dira. Hau posiblea da energia-emaile bezala erabiltzen diren lantanidoak milisegundo ordeneko energia emisio luzea dutelako (Degorce et al., 2009).
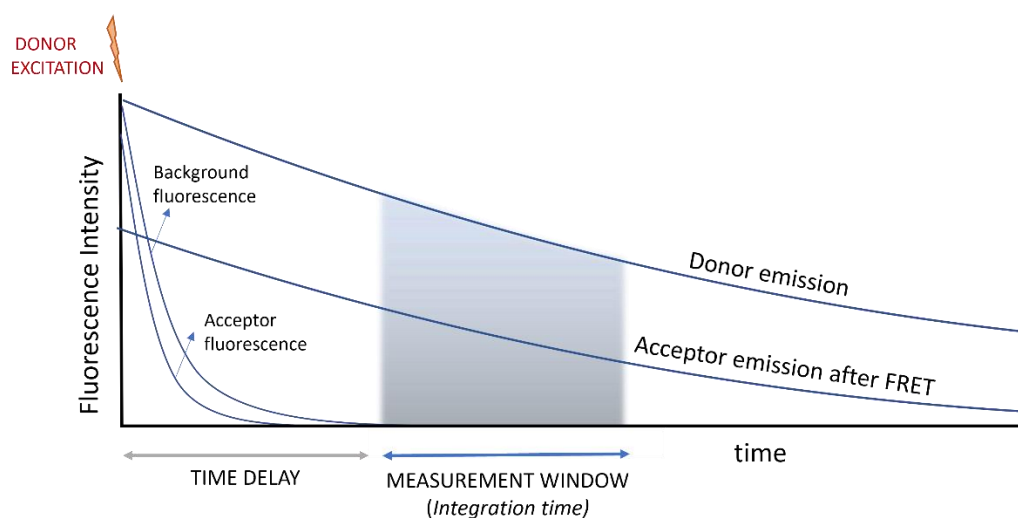
9. irudia. *"Time-resolved FRET" metodologiaren aurkezpena. Lagina laserrarekin kitzikatzen denetik seinalea hartu arte igarotako denbora tarteak aukera ematen du hasieran eman daitezkeen eta FRET-etik ez datozen fluoreszentzia seinaleak baztertzeko. Energia emaile moduan jarduten duten lantanidoak (Europioa edo Terbioa) denboran luzea den emisioa dutenez, FRET energia -hartzaileak emailearen energia xurgatzen jarraituko du zenbait milisegundotan zehar.*

Lantanidoak erabiltzen dira energia-emaile bezala TR-FRET metodologian. europio edo terbio ioien fluoreszentzia handitzeko, ioi hauekin sortutako kelatoak edo kriptatoak erabiltzen dira hauen fluoreszentzia propietateak hobetzeko. Modu honetan, energiaren metaketa eta transferentzia propietateak hobetzen dira. Terbioak igortzen duen energia europioarena baino 10 aldiz handiago da, beraz, TR-FRET-ean erabiltzeko aproposagoa da. Gainera, lantanidoen kriptato edo kelatoak oso egonkorrak direnez, entsegua baldintza desberdinetan burutzea posible da.

TR-FRET -EN APLIKAZIOA LIGANDO-HARTZAILE LOTURA IKERTZEKO

HTRF emission ratio: $\frac{aceptor\ emission}{donor\ emission} \times 10000$
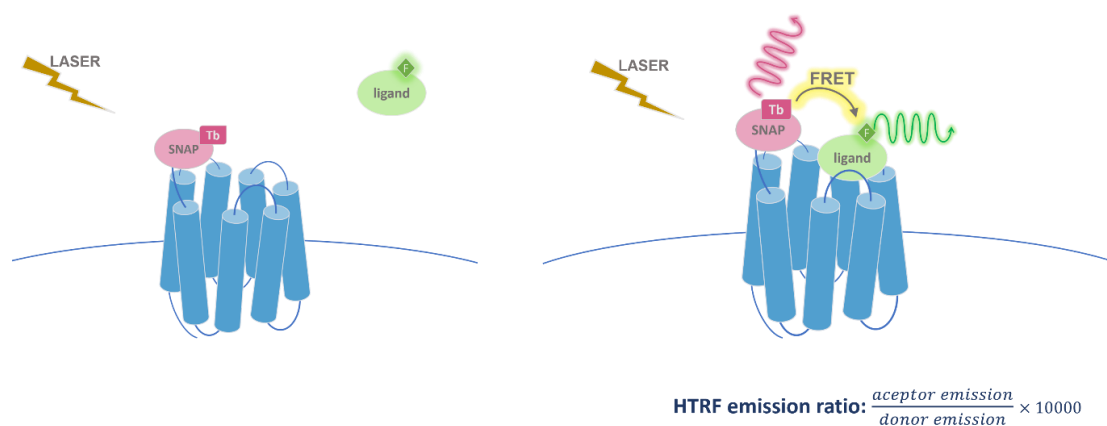
10. irudia. *TR-FRET printzipioaren irudikapen eskematikoa ligando eta hartzaileen arteko lotura entseguetan. Irudian, Terbioareekin (Tb) markatutako GPCR bat ageri da, energia emaile gisa jarduten duena, eta fluoroforo batekin (F) lotutako ligandoa, hartzaile moduan jardungo duena. Laser-iturriak terbioa kitzikatzen duenean, energia ligando fluorezenteari transferituko zaio eta FRET gertatuko da energía hartzailea eta emialea gertu egonez gero ("10 nm"). FRET (gezi berdea) ematean HTRF emisioen zatidura kalkulatuko da energía hartzailearen (ligandoaren fluoroforoa) eta energía emailearen (terbioa) arteko zatiketa eginez.*

TR-FRET-ek eskaintzen dituen abantailez baliatzeko, beharrezkoa da hartzaileak aldatzea eta zelulaz kanpoko N-terminalean SNAP markaketa jartzea. SNAP proteinak modu kobalentean erreakziona dezake terbioa (energia-emailea) lotzeko (Keppler et al., 2003). Erreakzio itzulezin horri esker, FRET energia-emaile gisa diharduen molekula luminiszente batekin markatu ahal izango dira hartzaileak (Maurel et al., 2008).

Estrategia hau CB1 eta CB2 giza kanabinoide hartzaileei lotzen diren konposatuen lotura detektatzeko erabiltzen dugu. Nabarmendu behar da CB1 hartzaileak N-terminal zelulaz kanpoko domeinu oso luzea duela, nahiko arraroa A klaseko GPCR familiaren artean. Hori dela eta, badirudi ezinbestekoa dela zelulaz kanpoko eremuan aminoazido-sekuentzia laburtzea FRET seinalea lortzeko. Hartzailearen proteina-sekuentziaren ezaugarriek eta ligandoaren lotura lekuak mugatu egingo dute estrategia hori erabiltzea ligandoen lotura hautemateko, Izan ere, emailearen (SNAP-i lotutako terbioa) eta hartzaile gisa jarduten duen ligando fluoreszentearen arteko distantzia laburra funtsezkoa da FRET seinalea lortzeko.

"MOTUSLKY & MAHAN" EREDUA: ASOZIAZIO ENTSEGU ZINETIKO LEHIAKORRAK MARKATU GABEKO LIGANDOEN PARAMETRO ZINETIKOAK KALKULATZEKO

Motuslky eta Mahan zientzialariek 1984 urtean proposatutako metodologia aplikatu zen kannabinoide "hotz"-en parametro zinetikoak kalkulatzeko (Motulsky & Mahan, 1984). Modelo honetan, lotura esperimentu konpetitiboen bitartez eta modelo matematiko bat erabiliz, markatu gabeko edo ligando hotzen parametro zinetikoak kalkulatu daitezke. Orain dela gutxi arte, isotopo erradioaktiboekin markatutako ligandoak erabili izan dira gehien bat esperimentu mota hauek burutzeko. Dena dela, lan honetan fluoreszentziarekin markatutako ligandoak erabiltzen dira, TR-FRET teknologiak eskaintzen dituen abantailak direla eta. Erradioligandoekin burutako esperimentuekin alderatuta, TR-FRETen bidez hartzaile eta ligando fluoreszentearen arteko lotura neurtu daiteke eta kasu honetan, ez da laginaren iragazketa burutu behar, bolumen txikiagoekin lan egitea ahalbidetzen du, efizientzia handiagoarekin egiten da lan, eta hasierako denborak neurtzeko erraztasuna eskaintzen du metodo honek.

Metodologia honetan, markatutako ligandoaren konzentrazio bakarra erabiltzen da, [L], eta ligando hotzaren [B] konzentrazio desberdinak gehitzen dira. Modu honetan, ligando fluoreszentea [L] eta ligando hotza [B] aldi berean gehitzen dira, bien arteko lehiaketa bat sortuz hartzailera lotzeko. Modu honetan, lehiaketa hori eman ondoren hartzailera lotu den ligando fluoreszentea neurtu ahal izango dugu. Lotura lehiakor honen ondorioz, bi motatako hartzaile-ligando konplexuak lortuko dira; batetik, ligando hotzekin lotutako hartzaileak egongo dira [BR] , eta bestetik, ligando fluoreszenteekin lotutakoak [LR].

$$[R] + [L] + [B] \; \underset{\leftarrow}{\rightarrow} \; [LR] + [BR] \qquad (2.16)$$

Lehiatzen ari den [B] ligando hotzaren propietate zinetikoak eta konzentrazioak definituko du [LR] sorreraren abiadura.

Aurrekoa kontuan hartuta, posible izango da ez-markatutako ligando hotzen lotura eta disoziazio abiadurak kalkulatzea, hau da, asoziazio eta disoziazio

konstanteak, Motulskyk and Mahanek (1984) deskribatutako ekuazio hau erabiliz:

$$K_A = k_1[L] + k_2$$

$$K_B = k_3[I] + k_4$$

$$S = \sqrt{((K_A - K_A)^2 + 4 \cdot k_1 \cdot k_3 \cdot L \cdot I \cdot 10^{-18})}$$

$$K_F = 0.5 * (K_A + K_B + S)$$

$$K_S = 0.5 * (K_A + K_B - S)$$

$$Q = \frac{B_{max} * K_1 * L * 10^{-9}}{K_F - K_S}$$

$$Y = Q \cdot \left(\frac{k_4 \cdot (K_F - K_S)}{K_F \cdot K_S} + \frac{k_4 - K_F}{K_F} \; exp^{(-K_F \cdot X)} - \frac{k_4 \quad K_S}{K_S} \; exp^{(-K_S \cdot X)} \right) (2.17)$$

Hurrengo parametroak definituta egon beharko dute: X = denbora (min), Y = lotura espezifikoa (HTRF ratioa: 520nm/620nm*10,000), $k_1 = k_{on}$ (M^{-1} min^{-1}), k_2 = fluoreszentziadun ligandoaren k_{off} (min^{-1}), L = erabilitako fluoreszentziadun ligandoaren konzentrazioa (nM) eta I = ligando hotzaren kontzentrazioa (nM). Behin parametro guzti horien balioak finkatuta, posible izango da lotura abiadura konstantea (k_3=ligando hotzaren kon) and disoziazio abiadura konstantea (k_4= ligando hotzaren k_{off}) definitzea markatu gabeko ligandoarentzat, eta baita B$_{max}$ (orekan ematen den lotura espezifiko maximoa, HTRF ratio unitatean: 520 nm/620 nm *10,000).

Oreka disoziazio konstantea (K_d), ligandoen afinitatea definitzen duen parametroa da, eta honela deskribatu dezakegu:

$$Kd = \frac{Koff}{Kon} \qquad (2.18)$$

Motulsky eta Mahan metodologia aplikatuz kalkulatutako k_{on} eta k_{off} parametroek K_d kalkulatzea baimenduko dute.

SEINALEZTAPEN ENTSEGUAK ZELULETAN BRET ERABILIZ
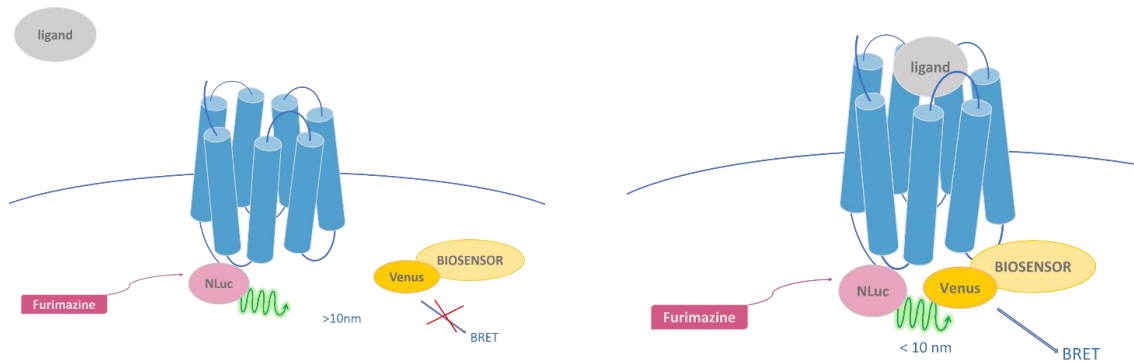
11. irudia. BRET entseguen printzipioaren adierazpen eskematikoa. GPCR hartzailearen C-muturrak Nluc entzima du fusionatuta, argia sortuko duena furimazina substratua medioan dagoenean. Biosentsoarea, berriz, Venus proteina fluoreszentearekin dago fusionatuta. Hartzailearen eta biosentsorearen arteko elkarrekintza estua ematen denean energia-transferentzia gertatuko da eta BRET energia neurtu ahal izango da.

Gure esperimentuetan, NanoLuc luziferasa entzima fusionatu genuen hartzailearen C-muturrean, eta horrek argia sortuko du furimazinarekin erreakzionatzean, energia-emaile moduan jokatuz (ikusi 11. irudia). Bestalde, erabilitako mGsi eta β-arrestina biosentsoreak eraldatu egin dira Venus proteina fluoreszentea lotuz. Venus proteina hori erresonantzia energia-hartzaile gisa jardungo du gure sisteman.

miniGsi akoplamendua neurtzeko entseguak

mGsi akoplamendu entseguak HEK293 T/17 zelulak erabiliz egin ziren; zelula horiek, hartzaileak (zelula barneko terminalean Nluc entzima fusionatuta dutenak) eta Venus proteina batekin fusionatutako mGsi proteinak espresatzen zituzten. miniG proteinak eraldatutako G proteinen alfa azpiunitateak dira, eta jatorriz GPCRak egonkortzeko eta haien egitura egoera aktiboan kristalizatzeko helburuarekin sortu ziren (Carpenter & Tate, 2016). Lan honetan, mGsi proteina erabili egin da; izan ere, miniG proteina azpimota horrek selektiboki imitatzen ditu G $_{i/o}$ azpifamiliako proteinak (Nehmea et al., 2017), CB1 eta CB2 hartzaileei lotzen zaizkien G proteina nagusiak.

Zelulak transfektatu egin ziren BRET erabiliz mGsi akoplamendua ebaluatzeko behar ziren elementuak espresatzeko, eta entseguak transfekzioa burutu eta 48 ordura egin ziren, zelulek proteinak adierazteko denbora nahikoa izan zezaten.

Zelulen medioa xurgatu egin zen, eta zelulak behin garbitu ziren HBSS tanpoia erabiliz. Entseguan erabilitako tanpoiak HBSS, 5 mM HEPES eta % 0,5 BSA (pH 7,4) zituen. Furimazina tanpoiari gehitu zitzaion 8 µM-ko azken kontzentrazioa lortzeko, plakari gehitu aurretik. Plaka irakurgailuan sartu zen (aurrez aurretik 37 °C-tara berotu zen) behin furimazina gehituta zelulak 15 minutuz inkubatu ziren konposatuak gehitu aurretik, luminiszentzia egonkortzeko.

β-arrestina 2 erreklutamendua neurtzeko entseguak

β-arrestina 2-ren erreklutamendu entseguak burutzeko, HEK TR zelula lerro egonkorrak erabili ziren, bai hartzaileak (zelula barneko terminalera Nluc bat fusionatuta zutelarik), bai Venus proteina batekin fusionatutako β-arrestin 2 proteina espresatzeko.

CB1 hartzailea eta biosentsorea adierazten dituen HEK TR zelula lerroa (HEKTR-SNAP-CB1-Nluc_βarr2-Venus) FACS (*Fluorescence activated cell sorting*) bidez hautatu zen seinale leiho handieneko zelula lerroa hautatzeko. CB2 eta hartzailea espresatzen zuen zelula lerroa biosentsore eta hartzaile DNA ratio desberdinekin sortutako hiru zelula lerroetatik aukeratu zen.

Zelulen medioa xurgatu egin zen, eta zelulak behin garbitu ziren HBSS tanpoia erabiliz. Entseguan erabilitako tanpoiak HBSS, 5 mM HEPES eta % 0,5 BSA (pH 7,4) zituen. Furimazina tanpoiari gehitu zitzaion 8 µM-ko azken kontzentrazioa lortzeko, plakari gehitu aurretik. Plaka irakurgailuan sartu zen (aurrez aurretik 37 °C-tara berotu zen) behin furimazina gehituta zelulak 15 minutuz inkubatu ziren konposatuak gehitu aurretik, luminiszentzia egonkortzeko.

HARTZAILEEN INTERNALIZAZIOAREN NEURKETA DERET ERABILIZ

DERET (*Diffusion-Enhanced Energy Transfer*) metodoak egoera berezi batzuetan energia-emaile eta energia-hartzaile bikote baten artean gertatzen den erresonantzia transferentzia du oinarri bezala. Teknika hori hartzaileen internalizazioa aztertzeko erabili da (Buenaventura et al., 2018; Roed et al., 2014), eta GPCRen barneratzea modu dinamiko eta zehatzean monitorizatzeko metodo baliotsua da (Levoye et al., 2015). Kasu horretan, fluoreszeina erabiltzen da energia-hartzaile bezala jokatzen duen molekula gisa. Molekula energia-emailea

terbioa da, eta hartzailearen zelulaz kanpoko SNAP proteinari lotuta egongo da. Fluoreszeina maila mikromolarreko kontzentrazioan egongo da ingurunean eta terbioak igorritako energia modu esanguratsuan xurgatzeko ahalmena edukiko du. Kondizio horiei esker, emailearen emisioan aldaketa bat monitorizatu ahal izango da, hartzaileak inguruan duen fluoreszeinaren arabera. Hartzailea mintzean dagoenean, ingurunean energia-hartzaile molekula (fluoreszeina) ugari egongo dira eta terbioak igortzen duen energiaren parte bat xurgatuko du. Zelula barnera internalizatzen diren hartzaileek, berriz, terbioaren seinalea igorriko dute fluoreszeinaren energia xurgapena gertatu gabe (ikusi 12. irudia)
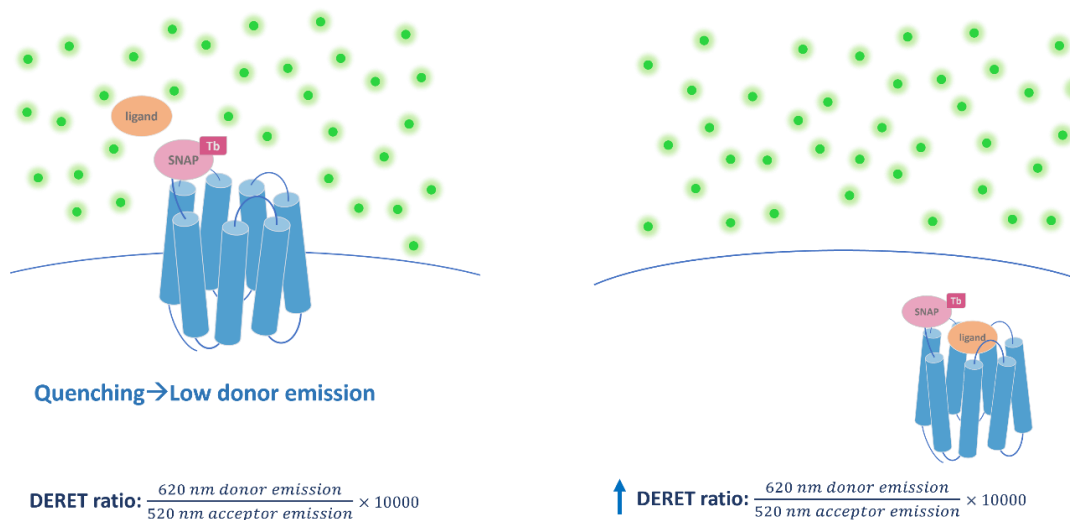
12. irudia. *DERET printzipioaren irudikapena. Gainazaleko hartzaileek terbioa (energia-emailea) lotuta dute. Zelulak fluoreseina kontzentrazio handiarekin (energia-hartzailea) daude kontaktuan beren gainazalean. Fluoreszeinak hartzaileetatik datorren terbio seinalearen parte xurgatuko du, eta horrek energia emailearen/hartzailearen arteko erlazioa txikiagotzea eragingo du (DERET ratioa). Gainazalean dauden hartzaileak zelula barnera internalizatzean, terboiaren emisioa ez da gutxituko fluoreszeinaren xurgapenagatik, eta ondorioz, DERET ratioa handitu egingo da.*

3. EMAITZAK

KONPOSATU KANNABINOIDEEN PARAMETRO ZINETIKOEN DETERMINAZIOA "MOTULSKY ETA MAHAN" METODOLOGIA APLIKATUZ

LIGANDOEN PARAMETRO ZINETIKOEN DETERMINAZIOA BALDINTZA FISIOLOGIKOETAN CB1 HARTZAILERA LOTZEAN

D77 ligando fluoreszentea erabiliz zen CB1 hartzailean asoziazio esperimentu lehiakor zinetikoak burutzeko. Esperimentuetan erabilitako D77 kontzentrazioa 600 nM-koa izan zen, 1,5 aldiz K_d gutxi gorabehera. D77-ren asoziazioa TR-FRET erabiliz monitorizatu zen kannabinoide hotz konzentrazioa desberdinen presentzian. Datuak globalki analizatu ziren GraphPad Prism erabiliz, eta asoziazio abiadura konstantea (k_{on}) eta disoziazio abiadura konstantea (k_{off}) kalkulatu ziren konposatu kannabinoide desberdinetarako.

Konposatu kannabinoide hotzak erabili ziren CB1 lotzeko D77 molekula fluoreszentearekin lehian, eta D77-ren lotura erakusten duten kurbak lortu ziren (ikus 13. irudia). Kurba horiek erakusten dute D77 loturaren inhibizioaren handipena lehian dagoen kannabinoide konposatu hotzaren kontzentrazioa handiagoa den einean. HU-210 ligandoarekin lortzen den konpetizio kurbak forma berezia erakusten du, non D77-ren loturaren handipena eta ondorengo txikitzea ikusten diren. Forma hau duten kurbak ligando hotzaren disoziazioa molekula fluoreszentearena baino geldoagoa denean lortzen dira. Gainerako kurbek D77 lotura pixkanaka handitzen dela erakusten dute, eta horrek adierazten du konposatu hotzak azkarrago disoziatzen direla molekula fluoreszentea baino.

Asoziazio esperimentu lehiakor zinetikoetatik parametro zinetikoak lortu ziren entseguetan erabilitako zazpi ligando kannabinoide hotzetarako. Modu honetan, asoziazio abiadura konstantea eta disoziazio abiadura konstateak kalkulatu ziren (k_{on} eta k_{off}) Motulsky eta Mahan modeloa aplikatuz, eta baita finkapen denbora ($1/k_{off}$), 1.taulan aurkitu daitezkeenak.
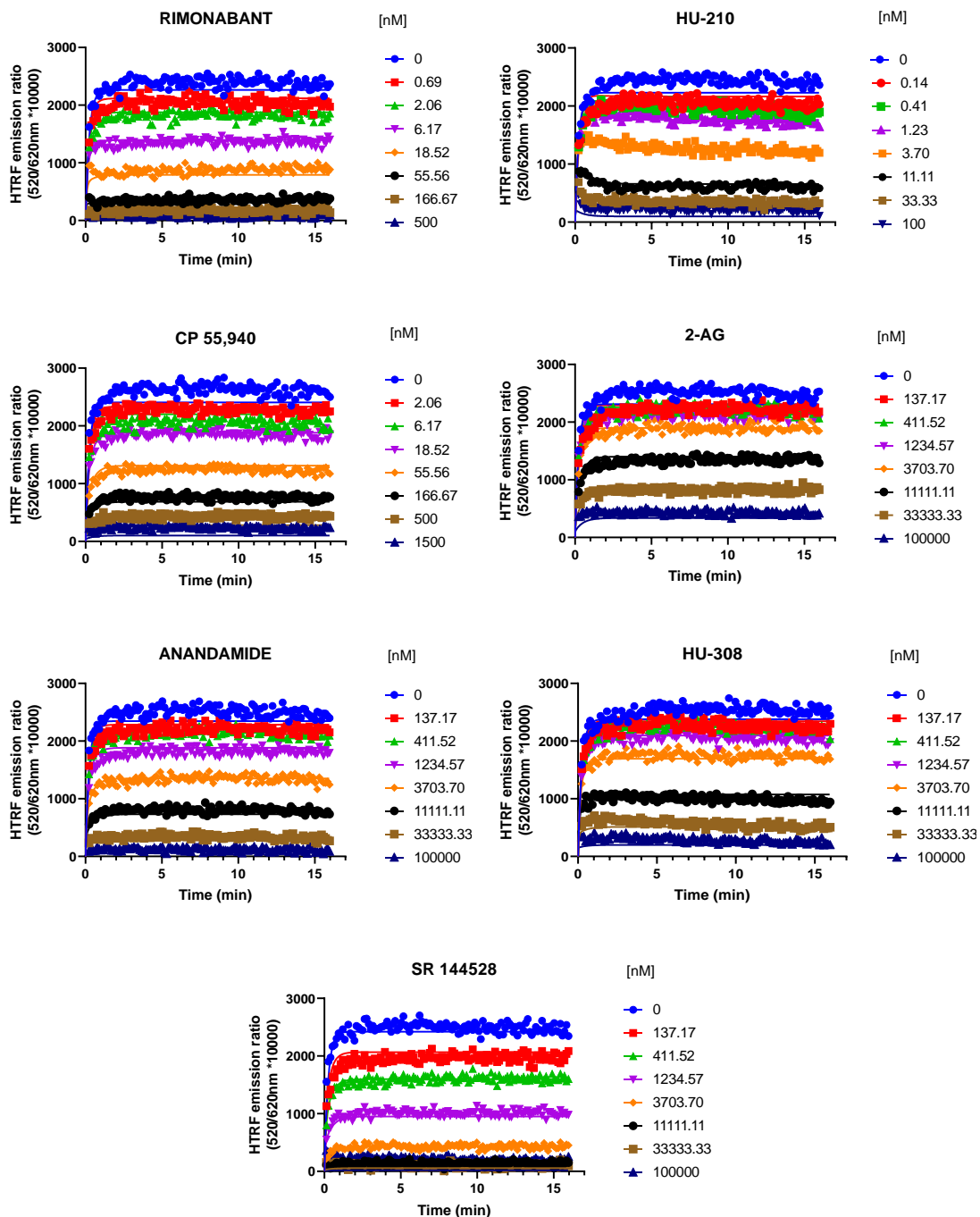
13. irudia. *Asoziazio lehiakor zinetiko esperimentuetatik lortutako kurbak. D77-ren asoziazioa CB1 hartzailera erakusten duten kurbek, 7 kanabinoide ligando desberdin erabiliz (37 °C). Esperimentuak egiteko, D77 (600 nM) molekula fluoreszentearekin hartzailera lotzeko lehiatzen duten kannabinoideen kontzentrazio gorakorrak erabili ziren.*

.
1. taula
Motulsky eta Mahan entseguetatik lortutako 7 konposatu kannabinoideen parametro zinetikoak CB1-era lotzean 37 °C-tan. Erakutsitako datuak era independentean burututako 4 esperimenturen emaitzaren batez bestekoak dira ± SEM (batez bestekoaren errore estandarra).

CB1 (37°C)	k_{on} (M^{-1} min^{-1})	k_{off} (min^{-1})	Finkapen denbora (Rt)	
			(min)	(s)
Rimonabant	$(5.0 \pm 0.5) \times 10^8$	2.2 ± 0.1	0.45 ± 0.03	**27 ± 2**
HU-210	$(3.8 \pm 0.1) \times 10^8$	0.85 ± 0.02	1.18 ± 0.03	**71 ± 2**
CP-55940	$(1.5 \pm 0.1) \times 10^8$	5.6 ± 0.3	0.18 ± 0.01	**10.8 ± 0.7**
2-AG (N=3)	$(1.4 \pm 0.5) \times 10^6$	6.7 ± 0.4	0.15 ± 0.01	**9.0 ± 0.5**
Anandamida	$(2.4 \pm 0.5) \times 10^6$	5.4 ± 0.6	0.19 ± 0.02	**12 ± 1**
HU-308	$(6.6 \pm 0.8) \times 10^5$	2.9 ± 0.3	0.35 ± 0.04	**21 ± 2**
SR144,528	$(1.4 \pm 0.2) \times 10^7$	5.0 ± 0.7	0.21 ± 0.03	**13 ± 2**

Konposatuen disoziazio-profilari dagokionez, disoziazio profil azkarrena duten konposatuak CP 55940, 2-AG, anandamida eta SR 144528 dira, eta hauek 10 s inguruko finkapen denbora dute CB1 hartzailean. HU-210-k du disoziazio profil motelena (k_{off} txikia) 70 s inguruko finkapen denborarekin, eta, ondoren, rimonabant (Rt=27 s) eta HU-308 (Rt=21 s) konposatuek.

Asoziazio profil azkarrena zuten konposatuak rimonabant, HU-210 eta CP 55940 izan ziren, 5, 3,8 eta 1,5 x 10^8 M^{-1} min^{-1}-ko k_{on}-arekin. 2-AG eta anandamida konposatu endokannabinoideak antzeko asoziazio abiadura konstanteak izan zituzten (k_{on} 1,4 eta 2,4 x10^6 M^{-1} min^{-1}, hurrenez hurren). Asoziazio geldoena zuen konposatua HU-308 izan zen (k_{on} 6,6 x 10^5 M^{-1} min^{-1}).

EMAITZAK

PARAMETRO ZINETIKOETATIK LORTUTAKO AFINITATE BALIOAK

Motulsky eta Mahan metodoa erabiliz lortutako parametro zinetikoak (1. taulan ageri direnak) konposatu kannabinoideen disoziazio-konstanteak kalkulatzeko erabili ziren. Horrela, disoziazio - eta asoziazio -konstanteak zatituz ($K_d=k_{off}/k_{on}$), afinitatea kalkulatu ahal izan zen (ikusi 2. taula).

HU-210 agonista ez-selektiboak CB1 hartzailearekiko afinitate handiena erakutsi zuen (K_d =2,2 nM) . Rimonabantek eta CP 55,940-k 4,6 eta 37 nM-ko K_d balioa dute, hurrenez hurren; SR 144,528-ren afinitatea 375 nM-koa izan zen. 2-AG eta anandamida bi konposatu endokannabinoideen afinitatea mikromolar tartean kokatu zen (K_d 5,8 eta 2,3 µM, hurrenez hurren). Kannabinoide endogenoen antzera, HU-308 konposatuak, CB2 agonista selektiboa dena afinitate txikia erakutsi zuen CB1 hartzailearekiko (K_d 4,5 µM).

2 taula

Konposatu kannabinoideen afinitate balioak CB1-era lotzeko 37 °C-tan. Motulsky eta Mahan metodologia erabiliz lortutako k_{on} eta k_{off} parametro zinetikoetatik abiatuta kalkulatu zen Kd zinetikoa. Eskuineko zutabean, afinitate-balioen eraldaketa logaritmiko negatiboa (pKd) ageri da. Erakutsitako datuak era independentean burututako 4 esperimenturen emaitzaren batez bestekoak dira ± SEM (batez bestekoaren errore estandarra).

| CB1 (37°C)	K_d zinetikoa (nM)	pK_d (M)
Rimonabant	4.6 ± 0.6	8.35 ± 0.06
HU-210	2.23 ± 0.03	8.65 ± 0.01
CP-55940	37 ± 2	7.44 ± 0.03
2-AG (N=3)	5882 ± 1573	5.3 ± 0.1
Anandamida	2323 ± 172	5.64 ± 0.03
HU-308	4514 ± 76	5.34 ± 0.01
SR144,528	375 ± 12	6.43 0.01

LIGANDOEN PARAMETRO ZINETIKOEN DETERMINAZIOA BALDINTZA FISIOLOGIKOETAN CB2 HARTZAILERA LOTZEAN

D77 ligando fluoreszentea erabiliz zen CB2 hartzailean asoziazio esperimentu lehiakor zinetikoak burutzeko. Esperimentuetan erabilitako D77 kontzentrazioa 900 nM-ekoa izan zen, 2 aldiz K_d gutxi gorabehera. D77-ren asoziazioa TR-FRET erabiliz monitorizatu zen kanabinoide hotz konzentrazioa desberdinen presentzian. Datuak globalki analizatu ziren GraphPad Prism erabiliz, eta asoziazio abiadura konstantea (k_{on}) eta disoziazio abiadura konstantea (k_{off}) kalkulatu ziren konposatu kannabinoide desberdinetarako.

Asoziazio azkarrena erakutsi zuten konposatuak CB2 hartzailera HU-210, CP 55,940 eta SR 144,528 izan ziren; beren k_{on} 2.6, 4.4, and 2.5 $\times 10^8$ M^{-1} min^{-1} izan zen. HU-308 konposatua izan zen hurrengo azkarrena, 5.6 $\times 10^7$ M^{-1} min^{-1}-ko k_{on} asoziazio konstantearekin. 2-AG eta anandamida konposatu endokannabinoideak antzeko asoziazio erakutsi zuten, aurrekoak baino geldoagoa (k_{on} 1.2 $\times 10^7$ eta 9.7 $\times 10^6$ M^{-1} min^{-1}, hurrenez hurren), rimonabanten antzerakoa (k_{on} 9 $\times 10^6$ M^{-1} min^{-1}).

Konposatuen disoziazio profilari dagokionez, azkarrenak 2-AG, rimonabant eta anandamida izan ziren, eta beraz, finkapen denbora laburrena erakutsi zutenak CB2 hartzailean, ~4 s (2-AG) and ~10s-koa. CP 55,940, HU-308 eta SR 144,528 disoziazio geldoagoa erakutsi zuten, 33 s, 40 s eta 87 s-ko finkapen denborarekin hurrenez hurren. HU-210 izan zen konposatu guztien artean disoziatzen mantxoena, 20 min-ko finkapen denbora zuelarik.

Motulsky and Mahan asoziazio lehiakor esperimentu zinetikoetatik kalkulatutako parametro zinetiko guztiak (k_{on}, k_{off} eta finkapen denbora) CB2 hartzailerako (ikusi 14. irudia) 3.taulan aurki daitezke.
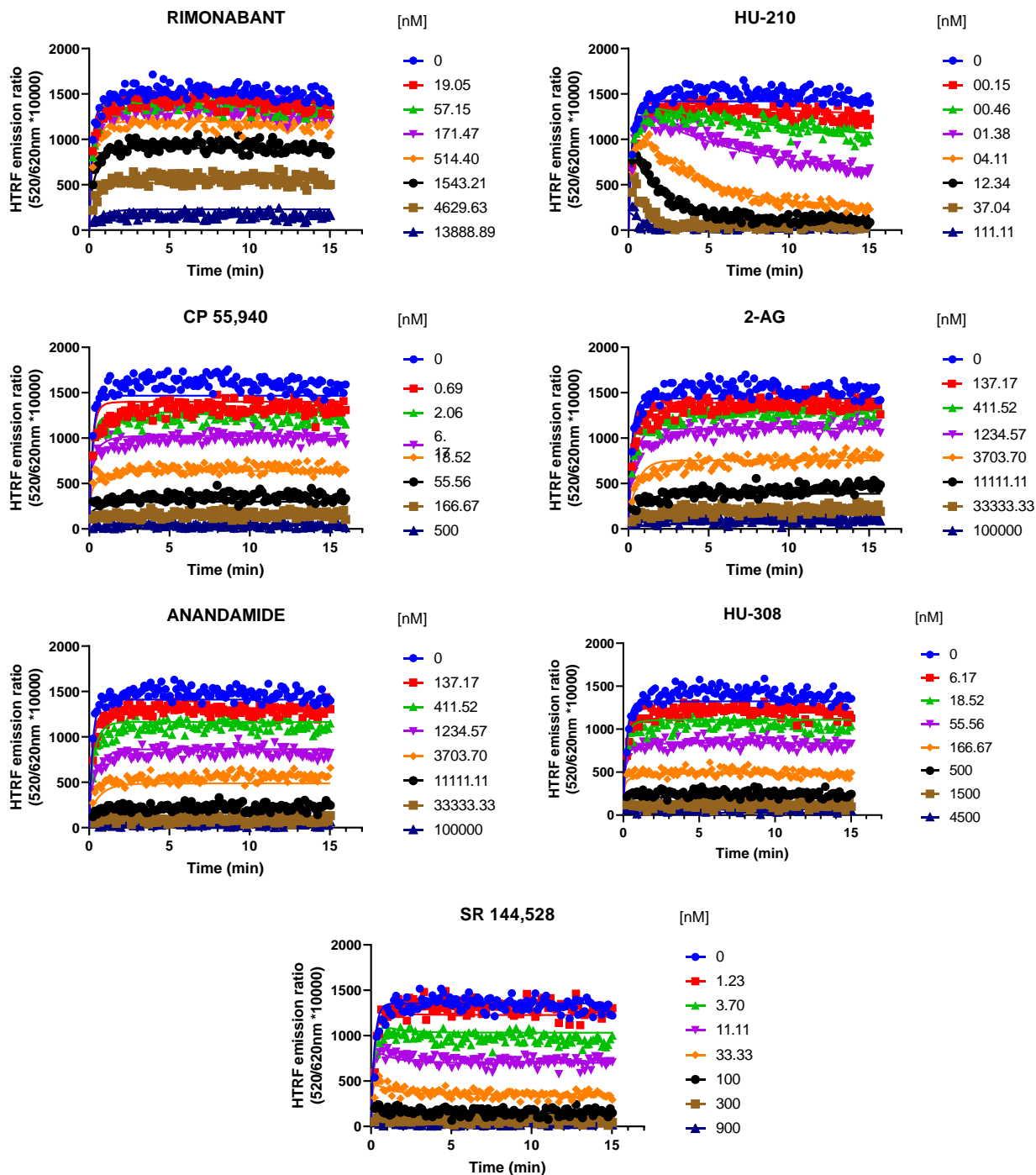
14. irudia. *Asoziazio lehiakor zinetiko esperimentuetatik lortutako kurbak. D77-ren asoziazioa CB2 hartzailera erakusten duten kurbek, 7 kanabinoide ligando desberdin erabiliz (37 ºC). Esperimentuak egiteko, D77 (900 nM) molekula fluoreszentearekin hartzailera lotzeko lehiatzen duten kannabinoideen kontzentrazio gorakorrak erabili ziren.*

3. taula
Motulsky eta Mahan entseguetatik lortutako 7 konposatu kannabinoideen parametro zinetikoak CB2-ra lotzean 37 °C-tan. Erakutsitako datuak era independentean burututako 4 esperimenturen emaitzaren batez bestekoak dira ± SEM (batez bestekoaren errore estandarra).

CB2 (37°C)	k_{on} (M^{-1} min^{-1})	k_{off} (min^{-1})	Finkapen denbora (Rt)	
			(min)	(s)
Rimonabant	(9 ± 1) x10^6	6.4 ± 0.7	0.16 ± 0.02	**10 ± 1**
HU-210	(2.6 ± 0.2) x10^8	0.051 ± 0.002	20 ± 1	**1190 ± 67**
CP-55940	(4.4 ± 0.5) x10^8	1.9 ± 0.1	0.55 ± 0.04	**33 ± 3**
2-AG	(1.2 ± 0.2) x10^7	14 ± 2	0.07 ± 0.01	**4.4 ± 0.7**
Anandamida	(9.7 ± 0.4) x10^6	6.1 ± 0.7	0.17 ± 0.02	**10 ± 1**
HU-308	(5.6 ± 0.3) x10^7	1.5 ± 0.1	0.66 ± 0.04	**40 ± 2**
SR144,528	(2.5 ± 0.2) x10^8	0.69 ± 0.03	1.46 ± 0.07	**87 ± 4**

PARAMETRO ZINETIKOETATIK LORTUTAKO AFINITATE BALIOAK

Motulsky eta Mahan metodoa erabiliz lortutako parametro zinetikoak (3. taulan ageri direnak) konposatu kannabinoideen disoziazio-konstanteak kalkulatzeko erabili ziren. Horrela, disoziazio eta asoziazio -konstanteak zatituz ($K_d=k_{off}/k_{on}$), afinitatea kalkulatu ahal izan zen (ikusi 4. taula).

4. taula
Konposatu kannabinoideen afinitate balioak CB2-ra lotzeko 37 °C-tan. Motulsky eta Mahan metodologia erabiliz lortutako k_{on} eta k_{off} parametro zinetikoetatik abiatuta kalkulatu zen K_d zinetikoa. Eskuineko zutabean, afinitate-balioen eraldaketa logaritmiko negatiboa (pK_d) ageri da. Erakutsitako datuak era independentean burututako 4 esperimenturen emaitzaren batez bestekoak dira ± SEM (batez bestekoaren errore estandarra).

CB2	K_d zinetikoa (nM)	pK_d (M)
Rimonabant	701 ± 52	6.16 ± 0.03
HU-210	0.20 ± 0.02	9.71 ± 0.05
CP-55940	4.27 ± 0.24	8.37 ± 0.02
2-AG (N=3)	1213 ± 109	5.92 ± 0.04
Anandamida	632 ± 52	6.20 ± 0.04
HU-308	27.5 ± 1.5	7.56 ± 0.02
SR144,528	2.82 ± 0.16	8.55 ± 0.03

HU-210 agonista ez-selektiboak erakutsi zuen afinitate handiena CB2 hartzailera lotzeko, bere afinitate balioa 0.2 nM zelarik. SR 144,528, CP 55940 eta HU-308-k 2.8, 4.2 nM and 27.5 nM-ko afinitatea aurkeztu zuten CB2 hartzailera lotzeko, hurrenez hurren. Rimonabantek 701 nM-ko afinitatea izan zuen, anandamidaren antzekoa (632 nM). Afinitate baxuena izan zuen konposatua 2-AG izan zen, 1.2 µM-ko K_d-a zuelarik.

PARAMETRO ZINETIKOAK ETA OREKA-AFINITATEA

Korrelazio analisi bat burutu genuen CB1 eta CB2 hartzaileetara lotzeko konposatuentzako lortutako parametron zinetikoekin (k_{on} and k_{off}) eta hauek orekan duten afinitatearekin. Hau eginez, CB1 eta CB2 hartzaileetan asoziazio eta

disoziazio abiadurek afinitatea zehazteko orduan jokatzen duten papera ikertu nahi izan genuen (ikusi 15.irudia).
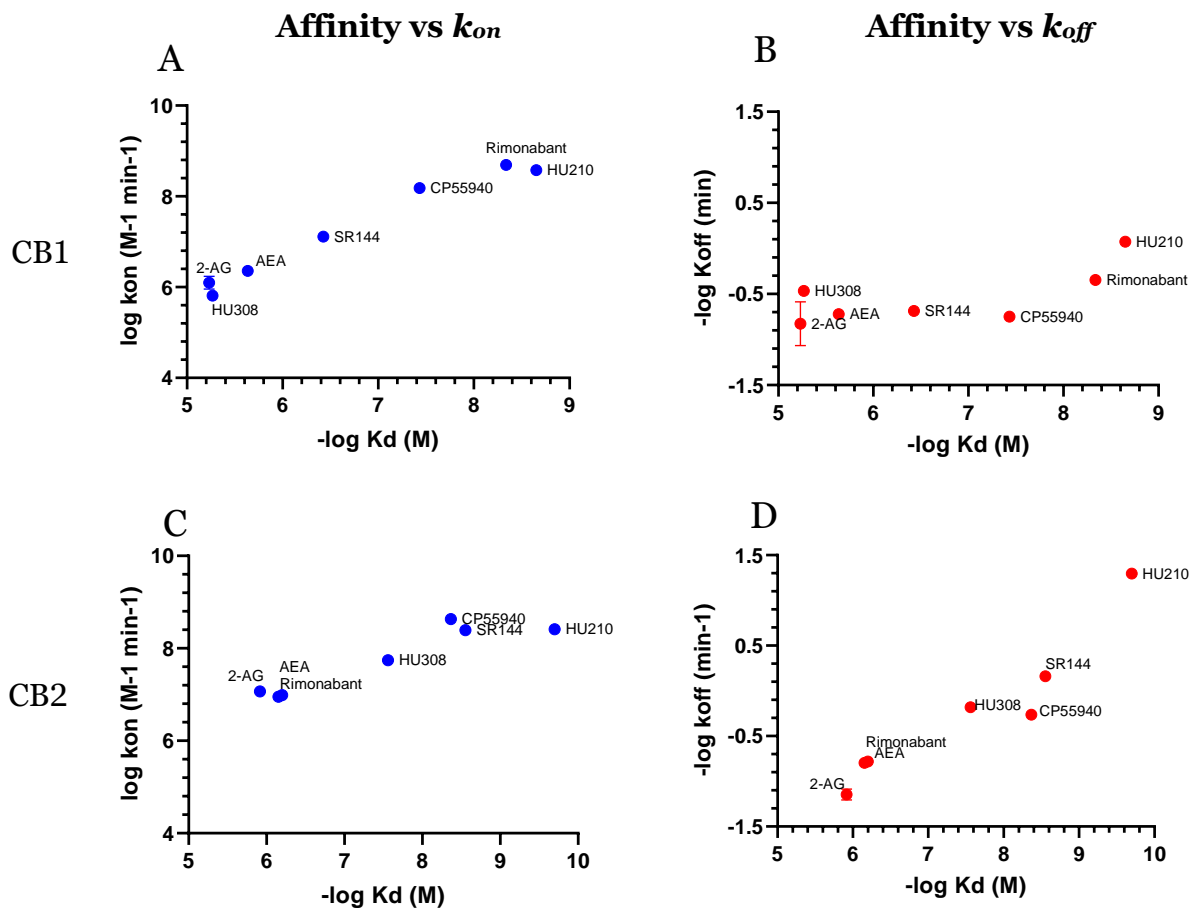
15. irudia. *Oreka afinitatearen (K_d) eta parametro zinetikoen (k_{on} eta k_{off}) arteko korrelazio grafikoak CB1 hartzailerako (A and B) and CB2 hartzailerako (C and D), 37 °C-tan neurtuta. Korrelazioa burutzeko balio guztiak beren aldaera logaritmiko negatiboetara transformatu ziren. Pearson-en korrelazio analisia erabili zen parametroen arteko erlazioa ikertzeko. Grafikoetan aurkezten diren datuak 4 esperimentu independenteen batez-bestekoak dira, eta errore barrek SEM erreflexatzen dute. P balioa < 0.0001***(A) eta < 0.0023**(C) izan zen -logKd eta log k_{on}-en korrelaziorako CB1 eta CB2 hartzaileetarako, hurrenez hurren (Pearson-en koefientea CB1 -0.985 eta CB2 -0.931). (B) -log k_{off} eta -log K_d ez dute korrelazio esanguratsurik aurkezten CB1 hartzailerako (p balioa= 0.08). (D) -log k_{off} and -log K_d balioek korrelazio esanguratsua dute CB2 hartzailerako, p balioa = 0.0015** delarik.*

Afinitate balioek eta asoziazio abiadura konstanteek korrelazio sendoa erakusten dute CB1 eta CB2 hartzaileen kasuan, transformatutako balioak erabiliz (pK_d vs log k_{on}) analisia gauzatu dugunean. Asoziazio abiadura konstanteak, berriz, soilik CB2 hartzailearen kasuan aurkezten du esanguratsua den korrelazioa afinitatearekin, eta ez CB1-en kasuan. Emaitza hauek iradokitzen duten k_{on} izango litzatekeela afinitatea determinatzeko parametrorik garrantzitsuena CB1

EMAITZAK

hartzailean, eta ez disoziazio abiadura konstantea (k_{off}). CB2 hartzaileetan, berriz, k_{on} eta k_{off} parametroek izango lukete pisua afinitatea determinatzeko garaian.

ESPERIMENTU LEHIAKORRAK OREKAN

Esperimentu lehiakorrak burutu ziren oreka-baldintzetan gure konposatu kannabinoideen disoziazio-konstantea (pK_i) kalkulatzeko. D77 markatzaile fluoreszentearen eta CB1 eta CB2 hartzaileen arteko lotura TR-FRET erabiliz monitorizatu zen, ligando kannabinoide hotzen kontzentrazio gorakorren presentzian, eta IC_{50} parametroak kalkulatu ziren lortutako kurbetatik. Ondoren, Cheng-Prusoff-en ekuazioa erabili zen K_i kalkulatzeko kurbetatik lortutako IC_{50} balioetatik abiatuta.
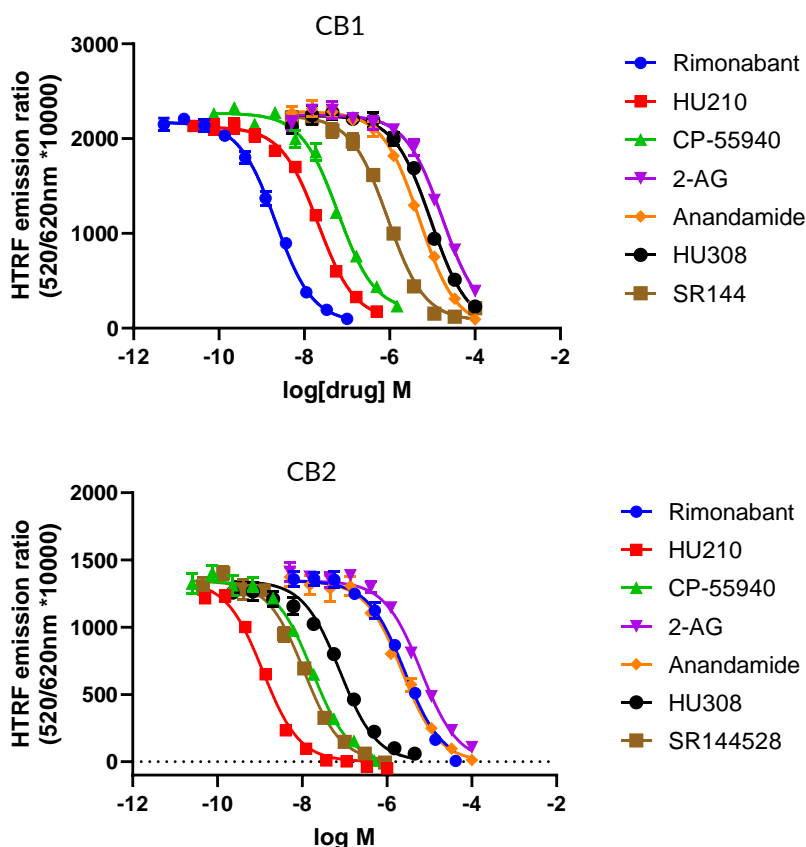
16. irudia. *Oreka egoeran lortutako konpetizio kurbak D77 ligando fluoreszentearekin lehiatzen duten 7 konposatu kannabinoideekin CB1 eta CB2 hartzaileetarako. D77 ligando fluoreszentearen 600 eta 900 nM erabili ziren CB1 aeta CB2 hartzaileen kasuan, hurrenez hurren.*

5. taula
Ligando kannabinoideetarako lortu ziren disoziazio oreka konstanteak, pKi. Erakusten diren datuak 4 esperimentuetan lortutako balioen batez-bestekoa ± SEM dira.

	$\mathbf{p}K_i$	
	CB1	CB2
Rimonabant	8.98 ± 0.05	5.9 ± 0.1
HU210	8.0 ± 0.1	9.48 ± 0.08
CP 55,940	7.5 ± 0.3	8.2 ± 0.1
2-AG	5.1 ± 0.3	5.7 ± 0.2
Anandamida	5.59 ± 0.04	6.0 ± 0.1
HU 308	5.41 ± 0.02	7.5 ± 0.1
SR 144,528	6.43 ± 0.01	8.47 ± 0.09

PARAMETRO ZINETIKOETATIK LORTUTAKO AFINITATE BALIOEN (K_d) ETA OREKA ESPERIMENTU LEHIAKORRETATIK LORTUTAKO AFINITATE BALIOEN (K_i) ARTEKO KONPARAZIOA

Konposatu kannabinoideen disoziazio-konstanteak kalkulatzeko, esperimentu zinetikoetatik lortutako parametroen zatidura (K_d *zinetikoa* $= k_{off}/k_{on}$) edota orekan egindako esperimentu lehiakorretatik kalkulatutako afinitate balioak (K_i) hartu ziren kontuan. Bi balioak konparatu egin ziren, CB1 edota CB2 hartzaileentzat lortutako datuak erabiliz.
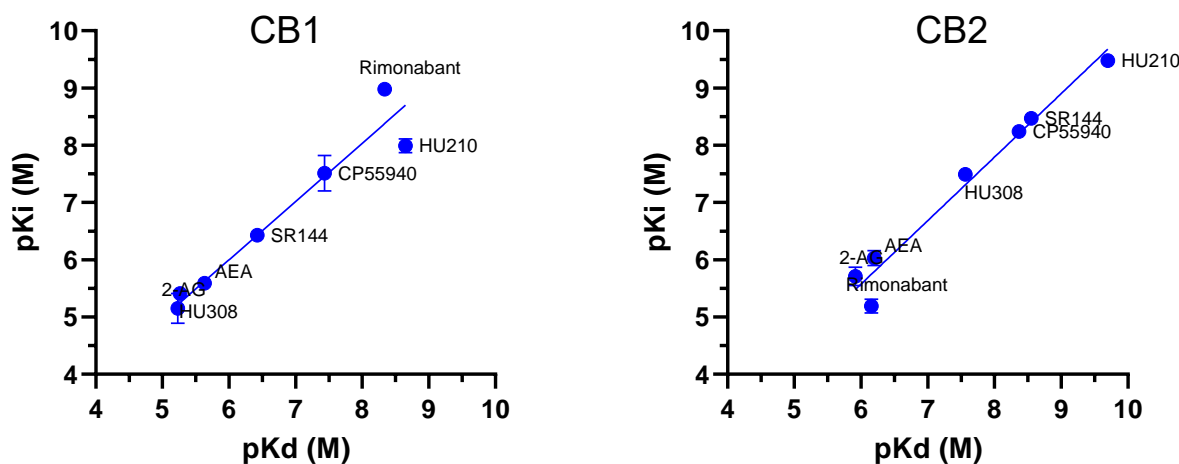
17. irudia. *Esperimentu zinetikoetatik (pK$_d$) eta oreka esperimentu lehiakorretatik (pK$_i$) lortutako afinitate balioen arteko korrelazio grafikak, CB1 eta CB2 hartzaileentzat.*

17. irudian ikusi daitekeen moduan, esperimentu zinetikoetatik lortutako K_d balioek korrelazio sendoa erakutsi zuten orekan burututako esperimentu lehiakorren bidez lortutako Ki balioekin, hala, Pearson-en korrelazio-koefizientea r=0,97 (P=0,0004) eta r=0,98 (P'0,0001) izan zen CB1 eta CB2 hartzaileen kasuan, hurrenez hurren. Emaitzek erakusten dute, bi esperimentu motak erabiliz oso antzeko balioak lorzten direla.

β-ARRESTINA 2 ERREKLUTAMENDUA CB1 ETA CB2 HARTZAILEETARA

β-arrestina 2-ren erreklutamendua CB1 edo CB2 hartzaileak eta β-arrestina 2 biosentsorea espresatzen zuten HEK TR zelula lerro egonkorretan aztertu zen, BRET erabiliz. Ligando kannabinoideak konzentrazio gorakorretan gehitu ziren, 10 μM-ko kontzentrazio maximoa erabiliz, 2-AG eta AEA endokannabinoideen kasuan izan ezik, non gehieneko kontzentrazioa 30 μM izan baitzen. BRET seinalea detektatu zen, eta dosi-erantzun kurbak sortu ziren ligandoa gehitu eta 15 min-ra lortutako datuekin (ikusi 18. irudia).

CB1 hartzailearen kasuan, HU-210 konposatuak du potentzia balio altuena β -arrestina 2-ren erreklutamendua induzitzeko, eta CP 55,940-k baino ~10 % handiagoa den efektu maximoa erakusten du. 2-AG eta anandamida konposatu endogenoek potentzia ahula dute seinaleztapen bide hau aktibatzeko, nahiz eta

hauek sortzen duten efektu maximoa oso desberdina izan. Anandamida agonista partzial moduan agertzen da, CP 55,940-k lortzen duen efektuaren % 70-a lortuz, baina 2-AG-k, ordea, CP 55,940-k lortzen duen %175-ko efektua eragiten du erabilitako kontzentrazio altuena kontuan hartuz. Nahiz eta rimonabant alderantzizko agonista bezala definitzen den, ezin izan dugu ikusi maila basalen gutxitzea entsegu hauetan. Erabili diren agonisten potentzia ordena β -arrestina 2 erreklutamendua induzitzeko honakoa izan da: HU-210≈ CP 55,940 > anandamida > 2-AG. Konposatu agonisten potentziaren balioak eta eragindako efektu maximoen balioak 6.taulan aurkitu daitezke.

6. taula
β-arrestina 2 erreklutatzeko agonista kannabinoideen potentzia eta efektu maximoen balioak (pEC$_{50}$ eta E$_{max}$) CB1 eta CB2 hartzaileak estimulatzean. Konposatuek eragindako efektu maximoa (E$_{max}$) CP 55,940 agonista erreferentzia moduan erabilita (% 100-ko eranztuna) kalkulatu zen. Datuak independenteki burututako ≥3 esperimentuen batez bestekoa ± SEM adierazten dute.

CB1	pEC$_{50}$	E$_{max}$	CB2	pEC$_{50}$	E$_{max}$
HU-210	8.21 ± 0.15	114 ±3	HU-210	9.19 ± 0.17	77 ±8
CP 55,940	8.03 ± 0.17	100	CP 55,940	8.95 ± 0.16	100
2-AG	4.81 ± 0.23	212 ± 45	2-AG	5.6 ± 0.32	102 ± 9
AEA	5.70 ± 0.27	63 ±8	AEA	6.6 ± 0.65	44 ± 12
			HU-308	7.72 ± 0.23	89 ± 9

CB2 hartzaileen kasuan, HU-210 eta CP 55,940 konposatuek erakutsi zuten potentzia altuena β-arrestina 2 erreklutatzeko. HU-210-ren efektu maximoa CP 55,940 erreferentzia agonistarekin lortutakoaren ~90 % izan zen. HU-308-k HU-210 and CP 55,940 baino potentzia eta efektu maximo baxuagoa erakutsi zuen, hala nola, CP 55,940-k lortutako efektu maximoaren % 77a. 2-AG eta AEA bi konposatu endogenoek erakutsi zuten potentziarik baxuena β -arrestina 2 erreklutatzeko. Hala ere, erabilitako konposatuen artean anandamidak E$_{max}$ baxuena eragin zuen arren, 2-AG izan zen efektu maximo altuena induzitzeko gai izan zen konposatua (CP 55,940-k eragindako efektu maximoaren % 134) nahiz eta potentzia baxua izan. Erabilitako agonisten potentzia ordena β-arrestina 2 erreklutatzeko CB2 hartzailera lotzean honakoa izan zen: HU-210≈CP 55,940 > HU 308 >anandamida> 2-AG.

EMAITZAK
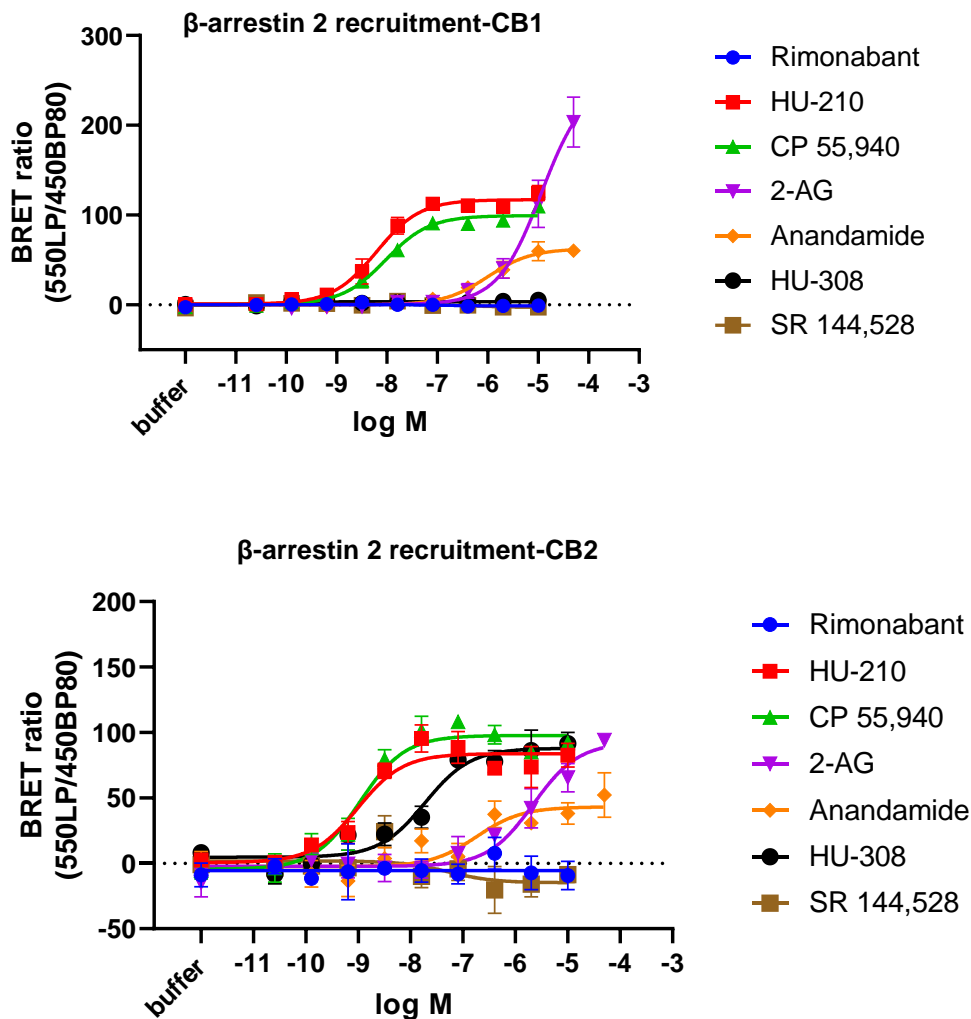
18. irudia. *Ligando kannabinoideek β -arrestina 2 erreklutamendua CB1 eta CB2 hartzaileetara induzitzeko duten gaitasuna erakusten duten dosi-erantzun kurbak. Datuak ligando kannabinoideak gehitu eta 15 min-tara, 37 °C -tan, lortu ziren. Lortutako BRET ratioak normalizatu egin ziren CP 55,940 erreferentzia agonista gisa erabiliz (% 100-eko erantzuna). Erakutsitako datuak independenteki egindako ≥3 esperimentuen batez bestekoa ± SEM irudikatzen dute.*
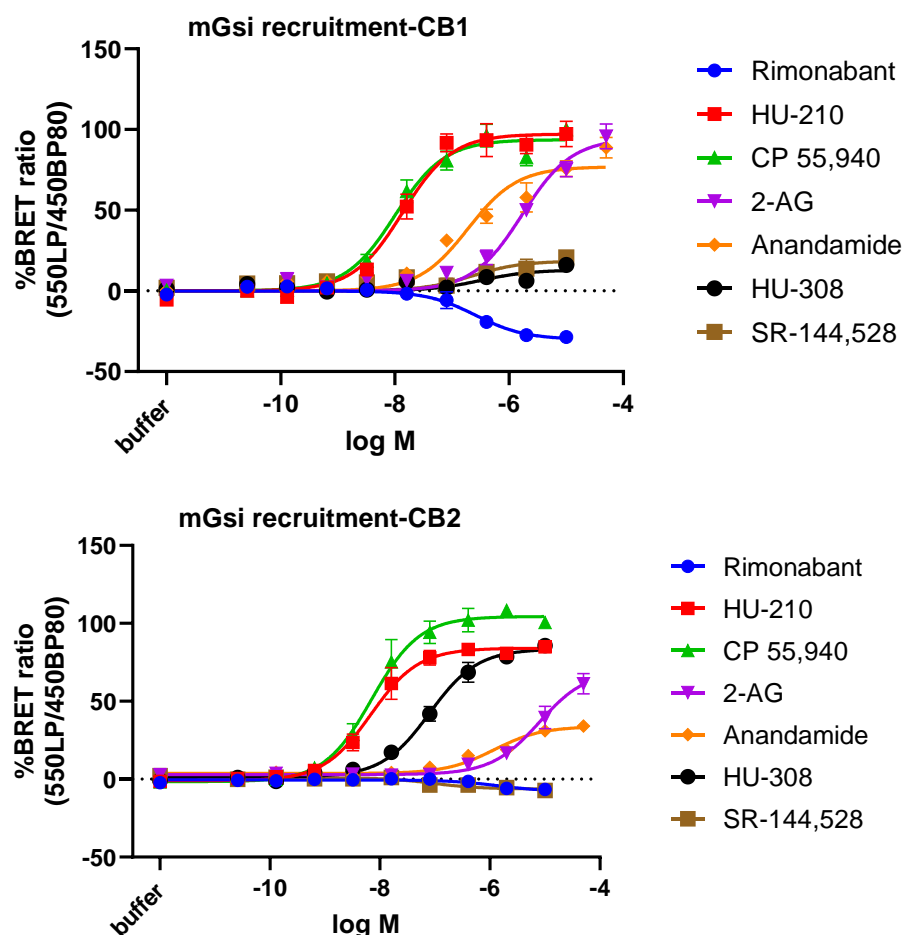
mGsi-REN AKOPLAMENDUA CB1 ETA CB2 HARTZAILEETARA

MiniGsi proteinen akoplamendua CB1 edo CB2 hartzaileak eta mGsi biosentsoreak modu iragankorrean espresatzen zuten HEK 293 T17 zeluletan aztertu zen, BRET erabiliz. Ligando kannabinoideak gero eta kontzentrazio handiagoetan gehitu ziren; 10 μM-ko kontzentrazio maximoa erabili zen, 2-AG

eta AEA endokannabinoideen kasuan izan ezik, non gehieneko kontzentrazioa 30 µM izan baitzen. BRET seinalea detektatu zen, eta dosi-erantzun kurbak sortu ziren ligandoa gehitu eta 15 min-ra lortutako datuekin (ikusi 19. irudia).

CB1 hartzailearen kasuan, bai CP 55,940-k eta bai HU-210-k agonismo totala erakutsi zuten mGsi akoplamendurako, eta baita 2-AG konposatu endogenoak ere. Anandamidak mGsi akoplamendua induzitzeko potentzia handiagoa duen arren CB1 hartzaileetan 2-AG-k baino, erantzun maximoa agonista totalak lortutakoa baino txikiagoa izan zen, eta CP 55,940-k sortutako erantzun maximoaren %~80 baino ez zen lortu anandamidarekin.

19.irudia. *Ligando kannabinoideek miniGsi proteinen akoplamendua CB1 eta CB2 hartzaileetara induzitzeko duten gaitasuna erakusten duten dosi-erantzun kurbak. Datuak ligando kannabinoideak gehitu eta 15 min-tara, 37 ºC -tan, lortu ziren. Lortutako BRET ratioak normalizatu egin ziren CP 55,940 erreferentzia agonista gisa erabiliz (% 100-eko erantzuna). Erakutsitako datuak independenteki egindako 4 esperimentuen batez bestekoa ± SEM irudikatzen dute*

EMAITZAK

Rimonabantek alderantzizko agonistaren propietateak ditu, izan ere mGsi akoplamendu basala % 30ean inhibitzeko gaitasuna du, CB1 hartzailearen aktibitate konstitutiboa agerian jartzen. CB2-rako seelktiboak diren HU-308 eta SR-144,528, mGsi akoplamendu oso ahula eragiten dute kontzentrazio handietan, agonismo partzial oso ahula eraginez CB1 hartzaileetara lotzean. Hala ere, BRET seinalearen igoera agonista totalaren erantzunaren % 20 baino txikiagoa da, eta EC_{50}-ren balioen kuantifikazioa ezin izan zen konfiantzaz egin. 7. taulan aurkitu daitezke agonista kannabinoideen potentziaren balioak (pEC_{50}) eta sortutako efektu maximoen balioak (E_{max}) mGsi akoplamendua induzitzeko. CB1 hartzaileetara mGsi akoplamendua eragiten duten agonisten potentzia ordena honakoa izan zen: HU-210≈CP 55,940 > anandamida> 2-AG.

CB2 hartzaileen kasuan, CP 55,940 konposatuak bakarrik erakutsi zuen agonismo totala mGsi akoplamendua aktibatzeko; HU-210, 2-AG, anandamidak eta HU-308 konposatuek, berriz, agonismo partziala erakutsi zuten, CP 55,940 -k eragindako aktibazio maximoaren % 80, % 66, % 30 eta % 55,76a eraginez, hurrenez hurren. CB2 hartzailearentzat selektiboa den HU-308 konposatuak HU-210 konposatuaren oso antzeko efektu maximoa eragin zuen, nahiz eta HU-308 konposatuak, HU-210k baino 10 aldiz potentzia baxuagoa duen efektua sortzeko. 2-AG eta anandamida agonista endogenoek potentzia txikia erakutsi zuten, CB1 hartzaileetan ikusitakoaren antzekoa, baina eragin maximo txikiagoa izan zuten CB2-aren kasuan. SR 144,528 konposatua alderantzizko agonista da, baina kasu honetan erantzun basalaren jeitsipen oso txikia eragiteko gai besterik ez da. Honek agerian jartzen du, CB2 hartzailean ikusi daitekeen aktibitate konstituzionala oso baxua dela CB1-arekin ikusten dugunaren aldean. Erabilitako agonistek CB2 hartzaileetara mGsi akoplamendua eragiteko potentzia ordena honakoa izan zen: HU-210≈CP 55,940 > HU 308 >anandamida> 2-AG.

7. taula
mGsi proteinaren akoplamendua induzitzeko agonista kannabinoideen potentzia eta efektu maximoaren balioak (pEC$_{50}$ eta E$_{max}$) CB1 eta CB2 hartzaileak estimulatzean. Konposatuek eragindako efektu maximoa (E$_{max}$) CP 55,940 agonista erreferentzia moduan erabilita (% 100-ko erantzuna) kalkulatu zen. Datuak independenteki burututako 4 esperimentuen batez bestekoa ± SEM adierazten dute.

| CB1	pEC$_{50}$	E$_{max}$	CB2	pEC$_{50}$	E$_{max}$
HU-210	7.91 ± 0.06	107 ± 8	HU-210	8.32 ± 0.03	80 ± 1
CP 55,940	8.00 ± 0.06	100	CP 55,940	8.29 ± 0.03	100
2-AG	5.66 ± 0.13	98 ± 8	2-AG	5.22 ± 0.08	66 ± 3
AEA	6.51 ± 0.15	78 ± 6	AEA	6.16 ± 0.13	30 ± 4
			HU-308	7.27 ± 0.08	76 ± 4

CB1 ETA CB2 HARTZAILEEN INTERNALIZAZIOA AGONISTEKIN ESTIMULATU OSTEAN

CB1 eta CB2 hartzaile kannabinoideen internalizazioa hartzaileak espresatzen zituzten HEK TR zeluletan ebaluatu zen, kanabinoideak lotzen zituzten zazpi ligandoekin estimulatu ondoren. Internalizazio prozesua dinamikoki ebaluatu zen 60 minutuz, DERET (*Difusion Enhanced Resonance Energy Transfer)* erabiliz.

Dosi-erantzun kurbak lortzeko, ligandoak gehitu eta 15 minututara lortutako datuak erabili ziren, une horretako EC_{50} eta efektu maximoa zehazteko. Lortutako datuak CP 55,940 erabiliz normalizatu ziren (CP 55,940 % 100-eko erantzuna), eta ligandorik erabili gabe antzeman zen internalizazio basala kontuan hartu zen, balio guztietatik hau kendu eta bakarrik ligandoek sortutako internalizazioa kalkulatzeko.

Lortutako dosi-erantzun kurbek erakusten dutenez, hartzaile kannabinoide bakoitzarentzat agonista gisa deskribatutako ligandoek kontzentrazioaren araberako internalizazio-profila sortu zuten (ikusi 20. irudia).

HEK TR-CB1 espresatzen zuten zeluletan, 2-AG kannabinoide endogenoak eragin zituen barneratze maila handienak, hala nola CP 55,940-k sortutako erantzunaren % 166 ± 16, nahiz eta potentzia txikia izan (EC_{50}= 1,7 µM). Bai HU-210 konposatuak eta bai anandamidak CP 55,940-ren antzeko internalizazio mailak sortu zituzten (104 ± 5 eta 105 ± 12, hurrenez hurren), baina HU-210 25 aldiz potenteagoa izan zen CB1 hartzaileen internalizazioa eragiteko anandamida baino. HU-308-k CB1 hartzailearen internalizazio oso ahula eragin zuen, CB2-rekiko selektiboa baita eta CB1 hartzailearekiko oso afinitate txikia baitu. Rimonabantek alderantzizko agonismoa eragiten du bide honetan, internalizazio basala murrizteko gaitasuna erakutsiz.
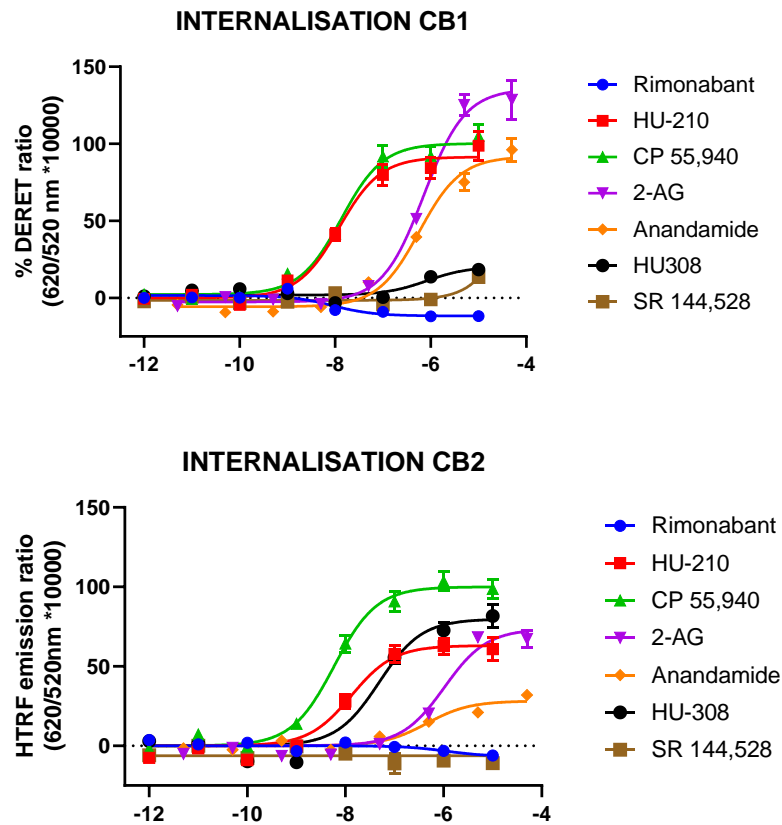
20. irudia. *CB1 eta CB2 hartzaileen internalizazioaren dosi-erantzun kurbak ligando kannabinoideak gehitu eta 15 min-ra, 37 ºC -tan. Lortutako DERET ratioak normalizatu egin ziren CP 55,940 erreferentzia agonista gisa erabiliz (% 100-eko erantzuna). Erakutsitako datuak esperimentu bakarretik lortutako 6 irakurketa desberdinen batez bestekoa ± SEM irudikatzen dute.*

EMAITZAK

CB2 hartzailea espresatzen zuten HEK TR zeluletan, CP 55,940 izan zen efektu handiena eragin zuen konposatua, eta baita potentzia altuena erakutsi zuena (EC_{50} 12 nM) hartzaileak barneratzeko. 2-AG eta AEA konposatu endogenoek bakarrik % 80 eta 20eko eragina izan zuten ,hurrenez hurren, hartzaileak internalizatzeko CP 55,940-rekin alderatuta, eta µM tarteko potentzia baxua erakutsi zuten. HU-210 konposatuak % 64-ko internalizazio maila eragin zuen CP 55,940-rekin konparatuz, baina biek antzeko potentzia izan zuten (EC_{50} =16 nM eta EC_{50} =13 nM, HU-210 eta CP 55,940-rako hurrenez hurren). HU-308 konposatuak %~86-ko internalizazioa eragin zuen eta potentzia EC_{50}=95nM-koa izan zen.

8. taula
CB1 eta CB2 hartzaileen internalizazioa induzitzeko agonista kannabinoideen potentzia eta efektu maximoaren balioak (pEC_{50} eta E_{max}). E_{max} -en balioak CP 55,940 agonista erreferentzia moduan erabilita (% 100-ko erantzuna) kalkulatu ziren. Datuak independenteki burututako 4 esperimentuen batez bestekoa ± SEM adierazten dute.

CB1	pEC_{50}	E_{max}	CB2	pEC_{50}	E_{max}
HU-210	7.80 ± 0.07	104 ± 5	HU-210	7.80 ± 0.05	64 ± 5
CP 55,940	7.64 ± 0.08	100	CP 55,940	7.9 ± 0.2	100
2-AG	5.7 ± 0.1	166 ± 17	2-AG	5.9 ± 0.2	82 ± 4
AEA	6.4 ± 0.2	105 ± 12	AEA	5.6 ± 0.3	20 ± 5
			HU 308	7.02 ± 0.09	86 ± 4

AGONISTA KANNABINOIDEEN SELEKTIBITATE FUNTZIONALA

Agonista kannabinoideek eragindako agonismoaren biderapena kalkulatu genuen CB1 eta CB2 hartzaileetara lotzean. Horretarako, mGsi akoplamendu, β-arrestina 2 erreklutamendu eta internalizazio entseguetan lortutako erantzunak kontuan hartu ziren. CB1 hartzailera lotzean, HU-210, CP 55940 eta anandamida konposatuek eragindako erantzunak analizatu ziren. CB2 hartzailearen kasuan, berriz, HU-210, 2-AG, AEA eta HU-308 konposatuen erantzunak hartu ziren kontuan.

Hiru seinaleztapen entseguetatik lortutako datuak modelo operazionala erabiliz analizatu ziren, $\log(\tau/KA)$ parametroa lortuz konposatu eta bide bakoitzerako. Agonista bakoitzerako bide bakoitzean lortutako transdukzio ratioak (τ/KA) konparatu egin ziren erreferentziazko agonistarekin. Horrela, transdukzio ratioen aldaketak $(\Delta\log(\tau/KA)_{lig-ref})$ kalkulatu ziren ligando bakoitzarentzat seinaleztapen bide bakoitzean erreferentziazko ligandoarekiko. 2-AG eta CP 55,940 konposatuak erabili ziren erreferentziazko ligando gisa CB1 eta CB2 hartzaileetarako, hurrenez hurren. Ondoren, $\Delta \log(\tau/KA)$ balioak erabili ziren $\Delta\Delta\log(\tau/KA)_{1-2}$ kalkulatzeko bi bide desberdinen artean, eta agonismoaren biderapena erreflexatzen duen balioa edo "*bias*" $(10^{\Delta\Delta\log(\tau/KA)_{1-2}})$ kalkulatu zen. Modelo operazionala aplikatuz agonisten biderapena islatzen duten balioak 9.taulan aurki daitezke. 21. irudian modu grafikoan islatzen da ligandoek bide bat ala beste aktibatzeko duten joera.

9. taula
*CB1 eta CB2 hartzaileetan eragiten duten agonisten $\Delta\Delta\log(\tau/KA)_{1-2}$ eta "bias" $(10^{\Delta\Delta\log(\tau/KA)_{1-2}})$ balioak. Izartxoa * duten balioek estatistikoki esanguratsua den joera aurkeztu duten bide bat bestearen aurretik aktibatzeko.*

CB1	mGsi-Intern		mGsi- β-arr2		β-arr2 -Intern	
	$\Delta\Delta\log(\tau/KA)$	Bias	$\Delta\Delta\log(\tau/KA)$	Bias	$\Delta\Delta\log(\tau/KA)$	Bias
2-AG (ref)	0	1	0	1	0	1
HU-210	0.82*	6.57*	-0.18	0.65	1.00*	9.97*
CP 55,940	0.81*	6.40*	0.11	1.28	0.70*	5.00*
AEA	0.65*	4.43*	0.28	1.92	0.36	2.31
CB2	**mGsi-Intern**		**mGsi- β-arr2**		**β-arr2 -Intern**	
	$\Delta\Delta\log(\tau/KA)$	Bias	$\Delta\Delta\log(\tau/KA)$	Bias	$\Delta\Delta\log(\tau/KA)$	Bias
CP 55,940 (ref)	0	1	0	1	0	1
HU-210	-0.24	0.57	0.24	1.75	-0.48*	0.33*
2-AG	-0.49*	0.32*	0.09	1.24	-0.58*	0.27*
AEA	-0.24	0.57	0.02	1.04	-0.26*	0.55*
HU-308	-0.34*	0.45*	-0.02	0.95	-0.32	0.47

EMAITZAK

Aztertutako konposatu guztiek joera esanguratsua dute aztertutako erantzun batzuk besteen aurrean aktibatzeko. CB1 hartzailean jarduten duten konposatuek ez zuten inolako lehentasunik erakutsi mGsi eta β-arrestina 2 erreklutamendua aktibatzearen artean, baina guztiek lehentasuna izan zuten mGsi akoplamendua induzitzeko, internalizazioarekin alderatuta. HU-210 eta CP 55,940-k β-arrestina 2-ren erreklutamendua eragiteko joera dute, internalizazioarekin alderatuta, eta baita AEA-k, nahiz eta azken honek ez duen estatistikoki esanguratsua den baliorik lortu analisian.

CB1 hartzaileetan gertatzen den antzera, CB2 hartzailean jarduten duten konposatuek ez zuten joerarik erakutsi mGsi eta β-arrestina 2 erreklutamendua aktibatzearen artean. 2-AG eta HU-308 konposatuek internalizazioa induzitzeko joera aurkeztu dute, mGsi akoplamenduarekin alderatuta. HU-210, 2-AG eta AEA konposatuek lehentasuna dute internalizazioa eragiteko β-arrestina 2 erreklutamenduarekin konparatzean.
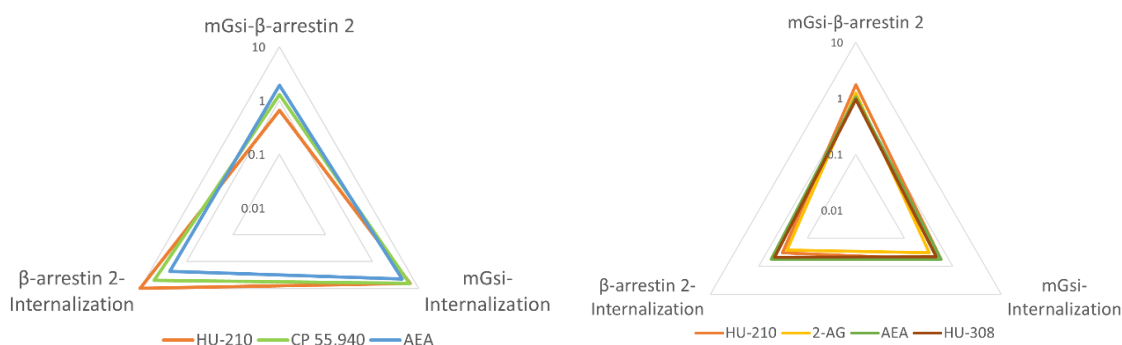

21. irudia. *Konposatu agonistek bide bat edo beste aktibatzeko duten lehentasuna erreflexatzen duen grafikoa. 2-AG eta CP 55,940 konposatuak erreferentziazko konposatuen moduan erabili ziren CB1 eta CB2 hartzaileen kasuan, hurrenez hurren, modelo operazionala aplikatu eta agonisten biderapena kalkulatzeko. Radar-grafiko gisa adierazten dira mGsi akoplamenduaren, agonistek eragindako internalizazioaren eta β-arrestina 2 erreklutamenduaren arteko agonisten "bias" balioak ($10^{\Delta\Delta log\ (\tau/KA)\ 1-2}$).*

Aztertutako erantzunetako bat aktibatzeko joera orokorra ikusten da hartzaileetako bakoitzean. CB1 hartzailean eragiten duten agonisten kasuan, estatistikoki esanguratsuak diren balioak joera mGsi-ren aldekoa dela islatzen dute; aldiz, kontrakoa gertatzen da CB2 hartzailearen kasuan, non agonistek lehentasuna baitute internalizazioa eragiteko β-arrestina 2 edo mGsi akoplamenduaren gainetik biderapena esanguratsua den kasu guztietan.

AGONISTEN FINKAPEN DENBORA ETA ERAGINKORTASUNAREN ARTEKO ERLAZIOA

Eraginkortasun balioak (τ) modelo operazionaletik eratorritako log R-tik (log R=log τ/KA) abiatuta kalkulatu ziren agonista bakoitzarentzat, eta finkapen denborarekin (Rt=1/k_{off}) duen erlazioa aztertu zen Pearson-en korrelazio-azterketa aplikatuz (bi-mutur).

CB1 hartzailearen kasuan, lau agonisten eraginkortasuna, HU-210, CP 55,940, 2-AG eta anandamida, honela kalkulatu zen: mGsi akoplamendua, β-arrestina 2 erreklutamendua edo internalizaziorako τ (tau), ligandoa gehitu eta 15 minutura. CB2-rako analisiak agonista berak ditu, baina baita HU-308 agonista selektiboa ere; hau da, bost konposatu guztira.
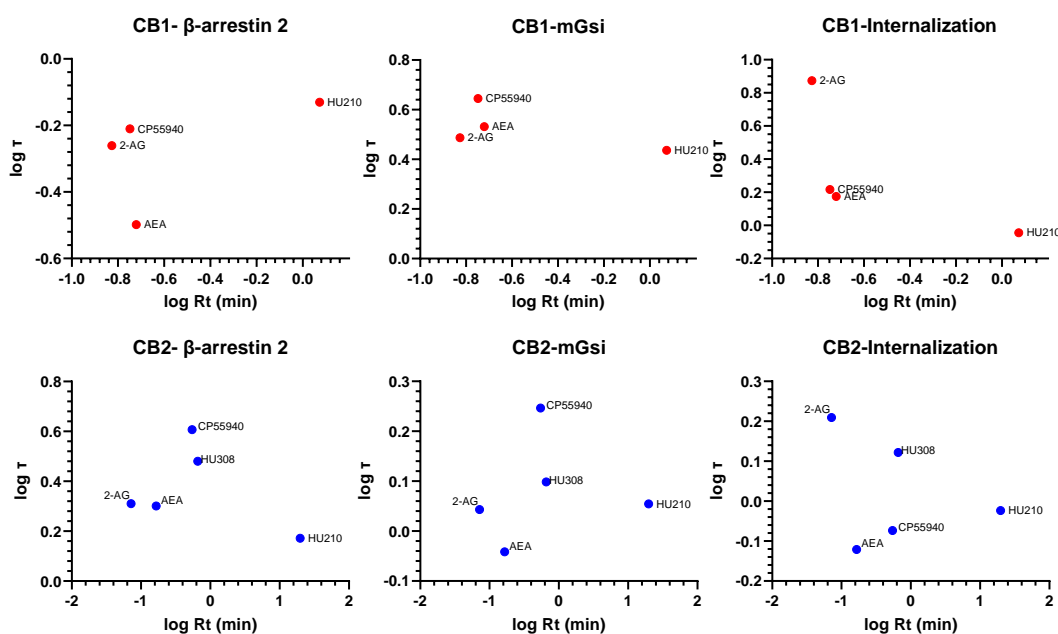
22. irudia. *Agonista kannabinoideen finkapen denbora (Rt) eta bide bakoitzean azaltzen duten eraginkortasuna (tau) erlazionatzen dituzten grafikoak CB1 eta CB2 hartzaileetan. Pearson korrelazio analisia erabili zen bi parametroen arteko erlazio lineala ote zegoen analizatzeko eta ez zen erlazio esanguratsurik aurkitu bi balioen artean ikertutako hiru seinaleztapen bideentzat ez CB1-ean ezta CB2-an ere.*

Korrelazio hori erabiliz, aztertu nahi izan genuen ea CB1 eta CB2 hartzaileekin elkartzen diren agonisten kasuan, hartzaile-agonista konplexuaren iraupenak

EMAITZAK

(hau da, finkapen denbora =Rt) eragina izan dezakeen aztertutako erantzunak aktibatzeko eraginkortasunean.

22. irudian ikusi daitekeenez, ez zen korrelazio esanguratsurik aurkitu aztertutako konposatu multzorako bi parametroen artean. Eraginkortasuna (τ) parametroak ez zuten korrelazio esanguratsurik erakusten ligandoen finkapen denborarekin (Rt) aztertutako kasuetan.

4.ONDORIOAK

ONDORIOAK

Aurreko atalean azaldutako emaitzak kontuan hartuta, honako hauek dira tesi honen ondorio nagusiak:

1. TR-FRET metodologian oinarritzen den entsegu berri bat garatu da, ligando kannabinoideen parametro zinetikoak kalkulatzeko CB1 eta CB2 hartzaileetan lotzean.

     1.1. D77 ligando fluoreszenteak profil zinetiko aproposa erakusten du CB1 eta CB2 hartzaileetara lotzean, eta honek "Motulsky eta Mahan" metodologia aplikatzea baimentzen du. D77 ligandoak afinitate egokia eta disoziazio profil azkarra du.

     1.2. Entsegu hau konposatu kannabinoideen parametro zinetikoak zehazteko HTRF metodologia erabiltzen duen lehen entsegua da. Gainera, bere errendimendu altua kontuan izanik, eskala handian erabiltzea posible izango da konposatu kannabinoideak zinetikoki karakterizatzeko.

     1.3. FRET seinaleztapena lortu ahal izateko, CB1 hartzailearen N-muturraren lehen 90 aminoazidoak ezabatu dira, beraz, CB1 $_{91-472}$ aldaera erabili da ligandoen parametro zinetikoak kalkulatzeko.

2. Zazpi ligando kannabinoide desberdin CB1 eta CB2 hartzaileetara lotzean azaltzen dituzten asoziazio eta disoziazio abiadura konstanteak (k_{on} eta k_{off}) kalkulatu dira, afinitate baxua duten 2-AG eta anandamida konposatu endokanabinoideak barne.

     2.1. Zinetikaren bidez lortutako afinitate-balioek (K_d zinetikoa) korrelazio estua dute orekan gauzatutako lehiaketa esperimentuen bidez lortutako K_i balioekin, eta horrek adierazten du Motulsky eta Mahan metodologiaren bidezko determinazio zinetikoa modu egokian egin dela.

     2.2. Garatutako metodologiak lotura zinetika parametroen determinazioa tenperatura fisiologikoan egitea ahalbidetzen du (37 °C-tan). Honek parametro zinetikoak zeluletan burututako seinaleztapen entsegu desberdinekin erlazionatzea baimentzen du, orokorrean 37 °C-tan gauzatzen baitira entsegu hauek.

2.3. CB1 hartzailearen kasuan, badirudi k_{on} asoziazio abiadura konstantea dela afinitatea bideratzen duen parametro nagusia; CB2 hartzailerako , berriz, k_{on} eta baita k_{off} konstanteek aurkezten dute korrelazioa afinitatearekin erabilitako konposatu multzoaren parametroak aztertu direnean.

3. Konposatu agonistek β-arrestina 2-ren erreklutamenduan, mGsi-ren akoplamenduan eta internalizazioan sortutako erantzuna ebaluatu da, eta eredu operazionala aplikatu da bideratutako agonismoa kuantifikatzeko. CB1 eta CB2 hartzaileekin elkartzean, agonista kannabinoideek bideratutako agonismoa aurkeztu dezakete, baina aztertutako agonistek ez dute joera sendorik aurkeztu bide bat selektiboki aktibatzeko beste baten gainetik.

3.1. Honako hau izan da CB1 hartzaileetan β-arrestina 2 erreklutatzeko eta mGsi akoplamendua eragiteko konposatuen potentziaren ordena: HU-210≈CP55,940 > anandamida > 2-AG. CB2 hartzaileen kasuan, potentziaren ordena honakoa izan zen: HU-210≈CP 55,940 > HU-308 >anandamida> 2-AG

3.2. Hartzaileen internalizazioa eragiteko agonisten potentziaren ordena honakoa izan zen CB1 hartzaileetan: HU-210≈CP 55,940 > anandamida> 2-AG. CB2 hartzaileetan, potentziaren ordena honakoa izan zen: HU-210≈CP 55,940 > HU-308 >anandamida≈2-AG.

3.3. Neurtu diren hiru erantzunetan, konposatuen potentzia-balioen ordena oso antzekoa izan den arren, konposatuen eraginkortasun maximoa aldatu egin da bideetan zehar. CB1 hartzaileetan, CP 55,940 eta HU-210 mGsi akoplamendua eragiteko bakarrik jardun dira agonista oso gisa. 2-AG konposatuak, berriz, β-arrestina 2 lotzeko eta internalizazioa eragiteko izan du efektu maximoa. CB2 hartzaileetan, berriz, CP 55,940 konposatuak agonista oso gisa jokatu du kasu guztietan, eta 2-AG konposatuak, agonista osoaren portaera erakutsi du soilik β-arrestina 2-ren erreklutamenduan.

ONDORIOAK

4. Azterketa honetarako hautatutako konposatuak aztertu ondoren, ezin dugu baieztatu ligandoen lotura zinetikek edo finkapen-denborek eragin zuzena dutenik CB1 eta CB2 hartzaileak aktibatzean ligandoek aurkezten duten eraginkortasunean (τ).

    4.1. Aztertutako hiru seinaleztapen bideetan, log τ balioek ez dute korrelazio esanguratsua aurkezten finkapen-denborarekin; β-arrestina 2 erreklutamendua, mGsi akoplamendua eta internalizazioa aztertzean lortu diren korrelazioaren R^2-ren balioak honakoak izan dira, CB1 hartzaileetarako: 0.31, 0.38 eta 0.45, hurrenez hurren; eta CB2 hartzailerako: 0.11, 0.02 eta 0.09.

    4.2. Hala ere, lan honetan erabili diren konposatu agonista kannabinoideen kopurua mugatua da eta, beraz, agonista gehiago erabiliko dituzten etorkizuneko azterketek aukera emango dute zinetikak kannabinoideen eraginkortasunean duen garrantzia sakonago aztertzea.

BIBLIOGRAFIA

Testuan agertzen diren erreferentzia bibliografikoak "REFERENCES" atalean aurkitu daitezke, 123. orrialdetik aurrera.